

博士論文（要約）

A Framework Toward Better Specification
of the Building Envelope Characteristics
with Respecting Cooling Demands

(冷房負荷を中心とした外皮性能の特性
評価の改善に向けたフレームワーク)

イドリス ヤシン

i. Acknowledgements

I would like to express my sincere thanks to the MEXT, the Ministry of Education, Culture, Sports, Science and Technology for giving me this priceless opportunity to continue my study journey.

I would like to pass my gratitude to my advisor Professor Mae for all the great opportunities that he have provided.

I would like also to send thanks to all my labmates for their continuous support of my Ph.D study.

Last but not least, to my beloved, mother, father, brother and sisters, and my children, and to all the amazing people whom I have lived with,

And for the person who held me up along this path,
my beloved wife.

Thank you

ii. Table of Contents

i.	Acknowledgements.....	3
ii.	Table of Contents.....	4
iii.	List of tables	6
iv.	List of figures.....	6
	Chapter 1.....	15
1.	Introduction and Literature Review.....	15
1.1	Introduction	17
1.1.1	The increasing need for cooling.....	17
1.1.2	The role of the building envelope in reducing cooling loads.....	21
1.1.3	The problem statement.....	25
1.1.4	The thesis structure	31
1.2	Literature review.....	33
1.2.1	The scope of the literature survey.....	33
1.2.2	Research on the envelope core	34
1.2.3	Research on the envelope external skin.....	41
1.2.4	The Framework outlines	52
	Chapter 2.....	54
2.	Before the Simulation	54
2.1	Reasons behind employing EnergyPlus	56
2.2	Weather files reliability investigation	58
2.3	Testing the layer segmentation process influence on the layer config.....	65
	Chapter 3.....	74
3.	The layer configuration influence on the anti-insulation (JOURNAL ARTICLE).....	74
	Chapter 4:	76
4.	The number of layers' influence on the anti-insulation (Simulation).....	76
4.1	Preface and Objectives	78
4.2	Methodology and Simulation setup.....	78
4.3	Results and discussion	81
4.4	Conclusion.....	89

Chapter 5:	91
5. The number of layers' influence on the dynamic thermal behaviour. (Experimenting)	91
5.1 Introduction	93
5.2 Thermal Mass material selection.....	96
5.3 Experimental setup	100
5.3.1 The base configurations.....	101
5.3.2 The Peltier device, and the Rig setup	103
5.3.3 Thermal conditions setup	106
5.4 Results and discussion	108
5.5 Conclusion.....	118
Chapter 6:	120
6. Reflective paints study	120
6.1 Introduction	122
6.2 First experiment (inspection).....	122
6.2.1 Experimental setup and methodology	122
6.2.2 Results and Discussion	126
6.3 Second experiment	134
6.3.1 Methodology.....	134
6.3.2 Results and Discussion	139
6.4 Conclusion.....	151
Chapter 7:	153
7. Conclusion.....	153
7.1 Summary of the findings	154
7.2 The concluded framework	156
7.3 Limitation and further work	158
Bibliography	161

iii. List of tables

All tables are for Chapter 3, which has been “masked” from this abridged version of thesis.

iv. List of figures

Figure 1-1. The Title keywords are elaborated in individual sections. These what compose the main parts of the introduction section.	17
Figure 1-2. Some climate change observations provided by the Synthesis Report. Contribution of Working Groups I, II and III to the Fifth Assessment Report of the Intergovernmental Panel on Climate Change IPCC (Contribution of Working Groups I & IPCC 2014).....	18
Figure 1-3 Population distribution by size class of settlement and region, 2016 and 2030 (United Nations, Department of Economic and Social Affairs 2016).....	19
Figure 1-4. Sketch of urban heat island profile in Singapore. (Priyadarsini et al. 2008).....	20
Figure 1-5. Worldwide residential energy consumption.	21
Figure 1-6. U.S. primary energy consumption (quads)	22
Figure 1-7 Classification of Passive cooling approaches in the energy-efficient building by (N. B. Geetha 2012). The shaded parts are highlighting the passive approaches that the envelope can interplay with.....	23
Figure 1-8. Staged maximum adoption potential and staged payback in 2030 for priority windows and building envelope technologies in the residential (R) and commercial (C) building sectors. Provided by (US Department of Energy 2014b).....	24
Figure 1-9 Participants’ (ZEB Optimization experts) choices of optimization objective functions. Source: (Attia et al. 2013).	25
Figure 1-10 The Thesis framework outlines, and the envelope specification issues to address and advance	26
Figure 1-11 The periodic heat flow through a light and heavy wall of the same U-value. Produced by (Roaf et al. 2007) and referenced to (Szokolay 2007).	28
Figure 1-12 The optimum insulation thickness have no upper limits and can be increased once the insulation cost is decreased or when the energy cost increases (Kaynakli 2012).....	29
Figure 1-13 Envelope insulation material cost and performance targets (US Department of Energy 2014b).	29
Figure 1-14 the envelope is only described by the type and thickness of the heat insulating material. Reference (Japan Sustainable Building Consortium 2011).....	31
Figure 1-15 The key issue that are addressed by this research.....	32
Figure 1-16 Envelope component's Typologies as being studied in the literature. The highlighted parts are within study scope.....	33
Figure 1-17 The schematic representation of time lag ϕ and decrement factor f . Whereas t_{To}^{max} and t_{Te}^{max} (h) represent the time in hours when inside and outside surface temperatures are at their maximums, respectively.(Asan 2006).	36

Figure 1-18 Combined effects of Heat Capacity ρ (kJ/Km ²) and Thermal Conductivity k (W/mK) on; [a] Time Lag [b] Decrement Factor	38
Figure 1-19 ORNL Thermal Mass Calculator - Dynamic Benefits of the Massive Systems (DBMS)	40
Figure 1-20 Comparison of solar and earth radiations wavelengths.....	42
Figure 1-21 Solar energy distribution. Source: (Haavi et al. 2012)	43
Figure 1-22 Spectra for (a) blackbody exitance at four temperatures, (b) extra-terrestrial solar irradiance, (c) typical Absorptance across the atmospheric envelope, (d) relative sensitivity of the human eye and relative photon efficiency of photosynthesis in green plants. Source: (Granqvist 1981).	44
Figure 1-23 Emissivity/absorptivity of the photonic radiative cooler from the ultraviolet to the mid-infrared.	44
Figure 1-24 Generalised compositions of pigmented liquid coatings and manner of film formation. Source (H. E. Ashton 1966):	45
Figure 1-25 Types of spectrally selective paints.	46
Figure 1-26 Climate effect on cooling and heating load changes when altering roof solar reflectance from 0.2 to 0.65. (Synnefa et al. 2007)	47
Figure 1-27 Variation of yearly cooling and heating transmission loads versus insulation thickness with respect to solar absorptivity varying from 0 to 1. (Ozel 2012).	47
Figure 1-28 Variation of yearly averaged Time Lag and Decrement Factor versus insulation thickness with respect to solar absorptivity varying from 0 to 1.(Ozel 2012).	49
Figure 1-29 Time lag (φ_{max}) VS. Solar absorptivity (α_{solar}) for the wall formations with insulation as (a) one layer and (b) two layers.(Kontoleon & Bikas 2007).....	50
Figure 1-30 Values of sol-air temperature over time with respect to Solar Absorbtivity values. (Kontoleon & Bikas 2007).	50
Figure 1-31 Time Lag and Decrement Factor values VS solar absorptivity for a two insulation layer's wall configurations at different wall orientations;	52
Figure 2-1 Summary of research on optimisation of opaque envelope components.(Stevanović 2013).	56
Figure 2-2 Summary of a full review of optimisation of passive solar design strategies by (Stevanović 2013).	57
Figure 2-3 Optimisation tools order by use (right) and simulation tools ordered by use (left). The line thickness is proportional to the frequency of the pairings. (Attia et al. 2013).....	58
Figure 2-4 Internal Data Element Names (directly applicable to EPW). Source:(US Department of Energy 2015a) Page 14 of 144.	59
Figure 2-5 EPW Availability map. (Ladybug + Honeybee & Github n.d.)	60
Figure 2-6 Replacement values for the missing weather data. (US Department of Energy 2015c)	61
Figure 2-7 Tokyo- Mismatch between the calculated and the Given Horizontal IR radiation Intensity Wh/m ²	62

Figure 2-8 Las Vegas - Mismatch between the calculated and the Given Horizontal IR radiation Intensity	62
Figure 2-9 Khartoum, Sudan - Mismatch between the calculated and the Given Horizontal IR radiation Intensity.....	63
Figure 2-10 The [10 °C] CDD values obtained from the *.STAT file contents for HOUSTON BUSH INTERCONTINENTAL.	64
Figure 2-11 The CDD [10 °C] values as obtained from the AHSRAE commercial spreadsheet data for HOUSTON BUSH INTERCONTINENTAL.	64
Figure 2-12 the CDD [10 °C] variation between the *.STAT data and the AHSRAE commercial spreadsheet data for 13 climates.	65
Figure 2-13 Accuracy Sensitivity investigation various setups for the Layers Subdivision and heat balance calculation algorithm.....	66
Figure 2-14 Layers subdivision inputs to the EnergyPlus.....	66
Figure 2-15 Heat Balance Algorithm refinement fine-tuning is made by incorporating the “HeatBalanceSettings: ConductionFiniteDifference” object.	67
Figure 2-16 The [Conduction Finite Difference] calculation nodes are displayed in the *.EOI file	68
Figure 2-17 The Total, Maximum and Minimum variation between the different setups simulation results.....	69
Figure 2-18 The Hourly variation values between the fine-tuned models (C) and (D).....	70
Figure 2-19 Layer segmentation influence on the calculation results.....	70
Figure 2-20 Heat Balance Algorithm refinement influences on the calculation results.....	71
Figure 2-21 Simple layer subdivision and maximum model refinements influences on the calculation results.	72
Figure 2-22 Absolute Differences of cooling loads among the various setups.....	72
Figure 4-1 The base configurations and the occupancy profiles that will be used as references for layer segmentation/ dispersion evaluation.	79
Figure 4-2 The layer’s segmentation technique for the specific multiplication number.	80
Figure 4-3 The layers segmentation process for an example case of [IMI] with an insulation layer of 20 cm.	80
Figure 4-4 The Layer Configurations preference order for the Residential with continuous load occupancy profiles in two sample climates.	82
Figure 4-5 Taking the Base case [IMI] as a reference to evaluate the layer segmentation performance across the various insulation thicknesses.	83
Figure 4-6 Some of the derived segmentations have been simulated in Chapter 3. Shaded cells are for the borrowed results.....	83
Figure 4-7 Layer Configurations preference order for the Office occupancy profiles in two sample climates.	84
Figure 4-8 Taking the Baseline scenario [IM] as a reference to evaluate the layer segmentation performance under the Office occupancy profile, and across the various insulation thicknesses.	85

Figure 4-9 Layer Configurations preference order for the Office with continuous load occupancy profiles in two sample climates. For the base configuration of [MI].....	86
Figure 4-10 Taking the Base case [MI] as a reference to evaluate the layer segmentation performance across the various insulation thicknesses.	86
Figure 4-11 The PTI values for the Layer Configurations investigated under an Office with continuous load occupancy profiles in two sample climates. For the base configuration of [MI].....	87
Figure 4-12 Layer Configurations preference order for the Residential occupancy profiles for the two sample climates. For the base configuration of [IMI]	88
Figure 4-13 Taking the Base case [IMI] as a reference to evaluate the layer segmentation performance across the various insulation thicknesses.	88
Figure 4-14 The PTI values for the various Layer Configurations the Residential occupancy profile with the continuous load. Note, that [IM-4] with 20cm have very close PTI compared to much less insulation i.e. [IM] at only 5cm.	89
Figure 4-15 The PTI values for the various Layer Configurations the Residential occupancy profile with the continuous load. Note, that the base case [IM] at 5cm and 10 have an always saving Anti-insulation pattern (I) and have degraded to pattern (III) after some segmentation.	90
Figure 4-16 The PTI values for the various Layer Configurations the Residential occupancy profile with the continuous load. Note, that more layers segments yield higher PTIs where the effect is pronounced at lower insulation thicknesses.....	90
Figure 5-1 Time lags between the indoor and outdoor temperature in a Haveli in Jaisalmer India.....	94
Figure 5-2 The practicality constraint against maximum utilisation of conventional thermal mass materials in multi-layered envelope components.	95
Figure 5-3 Compound Decrement Factors and Time Lags for different building materials. The highlighted materials have high heat capacity capabilities, great time lag and low decrement factor values.	97
Figure 5-4 The heat capacity capabilities of a selected list of materials including various types of rubber and asphalt, together with the conventional thermal mass materials i.e. brick concrete and some rock types. Data are obtained from (Asan & Sancaktar 1998),(Thermtest Inc. 2016) and (MakeltFrom.com 2009).	98
Figure 5-5 The heat capacity capabilities of four best-performing types of rubber. Materials thermophysical property data are obtained from (Thermtest Inc. 2016) and (MakeltFrom.com 2009).	99
Figure 5-6 Young's modulus, E , against density, ρ . The design guidelines assist in the selection of materials for minimum weight, stiffness-limited design. (Data courtesy of Granta Design Ltd) Reference: (Cambridge University Engineering Department 2003).....	99
Figure 5-7 The heat capacity of the procured Butyl rubber compared to the base information.....	101

Figure 5-8 Two first sets were proposed for the experiment, where configuration either have an internal mass (rubber) or external mass.	102
Figure 5-9 the experimented configurations.	103
Figure 5-10 The Peltier device controlling dashboard and experimental units.	104
Figure 5-11 The heat flux meters are attached to the internal and external faces of the wall specimen.	105
Figure 5-12 The Butyl rubber and the Extruded Polystyrene (XPS) preparation and positioning of the Peltier device.	105
Figure 5-13 Various experimental device components.	106
Figure 5-14 The Experimental conditions, where the internal temperature is fixed, and the Sinusoidal Curve resembles the external temperature.	107
Figure 5-15 In the Peltier device the configuration can be altered by changing the heat flux direction instead of rearranging the layers.	108
Figure 5-16 The temperature distribution profiles for the various configurations. The effect of the rubber appears a Time Lag which is the slight shift between the peaks. While the insulation prevails in reducing the temperature -vertical gap (Decrement Factor).....	109
Figure 5-17 The heat flux curves of a sample configuration of [MI].	110
Figure 5-18 The individual internal and external heat flux patterns of the investigated configurations.	111
Figure 5-19 The outer and internal heat flux of the various configurations are plotted in the same graph for better referencing and comparison.....	112
Figure 5-20 The Decrement Factor values and ranking for the various configurations.	113
Figure 5-21 The internal heat flux curves are inverted as to better visualise the Time Lag (heat wave peak delay) about the external heat flux curve.....	114
Figure 5-22 The Time Lag values and ranking for the various configurations.	115
Figure 5-23 The Dynamic R-values of the various configurations compared to their (shared) nominal R-Value.	116
Figure 5-24 The Experimental conditions of a proposed initial transient experiment, where the internal temperature is fixed, and Sinusoidal curve resembles the external temperature.....	117
Figure 5-25 The sample case (configuration) that is used for testing the effect of the initial transient operation.	117
Figure 5-26 The experimental situation of a proposed initial transient experiment, where the internal temperature is fixed, and the Sinusoidal Curve resembles the external temperature.....	118
Figure 6-1 The importance of the external Skin – and its effect on the envelope performance.	123

Figure 6-2 The bare concrete tiles are used to investigate the measurement tool (Hioki 8422-50) reliability and error margin.....	124
Figure 6-3 The roof tiles are located in a way to minimise the shading effect of the surrounding context.....	124
Figure 6-4 The cornered tiles (1, 2, 9,10) are kept plain to monitor the shading effect. Meanwhile, the sealer base is applied over four tiles of the six tiles that will be painted.	125
Figure 6-5 The application of the paint base “Sealer” have an immediate influence on the surface temperature, where the difference between the plain tile and the tile with a sealer is about 15°K.	125
Figure 6-6 The six cases (permutations) are a named basis on the three parameters being investigated. The first parameter is the paint type either Normal paint or Solar paint. The second parameter is the paint colour (White, Grey and Black). The third parameter is either the paint is directly applied to the tile or applied on top of a sealer base.....	126
Figure 6-7 The first Infrared thermal photos showing the surface temperature variation than the reference tile i.e. the bare tile. Note that all the painted tiles are cooler than the bare concrete tile.....	127
Figure 6-8 The fluctuation range of surface temperatures. The average temperature is for the bare concrete tiles i.e. (C1, C2, C3 and C4).....	128
Figure 6-9 The fluctuation range of soffit temperatures. The average temperature is for the bare concrete tiles i.e. (C1, C2, C3 and C4). The results of the case of the Black Solar paint without sealer (S-B-F) are excluded due to reading errors., similar to what is seen in the solar white paint on a sealer, i.e. case (S-W-S).....	129
Figure 6-10 The tiles surface and soffit temperature averages are showing that the soffit temperature instantaneously follows the surface temperatures.....	130
Figure 6-11 the impact of using solar paint is studied by comparing the normal grey and solar grey paints in reference with the bare concrete tiles; where both are applied over a sealer base.....	130
Figure 6-12 the impact of using solar paint colour is studied by comparing the three colours of solar paints when applied over a sealer base.....	131
Figure 6-13 the impact of using solar paint colour without a sealer base is studied by comparing the white and black colours of solar paints.	132
Figure 6-14 the impact of having a sealer base on the black solar paint is studied by comparing the cases (S-B-S) solar black on sealer and (S-B-F) solar black on facial surface.	133
Figure 6-15 the impact of having a sealer base on the white solar paint is studied by comparing the cases (S-W-S) solar white on sealer and (S-W-F) solar white on the facial surface.	133
Figure 6-16 The second experiment investigated factors and the resultant permutation (cases) matrix.....	134

Figure 6-17 The cases/permutations name coding methodology	135
Figure 6-18 The second experiment is located at the less shaded area, where the sun exposure analysis confirmed that the location has full access to the solar radiation during the experimental period.	136
Figure 6-19 The tiles are placed over a cm XPS sheet that is suspended for the roof slab by a Styrofoam legs as to reduce the heat transfer for the roof to the tiles to the minimum degree.	137
Figure 6-20 A custom made plastic caps with an aluminium foil finishing are placed to protect the thermocouple probes from the direct sunlight throughout the day.	137
Figure 6-21 Temperature distribution Standard Deviation for sample tiles.	138
Figure 6-22 Temperature variation between the tiles surface and edges may exceed 5°K	139
Figure 6-23 Selecting the sample days through September 2016.....	140
Figure 6-24 The Top and bottom temperatures variation	141
Figure 6-25 The group of cases that have a soffit temperature that is hotter than their surface temperatures. The group consists of black paint, conventional paint and tiles without paint.....	141
Figure 6-26 The influence of the sealer is made by comparing the tile that only has a sealer together with the plain tile located on the eastern side.....	142
Figure 6-27 The result of the comparison between the plain (bare) concrete tile and the tile with sealer only.....	143
Figure 6-28 The sealer that was used in the second experiment was transparent. Unlike the first experiment where the sealer was white.....	143
Figure 6-29 Two sets (Group) of cases that either applies the sealer or without the sealer base (facial) are compared to study the influence of the sealer application on the solar paint temperature profiles.....	144
Figure 6-30 Maximum temperatures difference [without sealer - sealer base].....	145
Figure 6-31 Maximum temperatures difference [without sealer - sealer base] with weather conditions being considered.....	145
Figure 6-32 The solar paints reflection rates as per provided by the manufacturer. Source:(SCI-PAINT JAPAN INC. 2008).	146
Figure 6-33 Identification of the representative sunny (clear) and cloudy (overcast) days.....	147
Figure 6-34 Comparing the temperature profile for the glossy and matte finishes in a sunny and cloudy days.....	148
Figure 6-35 Comparing the temperature profile for the glossy and matte finishes in all the sampling ten days.....	148

Figure 6-36 The temperature variation is calculated by subtracting the glossy minus the matte Temp for all the three paint colours.	149
Figure 6-37 A closer look at the Glossy and matte paints temperature profile in the morning of the cloudy day.	150
Figure 6-38 The infrared portion of the solar spectrum is high in the early morning and overwhelmed by the visible components at noon. Source:(National Institute of Standards and Technology 2015).	150
Figure 6-39 The change in the solar spectrum portions in the various conditions, i.e. the NIR portion drops by the presence of the cloud.	150
Figure 6-40 Average, Maximum, and Minimum Temperature for the period (2nd~11th Sept.) for all the experimental permutations compared to the base cases i.e. the bare (plain) concrete tiles and the normal paints	151
Figure 7-1 the framwrok formulation.	157

Chapter 1

1. Introduction and Literature Review

This chapter narrates the research story and the need and importance of the research topic before delving into specific technicalities at later chapters. It is intended to shed light on the research problem within the most relevant up-to-date knowledge areas. This chapter is divided into two main sections. The first section is the broad introduction to the research; whereas each chapter will have its introduction as well. The second section is concerned with the literature review that was used to build the research questions and arguments. The literature review (relevant work) is used to identifying the research field and scope of interests, hence It is introduced in a wider perspective rather than reviewing detailed procedures, as these are elaborated among their specific chapters.

1.1 Introduction

In the beginning, the research is introduced by elaborating the research title keywords, whereas each of these keywords is addressed individually in a dedicated subsection. That is, the research title has four keywords which are; Framework, Better Specification, Envelope and Cooling. For a better understanding and better arguments coherence, the subsections are structured in a reversed order; i.e. the first subsection is concerned with the cooling and the increasing need for cooling. The second is to acknowledge the importance of the building's envelope from within the energy efficient and passive designs point of view. The third subsection embraces the phrase "toward better specification". Here, the key research problem; which is, how the envelope is being specified in the building's energy oriented codes (standards, and legislations) is tackled with quoting some known examples. The last part shows that this thesis research is aimed at providing a "framework" to solve the introduced problem.

Figure 1-1. is used to visualise the structure mentioned above. However, the introduction section encompasses the framework in the subsections 3 and 4 . in this venue, It is thought that it is equally important for the reader to understand the interrelation between the different chapters and components and how to allocate these components within the wider research scope. Showing the thesis structure is meant to avoid redundancy and repetition, and to keep the text at a reasonable size.

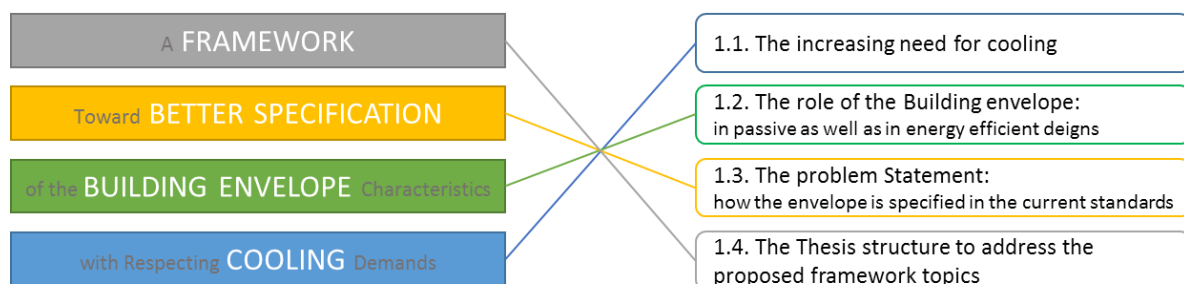


Figure 1-1. The Title keywords are elaborated in individual sections. These what compose the main parts of the introduction section.

1.1.1 The increasing need for cooling

It can be seen that the research is solely oriented towards tackling the cooling demands in buildings. The reason behind this started by a personal observation and discussion with concerned scholars and practitioners. It was noticed that the cooling needs are subsided, and energy savings during summer is not having enough research when compared to the winter heating needs. Attention to heating seemed to be a global trend. To support this argument, an interesting view was found, that might justify why the cooling demands are somehow aside when compared to the global attention in resolving the heating needs. (Masoso & Grobler 2008) has advocated that the adverse effects of the insulation "anti-insulation" is not having fair attention because most of the research/ers are based on North America and Europe where the winter heating needs is the major concern and is overshadowing

the need for cooling. The need for cooling can further diminish when a tradeoff between the cooling and heating needs arises. Such motives and attention to local needs are well understood, however, it is to understand that, even in the very cold climates, the summer cooling should have a better consideration in the near future, due to the following five facts that are forwarded by the same researchers early mentioned, in addition to other reports and researchers;

- i. The first issue that contributes to rising the cooling demands is the global warming caused by the climate change. Throughout the last century, it is observed that the land temperature is rising by 0.2°C per decade (Contribution of Working Groups I & IPCC 2014). Figure 1-2 shows some of the observations during this period as reported by the Intergovernmental Panel for Climate Change. Although such increase might not sound critical for many people. However, many researchers have been concerned with the cumulative and diverse risks that affect the ecological system, and many other where have also carried systematic analysis to predict such changes on the energy consumption penalties. For example, the simulations carried by (Jentsch et al. 2008) and (McLeod et al. 2013) have reported potential overheating risks inside buildings mainly because of the climate change. On the other hand, the need for heating is predicted to decrease based on detailed observations over 22 Chinese cities (Zhang et al. 2006). The climate change is also producing extreme and adverse climatic conditions that will contribute to increasing the peak loads. When the peak load increases, larger HAVC equipment capacities will be required, and in turn, the HVAC systems will have less COP (Coefficient of Performance) as well. Let alone, that the occurrence of simultaneous peak load will affect the electricity grid stability in addition to other negative implications.

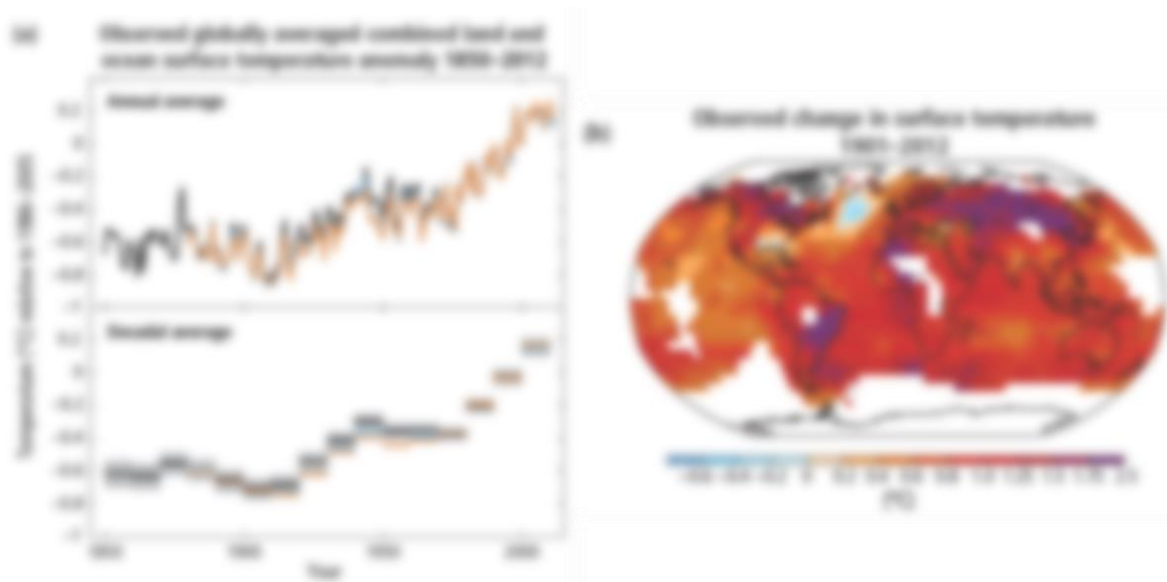


Figure 1-2. Some climate change observations provided by the Synthesis Report. Contribution of Working Groups I, II and III to the Fifth Assessment Report of the Intergovernmental Panel on Climate Change IPCC (Contribution of Working Groups I & IPCC 2014)

ii. The second issue that will increase the need for cooling goes back to the fact the most people are now living in cities, whereas the cities themselves have hotter microclimates compared to their surrounding suburbs. This increment in the cities temperature profile is known as the Urban Heat Island (UHI) effect. The interaction between both factors, i.e., People are migrating to cities, and the more people the city hosts, the hotter it become, and the more cooling energy will be consumed per capita. Such risks have driven many researchers to investigate the potential passive cooling techniques that can be applied a city scale. However, what it is to quote here is the very high-temperature increases due to these two factors. Figure 1-3 shows the current population on 2016 who living in the six contents, and the projected number at 2030. From this figure and as what have been reported by (United Nations, Department of Economic and Social Affairs 2016) that people are residing in cities will increase on account of the rural areas in all the world regions. On the other hand, and taking Singapore as an example, and as can be seen in Figure 1-4, the city CBD temperature is higher than the surrounding suburbs almost by 3°K. Moreover, this zone of the city have shown to stay at high temperatures i.e. 28°C even at midnight hours. Such increment will simply reflect on the Cooling Degree Days and subsequently on the cooling requirements. Some other extreme examples were also found in Indian cities as the heat island intensity has recorded a 10°C difference from the surrounding areas (Wong et al. 2011).

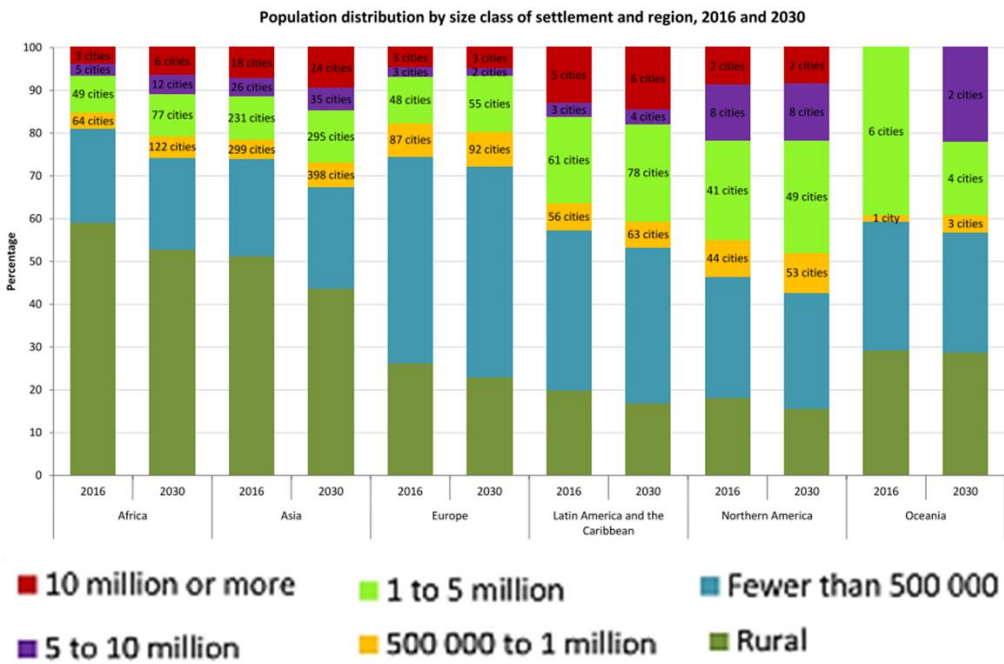


Figure 1-3 Population distribution by size class of settlement and region, 2016 and 2030 (United Nations, Department of Economic and Social Affairs 2016)

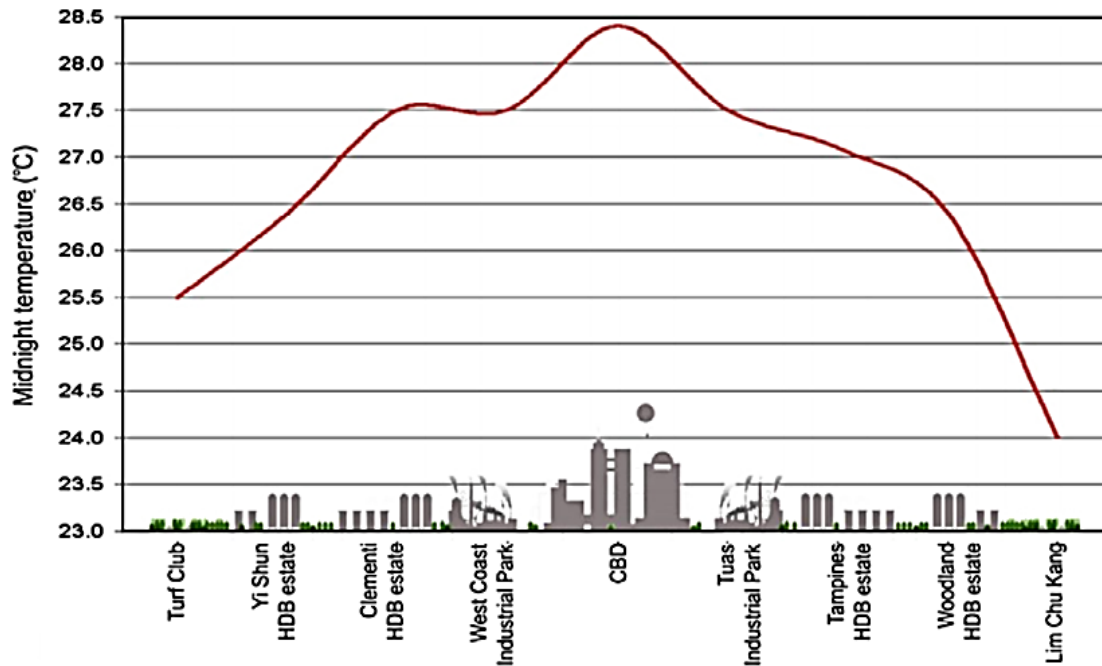


Figure 1-4. Sketch of urban heat island profile in Singapore. (Priyadarsini et al. 2008)

- iii. The third factor that entails higher cooling loads is found at the dwellings level this time. It is a by-product of having a very well sealed, airtight and very insulative buildings. Also, the use of the advance fenestrations that minimises the thermal bridges and reduce the heat transmission through them are all working towards keeping the internally generated heat inside the buildings. Such practices are driven by governmental bodies and some well known energy-saving institutions. A good example that has been quoted earlier is the study of (McLeod et al. 2013) that have reported and overheating risks in UK dwellings when applying the German passive house defensive strategies that are based on highly sealed and controlled envelope.
- iv. By the same token, the fourth factor that increases the need for cooling returns to the modern lifestyle that is based on using more equipment, especially in the office buildings. In such buildings, the cooling equipment is found to operate even in the very cold climates (Masoso & Grobler 2008). Particallury if such offices have deep zones that are far from the cold façade. In general, it can be said that in most of the commercial buildings, especially the crowded ones, like schools, markets, and so on, the need for cooling is mostly required. In such cases, the internal heat generation by the building occupants has a big contribution to the internal heat sources. Most designers might underestimate the magnitude of the human heat generation. However, it is to remind that a single male adult may generate 130W while setting and go up to 295W at light machine factory works (ASHRAE HOF 2013). It can be argued the effect of the internal heat generated by people be coupled with the fact that most of the people are moving to cities where the land prices are much higher. Hence the properties size allocated for a given activity is a bit confined. Therefore, gathering more people in smaller areas inflates the effect of the need for cooling is such dense modern spaces.

1.1.2 The role of the building envelope in reducing cooling loads

Having shown that cooling demand is growing, it is to elaborate that this growth is translated into significant amounts of energy being consumed for that mission i.e. cooling the buildings. The energy saving issues are a global concern and are one of this century critical issues. The international conventions in maintaining rational level of the energy consumptions are one way to reflect the importance of the energy saving topics. One known example in this regard is the Kyoto accord 1997 that is aimed at reducing energy consumptions and their correlated greenhouse gas emissions (e.g. carbon dioxide). One way for nations to meet such goals is through reducing the energy consumption in buildings. Figure 1-5 gives a good insight to the residential buildings share - let alone other building types- in the total energy consumption for many developing and developed countries. It can be seen that energy used in residential buildings is about 31% of the world's total energy consumption whereas it may reach 50% as in the case of Saudi Arabia.

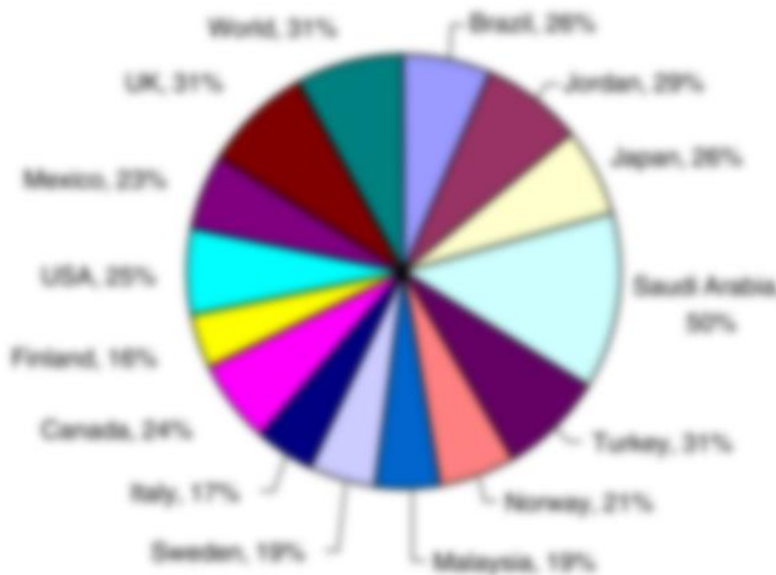


Figure 1-5. Worldwide residential energy consumption.

Collected and generated by (Saidur et al. 2007). (Data Sources: Meyers et al., 2003; Morelli, 2001; Boardman, 2004; Ueno et al., 2006; Almeida et al., 2001; Kamal, 1997, Lenzena et al., 2006).

Taken Saudi Arabia as an extreme example, more details about the energy consumption in buildings were provided by (Ministry of Industry and Electricity 2002). It was reported that two-thirds of the electricity is consumed in buildings whereas two-thirds of this amount is being consumed by air conditioners. Considering that Saudi Arabia has an extremely Hot and Dry Climate (International Code Council 2015), Alsanea shows that heat transmission through the building envelope contributes to a major portion of this AC loads. (Al-Sanea 2012) Breakdown the 30% AC load and presented that another two-thirds of the AC load are due the heat transmission through the building outer walls. Therefore, in this example, it can be calculated that 20% of the electric energy in Saudi Arabia is directly influenced and can be manipulated through the building envelope components.

Similar results have also been reported for the United States, where a recent report by (US Department of Energy 2014b) showed that the space cooling and heating in buildings contributes to about 15% of the primary energy end usages. Figure 1-6 gives more detailed records about the breakdown of the current status, and, similar to KSA, the energy that is being consumed in buildings is more than 40% of the primary energy consumption. This percentage is almost shared between the commercial and residential buildings, with a higher weight to the latter. However, it is to notice that in both building types, the cooling load is almost 15% for each. Therefore, in order reducing these demands (Al-Sanea & Zedan 2011) emphasize the role of the building envelope in cutting such huge amount of AC energy, as they stated the following *“Because building envelope is one of the most important design variables for effective energy conservation, building components (especially walls and roofs) must be designed to operate as passive systems over the lifetime of the building.”*



Figure 1-6. U.S. primary energy consumption (quads)

Source: Energy Information Agency 2013d; Office of Energy Efficiency and Renewable Energy 2011b; Office of Energy Efficiency and Renewable Energy 2011e

In order utilising the building to save energy, it is seen that the envelope needs to act in a passive way, meaning that, it should work in a way to aid the AC systems when the are shutoff as well as during their operation. To provide a better explanation to the above definition, the passive cooling methods strategies, as borrowed from (N. B. Geetha 2012) are presented inFigure 1-7. From this figure, it can be seen that there are three levels to achieve a passive cooling means for energy efficient buildings. Moreover, It can also be seen, that the building envelope have a profound involvement in each of these levels. i.e. in the level of protecting from the ambient environment, which can be

be met through appropriate envelope design and having an adequate amount of heat storage mediums within the envelope. For example, the incorporation of thermal mass and Phase Change Materials (PCM) have shown remarkable results in regulating the internal temperature i.e. shifting the heat wave and damping its peaks as shown by many studies, summarised in the work of (Samuel et al. 2013). The heat modulation (regulation) issues are explained in detail in later sections. Moreover, lastly, the building envelope properties can also be utilised in a way to dissipate the heat. This is mainly met by either storing the heat within the envelope when there is no potential heat sinks i.e. at summer noon, and then dissipating the heat either by night ventilation or by radiation to the night sky using radiative cooling. The combination of both strategies, i.e. thermal mass combined with the radiative systems has been reported to have profound cooling effects (Etzion & Erell 1991).

all things considered, it is found that the building's envelope determines, to a large extent, the cooling energy consumptions profiles, and this effect inflates at extreme climates. In another point of view, and despite that solar paints application is fairly cheap, it is to illustrate that investments and initial costs in the building envelope are huge and the payback periods for well-designed envelopes is quite long, as can be seen from Figure 1-8. However, it is also to notice that the energy savings out of the envelope materials are significant as well.

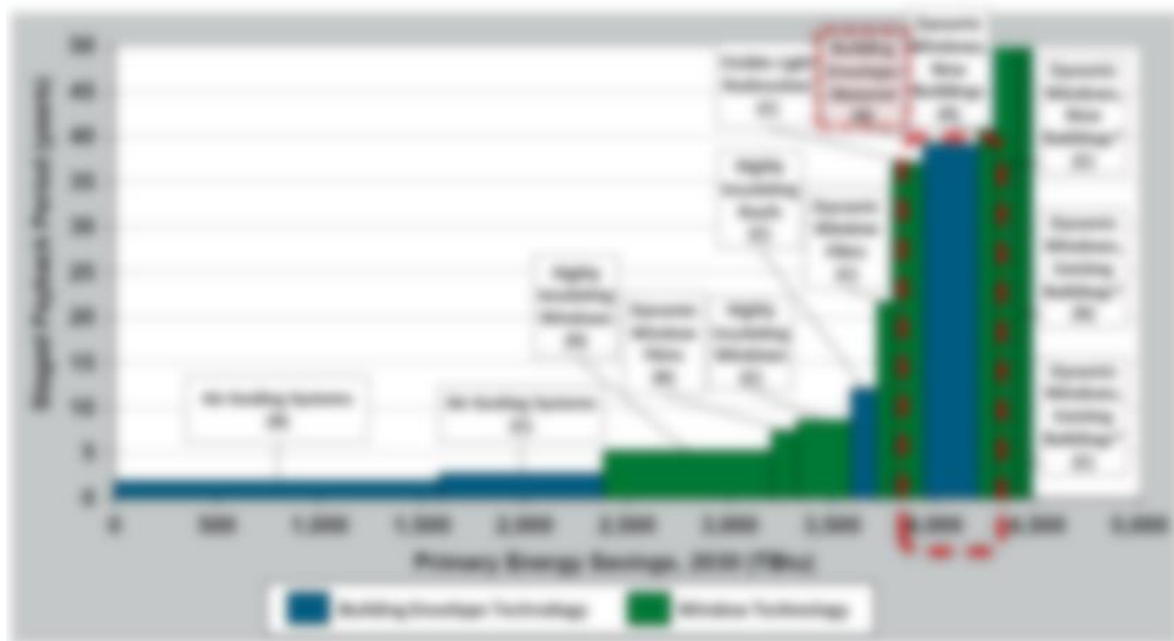


Figure 1-8. Staged maximum adoption potential and staged payback in 2030 for priority windows and building envelope technologies in the residential (R) and commercial (C) building sectors. Provided by (US Department of Energy 2014b).

For this reason, many recent studies, as summarised by (Stevanović 2013) are concerned with the optimisation process of the passive solar design in general, where a big portion of this goes to optimise the opaque components of the building envelope. The other two major concerns are not so far from this topic, as the author has classified the reviewed particular strategies articles into three

categories; the building form, the opaque components of the envelope and the transparent part of the envelope (Glazing) and their shading elements optimisation. In the same optimization manner, (Attia et al. 2013) have interviewed 28 experts in the field of the Zero Energy Buildings (ZEB) and building performance optimization (BPO) tools together with many recent article. At the end, it was founded that the Building envelope optimization is the third most optimized design variables where 50% of the interviewed experts are concerned with it. The ranking order of the participants interest is seen in Figure 1-9.

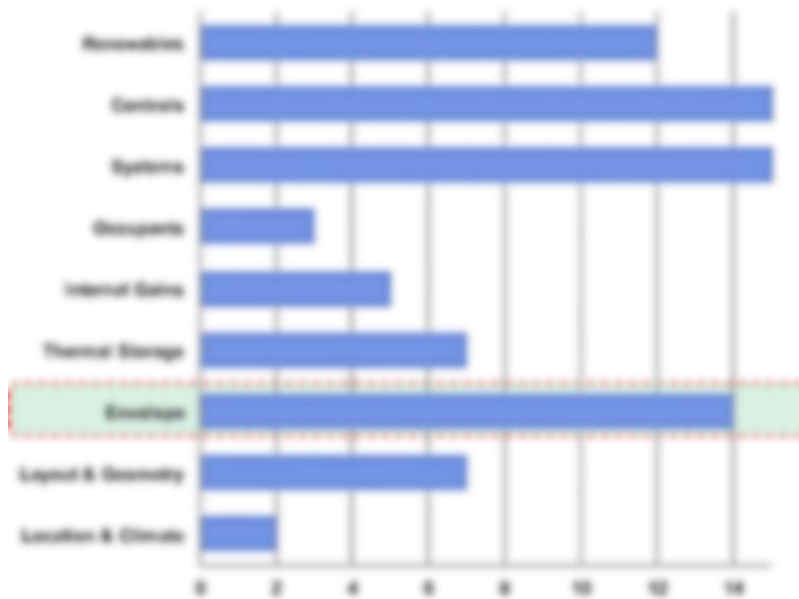


Figure 1-9 Participants' (ZEB Optimization experts) choices of optimization objective functions. Source: (Attia et al. 2013).

1.1.3 The problem statement.

Despite the decisive importance of the building envelope characteristics on the passive design and its related energy saving issues, it is noticed that the building envelope prescription is lacking some crucial points, especially when it comes to the characteristics that are related to its performance under summer/ cooling based conditions. In this subsection, the aim is to highlight the key points that are thought important and require better attention by both, scientists and practitioners, and legislation bodies/institutes. These lacking points are introduced with providing some supporting examples that show that building envelope prescription needs to be an update to comply with the increasing needs for cooling showed earlier.

To start with, an important and very recent document provided by the U.S. Department of Energy (US Department of Energy 2014b), is solely concerned with the envelope issues. The document is titled "Windows and Building Envelope Research and Development; Roadmap for Emerging Technologies". From this title, it can deduce that what is inside this documents is what the US government is targeting shortly about the envelope and windows matters. Under the section of "Barriers for Next-Generation Building Envelope Technologies - Residential Building Envelope P. 40" the first point stated that there is a lack of clear and holistic guidelines about the envelope specification. It was also stated that the way the building envelope materials are tested and evaluated

is not established. Moreover, it was emphasised that the commercial building envelope requires more building design and diagnostics tools.

However, In the same document i.e. (US Department of Energy 2014b), although it has raised many important topics regarding the building envelope, it is noticed that it carries the same message to the building stakeholders; that a proper building envelope only equals a better (usually means higher) insulated envelope. This message is clearly reflected by showing that the first topic that has the highest priority for Research and Development (R&D) in the building envelope is the envelope insulation materials. However, this thesis primary aim is to advocate that such envelope perceptions is inaccurate and would lead to significant energy losses if not corrected soon and incorporate concepts like the risks of anti-insulation, for example.

In fact, it seems that it is a common perception, which if a designer wants to achieve the maximum energy saving out of the building envelope, then one of the guaranteed ways is to invest as much as possible on insulation. This image is further enhanced when a designer refers to any green building (energy-saving) standard, guideline, code, or regulation, where the envelope is referenced by the minimal resistance value (R-value) or its equivalent weighted-area averaged U-value. The recommended high R-value is usually met by increasing the insulation material, and this is the reason behind overlooking the thermal mass materials in the building codes. Among much other consideration, it is to highlight that main motive behind such limited understandings can be fairly ascribed to the fact that most of these codes and standards are paying less attention to the cooling demands.

- **The envelope Specification is lacking the following measures.**
 - 1. Alert of Anti-insulation “overheating”, and maximum limit of insulation.**
 - 2. Specification of the minimum amount of required Thermal mass.**
 - 3. Specification of required Dynamic Thermal Properties instead of static ones “ Time-lag, Decrement Factor, and Dynamic R-value”.**
 - 4. The preferred envelope layers Configuration.**
 - 5. The preferred envelope Number of layers.**
 - 6. Lack of guidance about the surface properties (Reflectivity, Glossiness..)**

Figure 1-10 The Thesis framework outlines, and the envelope specification issues to address and advance

To cap it all, and clearly, state the initial points that this thesis is aiming to address and improve via providing a framework of advancements are summarised in Figure 1-10 above and listed in the following bullet points;

- The first issue that all the codes are not remarking is the risk of anti-insulation and overheating. The anti-insulation concept has firstly introduced by (Masoso & Grobler 2008), and since that time, even the researchers that cited that innovative article did not give any tangible advances to the topic and the issue was not reflected or hinted at any building code or regulation. However, some research like the one - introduced earlier in many times of its importance– by (McLeod et al. 2013) that showed the possible overheating penalties when incorporating the German Passive House standards in a UK dwellings.
- The second issue that is considered to be unrealistic in the available codes is that the recommended R-value is a nominal value and based on static behaviour. In such static conditions, the performance of a 1 cm insulation of a polystyrene slab equals te performance of 4 cm dense concrete slab, whereas both has a U-value of 2.17 W/m²K (Roaf et al. 2007). However, on the other hand, these two slabs have entirely different dynamic behaviours as can be seen in Figure 1-11; where the concrete slab yielded less internal heat fluctuations and also delayed the peak heat wave arrival time. Scholars agree that better analogy to the real behaviour of the envelope components is by evaluating the structure in a dynamic manner (Bojić & Loveday 1997).
- Moreover, still, with the dynamic behaviour, it is important to understand that when the envelope is undergoing a dynamic behaviour it needs to be evaluated using other distinct criteria. The Decrement Factor and the Time Lag are the two well known and established measures for this evaluation and are explained in detail in section 1.2.2. However, in general, the Decrement Factor describes the heat flux range arrived at the internal surface of the envelope as a ratio of the external heat wave fluctuation range. On the other hand, The Time Lag is a measure of the heatwave delay represented by a time value, and in essence, it indicates how long does the external change need to inflate the internal conditions, both principles are illustrated in Figure 1-11.
- The static perception about the envelope explains why the codes do not pay attention to the thermal mass materials which have profound effects on the dynamic thermal behaviour and less on the static calculations. Notwithstanding that comprising the thermal mass material is very common in traditional and vernacular architecture, and over the years, the heavily mass walls have provided a comfortable indoor temperature at many climates, e.g. the Desert Climates, Hot Arid Climates and on the Mediterranean Climates as well (Stazi et al. 2015). Hence, it is expected, at least in these climates, and it is logical that local building codes should advocate the use of this creditworthy passive strategy.
- To say nothing about that the Time lag is mainly met by providing adequate thermal capacity, which in turn is primarily enhanced via incorporating thermal mass materials. The time lag is not only necessary for cooling considerations but also for controlling the heating demands. (Al-Sanea & Zedan 2011) List the benefits when increasing the Time lag hours in three key points. Firstly, by shifting the peak load from its usual time, the grid stability will be improved because the load is going to be evened throughout the day. Secondly, by the shifting the peak demand from the peak (most severe) hours will increase the COP of the AC systems because they will operate in less severe conditions. Lastly, by reducing the peak loads, a smaller HAVC

equipment capacities will then be required. Hence, fewer ducts and installations are sizing. Moreover, by reducing, the equipment capacities, less capital and maintenance costs will be needed.

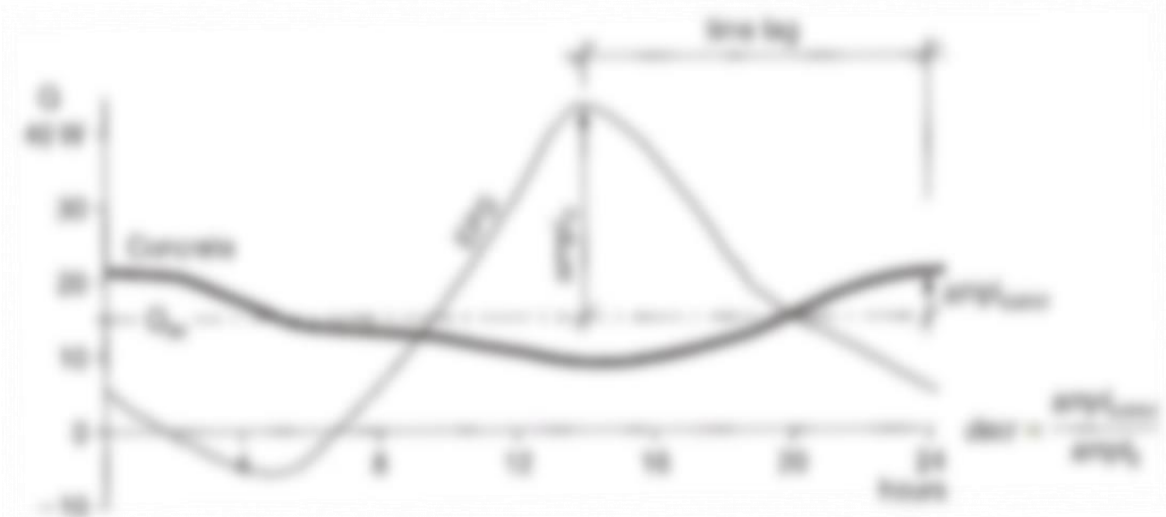


Figure 1-11 The periodic heat flow through a light and heavy wall of the same U-value. Produced by (Roaf et al. 2007) and referenced to (Szokolay 2007).

- In this regards, it is equally important to highlight the integration of the thermal mass into the building envelope should be coupled with the understanding that insulation layers are also crucial parts of the envelope. Moreover, they are mostly required to cut the transmission loads through the envelope. Subsequently, the envelope arrangement i.e. the layer configurations needs to be also taken into account when ascribing the envelope structure. As well be seen in detail in section 1.2.2. The envelope layer configurations have a direct effect on the dynamic thermal behaviours, and understanding this point is imperative if a standard wants to provide a practical envelope guidance to its audiences. Given these points, It is important to consider the dynamic thermal performance when designing the building envelope, and not only providing the nominal (static) R-value in the building codes.
- Another critical point in the standards is that they provide a minimum (lowest) R-value but do not provide any upper thresholds for that. Most probably, the green building legislations is leaving the upper insulation limits open as to be ceased by the installation costs. That is, the insulation (R-value) is provided and conceived as the minimum threshold, after that, the designer is to go through an optimisation process, where the cost of the insulation is weighted against the energy savings profits when comprising that insulation. Figure 1-12 is a typical illustration for the insulation point optimisation against the cost factors that introduced by many researchers e.g. (Kaynakli 2012) (Samuel et al. 2013) and (Ozel 2012).

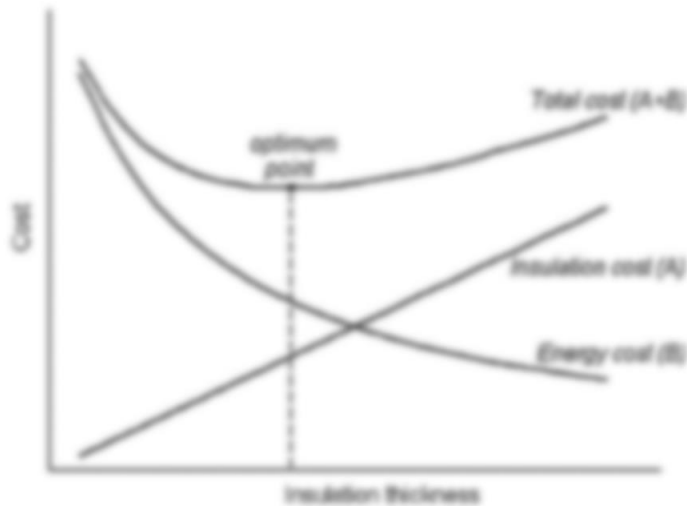


Figure 1-12 The optimum insulation thickness have no upper limits and can be increased once the insulation cost is decreased or when the energy cost increases (Kaynakli 2012)

- Moreover, also from this graph, it can be foreseen that when the insulation costs drops for any reason, i.e. governmental subsidies, industrial revolutions, and so on, the optimisation process will only result in heavily insulated envelopes. The same result of thick insulation can be obtained when the energy cost increases. Where both issues are happening, i.e. the insulation material costs are decreasing while the energy costs are increasing everywhere. In fact, the governments e.g. US are driving the industry to provide a double insulation resistance i.e. form (R-6) to (R-12) with only half price in the next decade, as shown in Figure 1-13 and as conveyed by (US Department of Energy 2014b). Moreover, US government encourages revolutionary insulation materials to pervade. For example, the DOE is encouraging the manufacturers to work on the drawbacks of the very powerful Vacuum Insulated Panels (VIP). Such systems have shown extraordinary resistive abilities, as only a 0.5cm of this panel have a conductivity of only 0.004 W/mK (Schiavoni et al. 2016). Therefore, under those circumstances, it is expected that the world will accommodate heavily insulated buildings that are projected to incur Anti-insulation and overheating problems.

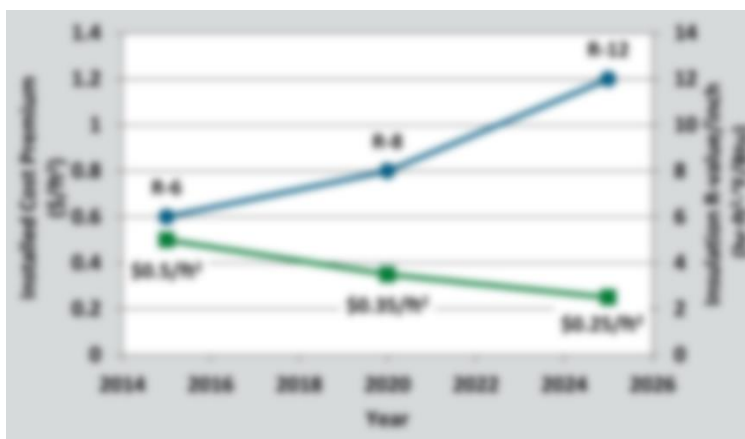


Figure 1-13 Envelope insulation material cost and performance targets (US Department of Energy 2014b).

- Therefore, it should be emphasised that the unseen Anti-insulation phenomenon needs to be understood and involved in the optimisation process to set the maximum threshold of the optimisation process. The anti-insulation issue is introduced to the literature and has been accredited as an actual behaviour, but scholars are still grappling about its existence. For this reason, and since anti-insulation is noted to be controversial, the thesis chapter that tackles this issue and proposes a mitigation technique for it has been compiled into a single article and submitted to the Energy and Buildings Journal, and at this moment (October 2017) it is under the second and final review. The article is titled “Anti-insulation Mitigation by Altering the Envelope Layers’ Configuration”.

After all, the examples of the upper provided practices are countless. Some of them are selected and briefly introduced to support the arguments and show the current trends in prescribing the envelope are dealing with an envelope with the same limited perspective, even at very developed and scientifically advanced countries, e.g., Japan, Germany and the United States.

In Japan, Figure 1-14 is a sample of on a climate-based recommended envelope properties found on the 16th page of the document translated into “energy conservation standards of housing” provided by (Japan Sustainable Building Consortium 2011). It is understood that the only measure to prescribe the building envelope is the (R-Value) with details about this value for the different envelope components i.e. (roof, walls, floors) and this value is varying based on the insulation material type and the allocated region of interests. In Germany, the very well known passive house standards are one of the most rigorous standards that consider having a fully insulated building is the sole way to reach the passive house energy saving targets. The standard is based on five principles that can be found at (Passive House 2016) whereas all of these principles are aiming to have a fully sealed envelope. To give an idea of the Passive House concept, it is to quote the following sentence from the same resource above: “*The most important principle for energy efficient construction is a continuous insulating envelope all around the building*”. The last example is globally inspiring standard, i.e. the ASHRAE (American Society of Heating, Refrigerating, and Air-Conditioning Engineers) standards, namely the ASHRAE 90.1 that is concerned with Energy Standard for Buildings Except Low-Rise Residential Buildings. The way this specification introduces the envelope is not falling away from the previous examples. Moreover, it echoes the same voice of encouraging the designers to come as much as possible of the insulation layers and proving minimum R-values that vary according to the climate zones where the building shall be erected. This can be seen in the envelope section (No 5) and more specifically in section (5.5 Prescriptive Building Envelope Option) Tables 5.5-1 through 5.5-8 in the document (ASHRAE 2013). In the end, it is to state that such standards are rapidly pervading around the world, and they are all hinting to stakeholders that better envelope only equals higher insulation. Moreover, this is what the research is aiming to amend and improve.

部 位		必要な熱抵抗の値 m ² ·K/W	断熱材の種類と厚さ(mm)							
			A-1	A-2	B	C	D	E	F	
屋根または天井	屋根	4.6	240	230	210	185	160	130	105	
	天井	4.0	210	200	180	160	140	115	90	
壁		2.2	115	110	100	90	75	65	50	
床	外気に接する部分	5.2	275	260	235	210	180	150	115	
	その他の部分	3.3	175	165	150	135	115	95	75	
土間床等の外周部	外気に接する部分	3.5	185	175	160	140	120	100	80	
	その他の部分	1.2	65	60	55	50	45	35	30	

部 位		必要な熱抵抗の値 m ² ·K/W	断熱材の種類と厚さ(mm)							
			A-1	A-2	B	C	D	E	F	
屋根または天井	屋根 Roof	4.6	240	230	210	185	160	130	105	
天井	天井 ceiling	4.0	210	200	180	160	140	115	90	
壁 wall		2.2	115	110	100	90	75	65	50	
床 floor	外気に接する部分	3.3	175	165	150	135	115	95	75	
	その他の部分	2.2	115	110	100	90	75	65	50	
土間床等の外周部	外気に接する部分	1.7	90	85	80	70	60	50	40	
	その他の部分	0.5	30	25	25	20	20	15	15	

Figure 1-14 the envelope is only described by the type and thickness of the heat insulating material. Reference (Japan Sustainable Building Consortium 2011)

1.1.4 The thesis structure

Having identified the key points that require attention in current building standards and codes; which need further improvements (as listed in Figure 1-10), this part is to clarify how these issues are approached across the thesis body text. In general, each of the advocated points (issues/concepts) is tackled in one or two chapters. However, it is to state that these points have gone to a last refinement and have been assembled into three key points and questions, which are;

- 1- The first concern is about the anti-insulation behaviour; and to which extent it can be mitigated by the hypothesised technique of altering the layer configurations, and what is the correlation between the anti-insulation and the number of the layers' segments.
- 2- How far the number of the layers' influence on the dynamic thermal behaviour of the envelope and how the big number of layers be assembled in real wall (practicality).
- 3- The role of using solar paint in reducing the solar heat gain.

The compilation of the various concepts inot these three issues was actually made after the literature review where the relevant works in improving the building standards have been considered as will be seen in next section. In the light of this notion, it is to give an idea of how these refined three issues concerns are handled and how they are correlated structured across the thesis, as can be generally observed in Figure 1-15 , and as per the following agenda.

The thesis is structured to avoid repetition, and follow a logical sequence in the investigation process. Therefore, all the literature review that perform the base of this field of study, together with

the key researchers is compiled in section 0 of this chapter. Subsequently. The main chapter, which contains the bulk work i.e. Chapter3, is immediately introduced after the literature reiview.. This chapter is under final revision, and therefore, it is used as the base for the subsequent investigations. Being a full article, it contained a fair amount of literature review, and thus, the literature arguments about the anti-insulation is not elaborated in section 0.

Therefore, Chapter 2 is fully allocated to deal with the first issue, that is, how to mitigate the anti-insulation by reconfiguring the envelope layers' order. The next chapter i.e. Chapter 4 Is also tackling the anti-insulation issue, but this time, the number of layers', instead of their order, is the subject of the investigation. Again, similar to the accredited simulation methodology and the findings being submitted for pair review in Chapter 2, Chapter 3 reused the simulation models to investigate the influence of the layers' number on anti-insulation.

Moving forward, to better understand the role of the number of layers' segment on the dynamic thermal behaviour, and to provide practical solutions for the multi layering technicalities, especailly if a construcion is to comprise more than three layers, Chapter 5 is formlized to study this issue by conducting an experiment. it used an experimental method not only to explore different research techniques, but also to demonstrate that same findings can be achieved by different means. On other aspect, the next chapter, Chapter 6 also uses an experimental investigation, but this time, the investigated issue is moved from the building envelope core to the building external skin, where the impact of the different solar paints is studied. Lastly, Chapter 07, the conclusion chapter contains the summary of all the key findings, put them as framework guidelines, and discuss the whole research limitations, and what can be done in the future research.

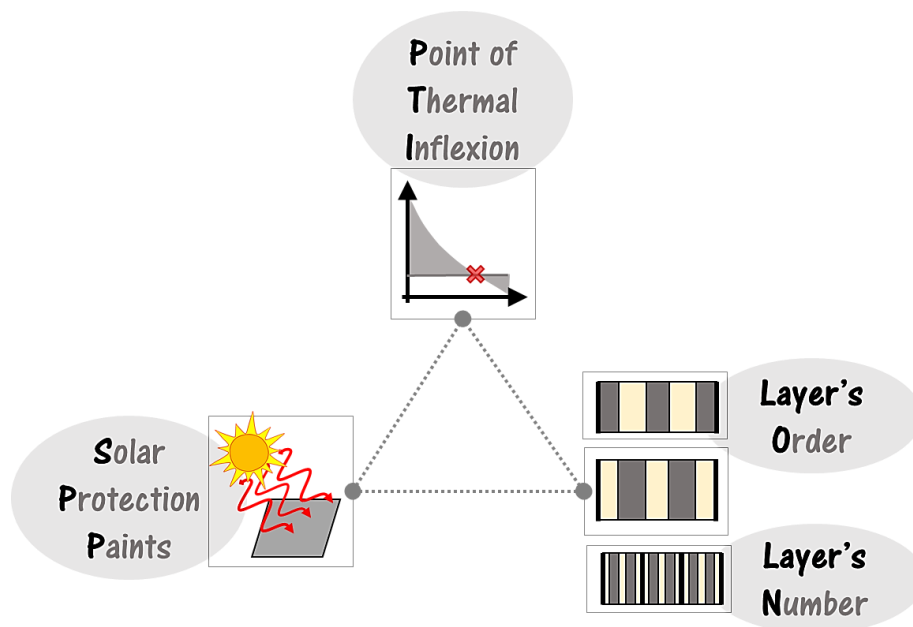


Figure 1-15 The key issue that are addressed by this research.

1.2 Literature review

The literature review is not allocated at a separate chapter because the aim of this survey is meant to give a broader outline about the envelope research, where further details are found in the relevant sections and among the text whenever arguments need literature support. In general, this section is subdivided into four subsections and furtherly into small topics (headings) as to keep the literature reviews sorted and traceable.

1.2.1 The scope of the literature survey

This introductory part is introduced to give an insight about the literature fields that is being surveyed herewith. Since the framework of this research is based on three issues, shown earlier in Figure 1-15, it was important to identify which sort of literature articles that tangent these three topics. Starting from this objective, the first literature surveys showed that the envelope is being typified into some thought of bundles. That is, in literature, it was found that envelope is categorised into basic three bundles. One is the envelope components boundary conditions, i.e. roof wall and floors, where the floors, for example, are not exposed to solar radiation while the roof has the big portion of it. The second typology is the layer exposures within this component and can be sorted as the construction core, and surface (skin). Lastly, the components are also sorted based on their (solar admittance) optical properties as either they are considered opaque or transparent/translucent.

From within these categories, the thesis has paid attention and focused on some of these typologies, as based on the research objectives. Figure 1-16 shows the scope of the study, and by turn, it demonstrates the literature field of survey. For instance, only the opaque parts are studied, as the transparent have to deal with other factors related to the glass, and accompany the studies about the daylight and solar gains which have another set of factors that is out of the objectives of this reach. Moreover, it is to highlight this research is not concerned with issues and studies are concerned with the geometries setups. e.g. the studies that are concerned with the volume to the area ratios and its impact on the various energy saving/loss measures, and so forth for all the other optimisation studies that comprise the spatial dimensions, and proportions.

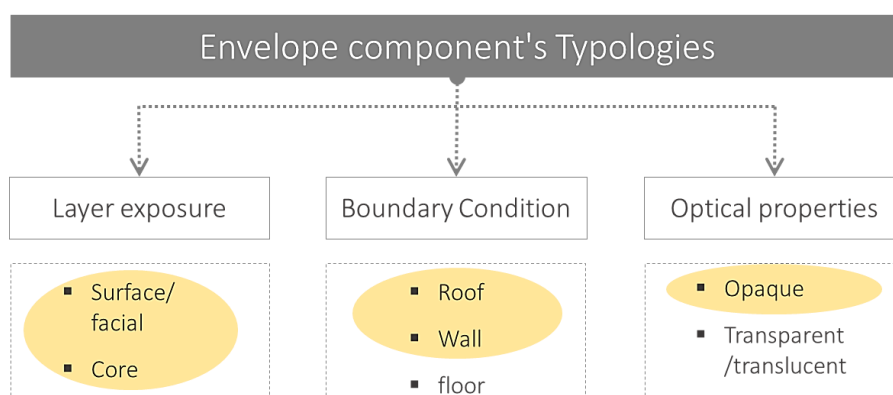


Figure 1-16 Envelope component's Typologies as being studied in the literature. The highlighted parts are within study scope.

Lastly, it is to state that the literature being surveyed herewith are not including the methodology issues, i.e. the simulation software, the selected model's setup and so on. These are reviewed at relevant parts of the thesis. For example, the simulation algorithms identification and selecting the weather files are all introduced in later sections.

1.2.2 Research on the envelope core

Research concerned with the construction core are seemed to be interested in evaluating the various layer configurations and arrangements. Many types of research were dedicated to understanding and examine the various configurations performance under several operational conditions. The research about the envelope core is noticed to focus on the various permutation of the thermal mass and insulation materials, i.e. the ratio and the position of each on the structural composition (Ozel 2014),(Bojic et al. 2001) and (Al-Regib & M.Zubair 1995). In essence, the incorporation of these two materials is intended to increase the envelope resistance and to increase the heat capacity various components as well. In turn, such dynamic behaviour enhancements are met by using the insulation and thermal mass materials due to their resistive and capacitive thermophysical properties, respectively (Asan & Sancaktar 1998).

For the Thermal mass and insulation materials, altering the location and the share of one material will influence the other's performance, as well as the overall envelope dynamic performance, since they are strongly interrelated. (Al-Sanea & Zedan 2011) stated that: *"Thermal characteristics under dynamic conditions are affected by relative locations (Distribution) of thermal mass and insulation layers. Accordingly, it is important to study effects of thermal mass and insulation separately as well as interactively (as a complete system) where either material influences effects of the other."* For this reason, there is a huge number of research that have been carried out to canvas the -almost endless- permutation possibilities when composing the wall out of these two materials.

Here, it is equally important to report that the findings among the different studies were sometimes contradicting, and recommendations are somehow conflicting. Many authors have also reported such complications. For example (Bond et al. 2013) have highlighted that there are no clear guidelines for the way the walls are being assembled as the evaluation criteria are ambiguous and might disagree even within the same research. By the same token, (Stazi et al. 2015), have reviewed many articles concerned with the dynamic performance of the various wall arrangement where he noticed that these studies do not have multidisciplinary evaluation criteria that cover all the energy saving aspects. For example, the studies being concerned with the insulation and mass optimisation and focus on cooling does not usually consider the heating aspects, and so forth. However, the scholars have ascribed such mismatch between the literature findings to the variations in the operational factors. The operational factors, and in general, are governed by the AC operation conditions, and to the cyclic patterns of the external conditions (Al-Sanea & Zedan 2011) and (Stazi et al. 2015). Based on these issues, the literature review about the core is being sectioned into five headings to explain such key operational concepts, as in the following.

a) *Dynamic and steady-state conditions.*

At the very first beginning, it was shown that the principal problem with the current standards, is their narrow perception of the envelope properties as being considered and dealt with in a steady-state perspective. Moreover, on the steady-state conditions, the heat flow calculation based on the nominal conductivity of the material, where the other properties like the specific heat and the density are not considered. On the other hand, the dynamic behaviour does incorporate such properties. Furthermore, the dynamic behaviour can be sorted into two categories (Corrado & Paduos 2016); either a dynamic thermal characterization under the steady-periodic condition or a dynamic thermal characterization under sinusoidal conditions. The former is studied by (Kontoleon & Bikas 2007), (Kontoleon & Eumorfopoulou 2008)(Al-Sanea & Zedan 2001) where the boundary conditions can be periodic but not necessary sinusoidal (Corrado & Paduos 2016). However, the sinusoidal cyclic conditions are better resembling the natural heat fluctuation as driven by the external temperature fluctuation over the day, which is an ordinary product if the sun travels across the Skydome, and it is commonly used by researchers (Ozel 2014). The external temperature in such cases usually incorporates the solar radiation effect in addition to the air temperature. Thus it is very common using the Sol-air temperature for such purposes. The sol-air equation can be found elsewhere in (Kuin et al. 1998).

b) *AC operations patterns (initial transient and continuous).*

Having specified the external conditions, this part is concerned with the internal conditions. The AC operational pattern is coupled with the energy that the equipment consumes, on its capacity, and on its COP as well. In principle, the AC can operation can be perceived in two ways; either initial transient or continuous operation. For the purpose of differentiating between the two operations, it is to consider two issues; the first is the AC working and shutoff period, and the second is the length of the normal thermostat pauses. (Al-Sanea et al. 2012) Distinguish the initial transient condition by its intermittent AC operation, and it arises when the equipment is shut off for extended periods of time. On another hand, the steady periodic condition is distinguished by its smooth operation as when the weather dominates the operation schedule, and the AC is operated for a prolonged time without major interruption of the short thermostat pauses. Eventually, as per the same authors above, it was reported that the best-performing layer configurations are subjected to the AC operation – together with the external environmental conditions.

However, it can be seen that there is no clear operation period (length) after which the initial transient is considered to switch into a continuous operation and vice-versa. This grey area between the two operations is still untackled and needs further systematic research. In fact, the misunderstanding between the two operations led to erroneous judgments as will be seen in the next points; when introducing the research that specifically looked at the AC operation under the initial transient equipment operation.

c) Dynamic thermal performance evaluation. (Time Lag & Decrement Factor).

In order evaluating the dynamic thermal behaviour of the constructions, the scholars have developed many evaluation criteria. The founded evaluation criteria are the Decrement Factor, the Time Lag, the damping effect, The Standard Deviation, and the basic total energy consumption and peak loads. However, throughout the literature, almost all the researches have considered the Time Lag and Decrement Factors as a base evaluation measure. The reliance on these tow factors can be ascribed to the fact that the decrement factor and the time lag does not change and are fixed values for any given wall composition made of specific materials. Therefore, they can be considered as a fingerprint for that specific composition i.e. if construction has decrement factor of 0.5 this means it will always be 0.5 regardless of the external environment (Threlkeld 1970) and (Burns et al. 1991).

Figure 1-17 is to depict this general concept of both measures as provided and defined by (Asan 2006). As in this figure, the Time Lag [ϕ] is defined as the “the time it takes for the heat wave to propagate from the outer surface to the inner surface” whereas the decrement factor [f] is “the decreasing ratio of its amplitude during this propagation”. Furtherly the author has also provided equations for both factors as; as for the decrement factor, it will equal. Besides, the Time lag equations are shown below, and it depends on the variation between the external and internal temperatures – accounting for the delay hours if exceeded 24hr.

$$\phi = \begin{cases} t_{T_o}^{\max} > t_{T_e}^{\max} \Rightarrow t_{T_o}^{\max} - t_{T_e}^{\max}, \\ t_{T_o}^{\max} < t_{T_e}^{\max} \Rightarrow t_{T_o}^{\max} - t_{T_e}^{\max} + P, \\ t_{T_o}^{\max} = t_{T_e}^{\max} \Rightarrow P, \end{cases} \quad \text{Eq. 1}$$

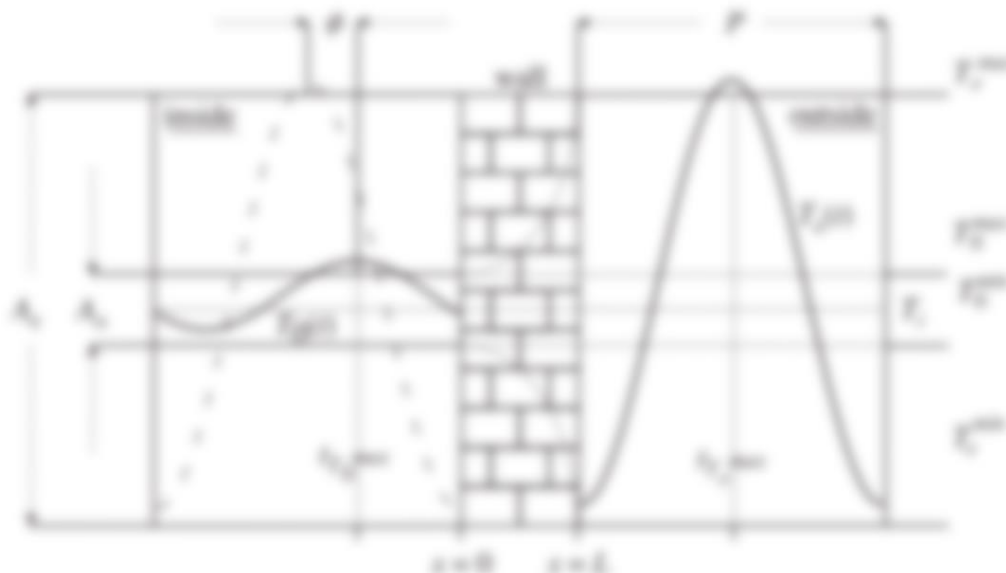


Figure 1-17 The schematic representation of time lag ϕ and decrement factor f . Whereas t_o^{\max} and t_e^{\max} (h) represent the time in hours when inside and outside surface temperatures are at their maximums, respectively.(Asan 2006).

Based on these definitions, the various studies targeted reducing the Decrement Factor and increasing the Time Lag of the developed configurations. As by reducing the Decrement Factor, the internal temperature would be more stable, hence, the AC operation will become more steady. Also, by reducing the Decrement Factor, the peak load (maximum amplitude) will be dampened as well. Thus, the equipment size will be reduced and will require less maintenance and ducting costs. On the other hand, the Time Lag is sought to be increased, as by increasing the time lag many benefits can be obtained, as listed earlier in section 1.1.3 earlier.

However, in reality, it can be argued that increasing the Time Lag might not always be favoured. Moreover, it is also to emphasise that there is a grey area, especially when thinking about Time Lags that exceed the 12 hours and moves toward 24 hours, where it can be questioned if the heat flux peak will arrive at the same time of the day. Despite that the wall provided a 24hrs delayed. Such questions lead to another complicated question that can be simplified in the following example. Assuming two walls with same decrement factor, but have a different time lag. Moreover, if the Time Lag of configuration A is only 5 hours, and for B is 10 hours, apparently B will be judged to be way better than A. However since the peak load at A will arrive at 5 pm (assuming that ambient peak is at 12 pm). For B the peak will arrive internal space at 10 pm. In this perspective, if we assumed that occupancy (and AC equipment) starts around 10 pm (typical bedroom), this means, that configuration B, will contribute to higher initial transient load as when compared to wall an (in which) the heat wave flux may have started descending already. Proving this example, and coupling it with the remained gray that keeps the goal of increasing time lag infinite, it may explain why when it comes to tradeoff between the Decrement Factor and the Time Lag, the researchers give priority to reducing the Decrement Factor, as can be hinted from (Bond et al. 2013).

To better understand how the various construction materials contribute to reducing the Decrement Factor and increase the Time Lag, and how these building materials practically meet this, It is to borrow the interesting investigation results carried by (Asan & Sancaktar 1998). The influence of the thermophysical properties of the Time Lag and the decrement factor have been investigated. Whereas the Heat Capacity values (kJ/Km^2) are obtained by multiplying the Density (kg/m^3) by the Specific Heat (J/kgK) of material while account for the material thickness (m) as well. Figure 1-18 shows the general findings of that research. Moreover, in conclusion, it is shown that to have a good thermal capacity, the construction material need to have a high specific heat, high density and low conductivity at the same time. Therefore, the Time Lag can only be increased by considering all these thermophysical properties, as can be seen in Figure 1-18-a. On the other hand, the less decrement factor can be achieved by only reducing the thermal conductivity without the need for increasing the heat capacity characteristic of the wall, which can be clearly seen in Figure 1-18-b. This physical attitude of materials can be a reasonable justification to recognise why the building envelope is being conceived as to be solely insulative; i.e. because Time Lag effect is not being considered important, and decrement factor can be achieved by just adding more insulation.

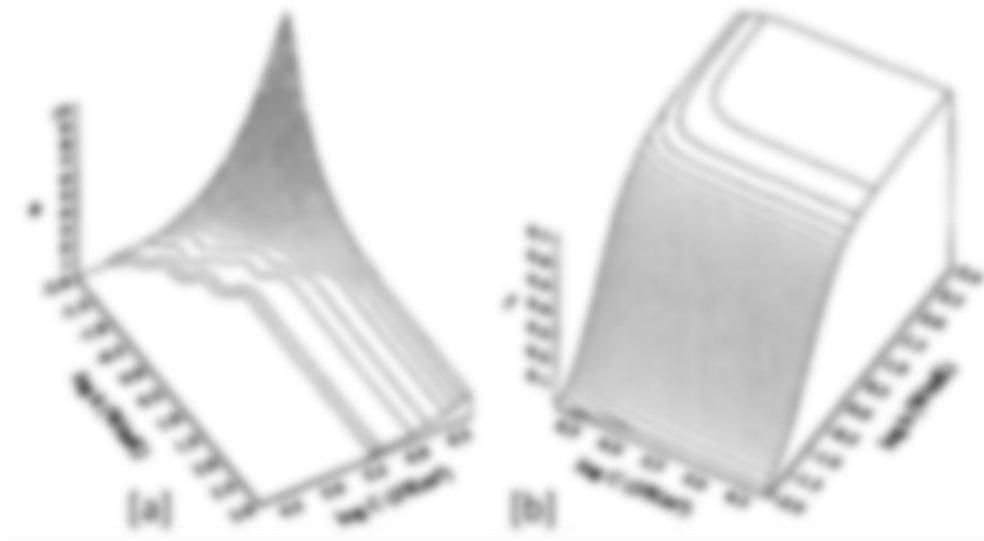


Figure 1-18 Combined effects of Heat Capacity ρ (kJ/Km²) and Thermal Conductivity k (W/mK) on;
 [a] Time Lag [b] Decrement Factor

d) Performance of configurations under various conditions.

The majority of literature concerned with the opaque building envelope enhancements have covered the issue of the layers configuration by one mean or another. However, as stated before, most of these researches come up with adverse conclusions and contradicting recommendations. Moreover, this part is intended to bring some of the adverse recommendations examples. However, also in this part, the literature have been sorted into two groups based on the AC operational conditions. i.e. the first paragraph goes through the fundamental research (as per cross refreshing in the subject area) that deals with the continuous AC operations. While the last paragraph -of this point- is covering the research that investigated the layer configurations performance under the initial transient conditions. Moreover, as being concerned with cooling, the review focuses on the cooling issues with preference to the studies carried out in hot climates.

Under the continuous operations, (Seth et al. 1981) compared the performance of two constructions that have the fixed amounts of thermal mass and insulation, while incorporating air cavity layers in between. The study was carried for Kuwait climate under hot summer days. The comparison showed that the configuration [IACAI]¹ yielded the best load levelling (decrement factor) as when compared to the counterpart configuration [CAIAC]. In another study by (Kossecka & Kosny

¹ IACAI = insulation/air/concrete/air/insulation slab.

In general, the naming code in this thesis starts from the outermost layer whereas [i] refers to insulation layer and [M] refers to a Thermal Mass layer. E.g. the configuration [MI] means that the Thermal Mass is located at the external surface of the envelope.

2002), similar arrangements were investigated under a continuously used residential building. The results were obtained from six US climates. However, the findings did agree with previous research of (Seth et al. 1981), as the configurations that have an insulation materials at its both external and internal faces was recommended, i.e. [IMI] have shown to yield the best thermal performance (the best temperature dampen), when compared to the [MIM] configuration.

By the same token, (Sodha et al. 1981) have studied the optimum air gap and insulation position within an air-conditioned single room in Delhi. The optimisation derived at by having the least concrete at the external layer i.e. [IM] the best load levelling could be obtained (decrement factor). Conversely, the different recommendation was concluded by (Bojic et al. 2001), whereas the authors have conducted a whole building simulation for residential flats in HongKong. Moreover, for the cooling purposes, they found that the highest decrease in the cooling demands can be attained by placing the insulation layers at the internal parts of the construction slabs i.e.[MI].

The same contradiction between findings was found under the initial transient AC operations too. For example, based on the study of (Bojic & Loveday 1997), the recommended arrangements for the intermittent cooling load operations can be ranked in the following order, starting from best, (i.e. lowest energy consumption) [IM] then [MIM] then [IMI] then [MI]. On the other hand, (Al-Sanea & ZEDAN 2001) results and recommendation for Riyadh scalding climate, showed that best-performing configurations would be ordered as [MI] then [IM]. However, in the end, it seemed like the latter researchers have tangent the reasoning behind these contradicting findings. As they have highlighted, that further studies are needed to examine the effects of the various AC starting times.

e) [Attempts to incorporate the Thermal mass and account for dynamic behaviours.](#)

Through the recent studies, it was found that some attempts have been carried out to account for the thermal mass, and the dynamic behaviour in general when specifying the envelope properties. Although these works are fully incorporated in current codes/compliance code, they seemed comprehensive and covered many of the inaugural issues that have been highlighted in Figure 1-10. After finding these researchers, the thesis objectives was then compiled and oriented to investigate the three key issues shown in Figure 1-15. In this part, these significant advancements in the specification of the building envelope are briefly overviewed as following.

The first and the major development belongs to the International Organization for Standardization, namely the document EN ISO 13786 titled “Thermal performance of building components-Dynamic thermal characteristics - Calculation methods” (UNI EN ISO 13786 2007). However, the paper is still limited to the sinusoidal boundary conditions, where it is based on evaluating the periodic thermal transmittance and the time delay (shift) to specify the dynamic performance of the building components. In the introduction, the document defined another two key concepts regarding the sinusoidal conditions. Firstly, it defines the Thermal admittance as ratio between the heat now rate to the temperature variations at the same boundary side. Secondly, it introduces the Thermal dynamic transfer; which is concerned with the ratio between the same quantifying measures (i.e. temperature or heat flux) of one side of the envelope over the same

measure on the other side. However, This standard seemed to draw the attention of other concerned researchers, and it is undergoing further extensions (Mazzeo et al. 2015).

Starting from the same Standard i.e. ISO 13786, and with reviewing additional resources, (Corrado & Paduos 2016) have developed a new scheme that accounts of the thermal inertia (Time Lag) and bears the dynamic thermal conditions instead of the old envelope parameters. The proposed approach have been developed using dynamic simulations whereas the realistic applications as well as the various contextual setups of the buildings e.g. the walls orientation and surfaces optical properties have all been incorporated. In the end, the simplified approach “new equivalent thermal parameter” was validated against the results of dynamic simulation models. Similar to the objectives of this thesis, the developed parameter, was targeting the enhancement of the technical standards and building indices.

While developing that new parameter (Corrado & Paduos 2016) have come across some recent innovative concepts that was carried by (Al-Sanea et al. 2012) i.e. “thermal mass energy-savings potential”, “dynamic thermal resistance” and “critical thermal-mass thickness” concepts. The following concept involves estimating the minimum amount of mass that a wall configuration may require in ordered obtaining a predetermined energy saving rates. Another important note to highlight, is that the critical thickness have been studied under and insulated envelope, where the location of the insulation have also been considered i.e. internal and external insulations, where the latter, i.e. [IM] yielded better results. Moreover, it is to note that the thickness of the thermal mass did not affect the energy saving rates in the summer, rather, increasing the mass amount have shown to have a profound effect on the cooling and heating loads occurred in the mild season. However, as expected, increasing the thermal mass have always reduced the peak load, reduced decrement factor, and delayed the heat transmission arriving at the inner envelope faces.

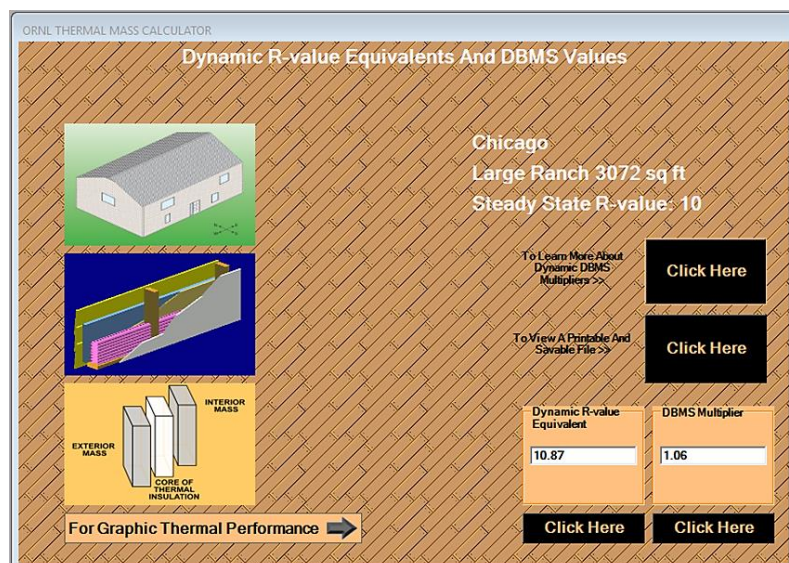


Figure 1-19 ORNL Thermal Mass Calculator - Dynamic Benefits of the Massive Systems (DBMS).

Resource: (ORNL ((Oak Ridge National Laboratory)) n.d.)

On the same regards, the (ORNL ((Oak Ridge National Laboratory)) n.d.) had an early interest, that goes back to 1995, in encouraging the use of thermal mass materials either concrete or masonry instead of wooden frame homes. In a comparison of both structural systems and assuming that same that both have the same Steady-state R-value, they have shown that 5% to 20% of the total building energy can be saved in the US homes when using the thermal mass instead. Moreover, based on early research, the laboratory have a developed a handy calculation tool that can provide the Dynamic Benefits of the Massive Systems (DBMS). The DBMS calculator interface is shown in figure xx, where the DBMS concept is an expression of the dynamic resistance (representing the real envelope performance under the dynamic conditions) divided by the nominal R-value (which based on the static conditions and provided by standards) of the same wall.

All things considered, the above-reviewed concepts seems interesting and fall within the close scope of the thesis research. Therefore, the thesis has well-thought-out that development and have been oriented to cover the tangent issues that have been introduced at the beginning of this section. Moreover, by the end of this section, the teaming issues are that the thesis aiming to cover have been reformed as to be;

- 1- Anti-insulation mitigation via the layer configuration reordering and by the number of the layers.
- 2- The practical application of incorporating the thermal mass in multi-layered walls.
- 3- The investigation of the solar protection paints effects on the overall envelope thermal performance.

1.2.3 Research on the envelope external skin

In this part of the thesis, the use of cool roof, protection paints, spectrally selective coatings, and similar other techniques, are covered in this section, which is limited to the optical properties of the external surfaces of the building envelope. In literature, the utilisation of Solar paints for cooling purposes is found to have broad applications. The applications range from the military uses to deceive the radars by changing the infrared frequencies (Sathish Kumar et al. 2016), and the use of the metal flakes paints applications in the automobiles to keep them comfortable. Moreover, the utilisation of these facial strategies extends to the application at the urban scale to mitigate the Urban Heat Island (UHI) effects by using at pavements (Akbari & Matthews 2012)(Synnefa et al. 2006)(Rosenfeld et al. 1995) and ending up with typical solar collector applications. Also, one of the known applications is the use of the low-emissivity layers wither in the opaque or transparent parts of the building to lessen the heat loss (exchange) via longwave (thermal) radiation. However, up to recent years, the effects magnitude of the low-e layers when applied the opaque envelope components on the building thermal performance is reported to be limited (Jelle et al. 2015).

These facial systems are also known as selective solar parts, where (Wijewardane & Goswami 2012) defined them as the paint that has high emittance at a certain frequency or within a particular frequency range. That is, for any opaque material the incident radiation equals the absorbed plus the reflected radiation, and according to Kirchhoff's law, the absorptivity (α) equals the emissivity (ϵ) at a

given frequency range. However, for different frequencies these values might not be equal. As the Solar absorptivity (short wave) of a material (α_{solar}) may either be (greater, equal, less) than what it emits at the long wave frequencies, known as at earth temperatures emissivity (ϵ_{temp}). The wavelength of both spectral ranges is shown in Figure 1-20. Therefore, based on this phenomenon, the spectral selectivity for energy efficient paint can be used for both purposes i.e. cooling and heating. As for the cooling (heat dissipation), the solar paints have an emissivity value (ϵ_{temp}) that is greater than solar absorptivity value (α_{solar}).

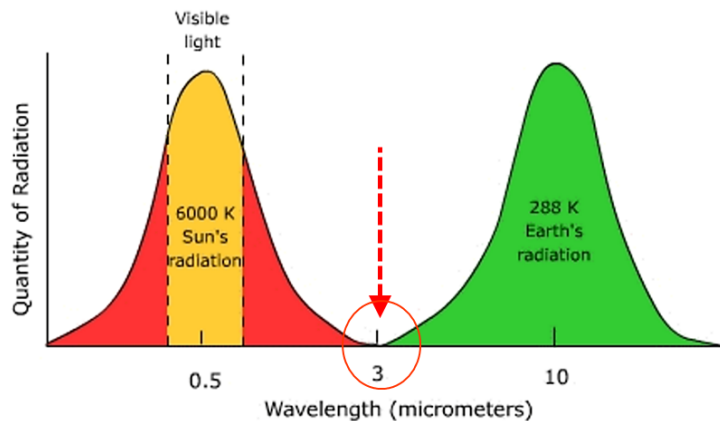


Figure 1-20 Comparison of solar and earth radiations wavelengths

Source: (Ritter 2012)

Therefore the basic principle behind both usages (either for cooling or heating) relies on the optical properties of the paint (or surface). As per (Dias et al. 2014) most of the paints show very high emissivity values, for example, conventional exterior paints have emissivity values around 0.90. However, the same article has demonstrated that there are two ways where cool paints may contribute to control the heat load of a building;

- 1- By reflecting the incident solar radiation and, which can be thought of as (mitigation).
- 2- By radiating the heat absorbed by emitting infrared (IR) radiation (can be considered as a heat dissipation strategy).

As for the first controlling measure (mitigation), authors have explained that it is possible to reflect a big portion of the solar heat without changing the surface colours. That is by manipulating the surface (paint) properties on the Near InfraRed band (NIR). Figure 1-21 shows that the NIR accounts for almost 52% of the solar spectrum. Therefore, most of the reflective paints are effective in this range and have very low Solar absorptance in the range of 700 to 2500nm (Haavi et al. 2012). In similar research (Smith et al. 2003) have demonstrated that such techniques can be used together with coloured paints, and is confined to using white colours as most people might think.

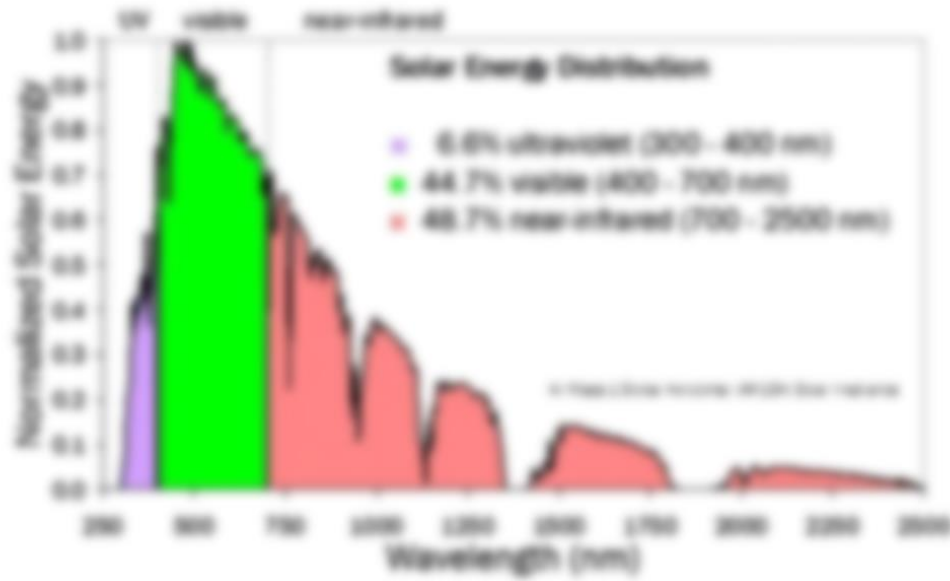


Figure 1-21 Solar energy distribution. Source: (Haavi et al. 2012)

On the other hand, the radiative paints (cooling by dissipation) works on the earth temperature heat wave bands, typically > 3000 nm (Meinel & Meinel 1976) and most of these paints are aiming to emit the radiation to the sky in the range of (8-13 μm) which is known as the atmospheric window (Catalanotti et al. 1975). The spectral window is where the atmosphere content of water vapour, Co2 and ozone can allow for the long wave radiation to pass to the cold sky in the outer space. Figure 1-22 plots this atmospheric window together with the typical spectral range of the black body (earth temperature), and other spectral ranges. In this aspect, and in ordered to emit the heat to the outer space, it is to remind that any object that contains heat (above absolute zero > -273 K emits some radiation. The radiation amount is therefore increased by the increasing of the body temperature. The relation between the body temperature and the amount of the radiated heat is governed by the Stefan-Boltzmann Law provided in equation blow, whereas (E) is the radiation power, (ϵ) is the surface emissivity, (σ) is the Stefan–Boltzmann constant (5.67 Exp–8) [W/m² K⁴] and (T) is the surface temperature in Kelvin Degrees [°K] (Albatici & Tonelli 2010);

$$E = \epsilon \sigma T^4 \quad \text{Eq. 2}$$

However, the net gain/loss is determined by balancing the outgoing and the incoming amounts of heat. Therefore, although building materials, emit more heat during the day (hotter during the day), they also receive a greater amount of heat from the sun. Hence, the net heat balance ends up with heating the surfaces. Some innovative systems could achieve extraordinary results and could have a net cooling effect even during the day. The photonic radiative cooler developed by (Raman et al. 2014) was able to cool during the day due to the very high emissivity on the atmospheric window while having almost no emissivity (absorptivity) at the solar band. Figure 1-23 shows the behaviour of the novel photonic radiative cooler from the ultraviolet to the mid-infrared range.

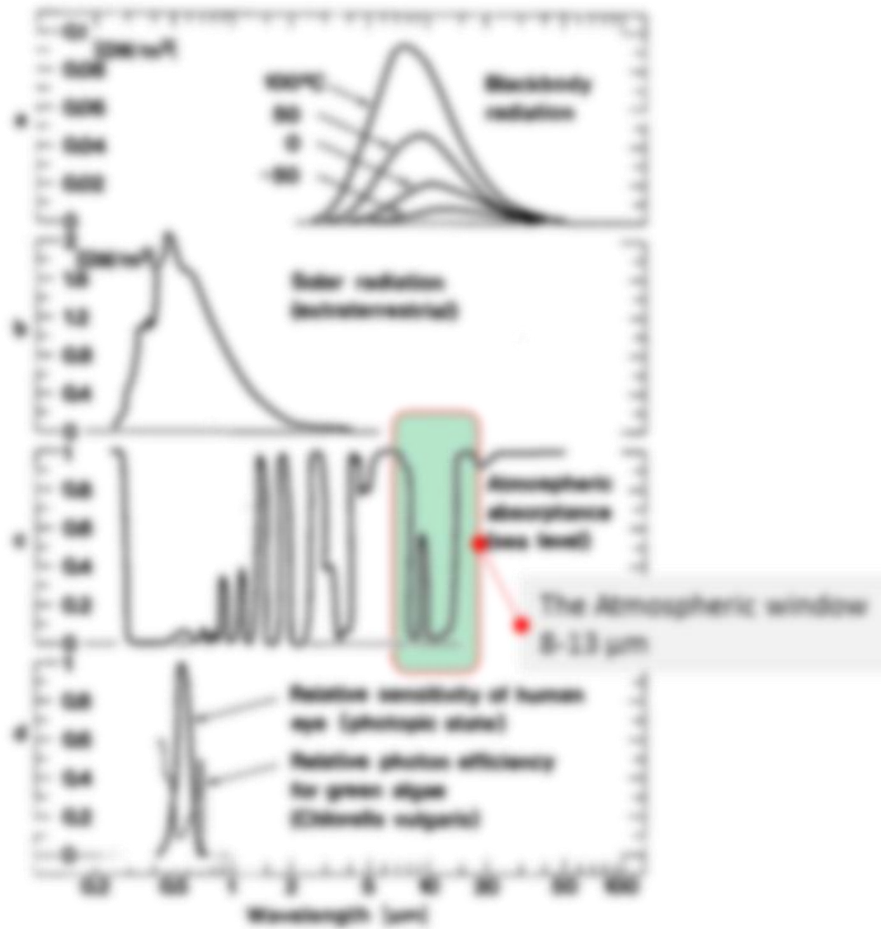


Figure 1-22 Spectra for (a) blackbody exitance at four temperatures, (b) extra-terrestrial solar irradiance, (c) typical Absorptance across the atmospheric envelope, (d) relative sensitivity of the human eye and relative photon efficiency of photosynthesis in green plants. Source: (Granqvist 1981).

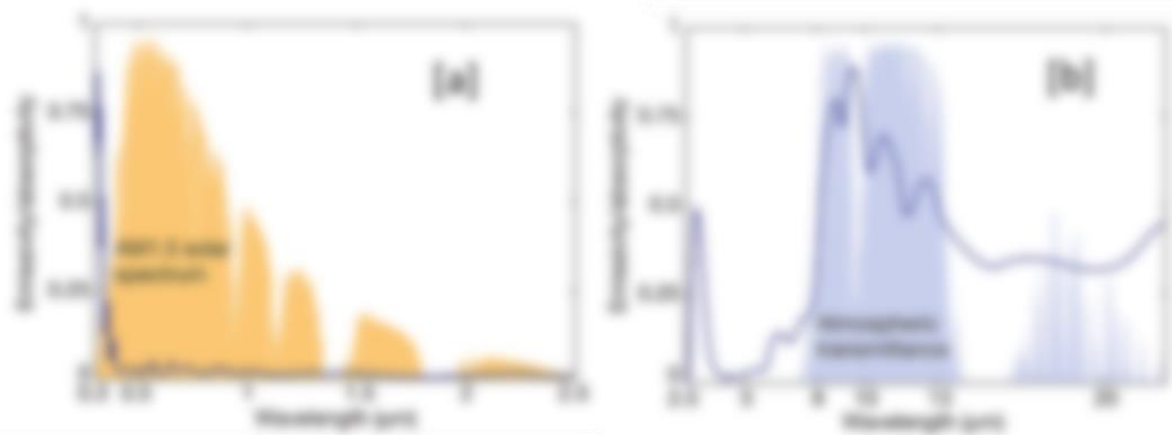


Figure 1-23 Emissivity/absorptivity of the photonic radiative cooler from the ultraviolet to the mid-infrared.

[a] Measured emissivity/absorptivity over optical and near- infrared wavelengths.

[b] Measured emissivity/absorptivity over mid-infrared wavelengths.

In contrast to such complex radiative systems, the conventional solar paint consists of four key components. The first is called the Pigment, whereas define it as a “*tiny insoluble particles included into the paint mainly to contribute colour by absorption and reflection of light*”(Gunde et al. 2003). The second component is the Resin or the binder, and from its name, it can be hinted that it is the paint’s film forming agent, that is either dissolved or dispersed in the solvent (Bullest & Prosser 1983). In turn, the Solvent is the major part of the dispersion chemical (Orel et al. 1990). The last paint component is the additives that are supplementary for enhancing the dispersion and the application properties of the paint i.e. the floating and the flooding (Orel et al. 1990). Figure 1-24 depicts this component and give an idea of how the paint is applied and its thickness is reduced after the solvent evaporates.

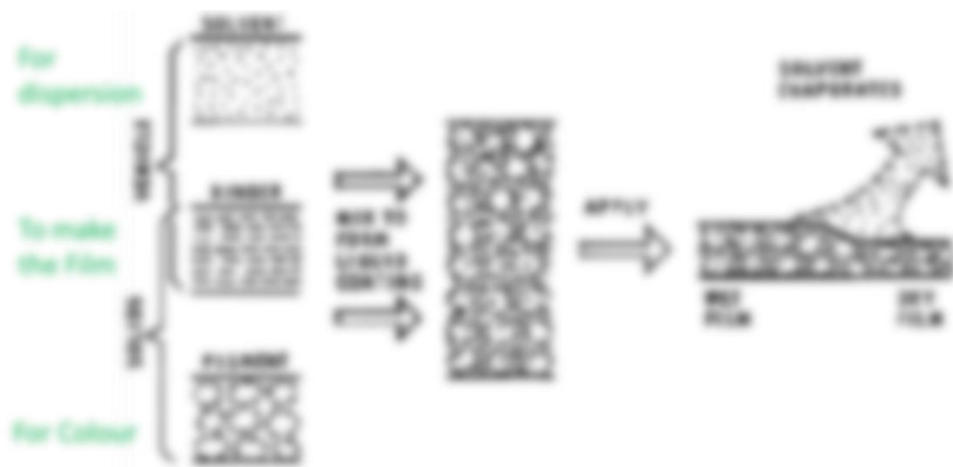


Figure 1-24 Generalised compositions of pigmented liquid coatings and manner of film formation. Source (H. E. Ashton 1966):

Based on this composition, the solvent-based paints are sorted into two types:

- 1- Thickness Sensitive Spectrally Selective (TSSS)
- 2- Thickness Insensitive Spectrally Selective (TISS)

Moreover, for the first category, The TSSS paint forms the upper layer, and it should be as thin as ($\sim 1-2 \mu\text{m}$) so it can be seen by the lower layer that is made of the infrared reflective metal surface (Wijewardane & Goswami 2012) (Orel et al. 1990). On the other hand, the TISS type does not have stratification since the pigment itself have an adequate emissivity at the IR band, while metal flakes of aluminium and bronze play the role of the reflective base layer(Wijewardane & Goswami 2012) (Orel et al. 1990). Figure 1-25 is prepared to illustrate the structure of both paint types as per the description provided by the above references.

Still, with the cooling oriented paints, it is important to state that for such systems that focus on the cooling load reduction either by increasing the emissivity or reducing the solar absorptivity would likely entail a heating penalties during the winter season. Therefore, the climates that have a reasonable amount of the heating demands needs to carry out a sensitivity analysis for such

drawbacks. For example, a climate based study made by (Synnefa et al. 2007) compares the cooling saving against the heating increase in different climates when the roof solar reflectance is increased to 0.65 instead of 0.2. Moreover, for the simulations flat roof house, it can be seen in Figure 1-26 that

some climates like Tokyo and Newyork, the increase in the heating needs almost abolished the benefits of the reduction in the cooling loads., besides, the heating needs in Mexico City have overwhelmed the cooling benefits. However, some scholars like (Akbari & Levinson 2008) are advocating that *“The winter heating energy penalty is usually smaller than the summer cooling energy savings because in winter the sun is low, the days are short, the skies are often cloudy, and heating occurs mainly in early morning and early evening”*. Moreover, as has been demonstrated by (Ozel 2012), that even in a relatively cold climate of Elazığ- Turkey, the influence of the solar absorptivity of the external face has little influence on the heating transmission loads at different insulation thicknesses as can be seen in Figure 1-27-a. Conversely, decreasing the solar absorptivity have a significant effect on the cooling transmission loads, especially at lower insulation thickness as seen in Figure 1-27-b.

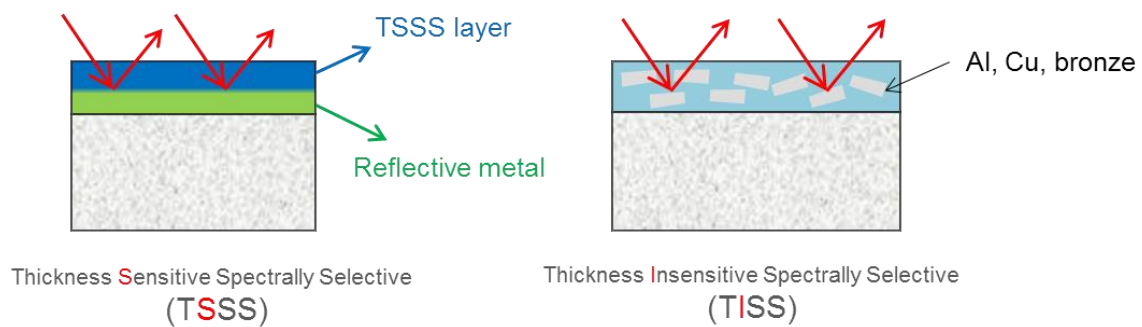


Figure 1-25 Types of spectrally selective paints.



Figure 1-26 Climate effect on cooling and heating load changes when altering roof solar reflectance from 0.2 to 0.65. (Synnefa et al. 2007)

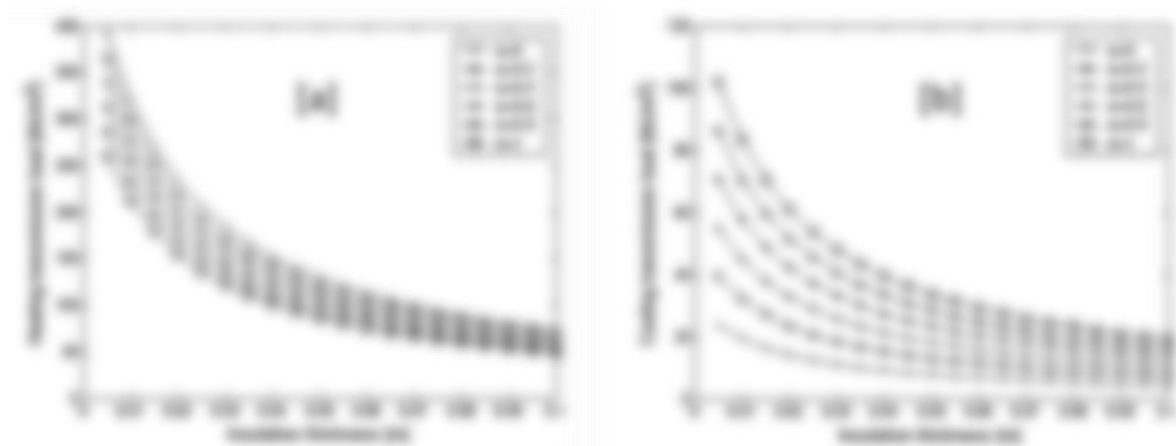


Figure 1-27 Variation of yearly cooling and heating transmission loads versus insulation thickness with respect to solar absorptivity varying from 0 to 1. (Ozel 2012).

All things provided, it is to declare that the aim of incorporating the spectral selective systems in this study has been directed as to protect the underneath core in the first place, then to cool it down as a second priority. The goal is set in this direction as to provide adequate protection to the

insulation materials if the envelope optimisation arrives at having outer layers of insulation. In their study, (Berdahl & Bretz 1997) have argued that the exterior skin should maintain the quality of the internal insulation at higher levels, and to protect the internal air contained within the insulation materials from rising to higher levels. This issue is of particular importance because of the contained air forms part of the insulation internal convective resistance, and if the air gets hot, it will degrade the insulation overall resistance (Griggs & Shipp 1988). Furthermore, due to such increase in the internal core layers temperature, especially the insulation layers, (Levinson et al. 1996) have supported the previous arguments and found that the insulation resistivity can be reduced by 10% to 20% during the summer when the roof temperature gets way higher the room temperature. Therefore when the envelope components are susceptible to such high temperatures, it is more practical to direct the aims to limit this heating rather than thinking about cooling it (Muselli 2010).

Lastly, it is quite important to review some of the scientific works that have coupled the external skin performance with the internal core dynamic performance. Moreover, it is to emphasise that such studies are very useful in understanding the holistic image. Since it was noticed that, due to the complexity, most of the research are either dealing with the outer skin or the inner envelope, but very few have looked at both properties as one system where each component affects the other. A good example of these research is the interesting work provided by (Etzion & Erell 1991), where the authors have explored the role of the thermal mass location on the cooling power of a radiative cooling system. In the results, it appeared that when the radiative system is coupled (attached) to the thermal Mass, the net and the effectiveness of the radiative cooling had much higher values that reached 35% when compared to the detached configurations. Also, the coupled configuration had the lowest average internal temperature. However, this did not deny the fact that coupling (directly attaching) the radiator to the mass have produced the greatest temperature standard deviation (fluctuation range, Decrement Factor).

By the same token, early studies have been concerned with evaluating the optical properties together with the envelopes dynamic thermal performance characteristics. For example, the Influence of the solar absorptivity on the Time Lag and Decrement Factor over the various insulation thicknesses was studied by (Ozel 2012). The findings of this research are borrowed and demonstrated in Figure 1-28, where it can be seen that solar absorptivity have a little effect on the Time Lag (Figure 1-28-a), and have no effects on the decrement factor (Figure 1-28-b). Moreover, the same study has demonstrated that the Solar absorptivity values have significant implications for the yearly transmission loads, and hence, on the energy savings, but these effects are not influencing the optimum insulation thickness and payback period. Therefore, It can be concluded that the study of the external skin properties can be isolated from the insulation optimisation process in the proposed framework.

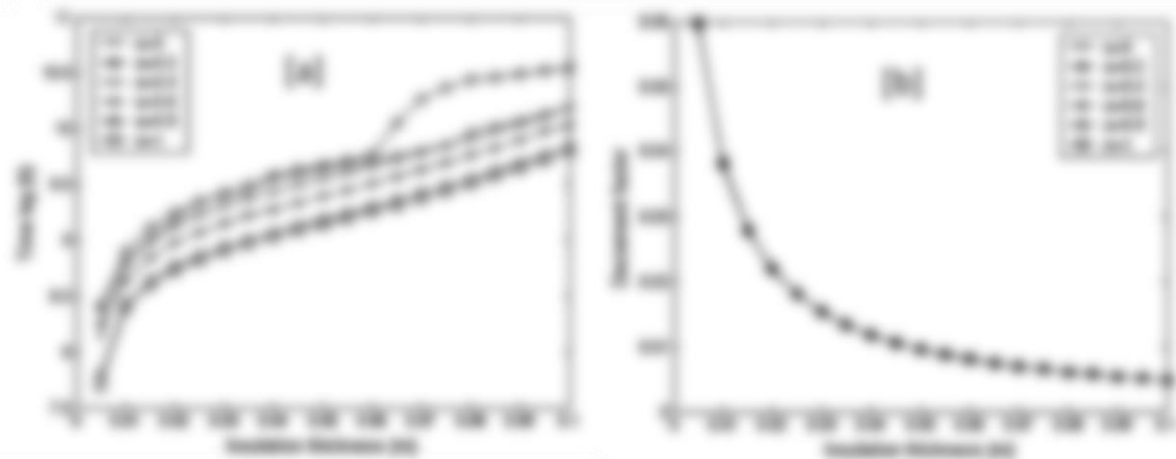


Figure 1-28 Variation of yearly averaged Time Lag and Decrement Factor versus insulation thickness with respect to solar absorptivity varying from 0 to 1.(Ozel 2012).

Conversely, the investigation of (Kontoleon & Bikas 2007) has derived at very different conclusions. The authors have also looked at the influence of the solar absorption ratio on Time Lag, Decrement Factor and temperature differences between the surfaces of a southern wall in a Mediterranean region when the coatings are applied at both (internal and external) surfaces. Moreover, the study have used six wall configurations in the investigated model wich are [IM], [MI], [MIM], [IMI], [IMIM] , and [MIMI]. The investigation argued that the maximum Time Lag can be greatly affected by the solar absorptivity across all the wall configurations, as has been provided in Figure 1-29. For the Decrement Factor, although the study emphasised that the solar absorptivity have a considerable effect on the temperature amplitudes (Decrement Factor), but the figures, however, does not tell that. As by referring to figure 7 in that study, the decrement factor only decreases by 0.002 for any given construction configuration. Rather, from that figure, it can be seen that the wall configuration has the greatest effect on the temperature fluctuation on the internal surfaces. Moreover, when comparing the Time Lag results of both studies i.e. (Ozel 2012) and (Kontoleon & Bikas 2007), it can be seen that the Time Lag results are quite similar, as the gap between the solar absorptivity (α_{solar}) of 1.0 and 0.0 is almost one hour in both studies. Despite that wall thickness in the latter study was 26cm while in the the former study it was limited to 10cm. Not to forget, that both studies have agreed that the optimum Solar absorptivity that yields the longest Time Lag is 0.2.

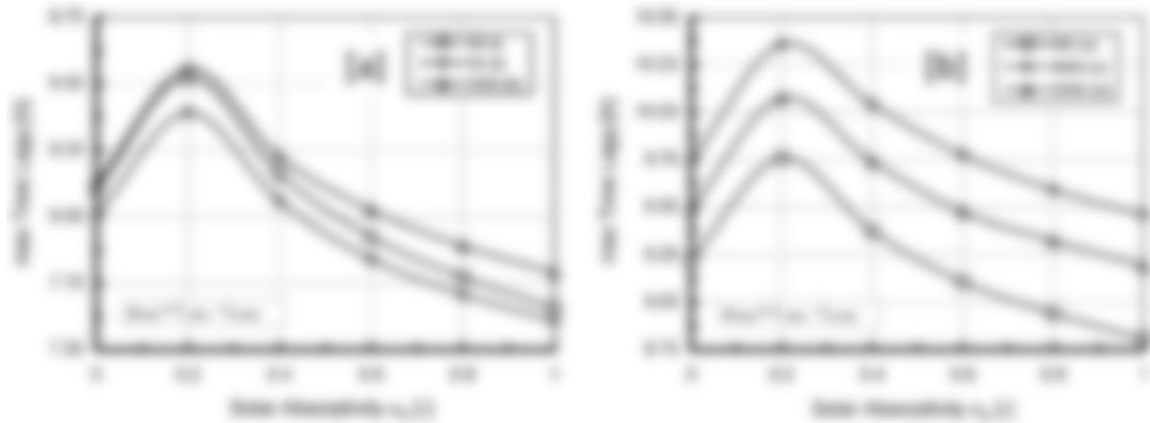


Figure 1-29 Time lag (ϕ_{max}) VS. Solar absorptivity (α_{solar}) for the wall formations with insulation as (a) one layer and (b) two layers.(Kontoleon & Bikas 2007)

The influence of the solar activity on the time lag can be attributed to the gap between the peak Sol-air temperature time, and the peak external ambient temperature time, as the former's peak usually takes place at noon i.e. 12:00, while the maximum ambient temperature is a little bit delayed to afternoon periods. The peaks gaps between these two temperatures have also been reported in the result's discussion by (Kontoleon & Eumorfopoulou 2008). Therefore, when the solar absorptivity is low, this means that the wall is less affected by Sol-air temperature, hence, the wall's external surface is mainly governed by the ambient temperature. Moreover, because that peak ambient temperature occurs at afternoon, then the walls with less solar absorptivity of, i.e., 0.2 shows the maximum time lag. In Figure 1-30, although it might be hardly observed, it can be seen that the Sol-air temperature peak for the surface with no solar absorptance seems to shift to the afternoon slightly. On the opposite, it can be anticipated and seen in the same figure that for surfaces with high solar absorptivity values, the surface peak temperature become more dependent on the Sol-air temperature, resulting in this nominal reduction in Time Lag.

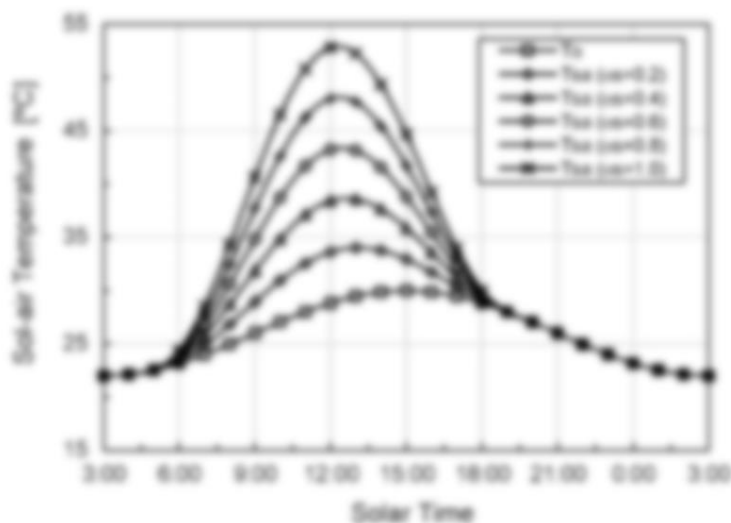


Figure 1-30 Values of sol-air temperature over time with respect to Solar Absorbtivity values. (Kontoleon & Bikas 2007).

On the study by (Kontoleon & Eumorfopoulou 2008), the single and the combined contributions of the wall orientation and surface solar absorptivity on manipulating the Time Lag and Decrement Factor was investigated in the Greek region summer climate conditions. This time, changing the wall orientation have produced an interesting results, where the Time Lag and Decrement Factor performance profiles have changed as a function of changing the Solar absorptivity from 0.0 to 0.1. As can be seen from the results of a three wall orientations presented in Figure 1-31, it is to point out that Northern Wall has shown the opposite effects on Time Lag and Decrement factors results when the Solar Absorptivity is increased, and it is entirely different from the South and East oriented walls. This differentiation may return to the fact that the northern wall is not influenced by the direct solar radiation, meanwhile, increasing the solar absorptivity will enhance the wall's emittance as well. As a result, when the solar radiation is blocked its emittance power will overwhelm the gain (absorptance) power. In turn, the Time Lag would increase by increasing the solar absorptivity while the Decrement Factor slightly increases by that absorptivity increment. Besides, it is also to consider that the peak incident solar radiation varies in accordance with the wall orientation, e.g. for the eastern wall, the peak incident radiation occurs at 8:00 instead of 12:00 as in the southern wall (Kontoleon & Eumorfopoulou 2008). Consequently, and as discussed earlier, this time variation between the peak incident radiation (Sol-air) and the ambient temperature would lead to different optimum wall configuration setups and different optimum solar absorptivity values as well.

Lastly, and regarding the paints application positions, it is to review the outcomes of (Azemati et al. 2013) research. The results showed that the coating with mineral particles has an important role in the thermal insulation. Also, it leads to a 17% decrease in energy consumption in moderate climates. More importantly, the previous study was based on investigating the coating application at different orientation as well as considering the internal and external surfaces. The results suggested that the best location for these surface coatings – i.e. in their study was ceramic coating and acrylic paint coating – is to apply them on both sides of the walls. That is to apply coatings on the internal and external surfaces, however, when taking the paints cost into consideration the priority goes to applying such coatings on the outer surfaces only.

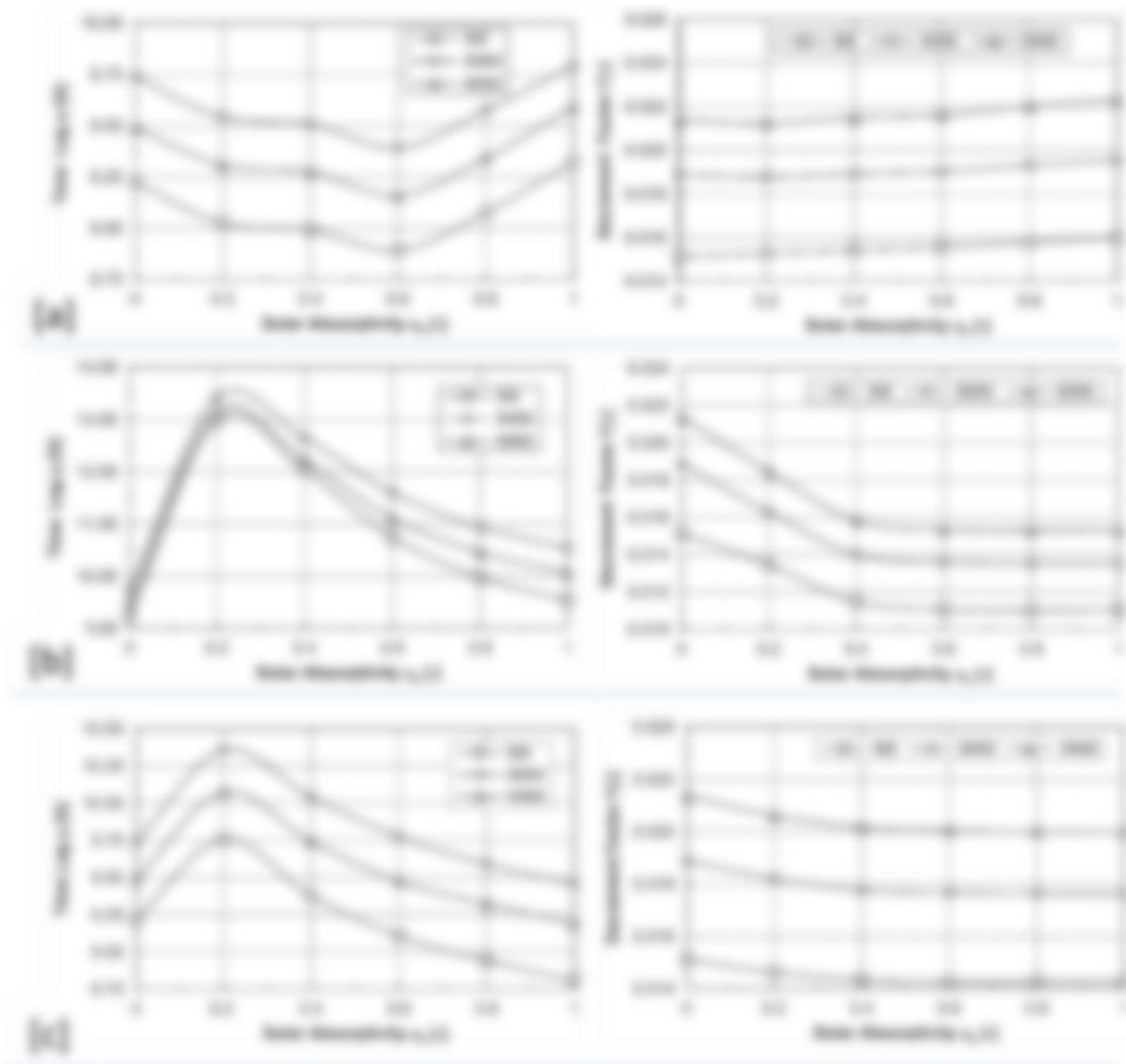


Figure 1-31 Time Lag and Decrement Factor values VS solar absorptivity for a two insulation layer's wall configurations at different wall orientations;

[a] North-Oriented Walls [b] East Oriented Walls [c] South Oriented Walls

Source: (Kontoleon & Eumorfopoulou 2008).

1.2.4 The Framework outlines

From the previous reviews, it was concluded that some of the proposed areas had been covered by new researchers and some standards, e.g. ISO 13786 have adopted, to some extent, the dynamic behaviour of the envelope and have accredited the importance of the thermal mass presence in the building envelopes. Such standards are not activated, and even little researchers and designers know about its existence. This situation might be a consequence of its sophisticated calculations and less rigorous objectives. However, it seems to be, there is a promising good start towards better specification of the building envelope.

Subsequently, since some objectives have been covered by other research, The aim of the thesis is limited to and revolved around investigating the untackled two issues which are; 1- the mitigation of anti-insulation and the effect of the layer configurations and the layer numbers on this behaviour. 2- providing a practical solution to the application of a multilayering envelope that is composed of more than two or three layers of insulation and thermal mass. At a later stage, the research has presented studies about another important issue related to the envelope surface properties which deemed to influence the envelope resilience against the first heat waves. That is, the surface properties of the envelope which have been addressed separately, but a link between this strategy and the envelope dynamic thermal performance was also introduced in the previous subsection. In summary, it is to confirm that Figure 1-15 represents the three key issues that the thesis is covering and aiming to provide a framework for, and improving its prescription in the building standards.

Chapter 2

2. Before the Simulation

This Chapter has embedded some of the early tests that were carried before starting the simulations, but not being published within Chapter 3 article. These early tests addresses the questions regarding the selection of the simulation software and its related issues including the weather files and reliability, weher all these issues are covered thoroughly in the follwing sections.

2.1 Reasons behind employing EnergyPlus

The discussions herein are meant to demonstrate why the Energyplus software was selected among all the other heat load calculation software, and also to show that it is the best matching - available- a tool for the purposes and objects of this research.

Historically, EnergyPlus is considered as one of the pioneer whole-building-dynamic-modeling simulation software. It's development started in 1996 by combining BLAST (Building Loads Analysis and System Thermodynamics) and DOE-2 building energy simulation programs. Hence it inherited both software best capabilities (US Department of Energy 2015b)(Crawley et al. 2001). The first version was realised 2001, and in this thesis, Version V8.4 is employed as being the latest edition. Since the first version, there was a lot of enhancement and tremendous contribution from the research society as motivated by being an open source software. Moreover, being open, there was any interface for the core engine. Hence, it has become very popular. Also, the modular structure of the energy plus enabled it to form having auxiliary programs that serve many-sided-purposes (Crawley et al. 2001). For example, to calculate the view factor, preparing the water data for compatibility with the software, or handling a huge number of inputs (permutations) via the parametric tool (US Department of Energy 2015a), which was a paramount feature that enabled simulating the 6500 cases for Chapter 3. As a result, the errors were always reported, shared and fixed, and software was kept up to date with latest researches findings and aligned with industrial revolutions. For example, EnergyPlus can simulate the Phase Changing Material PCM and variable thermal conductivity, unlike much other closed software that does not provide such simulation capabilities (US Department of Energy 2015b).

Figure 2-1 Summary of research on optimisation of opaque envelope components.(Stevanović 2013).

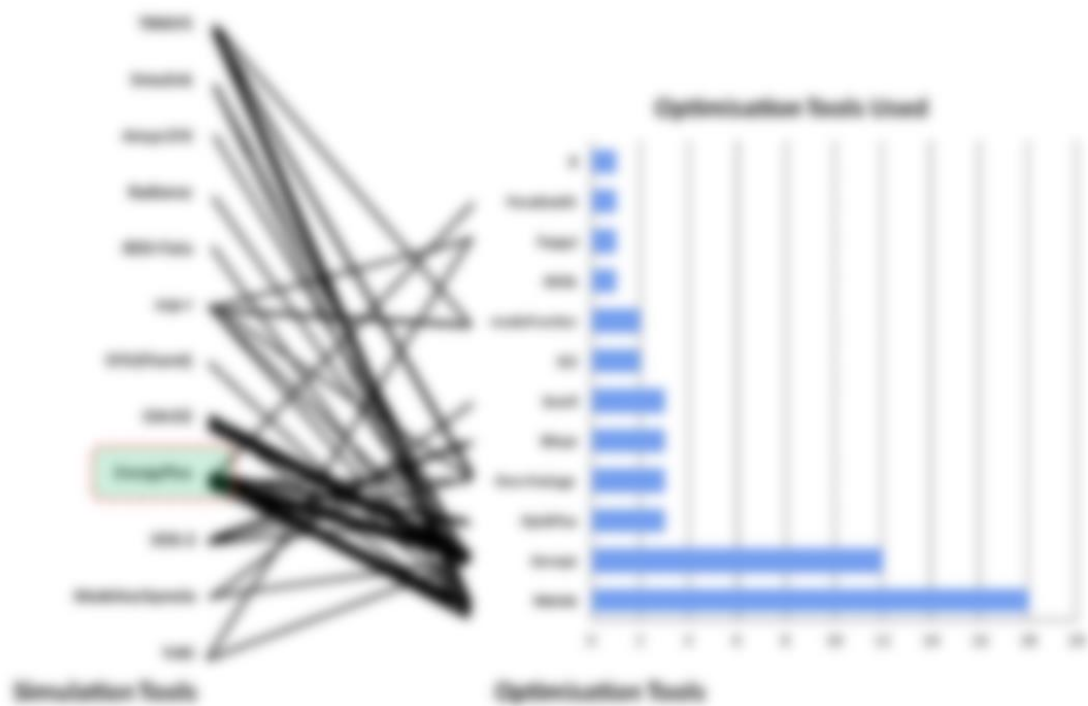


Figure 2-3 Optimisation tools order by use (right) and simulation tools ordered by use (left). The line thickness is proportional to the frequency of the pairings. (Attia et al. 2013)

2.2 Weather files reliability investigation

Having decided to employ the EnergyPlus software for all the simulations in this thesis, the second legitimate question was to examine the reliability of the climatic data that are built to comply with the software. The well Known EPW files (Energy Plus Weather Files) are specifically made to comply with the EnergyPlus.

The EPW files are basically made of another format of the weather data known as TMY2 (Typical Metrological Years)(US Department of Energy 2015a). The TMY, in turns, and as can be hinted from its name, is generated by composing a typical representative 12 months at a given location over a period – that is usually 30 years. Meaning that, to generate ethe TMY, the characteristic weather data of the solar radiation, dry-bulb temperature, dew point, and wind velocity are averaged over for each month over the 30 years (Wilcox & Marion 2008). The average values are then matched with the best resembling actual measured data of the specific month. Later, the whole year is composed from the representative month which is usually taken different form years (Crawley 1998).

In addition to the hourly climatic data, the TMY/EPW files embed other climatic and geographical information, like the Heating/Cooling Degree Days/Hours and the location coordinate respectively. However, some of this information are not necessarily used by the program, as can be seen in Figure 2-4. Such kind of data are incorporated as to be helpful when the weather files are converted into other weather data forms required by other simulation software. Moreover, these redundant data It can also be used in case some essential weather data are missing. That is, these

unused data are now utilised by the “Weather Converter”- auxiliary program in EnergyPlus – to supplement and calculate the core weather information data. Equally important to understanding is that the Weather Converter might also assign some default values for the missing data if it can not be generated due to lack of other formation data, as well be explained in detail in the following paragraphs.

Short Name	Long Name	Default EPW Units	Used by EnergyPlus
year	Year	-	n
month	Month	-	y
day	Day	-	y
hour	hour	-	y
minute	minute	-	n
datasource	datasource	-	n
drybulb	dry_bulb_temperature	C	y
dewpoint	dew_point_temperature	C	y
relhum	relative_humidity	%	y
atmos_pressure	atmospheric_pressure	Pa	y
exthorrad	extraterrestrial_horizontal_radiation	Wh/m2	n
extdirrad	extraterrestrial_direct_normal_radiation	Wh/m2	n
horirsky	horizontal_infrared_radiation_intensity_from_sky	Wh/m2	y
glohorrad	global_horizontal_radiation	Wh/m2	n
dirnorrad	direct_normal_radiation	Wh/m2	y
difhorrad	diffuse_horizontal_radiation	Wh/m2	y
glohorillum	global_horizontal_illuminance	lux	n
dirnorillum	direct_normal_illuminance	lux	n
difhorillum	diffuse_horizontal_illuminance	lux	n
zenlum	zenith_luminance	lux	n
winddir	wind_direction	degrees	y
windspd	wind_speed	m/2	y
totskycvr	total_sky_cover	tenths	n
opaqskycvr	opaque_sky_cover	tenths	n
visibility	visibility	km	n
ceiling_hgt	ceiling_height	m	n

Figure 2-4 Internal Data Element Names (directly applicable to EPW). Source:(US Department of Energy 2015a) Page 14 of 144.

Realising such facts, and understanding that EPW file may contain fabricated weather information for the missing data, it was important to investigate the effects of this process in the weather file reliability. From this point of view, the investigation started by checking one of the most important factors that especially affects the cooling load's calculation, which is the sky temperature. The sky temperature, and all its relevant components i.e. the Total sky cover (cloudiness) and the

Horizontal infrared radiation intensity are all affecting the radiative cooling to the night sky, whereas this cooling mechanism is very critical in climates with a clear sky and hot temperature, i.e. Hot and Dry climates. For these specific parameters, it was declared in the EnergyPlus Auxiliary Programs manual that values like the Horizontal Infrared Radiation Intensity are scarce (US Department of Energy 2015a); especially outside the US borders. Hence, even if the DOE provides a weather file, it might have contained some interpolated/processed/customised values, which need careful investigation.

Moreover, it also is important to understand that the weather files are not covering significant portions of the globe. Figure 2-5 draws attention to the voided zones that have no weather files ready made to incorporate into the EnergyPlus. Hence, other tools are required to generate the weather files for the targeted locations and then converting these weather files into the EPW format via the Weather Converter program. The METEONORM software is one of the profound tools that are commonly used to generate the weather files based on the irradiation interpolated data for the abandoned locations with no weather station/information (METEOTEST: et al. 2014). When using such assistant tools, the resultant weather files become even more susceptible to the weather customization inside the Weather Converter. Leading to more erroneous and misleading simulation results.

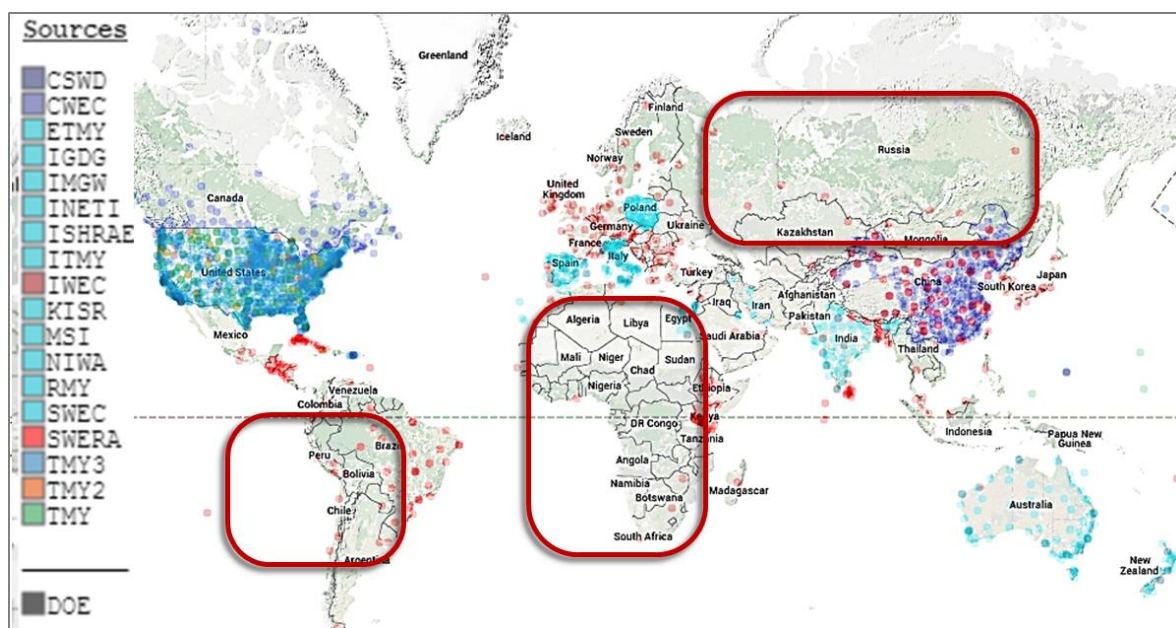


Figure 2-5 EPW Availability map. (Ladybug + Honeybee & Github n.d.)

For these reasons, the weather files examination is made to demonstrate the risks of using the weather files without systematic evaluation to their reliability in resembling the real weather conditions. As a start, the weather file of Tokyo [named: Tokyo Hyakuri 477150 (IWEC)] is obtained from the DOE-EnergyPlus weather data website (US Department of Energy n.d.). When opening the file in Microsoft-Excel, it was found that Opaque Sky Cover Value [Opaqskycvr] is assigned as (5) for all the 8760 hours of the year. Moreover, by referring to the Energy plus documentation –Input Output

Reference P.1521, it was found that (5) is the supplied value when the [Opaqskycvr] data are missing, as seen in Figure 2-6.

Missing Weather File Data		
The weather description of data contains "missing" descriptors, a new concept not introduced previously in our IDD conventions. In this case, it will be processed as though those values are "missing" in the weather conversions and/or EnergyPlus weather processing. This may not always be desirable though EnergyPlus will fill in "missing" value with something "appropriate". Eventually, these missing values will be available through the IDD and users will be able to supply their own values or EnergyPlus will calculate those values (such as radiation and illuminance) that are not a simple value replacement. Until then, the following are used:		
Table 44. Missing weather replacement values		
Data item	Supplied Value	Units
Dry-bulb Temperature	6	C
Dewpoint Temperature	3	C
Relative Humidity	50	%
Atmospheric Pressure	Standard** Barometric Pressure (altitude based)	Pa
Wind Speed	2.5	m/s
Wind Direction	180	Deg
Total Sky Cover	5	(tenths)
Opaque Sky Cover	5	(tenths)
Visibility	777.7	Km
Ceiling Height	77777	m

EnergyPlus Documentation Page 1521 of 1528

Figure 2-6 Replacement values for the missing weather data. (US Department of Energy 2015c)

Such data are imperative for the nocturnal sky radiation cooling since the Opaque Sky Cover value [N] is used to calculate the Sky emissivity, which, in turn, is used to calculate the Horizontal Infrared Radiation intensity in Wh/m² and the Sky temperature as well. These relations are shown in the following equations which are obtained for the Energy Plus documentation –Input Output Reference P.93 (Energy 2015).

$$Sky_{Temperature} = \left(\frac{Horizontal_IR}{Sigma} \right)^{.25} - Temperature_{Kelvin}$$

$$Horizontal_IR = Sky_{emissivity} \cdot Sigma \cdot Temperature_{drybulb}^4$$

Where ;

Horizontal_IR = horizontal IR intensity [W/m],

Sky = sky emissivity,

Sigma = Stefan-Boltzmann constant = 5.6697e-8 [W/m²-K⁴],

Temperature = drybulb temperature {K},

Whereas the sky emissivity is given by;

$$Sky_{emissivity} = \left(.787 + .764 \cdot \ln \left(\frac{Temperature_{dewpoint}}{273} \right) \right) \cdot (1. + .0224 N - .0035 N^2 + .00028 N^3)$$

Consequently, for the sake of testing the Tokyo weather file mismatches, the manually calculated Horizontal_IR [horzirsky] Value (using the equations above) is compared with the provided Horizontal_IR values in the weather file. Logically these values should be fairly identical, but because the Opaque sky values were not relative (missing) it is expected to see some mismatches. Indeed, as can be seen, from Figure 2-7, it is apparent that there is some discrepancy between the provided and calculated values of the Horizontal_IR.

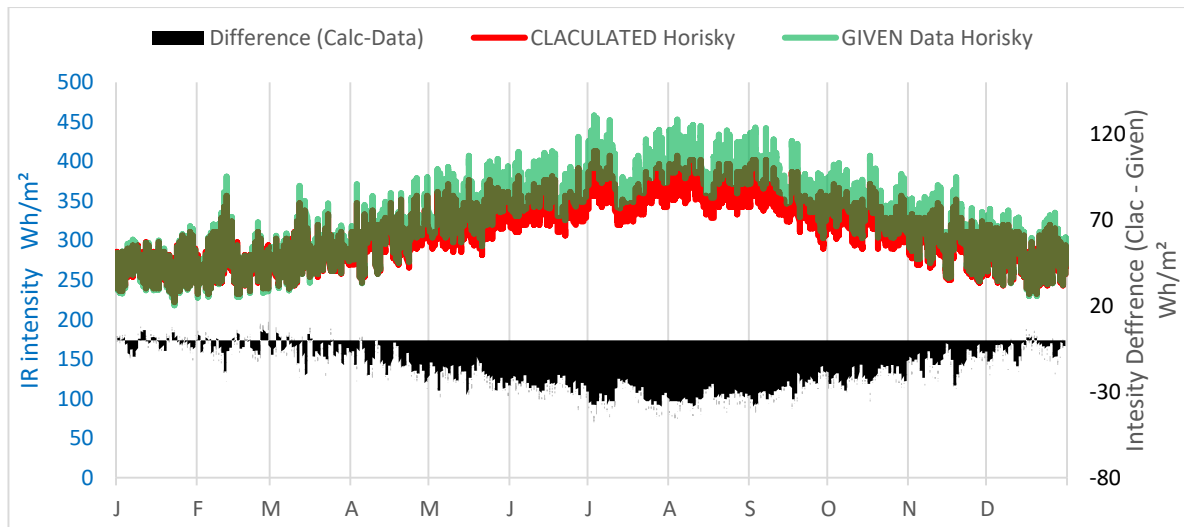


Figure 2-7 Tokyo- Mismatch between the calculated and the Given Horizontal IR radiation Intensity Wh/m²

Meanwhile, when the same exercise is done for some US cities, i.e. Las Vegas and Houston the deviation between the calculated and the provided data was either negligible or less than what is found in Tokyo data. Figure 2-8 demonstrates the same investigation results for Las Vegas, and it can be clearly seen that there is a great harmony between it is embedded and provided EPW file data.

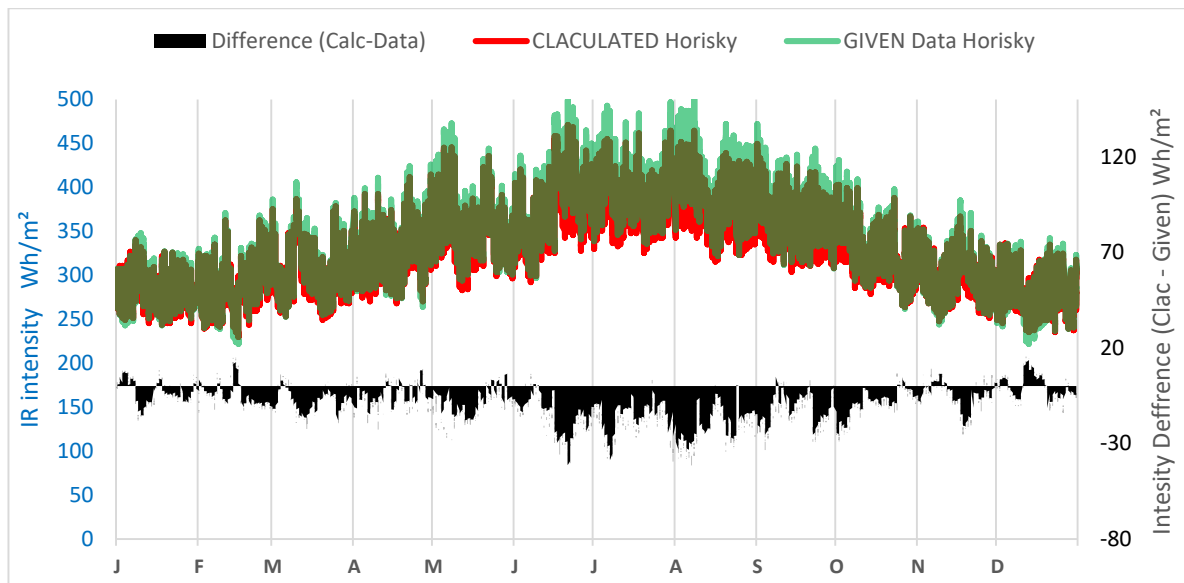


Figure 2-8 Las Vegas - Mismatch between the calculated and the Given Horizontal IR radiation Intensity Wh/m²

Moreover, an additional similar investigation is made for a third weather file, but this time the weather file was initially generated from the METEONORM software, then converted to the EPW file. Khartoum, Sudan was selected since the DOE does not provide EPW data for that location. The result is shown in Figure 2-9 and they demonstrate that the mismatch is prevalent throughout the year, unlike Tokyo which was dominant during the summer period, namely from June through October. Therefore, it can be concluded that for the sake of accurately simulating the night radiative cooling effects, and to account for the external surface radiative exchanges in general accurately, it is better to stick to the DOE Provided data within the United States, otherwise, it is to convey an inaugural sensitivity analysis for such cooling effects.

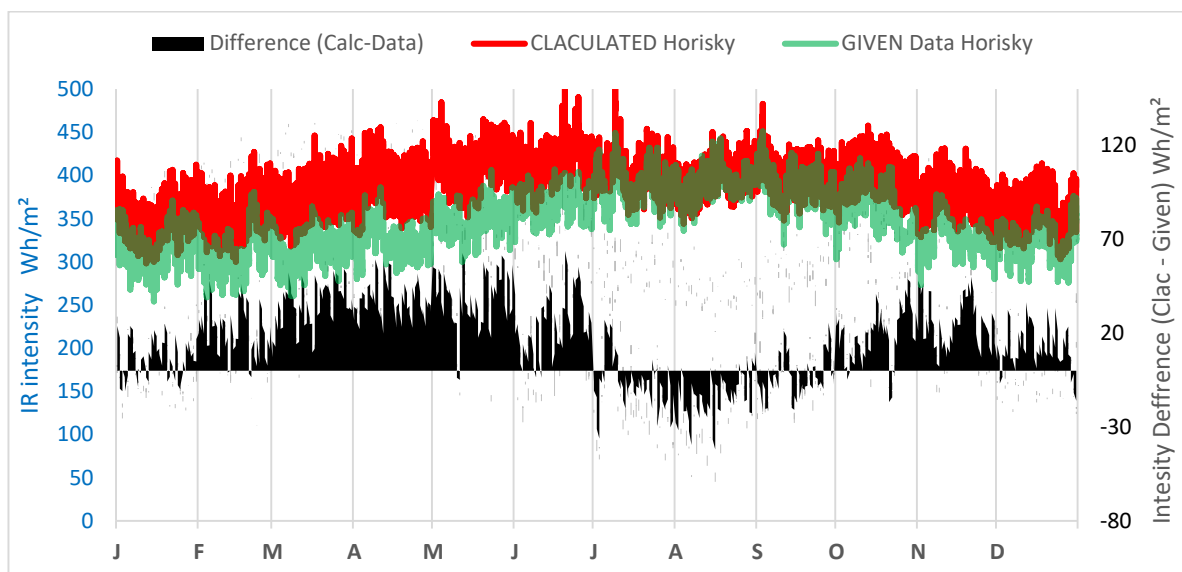


Figure 2-9 Khartoum, Sudan - Mismatch between the calculated and the Given Horizontal IR radiation Intensity

By the same token, another investigation has looked at the reliability of the other sensitive data provided by the EnergyPLUS weather files set and compare it with the other resources provided by the DOE. Namely, the Cooling Degree Days data of two sources are compared, i.e. from the Weather File Statistical Data and the from ASHRAE Standard saleable spreadsheets. The first resource of the Cooling degree days is the *.STAT file that comes with the EPW file package, along with the DDY [ASHRAE Design Conditions Design Day Data file]. However, the STAT format contains the weather file statistical summary of a bin file (Hirsch n.d.). The second source of the CDD/CDH data is the Commercially prepared spreadsheets provided by ASHRAE; some relevant documents can also be found in these references.(ASHRAE 2007)(ASHRAE 2012b).

The exploration was firstly made by opening the STAT file of a sample weather station of HOUSTON BUSH INTERCONTINENTAL AP. Moreover, from the state file, the CCD with a base temperature of [10°C] – values are presented in SI units. Moreover, as in Figure 2-10, the Annual CCD 10°C is 4089.

USA_TX_Houston_TMY3_ExportedEPW.stat - Notepad

File Edit Format View Help

- Displaying Heating/Cooling Degree Days/Hours from "Climate Design Data 2013 ASHRAE Handbook"
 - Monthly Standard Heating/Cooling Degree Days/Hours

	Jan	Feb	Mar	Apr	May	Jun	Jul	Aug	Sep	Oct	Nov	Dec
HDD base 10°C	39	20	6	0	0	0	0	0	0	1	7	36
HDD base 18.3°C	208	143	81	21	1	0	0	0	0	17	92	201
CDD base 10°C	98	126	221	320	462	532	585	586	491	360	201	107
CDD base 18.3°C	8	15	37	91	204	282	327	328	241	117	36	13
CDH base 23.3°C	27	64	184	632	1845	3082	3847	3855	2371	1006	223	42
CDH base 26.7°C	1	8	20	142	661	1395	1876	1936	1030	317	31	2

- 4089 annual (standard) cooling degree-days (10°C baseline)
 - 108 annual (standard) heating degree-days (10°C baseline)

- 1699 annual (standard) cooling degree-days (18.3°C baseline)
 - 762 annual (standard) heating degree-days (18.3°C baseline)

Figure 2-10 The [10 °C] CDD values obtained from the *.STAT file contents for HOUSTON BUSH INTERCONTINENTAL.

On the other hand, the ASHRAE supplied spreadsheet data, have shown that the CDD for the same base temperature equals 4043 as can be seen in Figure 2-11. It is apparent that when comparing the two data sources, there is a difference of 46 CDD. Despite that the two resources are using the same weather station data which is numbered WMO# 722430 [World Meteorological Organization reference number for the weather stations].

United States of America (USA)									
State					SI			Precip	Precip
LOCATION	WMO#	Lat	Long	CZ	Elev (m)	CDD10	HDD18	(mm)	(in)
HONDO MUNICIPAL AP	722533	29.36	-99.17	2B	284	3906	880	723	28
HOUSTON BUSH INTERCONTINENTAL	722430	29.99	-95.36	2A	32	4043	786	1262	50
HOUSTON WILLIAM P HOBBY AP	722435	29.65	-95.28	2A	14	4186	669	1340	53
HOUSTON/D.W. HOOKS	722429	30.07	-95.55	2A	46	4023	775	1187	47
HOUSTON/ELLINGTON	722436	29.60	-95.17	2A	12	4206	676	1356	53
JUNCTION KIMBLE COUNTY AP	747400	30.51	-99.77	3B	533	3521	1187	557	22
KELLY AFB	722535	29.38	-98.58	2A	208	4214	767	753	30
KILLEEN MUNI (AWOS)	722575	31.08	-97.68	2A	258	3777	1039	878	35

Figure 2-11 The CDD [10 °C] values as obtained from the ASHRAE commercial spreadsheet data for HOUSTON BUSH INTERCONTINENTAL.

The same exercise was done for another 13 climates, which are intended to be incorporated in the simulations, and there was always some variation between the two weather sources although they are originated from the same body i.e. ASHRAE. As to show the variation extent, Figure 2-12 is prepared to reflect the percentage of CDD variation between the STAT file and the ASHRAE commercial spreadsheets. The minimum variation was found in San Francisco climatic data as it was only 3 CDD which yield a negligible error percentage of 0.2%. Meanwhile, the maximum variation was 98 and have occurred in Riyadh city climatic data with a 1.6 % of the variation. Moreover, here, it is to note again, the Riyadh and Vancouver are the only two cities out of the US. Moreover, this might also support the previous argument that when using the climatic data of location beyond the US borders, it is to give an early investigation of the provided information before commencing the simulation.

Besides, and since Riyadh has a huge cooling needs i.e. huge CDD, it was not the highest variation percentage. Rather, the highest error as a percentage was found at Boise city with a 3.7% variation in tehCDD data, but with only 64 CDD.

Climate Zone	City	*.STAT provided data CDD [10°C]	Data from the ASHRAE spreadsheet CDD [10°C]	Varaition = STAT Data - ASHRAE		
				Error	Percentage	
(1A)	Miami, FL	5495	5447		48	0.9%
(1B)	Riyadh - KSA	6107	6009		98	1.6%
(2A)	Houston, TX	4089	4043		46	1.1%
(2B)	Phoenix, AZ	5116	5067		49	1.0%
(3A)	Memphis, TN	3165	3138		27	0.9%
(3B)	El Paso, TX	3306	3245		61	1.8%
(3C)	San Francisco, CA	1684	1681		3	0.2%
(4A)	Baltimore, MD	2169	2145		24	1.1%
(4B)	Albuquerque, NM	2326	2293		33	1.4%
(4C)	Salem, OR	1307	1289		18	1.4%
(5A)	Chicago, IL	1723	1689		34	2.0%
(5B)	Boise, ID	1751	1687		64	3.7%
(5C)	Vancouver, BC- Ca	968	951		17	1.8%

Figure 2-12 the CDD [10 °C] variation between the *.STAT data and the AHSRAE commercial spreadsheet data for 13 climates.

Besides, this variation have also been found for the Cooling Degree Days with the base temperature of [18.3°C] and Cooling Degree Hours CDH with base [23.3°C]. Similarly, the variation was also observed for Heating Degree Days HDD with all its provided base temperatures.

2.3 Testing the layer segmentation process influence on the layer config.

Similar to what will be shown later on in section 2.3 of chapter 3, a pre-simulation is carried out to determine the error margin of the further subdivision process on the energy simulation results. That is, to test the subdivision process and the algorithm refinement influence in te EnergyPLUS software results. The methodology is borrowed from Chapter 3. However, it can be briefly described as following. This inspection is evaluated by reporting the cooling and heating load difference between four setups as shown Figure 2-13.

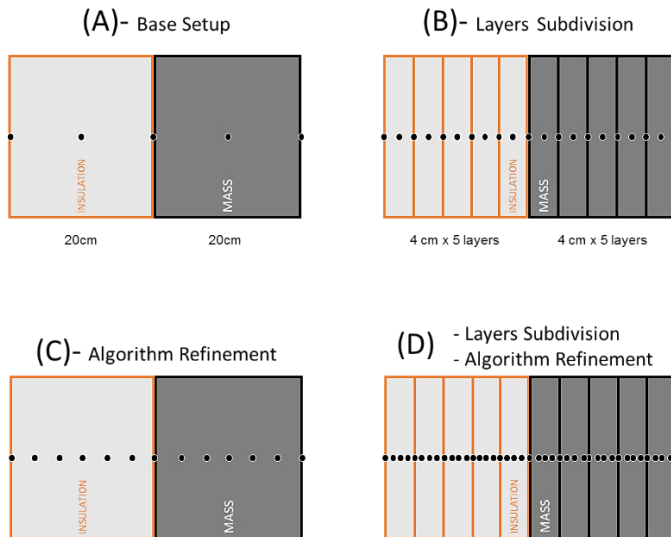


Figure 2-13 Accuracy Sensitivity investigation various setups for the Layers Subdivision and heat balance calculation algorithm.

The base case (Setup) for this survey is the simple configuration [IM]. Where the depth of the construction is kept at 20 cm too, this base setup is named (A). The first modification i.e. setup (B) is to subdivide the Brick and Insulation layers. It was proposed to have eight segmentations to comply with the maximum segmentation as in chapter 5, but due to the limitation in the fields of the number of layers in EnergyPlus to 10 fields, each single uniformed layer is replaced with five individual pieces instead. That is, each layer segment will be 4 cm thick, the input to the EnergyPlus then becomes as shown in Figure 2-14.

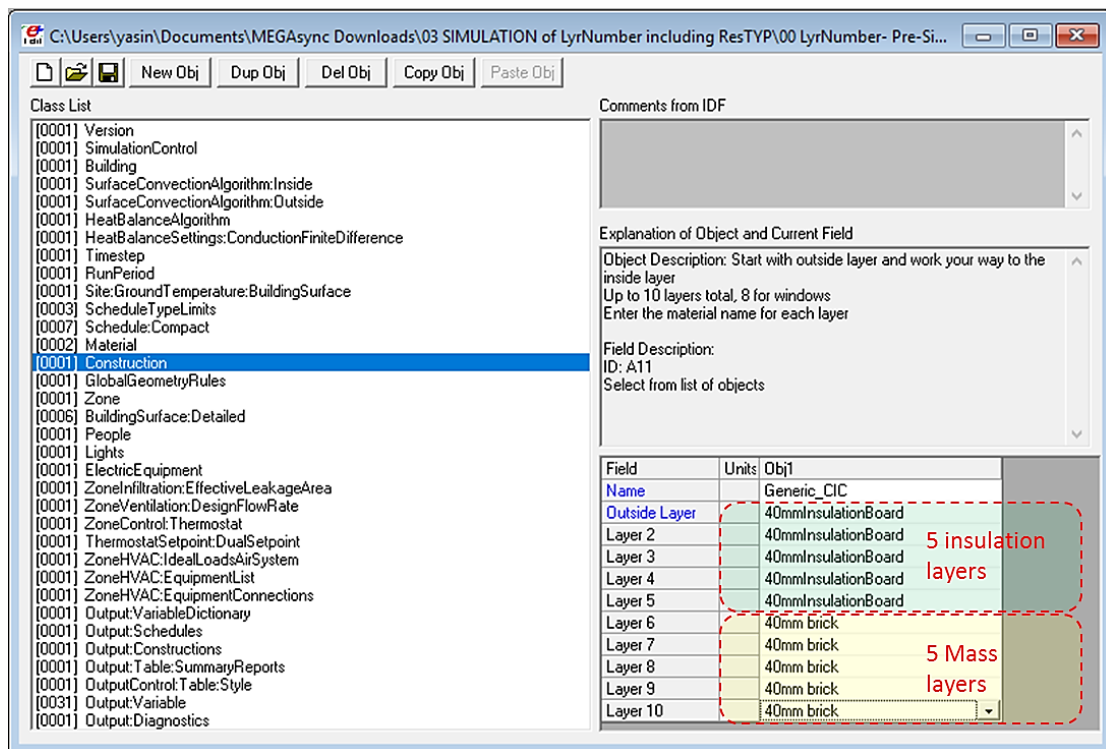


Figure 2-14 Layers subdivision inputs to the EnergyPlus

The second modification, shown as setup (C), is to refine the heat Balance Algorithm. This refinement is made by the fine-tuning is made by incorporating the “HeatBalanceSettings: ConductionFiniteDifference” object. Later on, more calculation nodes can then be added to the materials by changing the values of the “Space Discretization Constant”, the “Relaxation Factor”, and the “Inside Face Surface Temperature Convergence Criteria” from defaults to (1,0.01, 1 Exp-7) respectively as can be seen in Figure 2-15. Herre, it is worth mentioning that the number of nodes can be seen after the simulation is run for the first time, as by opening the *.eio file [EnergyPlus Invariant Output EIO². An example of this is shown in Figure 2-16 where the number of calculation nodes for the initial setup (A) is highlighted.

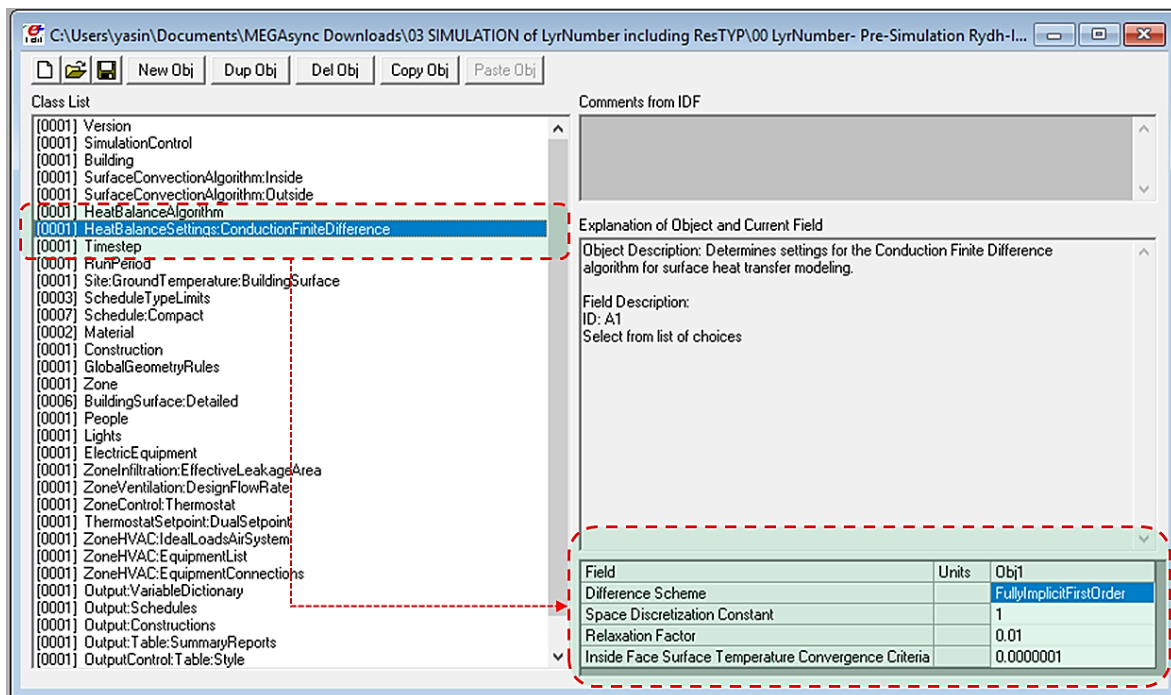


Figure 2-15 Heat Balance Algorithm refinement fine-tuning is made by incorporating the “HeatBalanceSettings: ConductionFiniteDifference” object.

² “The EnergyPlus Invariant Output (EIO) is a text file containing output that does not vary with time. For instance, location information (latitude, longitude, time zone, altitude) appears on this file.” (US Department of Energy 2015b)

```

ConductionFiniteDifference HeatBalanceSettings,FullyImplicitFirstOrder,3.00,1.00,2.0000E-003
! <Construction CondFD>,Construction Name,Index,#Layers,#Nodes,Time Step {hours}
! <Material CondFD Summary>,Material Name,Thickness {m},#Layer Elements,Layer Delta X,Layer Alpha/Delt/Delk**2,Layer Moisture Stability
! <ConductionFiniteDifference Node>,Node Identifier, Node Distance From Outside Face {m}, Construction Name, Outward Material Name (or Face)
Construction CondFD,GENERIC_CIC,1,2,39,1.666667E-002
Material CondFD Summary,200MMINSULATIONBOARD,0.2000,19,1.05263158E-002,0.31222372,0.00000000
Material CondFD Summary,200MMBRICK,0.2000,19,1.05263158E-002,0.31273141,0.00000000
ConductionFiniteDifference Node,Node #1,0.00000000,GENERIC_CIC,Surface Outside Face,200MMINSULATIONBOARD
ConductionFiniteDifference Node,Node #2,1.05263158E-002,GENERIC_CIC,200MMINSULATIONBOARD,200MMINSULATIONBOARD
ConductionFiniteDifference Node,Node #3,2.10526316E-002,GENERIC_CIC,200MMINSULATIONBOARD,200MMINSULATIONBOARD
ConductionFiniteDifference Node,Node #4,3.15789474E-002,GENERIC_CIC,200MMINSULATIONBOARD,200MMINSULATIONBOARD
ConductionFiniteDifference Node,Node #5,4.21052632E-002,GENERIC_CIC,200MMINSULATIONBOARD,200MMINSULATIONBOARD
ConductionFiniteDifference Node,Node #6,5.26315789E-002,GENERIC_CIC,200MMINSULATIONBOARD,200MMINSULATIONBOARD
ConductionFiniteDifference Node,Node #7,6.31578947E-002,GENERIC_CIC,200MMINSULATIONBOARD,200MMINSULATIONBOARD
ConductionFiniteDifference Node,Node #8,7.36842105E-002,GENERIC_CIC,200MMINSULATIONBOARD,200MMINSULATIONBOARD
ConductionFiniteDifference Node,Node #9,8.42105263E-002,GENERIC_CIC,200MMINSULATIONBOARD,200MMINSULATIONBOARD
ConductionFiniteDifference Node,Node #10,9.47368421E-002,GENERIC_CIC,200MMINSULATIONBOARD,200MMINSULATIONBOARD
ConductionFiniteDifference Node,Node #11,0.10526316,GENERIC_CIC,200MMINSULATIONBOARD,200MMINSULATIONBOARD
ConductionFiniteDifference Node,Node #12,0.11578947,GENERIC_CIC,200MMINSULATIONBOARD,200MMINSULATIONBOARD
ConductionFiniteDifference Node,Node #13,0.12631579,GENERIC_CIC,200MMINSULATIONBOARD,200MMINSULATIONBOARD
ConductionFiniteDifference Node,Node #14,0.13684211,GENERIC_CIC,200MMINSULATIONBOARD,200MMINSULATIONBOARD
ConductionFiniteDifference Node,Node #15,0.14736842,GENERIC_CIC,200MMINSULATIONBOARD,200MMINSULATIONBOARD
ConductionFiniteDifference Node,Node #16,0.15789474,GENERIC_CIC,200MMINSULATIONBOARD,200MMINSULATIONBOARD
ConductionFiniteDifference Node,Node #17,0.16842105,GENERIC_CIC,200MMINSULATIONBOARD,200MMINSULATIONBOARD
ConductionFiniteDifference Node,Node #18,0.17894737,GENERIC_CIC,200MMINSULATIONBOARD,200MMINSULATIONBOARD
ConductionFiniteDifference Node,Node #19,0.18947368,GENERIC_CIC,200MMINSULATIONBOARD,200MMINSULATIONBOARD
ConductionFiniteDifference Node,Node #20,0.20000000,GENERIC_CIC,200MMINSULATIONBOARD,200MMBRICK
ConductionFiniteDifference Node,Node #21,0.21052632,GENERIC_CIC,200MM BRICK,200MM BRICK
ConductionFiniteDifference Node,Node #22,0.22105263,GENERIC_CIC,200MM BRICK,200MM BRICK
ConductionFiniteDifference Node,Node #23,0.23157895,GENERIC_CIC,200MM BRICK,200MM BRICK
ConductionFiniteDifference Node,Node #24,0.24210526,GENERIC_CIC,200MM BRICK,200MM BRICK
ConductionFiniteDifference Node,Node #25,0.25263158,GENERIC_CIC,200MM BRICK,200MM BRICK
ConductionFiniteDifference Node,Node #26,0.26315789,GENERIC_CIC,200MM BRICK,200MM BRICK
ConductionFiniteDifference Node,Node #27,0.27368421,GENERIC_CIC,200MM BRICK,200MM BRICK
ConductionFiniteDifference Node,Node #28,0.28421053,GENERIC_CIC,200MM BRICK,200MM BRICK
ConductionFiniteDifference Node,Node #29,0.29473684,GENERIC_CIC,200MM BRICK,200MM BRICK
ConductionFiniteDifference Node,Node #30,0.30526316,GENERIC_CIC,200MM BRICK,200MM BRICK
ConductionFiniteDifference Node,Node #31,0.31578947,GENERIC_CIC,200MM BRICK,200MM BRICK
ConductionFiniteDifference Node,Node #32,0.32631579,GENERIC_CIC,200MM BRICK,200MM BRICK
ConductionFiniteDifference Node,Node #33,0.33684211,GENERIC_CIC,200MM BRICK,200MM BRICK
ConductionFiniteDifference Node,Node #34,0.34736842,GENERIC_CIC,200MM BRICK,200MM BRICK
ConductionFiniteDifference Node,Node #35,0.35789474,GENERIC_CIC,200MM BRICK,200MM BRICK
ConductionFiniteDifference Node,Node #36,0.36842105,GENERIC_CIC,200MM BRICK,200MM BRICK
ConductionFiniteDifference Node,Node #37,0.37894737,GENERIC_CIC,200MM BRICK,200MM BRICK
ConductionFiniteDifference Node,Node #38,0.38947368,GENERIC_CIC,200MM BRICK,200MM BRICK
ConductionFiniteDifference Node,Node #39,0.40000000,GENERIC_CIC,200MM BRICK,Surface Inside Face
! <Infiltration AirFlow Stats - Nominal>,Name,Schedule Name,Zone Name, Zone Floor Area {m2}, # Zone Occupants,Design Volume Flow Rate {m3/s},Volume Flow Rate/Floor Area {m3/s/m2},Volume Flow Rate/Exterior Surface Area {m3/s/m2},ACH - Air Changes per Hour,Equation A - Constant Term Coefficient {},Equation B - Temperature Term Coefficient {1/C},Equation C - Velocity Term Coefficient

```

Figure 2-16 The [Conduction Finite Difference] calculation nodes are displayed in the *.EOI file

The third modification, i.e. Setup (D) is made by incorporating both above mentioned modifications. Setup (D) will then have a much greater number of calculation nodes that are expected to increase the simulation stability, but, will also significantly increase the simulation time. Besides, It is thought to be useful comparing the chapter 3 pre-simulation results herewith. Therefore, the similar simulation conditions are applied, i.e. Riyadh was also selected as a sample city, where the constant cooling set-point was also kept at 22 °C. However, in this chapter, the occupancy schedule is set to residential occupancy with continuous load profile.

The Simulation results for the heating and cooling for the four setups (A, B, C and D) are all obtained and stored in a Comma Separated Values (CSV) File formats. Afterward, for the investigation and comparison, four different /techniques are used to investigate the influence of the three refined setups on the software calculation accuracy.

The first method is based on simple subtraction of the hourly data between the various setups. For example, when comparing two setups, for instance, configuration (A) and (B) cooling loads - written as (A) → (B)- the cooling load of each hour of setup (A) is subtracted from its counterpart in setup (B). Hence, the maximum [Max] variation will resemble the maximum found value where (A) is greater than (B), and vice versa for the minimum [Min] value, such variations are shown in Figure 2-17.

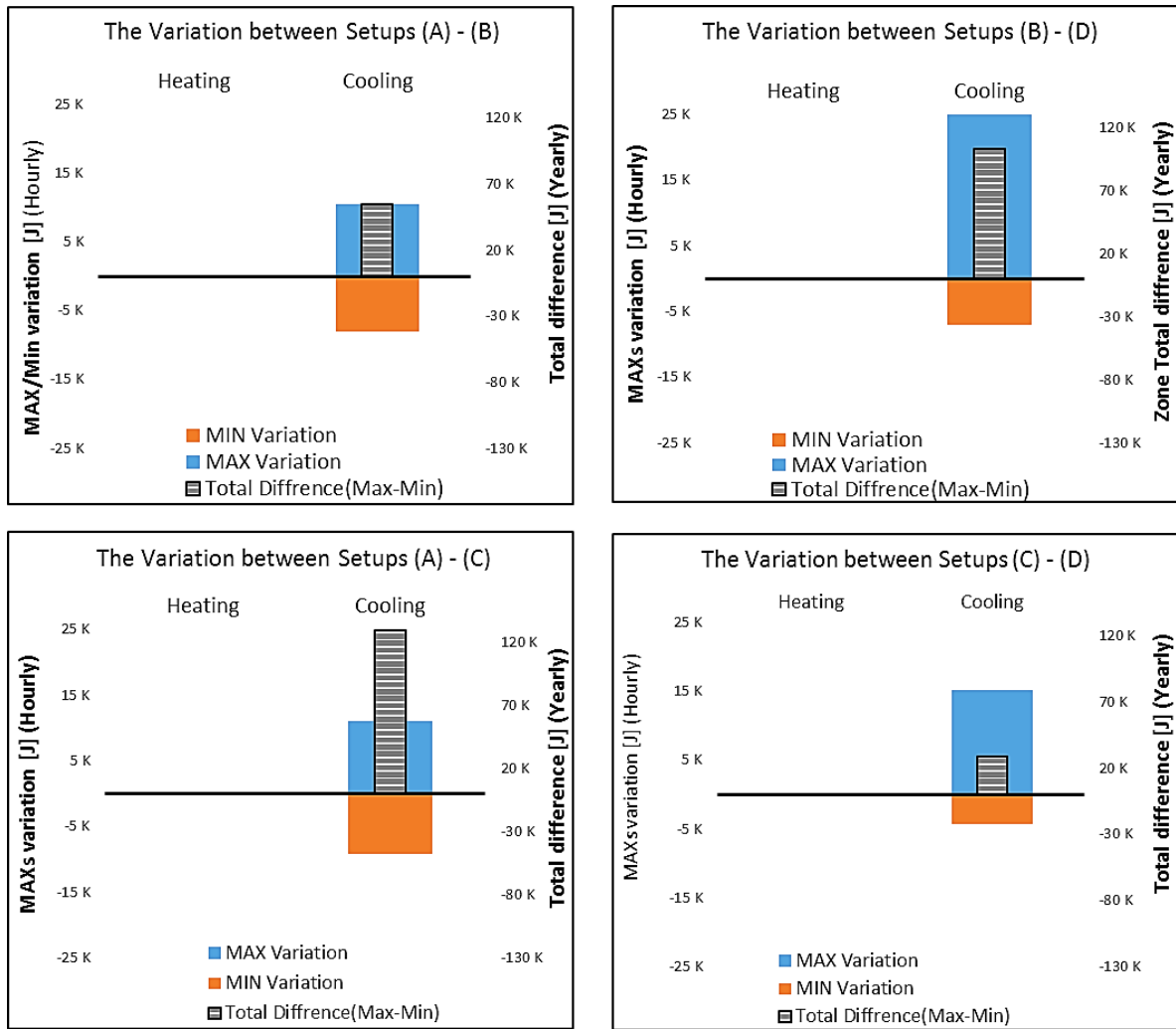


Figure 2-17 The Total, Maximum and Minimum variation between the different setups simulation results

Subsequently, The second is a way to evaluate the setups variations can be obtained by calculating the [Total Difference]. This difference is achieved by subtracting the [Max] and [Min] values, and if the results are positive this means that setup (A) cooling loads are overwhelming the setup (B) results. The total Difference is plotted on other side in the same Figure 2-17 provided above. Moreover, From these Figures, it can be seen that variation in the calculated heating load between the various setups is almost zero. This insignificant variation is attributed to the fact that Riyadh has very few heating demand hours throughout the year.

The third way to visualise the difference between the various setups was by directly plotting the variation between their corresponding hourly data in a year-based timeline. An example of such graphical variation between models (C)→(D) is seen in Figure 2-18; where the algorithm fine-tuned setups simulation results are compared. Moreover, from this comparison, it can be observed that the cooling loads being calculated via the most refined model (D) are greater than set up what is calculated in setup (C), especially in the summer season (an hour of years 2760 ~ 2670).

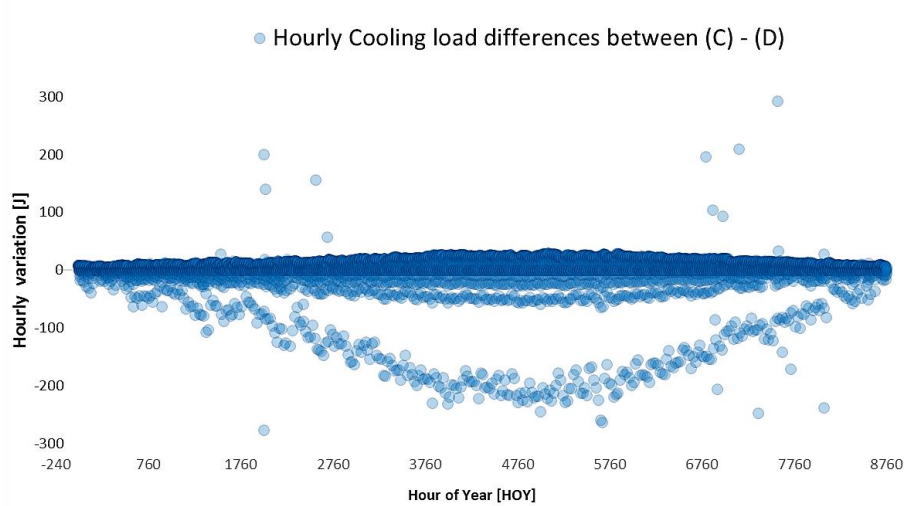


Figure 2-18 The Hourly variation values between the fine-tuned models (C) and (D)

Such technique enabled visualising the two modifications being applied to the model. For instance, to visualise the influence of the layer subdivision on the either the simple algorithm models (A and B) or among the refined algorithm models (C and D), the variations between them are plotted alongside as can be seen in Figure 2-19. Here, it can be seen the layer segmentation does not have profound affect the cooling load calculations, either among the simple algorithm models, i.e., (A and B) Or if the base model had undergone an initial algorithm refinement. Besides, it can also be noticed that the when subdividing the base model layers i.e. (A)→(B) it can be noticed that the setup (B) which has more layer segments had higher cooling loads calculations.

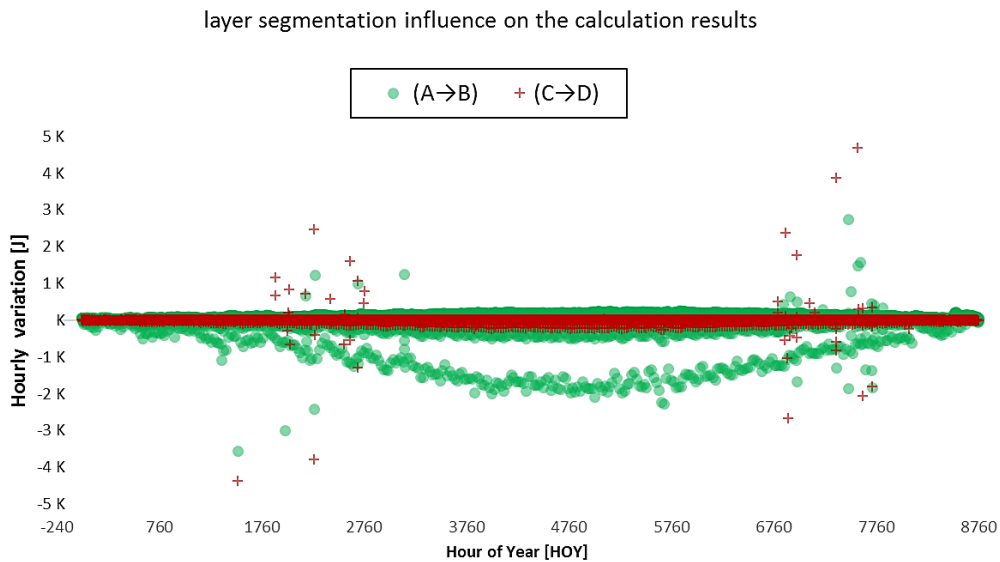


Figure 2-19 Layer segmentation influence on the calculation results.

Hourly variation between (A) → (B) VS (C) →(D).

Likewise, to for visualising the algorithm refinement influences on the EnergyPlus calculations, the modifications (A)→(C) and (B)→(D) are plotted on the same chart as in Figure 2-20. Moreover, from this figure, it can be seen that the algorithm modification on either a subdivided model (C and D) or in the block models (A and B) are not making a difference in the simulation errors. Meaning that, no matter how the layers are inserted (subdivided) if the model is refined there will be a significant variation between the simple algorithm models and the refined model where the latter yields the least cooling load calculations all over the year round.

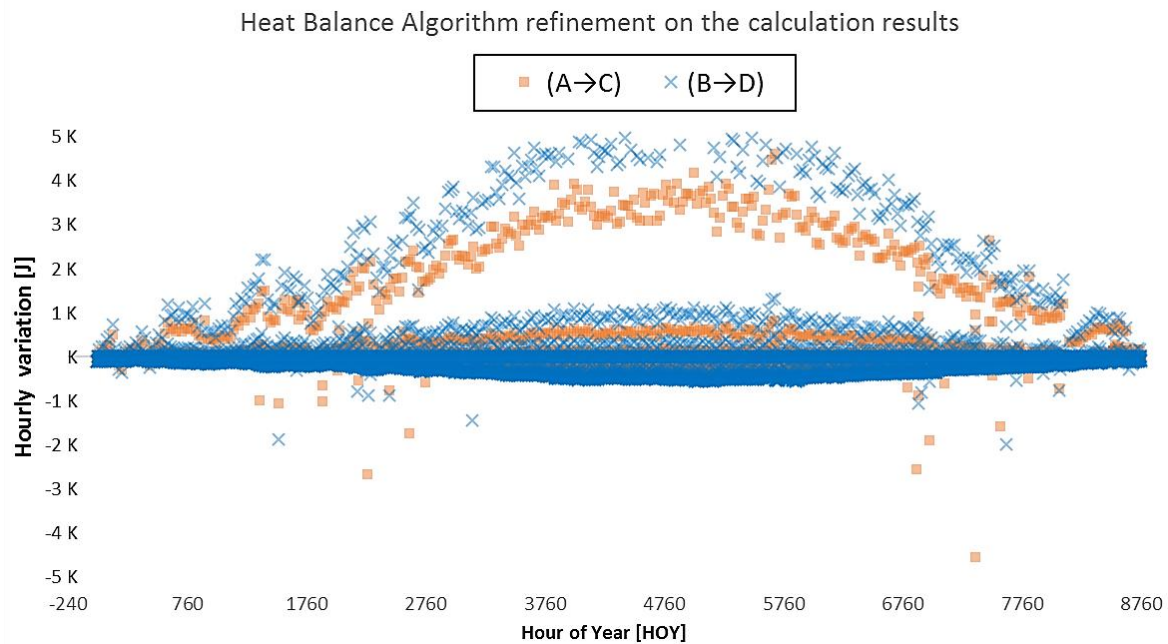


Figure 2-20 Heat Balance Algorithm refinement influences on the calculation results.

Hourly variation between (A) → (C) VS (B) →(D)

However, the two significant variations are plotted in Figure 2-21, which are the difference between either the simple layer subdivision modification, which will be applied through this research, i.e. (A)→(B) is compared to the most refined model i.e. (A)→(D). The results of this comparison would hint to which extent the model should be refined. Moreover, from Figure 2-21 It can be noticed that there is no significant difference between either modification, despite the invert effect. Therefore, initially, it can be said that the fine tuning process for the simulation models will not reduce the error margin when the layer subdivision is applied through this research.

Simple and Ultimate refinement influence on the calculation

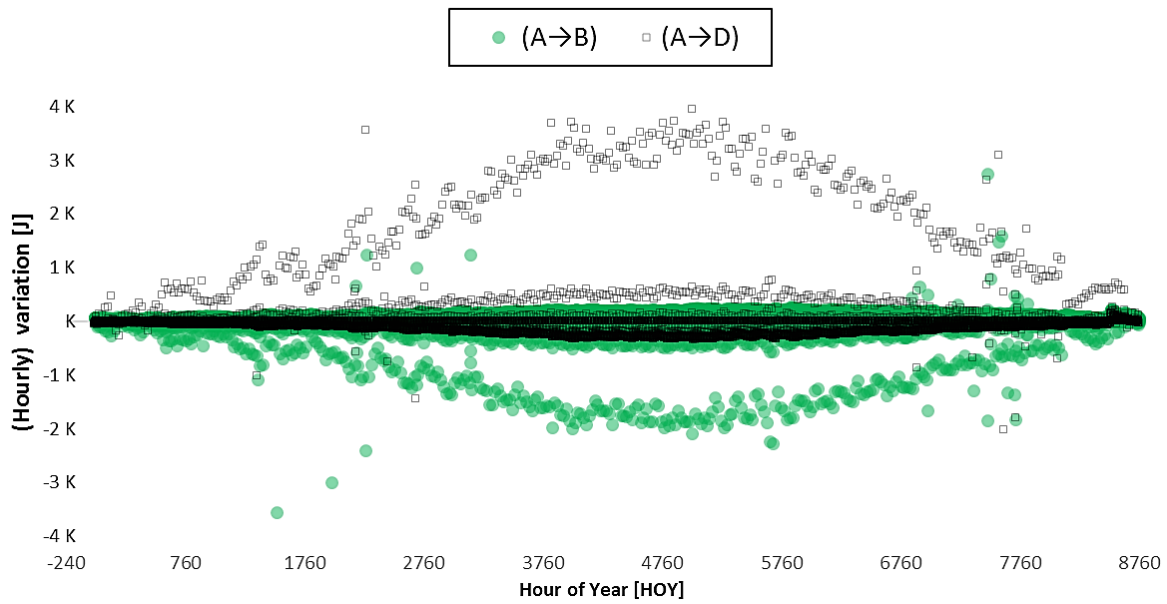


Figure 2-21 Simple layer subdivision and maximum model refinements influences on the calculation results.

Hourly variation between (A) →(B) VS (A) →(D)

To confirm the derived conclusion, another error evaluation technique is applied. This last technique is based on calculating and plotting the total absolute variation values. The process for such technique starts by subtract (A) from (B) - as example- for each of the 8760 individual hours, where the difference is expressed in an absolute difference. Consequently, the sum of the absolute differences for all the year is plotted as can be seen in Figure 2-22. At the end, the previous conclusion can be seen, validated there is no significant error reduction when comparing the (A→B) and (A→D) setups.

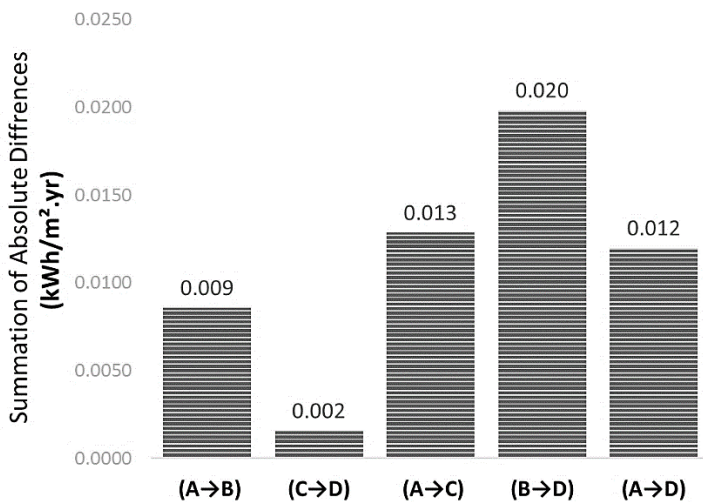


Figure 2-22 Absolute Differences of cooling loads among the various setups

Since the total Absolute, variation reflects the possible decisive error that might occur. Then the maximum error can be fairly obtained from this technique, i.e. the situation maximum error margin can be said as 0.02 kWh/m².Yr. Whereas the error that might arise from the subdivision process for the unrefined models i.e. (A)→(B), is just 0.009 kWh/m².Yr. It may sound logical to use a refined cmodels, as it can be observed that the deviation that caused by segmentation process is much less between refined algorithm models (C)→(D) when compared to the deviation between the models with the default algorithm (A)→(B). The load was 0.002 between the first setups and 0.009 ≈ 0.01 kWh/m².yr for the later. However, the time required for the refined models is almost 40 folds of the default ones. However, at the end, and apart from the shorter simulation time required by setup (A) and (B), but also, since the variation from (A→B) is still minuscule and therefore, the default Conduction Finite Diffrence algortihm is used for the simulation, while considering the 0.01 kWh/m².Yr as an sigmentaion/subdevisioin error margin.

Lastly, it is to state that the results of this section did not change a lot from chapter 3 variation study and error margins. Initially, as what will be seen later, the order of the variation magnitude between different setups was the same. Though It can be noticed that the deviation between (A) the default model and (B) has increased from 0.002 to 0.009 kWh/m².yr in t this chapter study. This incramnt in the errors magine was caused by the more layer segments that was adopted herwtih, i.e. 10 layers compared to 4 layers in chapter 5. Eventually having additional layers means ghaving more calculation nodes. Meanwhile, when comparing the two extreme setups (A) and (D), it was noticed that the variation has decreased by 0.001. In general, it can be seen that the change between the different setups is becoming more uninformed when compared to the variations in chapter 2 because, as explained earlier, the additional segmentations are producing more stable simualtions that is similar to those obtained when increasing the calcaultion nodes (i.e refining the simulation model).

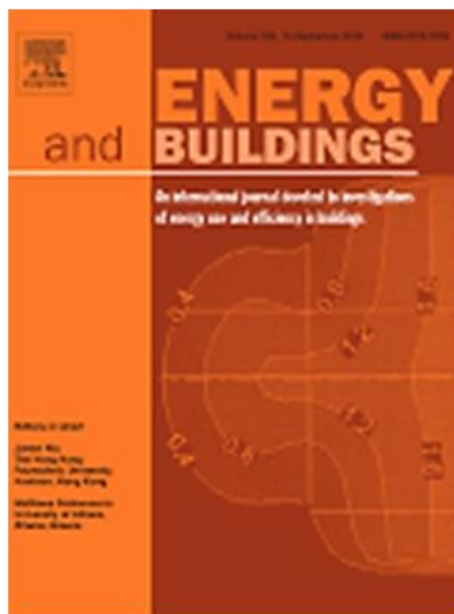
Chapter 3

3. The layer configuration influence on the anti-insulation (JOURNAL ARTICLE)

The contents fo this Chapter have been complied and submitted to the profound Energy and Buildings Journal under the title:

[Anti-insulation Mitigation by Altering the Envelope Layers' Configuration]

While writing these letters, on November the 2nd, the article has gone through the first revision where positive reviews have been forwarded by the Journal editor and the reviewers. The comments have been fully addressed and it this moment the article is going under the second revision.



Chapter 4:

4. The number of layers' influence on the anti-insulation (Simulation).

The contents of this chapter are a continuation of the previous chapter that dealt with the anti-insulation mitigation. However, the main difference is that Chapter 3 have investigated the layer configurations as a mitigation measure, while this chapter is examining the influence of the number of the layer segments on the anti-insulation. The subjected configurations and the environmental setups were also based on the findings of Chapter 3, as will be explained in detail in section 4.2.

4.1 Preface and Objectives

Before delving into the chapter contents, it is to point out that the basic idea behind the investigations herewith is inspired by the heuristic research provided by (Bond et al. 2013). The research outcomes have highlighted two interesting facts regarding the dynamic thermal behaviour of the multi-layered walls. Firstly, It was reported that the optimal dynamic results are obtained when the thermal mass and insulation layers are subdivided into thinner layers and are dispersed evenly through the wall configuration. Secondly, and most importantly, the study has revealed that there is an optimal point of that dispersion (subdivision), i.e. the infinite subdivision of layers will not guarantee the best performance, rather, there is a certain number of layer's subdivision where the best performance takes place.

Starting from these two pieces of evidence, and after demonstrating that the layer configurations could significantly contribute to mitigating the anti-insulation behaviour, it was intriguing to understand and examine how the layer dissipation (furtherly segmenting and subdividing) the Insulation and Thermal Mass layers of a given configuration. That is, the best performing configurations were borrowed from the (under publication) article. Subsequently, these configurations were subjected to multi subdivision process while maintaining their initial setup. For example, the configuration of [IMI] then becomes [IMIMI], where it can be noticed that the core mass layer has been furtherly subdivided into two layers while the peripheral boundaries (internal and external surfaces) are maintained the same.

The configurations selection process, the modifications, and simulation results have been covered, and conclusions are presented in the last part of this Chapter. Meanwhile, the important points that serve the formulation of the thesis framework are conveyed to the Chapter 7 [Conclusion] and discussed from a wider objectives point of view. Not to forget, that this Chapter and the following Chapter [5] are both concerned with layer dispersion. However, this chapter is based on simulation results and uses the anti-insulation and PTI "point of Thermal Inflexion" as evaluation criteria. Meanwhile, Chapter 4 builds on experimental investigations and utilises the standard dynamic thermal performance criteria i.e. the Time lag and Decrement factor as evaluation criteria.

4.2 Methodology and Simulation setup

In the beginning, it is to remind that the purpose of this Chapter is to investigate the influence of increasing the number of mass and insulation layers on the Anti-insulation behaviour. And as stated before, the literature have suggested that increasing the layer segments improve the dynamic thermal performance of the envelope components. Therefore, based on these two points, the best performing configurations that yielded the highest PTI is selected for each occupancy profile. This selection is also based on the advocated argument that increasing the number of layers means to increase the dynamic insulation and therefore having a negative effect on the anti-insulation and having lower PTI's. Therefore, the configurations [IMI, IM, MI] are used for this investigation as the base references, and they were subjected to the residential with continuous load, office profile and office with continuous

load occupancy profiles, respectively as per the findings provided in **Error! Reference source not found.**, Chapter 2.

Also, the configuration [IMI] was tested under the residential profile, although it is not the best performing configuration under this occupancy pattern. This random selection was made also to check the segmentation influence on the worst performing configurations as well. Apart from that, and as per what is provided in **Error! Reference source not found.**, Chapter 3, two cities were selected as representative climates fro the Hot and Cold climates, which are Houston and Albuquerque. The base configurations selection against their corresponding occupancy profiles loads is shown in Figure 4-1.

Case №	Climate	Occuopancy Profile	Base Configuration [Best Performing]*
1	Houston	Residential	I-M-I *
2	Houston	Residential+Load	I-M-I
3	Houston	Office	I-M
4	Houston	Office+Load	M-I
5	Albuquerque	Residential	I-M-I *
6	Albuquerque	Residential+Load	I-M-I
7	Albuquerque	Office	I-M
8	Albuquerque	Office+Load	M-I

* the best performing configuration under the Residential profile is [IM], however, this random selection is meant to investigate one of the worst performing cases as well

Figure 4-1 The base configurations and the occupancy profiles that will be used as references for layer segmentation/ dispersion evaluation.

In the second stage, the layer segmentation process is made for all the base configurations. Moreover, in this regards, and for the sake of coherence between this Chapter and Chapter 5, it was intended that this simulation should incorporate the same number of the investigated layers of Chapter 5. In Chapter 5, the maximum number of layer segments is 15. However, due to the limitation in EnergyPlus that allows only for ten layers to be inserted, the number of the investigated cases was confined to four processes for each instance, as can be shown in the sample case in Figure 4-2. Therefore, unlike the geometric progression of segments that have been used in chapter 5, the arithmetic progression of layers is used by adding two segments of insulation and mass at each case step.

City	Profile
Houston	Residential
Base Configuration	I-M-I
2 X	{I-M-I} - {M-I}
3 X	{I-M-I} - {M-I} - {M-I}
4 X	{I-M-I} - {M-I} - {M-I} - {M-I}

Figure 4-2 The layer's segmentation technique for the specific multiplication number.

By applying this segmentation process, if the PTI value of the selected cases is reduced, i.e. the performance is weakened, this will not only mean that the layer number have an effect on anti-insulation, but also it also proves that anti-insulation should be incorporated as an essential measure when optimising the number of the envelope layers. In this respect, it is important to emphasise that the overall length (material volume) of the mass and the insulation layers are equal among the similar cases. That is, The mass value is always fixed at 20 cm, but to plot the anti-insulation, the insulation varies from 5,10,15, and 20cm, as simulated before. Therefore, For the additional segmentation configurations, the insulation total thickness is constant for the same family branch, i.e. the 5 cm as a total insulation thickness is investigated in the [IMI],[IMIMI], [IMIMIMI], and [IMIMIMIMI] configurations, wherein the latter, for example, each insulation segment is 1 cm thick. Hence, any effects in the anti-insulation and on the PTI are solely made by this segmentation process. Moreover, to emphasise that point in a graphical overview, Figure 4-3 is produced for the same sample case of the baseline scenario of [IMI] layer configuration that might sound a bit conflicting to subdivide.

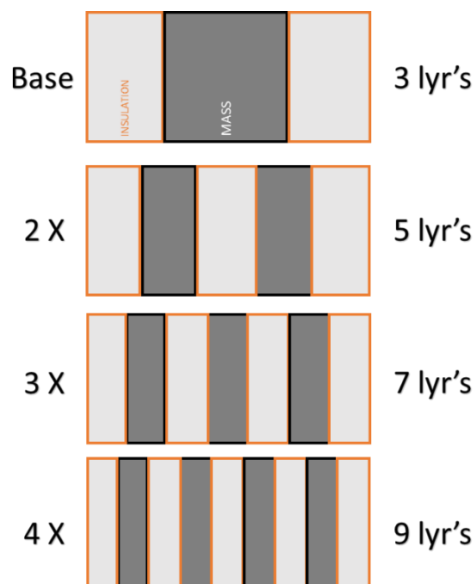


Figure 4-3 The layers segmentation process for an example case of [IMI] with an insulation layer of 20 cm.

Before illustrating the results, it is also to remind that Houston (2A) and Albuquerque (4B) are selected as sample cities, as in **Error! Reference source not found.**, Chapter 3. The results of the [IMI] under residential with continuous load schedule are at normal PTIs of the pattern (III) in Houston (26.5 ~ 28.4 °C) and having a pattern (I) always saving at 5 cm in the Albuquerque, and Normal PTI (III) in other conditions. The same behaviour of patterns applies for the normal residential occupancy profile

except that the best performing configuration is the [IM]. However, as stated before, the best performing configuration is the [IM], while the investigated configuration, i.e., [IMI] is not among the best three performing configurations, where it comes in the fourth. As can also be seen from the same figure, the situation is almost the same for both cities under the office schedule and the [IM] configuration, as in figure xx-b, except that the 10 cm for Albuquerque is a category (I) always savings. Lastly, for the [MI] configuration, and under the Office with continuous load profile, both cities had a PTI in the normal range (III) and for all insulation thicknesses.

4.3 Results and discussion

The results that were obtained from all the three occupancy profile cases are compared with the corresponding results as in Chapter 3. Whereas, the PTI of the base model is compared with the new ones that have additional segments. It is expected that the PTI values should decrease (anti-insulation performance decline), but in case otherwise observed, a further investigation might become a necessity and a detail justification will be needed. However, in this part, the results are presented as per the segmented layer performance and as per the occupancy profiles, they are subjected to. Moreover, it is to highlight that the illustration order will keep the least performing cases i.e. case [01] and [05] that belong to the typical residential profile to the end since the investigated configurations have shown adverse results.

f) Results under Residential with continuous load occupancy profile.

Firstly The segmentation results of the [IMI] configuration is presented under the residential with continuous loads occupancy profiles, i.e. cases [2] and [6] for Houston and Albuquerque respectively. In general, it is noted that the anti-insulation behaviour patterns of the various configurations did not change in relation with the climate type. Meaning that all the derived segmentations, i.e. [IMIx2], [IMI-3] and [IMIx4], had inherited their “mother” base configuration anti-insulation pattern. In Figure 4-4 it can be noticed that all the configurations have an Anti-insulation pattern [III], except for the Albuquerque case [6] at 5 cm where the derived and the mother configurations had pattern [I] which is always saving.

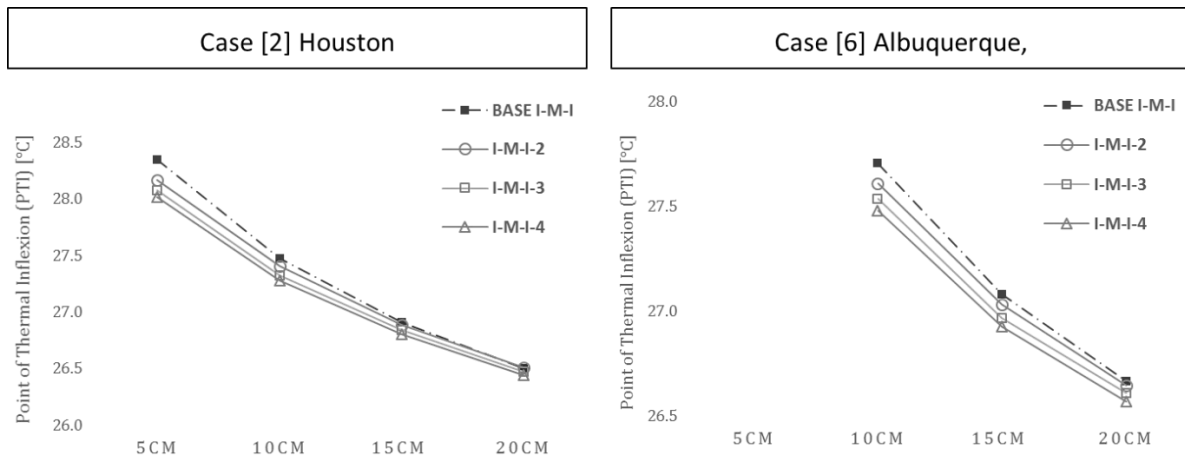


Figure 4-4 The Layer Configurations preference order for the Residential with continuous load occupancy profiles in two sample climates.

* The un-shown points in the graphs: e.g. the permutation of Albuquerque, Residential, [IMI], [IMI-2], [IMI-3] and [IMI-4] configurations at 5cm, were for Always energy saving and (I) pattern. i.e. there were no PTI.

From the same figure above, it can be noticed that the general trend is that adding more insulation yield the worst PTI performance for all configurations, i.e. the base case and its derived segmentation family produce lower PTI when their total insulation thickness increases from 5cm to 20cm. Also, it can also be seen that there is a clear performance order for all the configurations in both climates. Meaning that, at any given insulation thickness, the base configuration that has the least number of segments (i.e. 3) have better performance than the configuration with five layers. Meanwhile, the five layers have higher PTI when compared to the configuration with seven layers and so forth. Also, in both climates, it can also be seen that the variation of the resultant PTI between the segmented configurations was subtle. As to further pronounce this effect, Figure 4-5 has been developed with the base case [IMI] as to be the reference line. That is, the PTI value of the of the segmented configuration is subtracted from its corresponding mother case. By doing that, it can be seen that the maximum difference between the base case and the lowest PTI at configuration [IMI-4] was not more than 0.4°K, and this variation approached to zero at higher thicknesses.

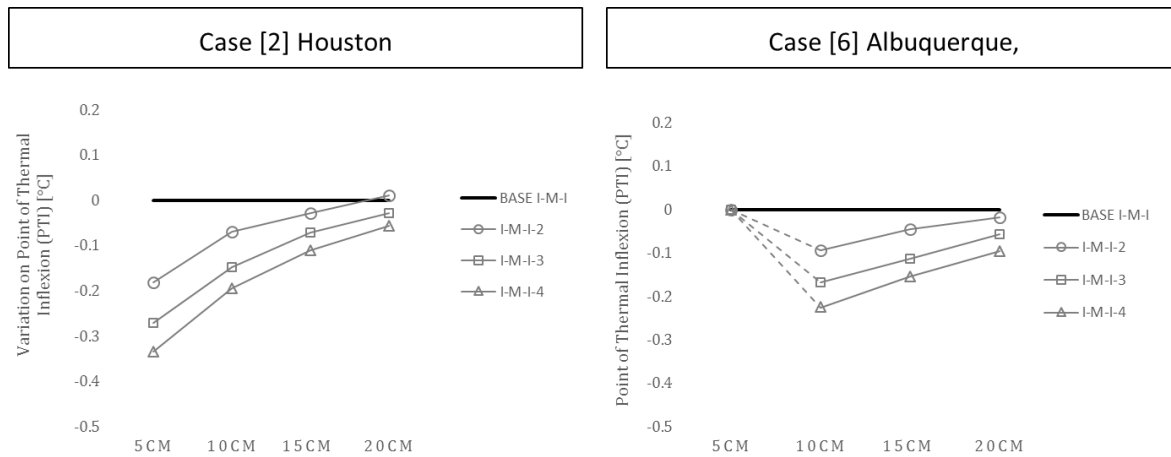


Figure 4-5 Taking the Base case [IMI] as a reference to evaluate the layer segmentation performance across the various insulation thicknesses.

* The missing points in the graphs: e.g. the permutation of Albuquerque, Residential, IMI, IM, and IMIM configurations at 5cm, were for Always energy saving and (I) pattern. i.e. there were no PTI.

For this occupancy profile, it is to confirm that when a configuration yielded a pattern [I] i.e. always saving, as in case [6] at 5 cm insulation, this pattern did not change and was consistent with the other segmented configuration at their 5cm setups. This means that the segmentation can be firmly incorporated into the “safe” climates and conditions undergoing the Residential profile with continuous loads since it will not change the anti-insulations behaviour pattern.

g) Segmentation results under the typical office profiles

The layer segmentation results of the Office occupancy profile are represented by cases [3] and [7] for Houston and Albuquerque respectively. For this occupancy profile, and as per the findings in Chapter 3 the best performing configuration was [IM]. Here, it is to note that the segmentation of the base configuration [IM] will arrive at the [IMIM]. Therefore the segmentation referred to as [IM-2] have been simulated earlier as configuration [IMIM]. Figure 4-6 is to highlight which layer segmentation has been borrowed from Chapter 3, and which segmented configurations have been conducted in this chapter.

Cases No	Occupancy Profile	Base Configuration	2-x	3-x	4-x
1,5	Residential	I-M-I	I-M-I-M-I	I-M-I-M-I-M-I	I-M-I-M-I-M-I-M-I
2,6	Residential+Loa	I-M-I	I-M-I-M-I	I-M-I-M-I-M-I	I-M-I-M-I-M-I-M-I
3,7	Office	I-M	I-M-I-M	I-M-I-M-I-M	I-M-I-M-I-M-I-M
4,8	Office+Load	M-I	M-I-M-I	M-I-M-I-M-I	M-I-M-I-M-I-M-I

Figure 4-6 Some of the derived segmentations have been simulated in Chapter 3. Shaded cells are for the borrowed results.

The first observation which can be seen in Figure 4-7, is that the segmentation process under this profile has changed some of the profile patterns particularly in the lower insulation levels, namely

at Albuquerque climate. Looking at the highlighted (in red) profiles lines, at all the derived configuration [2-x],[3-x] and [4-x] for the insulation thicknesses 5cm and 10cm, it can be noticed that they have turned the anti-insulation pattern from always savings pattern (I) to pattern (III). Moreover, this degradation in the configuration performance was not noticed in the residential with continuous load profile. However, such under-grading was limited to Albuquerque climate while the derived configurations in Houston have maintained the anti-insulation pattern of their base case.

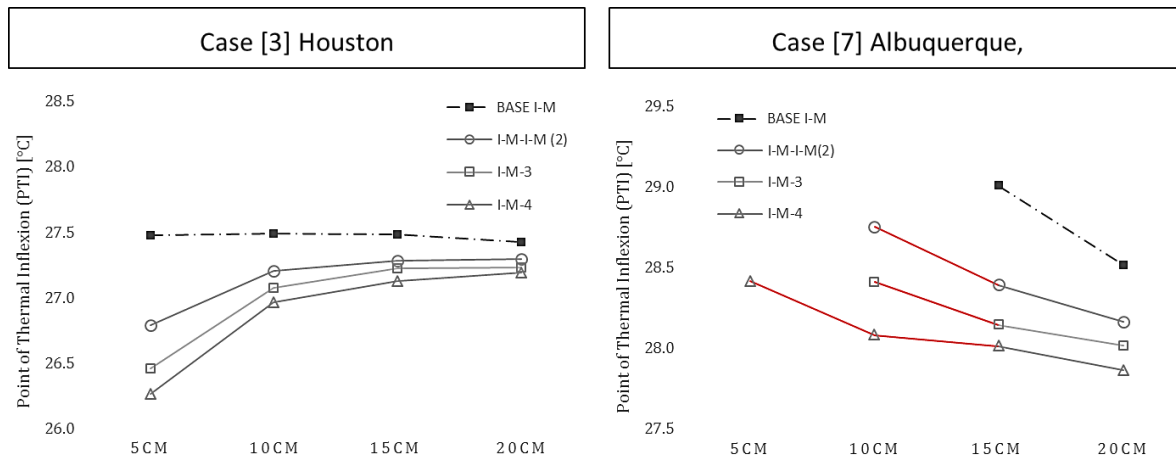


Figure 4-7 Layer Configurations preference order for the Office occupancy profiles in two sample climates.

* The missing points in the graphs are for the configurations that have an Always energy saving (I) pattern. i.e. there were no PTI.

Also, and different from residential with continuous load -case [2] - where the variation of the resultant PTI between the segmented configurations was subtle, the office occupancy profile for the Houston city the maximum variation jumped to 1.2°K as can be seen in Figure 4-8. The variation is increased by 300% as when compared to the residential with continuous load profile. This huge variation was apparent in Houston, and it can be ascribed to the fact that the base case [IM] have had an almost constant behaviour over all its insulation thickness.

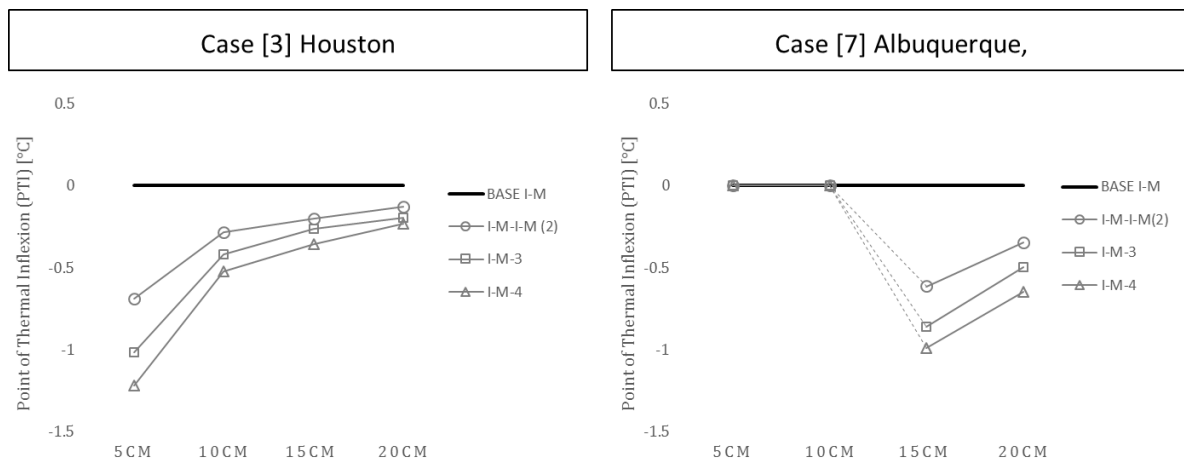


Figure 4-8 Taking the Baseline scenario [IM] as a reference to evaluate the layer segmentation performance under the Office occupancy profile, and across the various insulation thicknesses.

* The missing points in the graphs are for the configurations that have an Always energy saving (I) pattern. i.e. there were no PTI.

Moreover, in Houston climate, another important difference between the performance of the segmented configurations in the residential with continuous loads and the office profiles was noticed. As for the office profile, the higher insulation levels have produced higher PTI for the derived configurations. That is, when increasing the insulation from 5cm to 20 cm, the PTI of the segmented configurations [IM-2],[IM-3]and[IM-4] have increased accordingly. Moreover, gain, since that the PTI of the base case of the office is almost constant (around 27.5°C), then the multi-segmented layers dropped sharply at the lower insulation thickness, and thus producing better PTI (higher) at the thicker insulation levels. However, it is not to forget that the comparison is between two different wall configurations, i.e. [IMI] for residential with continuous load and [IM] for the office profiles. Hence the observations above, changes in respond to the insulation thickness, and may have been manipulated and have a link with the base configuration setup. Such judgement needs further extensive simulations to investigate all the base configurations among all the occupancy profiles and compare them with their derived multi-segment layer setups.

h) Segmentation results under Office occupancy profile with continuous loads

For the office with continuous load occupancy profile cases [4] and [8], it can be initially noted that the configurations performances under the both climates i.e. Houston and Albuquerque are almost identical. Also, it can be noted that the office with continuous load has yielded a different behaviour when compared to the office profiles that does not have a continuous load. Unlike the regular office profile, cases [3] and [7], the office profile with continuous load have shown more stable performance for the multi-segmented configurations when insulations increases where this behaviour can be attributed to the sharp deterioration in the base case itself [MI] when it insulation increases from 5cm to 20cm. In other words, and as can be seen in Figure 4-9, the [MI – 4] PTI was almost steady and around 23.5°C, while the base case i.e. [MI] have changed by 2°K between the 5cm and the 20 cm.

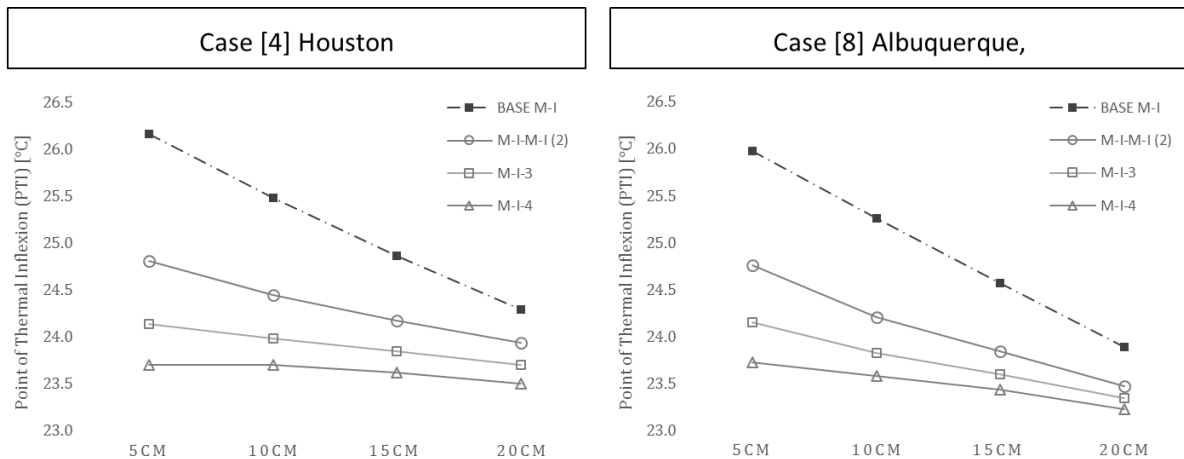


Figure 4-9 Layer Configurations preference order for the Office with continuous load occupancy profiles in two sample climates. For the base configuration of [MI]

* The missing points in the graphs are for the configurations that have an Always energy saving (I) pattern. i.e. there were no PTI.

Similar to the previous occupancy profiles, Figure 4-10 is prepared to further clarify the influence of the layer segmentation on the anti-insulation, with the base case [MI] various insulation levels are taken as reference values and present the y-axis = zero. Here, it can be seen that the variation in the base case [MI] and the configuration with maximum number of segments [MI-4] have increased to reach 2.4°K, and it is to highlight this increment is almost the double of what was found on the typical office profile that has no continuous load.

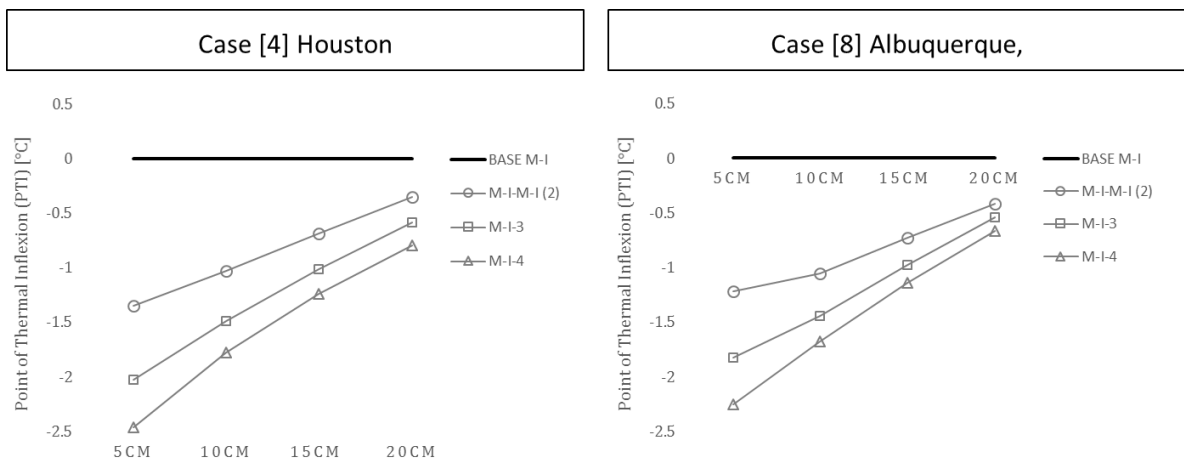


Figure 4-10 Taking the Base case [MI] as a reference to evaluate the layer segmentation performance across the various insulation thicknesses.

Moreover, another observation was found and may seem interesting is that the PTI of the configuration [MI-3] at a 5cm is slightly better than the PTI of the configuration [MI-2] but at 20cm of insulation. To show this observation better, the PTI values of all the configurations are plotted in a clustered column, where the two instances values are called out and can be seen in Figure 4-11. However, it is to note that this behaviour was solely observed at Houston Climate.

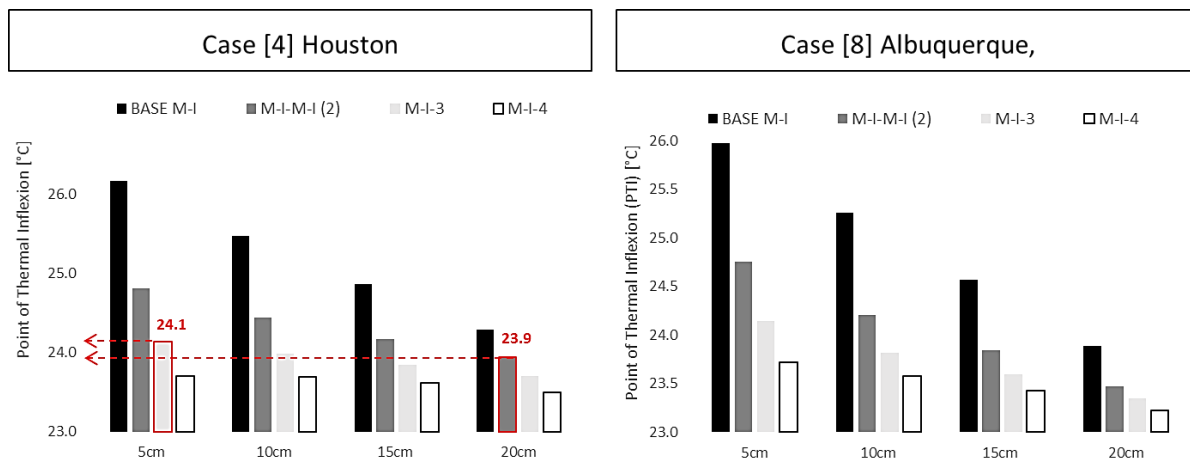


Figure 4-11 The PTI values for the Layer Configurations investigated under an Office with continuous load occupancy profiles in two sample climates. For the base configuration of [MI].

i) Results under Residential occupancy profile.

The results shown herewith are for the cases [1] and [4] for the Houston and Albuquerque climates respectively. The results are kept to the end since the selected base configuration under this occupancy profile, i.e. [IMI] was not the best performing configuration as can be seen Chapter 3. In fact, it was not even among the best three best performing settings. The reason behind exploring such configuration with negligible anti-insulation mitigation potentials is to study the influence of the layer segmentation on it. Meaning that, is the layer segmentation is going to degrade its mitigation potentials, as similar to the earlier cases, or it would be improved. Moreover, as a start, and analogous to the investigation techniques that carried for cases [2 to 4] and [6 to 8], the first investigation is made by plotting the PTI values for all the setups under both sample climates.

In Figure 4-12, it can be immediately noticed that the segmentation have, in fact, slightly enhanced the anti-insulation mitigation preference across all the insulation levels, and in both climates. Also, it can be seen that the variation in the PTI level between the various configurations – at a given insulation thickness- is not obvious at Houston, and better revealed in Albuquerque climate. Also, it can be seen that the anti-insulation pattern was not influenced by the layer segmentation process, i.e. the always saving, pattern (I) for the 5cm of Albuquerque was maintained across all the investigated configurations. Meanwhile, increasing the insulation of a given configuration is degrading the anti-insulation performance, i.e. increasing the insulation from 5cm to 20cm, for any configuration, have deteriorated its anti-insulation performance.

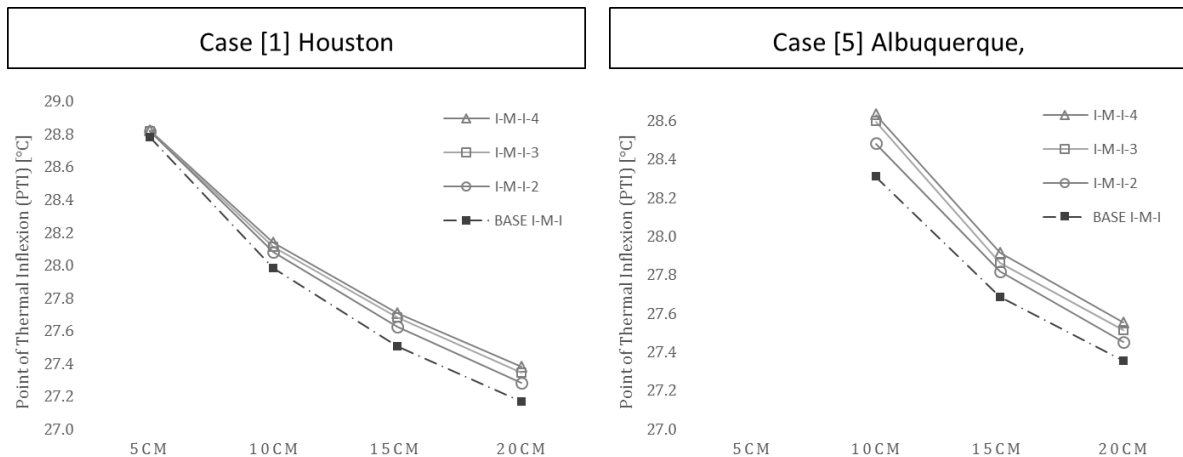


Figure 4-12 Layer Configurations preference order for the Residential occupancy profiles for the two sample climates. For the base configuration of [IMI]

* The un-shown points in the graphs are for the configurations that have an Always energy saving (I) pattern. i.e. there were no PTI.

Similar to what is conveyed in previous cases, Figure 4-13 is developed for this occupancy profile as to evaluate the improvement magnitude of the layer segmentation on the anti-insulation mitigation. From the provided results, another two unusual behaviours can be reported. Firstly, it can be observed that for Houston climate, increasing the insulation level from 5cm to 20cm has increased the PTI value. Secondly, when increasing the insulation, it was also found that the higher the insulation, the greater the performance gap between the various configurations, Which is firstly seen in this occupancy profile. Meanwhile, for the Albuquerque climate, although the variation between the configurations is a bit larger and more steady as when compared to the Houston case, it can also be seen that increasing the insulation level yields adverse effect on the configurations performance against anti-insulation behaviour.

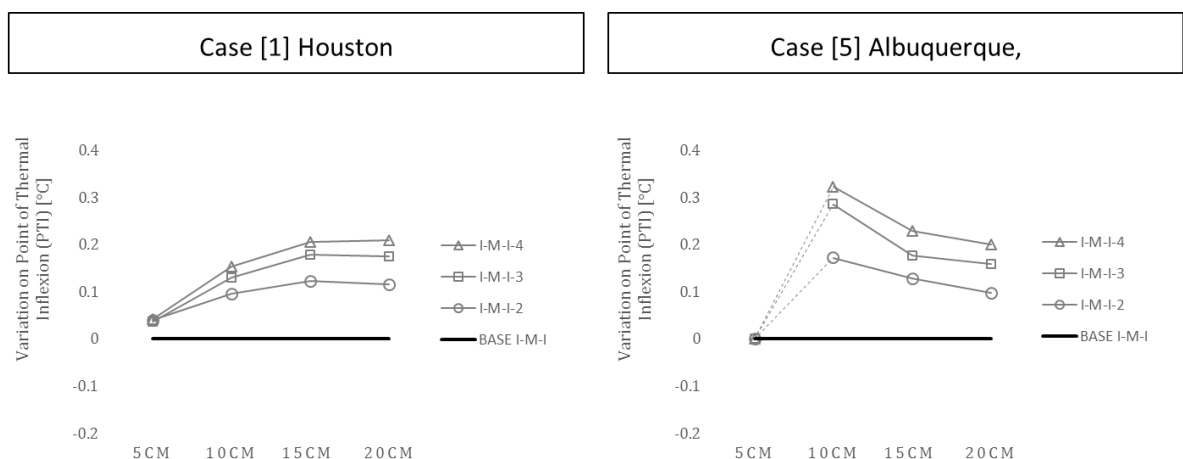


Figure 4-13 Taking the Base case [IMI] as a reference to evaluate the layer segmentation performance across the various insulation thicknesses.

* The missing points in the graphs are for the Always energy saving pattern (I). i.e. there were no PTI.

4.4 Conclusion

By the end, the general performance trends when increasing the layers segments can be sorted into two groups. The first is that if the best performing configuration is subjected to segmentation, then it is expected that its performance will degrade. On the other hand, if segmentation is applied to a least performing base configuration, then it is likely to yield better PTI results. However, It is important to remind that in some cases the layer segmentation has shown better results and could enhance the anti-insulation mitigation of a construction. An example of this can be seen in Figure 4-14 that represents the PTI values for the case [3]. As it can be seen that the [IM x 4] at 20 cm have higher PTI (better mitigation performance) when compared to to the [IMIM] at 5cm. This case can well be said that it represents the best scenario to mitigate anti-insulation via increasing the number of layer segments. As it enables higher PTI values while having very thick insulation levels at the same time.

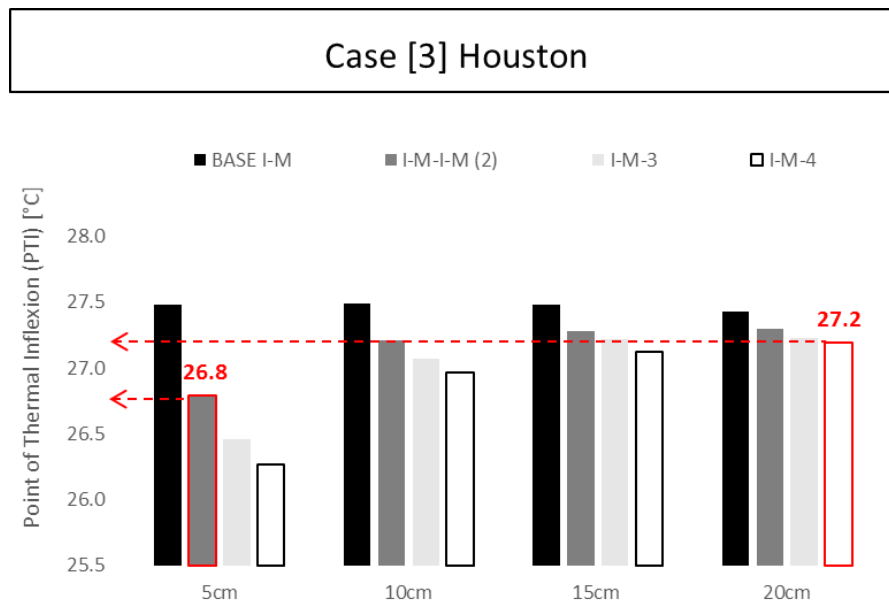


Figure 4-14 The PTI values for the various Layer Configurations the Residential occupancy profile with the continuous load. Note, that [IM-4] with 20cm have very close PTI compared to much less insulation i.e. [IM] at only 5cm.

Besides, as indicated above, and as what can be seen in Figure 4-11 of cases [4] and [8] for office profile with continuous loads as an example, the segmentation may result in significant degradation of the anti-insulation mitigation performance for a given thickness -with minor exceptions. Moreover, as in many sample cases, and as in Figure 4-15 below for case number [7], it can see that when the layers are segmented the anti-insulation pattern may degrade from always safe [I] to a lower anti-insulation pattern with a PTI at normal setpoint ranges (22~30). Therefore, it is difficult to say that the layer segmentations is always positive and will always enhance the anti-insulation mitigation, even if the initial base configuration showed a safe pattern (I) (always saving). Therefore, in conclusion, it can be said that adding more segment, needs a detailed investigation beforehand with considering the specific climates and occupancy profiles.

Case [7] Albuquerque

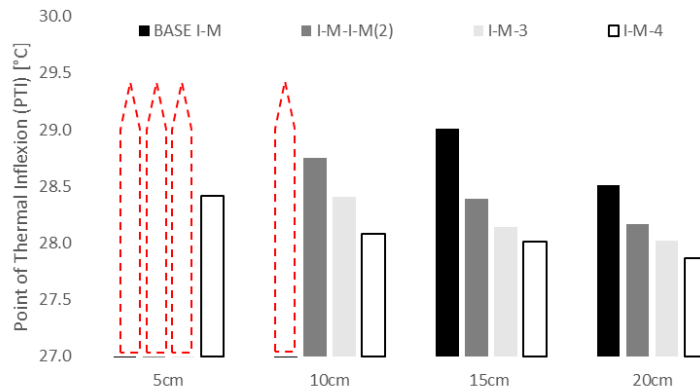


Figure 4-15 The PTI values for the various Layer Configurations the Residential occupancy profile with the continuous load. Note, that the base case [IM] at 5cm and 10 have an always saving Anti-insulation pattern (I) and have degraded to pattern (III) after some segmentation.

In opposite to previous cases, and as can be seen in Figure 4-16 for example [5] of Albuquerque climate at a residential occupancy profile, it was very clear that the segmented configuration [IMI-4] had always produced higher PTI compared to all other cases. Which can also be an example where increasing the wall segments may lead to better anti-insulation mitigation. However, in the end, it can be concluded that the approach of how anti-insulation could be manipulated and dampened have to be identified through a systematic consideration of the climate and the occupancy profile. As in some cases, the anti-insulation can be mitigated by increasing the number of segments while maintaining the higher insulation levels. In the other cases, the layer segmentation at lower insulation thickness may result in better PTI values.

Case [5] Albuquerque

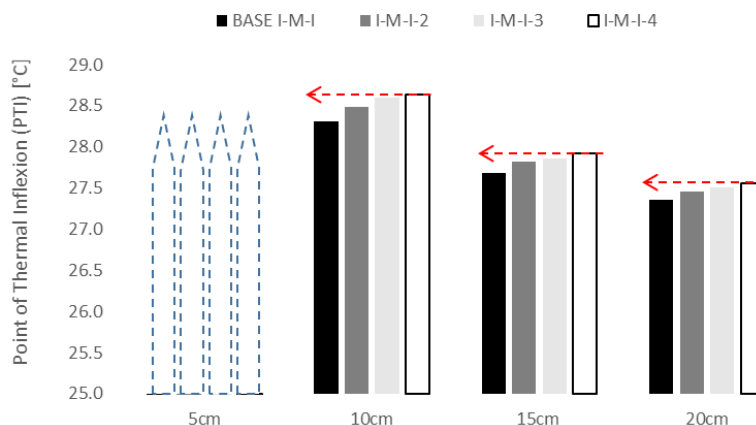


Figure 4-16 The PTI values for the various Layer Configurations the Residential occupancy profile with the continuous load. Note, that more layers segments yield higher PTIs where the effect is pronounced at lower insulation thicknesses.

Chapter 5:

5. The number of layers' influence on the dynamic thermal behaviour. (Experimenting)

As a continuation to the findings of previous Chapters 2 and 3, this chapter is aimed at studying the effect of the layer segmentation influence on the dynamic behaviour of the envelope opaque components. This time, the investigation was made via an experimental rig that is based on controlling and measuring the heat flow through the envelope specimen. Moreover, the chapter has introduced a novel method that provided a practical application of a thin thermal mass materials. The use of rubber as a very powerful thermal mass component that can also be produced at very thin layers have been tested using a thermocouple “Peltier” device that enables controlling the heat flux at both sides of the experimented specimen. The results, discussion and conclusions of a three layer configuration setups have been thoroughly covered and presented in the sections herewith.

5.1 Introduction

This Chapter deals with the thermal mass components of the building envelopes. It mainly focuses on these heat storage materials since its effective incorporation seems to be still limited to thick walls, and when it confined with such limitations, the privileges of having the thermal mass, in the building envelope will then vanish. As per what have been reviewed earlier, The importance of incorporating the thermal mass layers in the building envelope have been addressed in detail in Chapter 1. However, it is to remind that the thermal mass materials are majorly employed to increase the heat capacity of the building envelope. Whereas by increasing the heat capacity, lots of dynamics benefits can be obtained, like increasing the Time Lag and as well as reducing the Decrement Factor. In this respect, it is also to remind that increasing the Time Lag can solely be met by having adequate thermal storage "Mass" materials.

Also, as per what is Highlighted in literature, (Al-Sanea & Zedan 2011) has enumerated the benefits of increasing the Time Lag capabilities of the building envelope in three key points which are; firstly, is to increase the electrical grid stability by shifting the peak demands time and dampening the peak load. Secondly, shifting the peak load also helps in increasing the AC equipment Coefficient of performance, since the equipment are required to supply for peak operation at a less severe external conditions. Lastly, and based on the previous point, and as a result of reducing the peak demands, less HVAC equipment sizes will be needed. Hence, less ducting sizes will be required, less capital, as well as less maintenance operational costs, can be achieved.

Having said that thermal mass are the major envelope components that can shift the peak load "heat wave" arrival time. Hence, it is very welcomed in Mitteranean climates where the major concern is the high diurnal temperature ranges. In such climates, the incorporation of the very thick mass walls eliminates the need for insulation materials since the mass materials can provide heat resistance by "capacitive heat resistance" means, unlike the insulation materials that offer a "resistive heat capacities" (Roaf et al. 2007). In short, it is to say that the numerous benefit of utilising the thermal mass materials as the core envelope materials are well addressed in literature (Stazi et al. 2015) and they are also a genuine part of the vernacular architecture in the Hot Arid Climates and on the Mediterranean Climates as well.

On the whole, The use of thermal mass materials to supply for high time lags is very popular in climates with large diurnal ranges and where the basic aim is to supply for high Time Lags. A good example of such effect can be seen in Figure 5-1. This example shows a massive conventional walls and how they provide substantial Time lags between the indoor and outdoor temperature in a Haveli in Jaisalmer India, as surveyed by (MATTHEWS 2000). In this figure, the Time lag can reach up to two and half days on a ground floor level and can escalate to a seasonal variation in the basement where the heat that occurs at the moment in the ambient, its influence arrives inside the house after 23 days in average. Surprisingly, for the basement floor, (MATTHEWS 2000) have found that the Time lag in summer season may even jump to 91 days; i.e. a three months of heat daily.

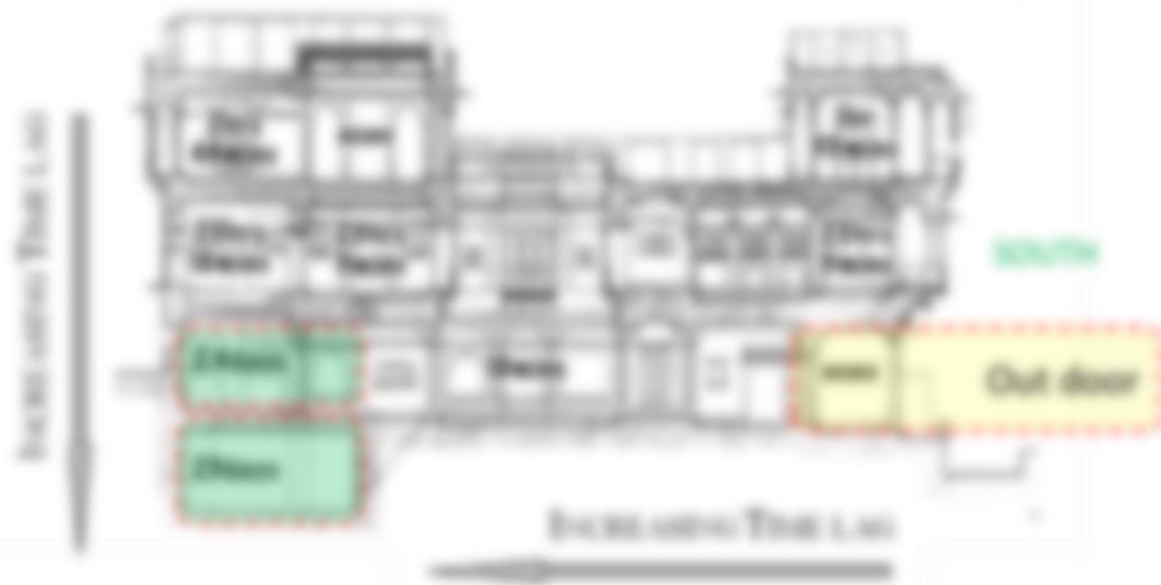


Figure 5-1 Time lags between the indoor and outdoor temperature in a Haveli in Jaisalmer India.

Source: (MATTHEWS 2000)

Also, from Figure 5-1, and as similar to the typical vernacular architecture, it can be noticed the thermal mass walls have always been very thick and cumbersome. Since these massive walls are constructed either from brick or adobe. Meanwhile, in the contemporary example, it is commonly found that concrete blocks are being used to supply for the heat capacity and thermal mass requirements. However, even in climates that require such kind of huge heat capacities, the extremely thick walls are no longer seems to be applicable in modern architecture, especially in cities where the land price is so high and when the plots are very small and/or narrow. Moreover, another concern of employing such massive construction may be hindered by the recent safety measures that overlook at the risks of these constructions during earthquakes. Therefore, a legitimate question would be of how to incorporate such very thick constructions in a modern settlement where such massive walls occupy vast areas of the typically small and expensive estates.

Even more, as shown in previous chapters, that a better thermal performance and greater Time Lags can be achieved if the building envelope thermal mass and insulation layers are furtherly subdivided into many small segments. This notion of layer segmentation was introduced by (Bond et al. 2013), and have been covered by simulation results in chapter 3. However, as has been depicted in Figure 5-2, a remained question is how to practically subdivide and disperse the thermal mass components into a small layer that may not exceed few centimetres/or maybe millimetres. The practicality issue was also reported by (Bond et al. 2013), whereas in their conclusion, the authors have shown that the fabrication issue of such multi-segmented walls needs to be furtherly studied.



What materials to use as thermal mass that can be produced in small thicknesses?

Figure 5-2 The practicality constraint against maximum utilisation of conventional thermal mass materials in multi-layered envelope components.

The practicality of producing finite thermal mass materials, especially when thinking about concrete /brick at that thickness, might not be a valid option in the construction industry. The reasons behind this practicality issue can be argued in two points;

- i. The conventional concrete/brick/rocks (e.g., granite, marble) are very stiff, and such rigid materials become very fragile at small thicknesses, that will be difficult to produce on site (delicate cutting) and will also be difficult to mobilise and handle. Moreover, even if these materials are produced at such thin segments, they cannot be used to cover large areas without supporting structural systems. In the end, this structural support will form the thermal bridges that will weaken the envelope overall thermal performance.
- ii. For the purpose of the experiment, the commercial earth-based tiles are not usually produced in a smooth back and front faces and without any textures or bevelled edges because these materials are typically are being applied at wet-based- application (e.g. on cement screeds). Such grooves are unwanted in the experiment, as they create an extra air gap that will influence the conductivity of the adjacent layer. Hence, the measured results will then be less reliable and would lead to erroneous judgements.

In conclusion, It is apparent that conventional materials can not be used in the thin and segmented wall. Therefore the initial target is to find and identify another way to enhance the thermal envelope capacity with an alternative thermal mass materials.

As a result, the original purpose was then to find a suitable material that has the proper thermal capacity (heat storage) but at the same time, can be produced at subtle thicknesses. Consequently, the first questions turned to be; how to identify the thermal storage characteristics of the material? Moreover, which materials can replicate the use of the brick and concrete blocks but have, if not better, the same heat storage capabilities? The upcoming section is dedicated to narrate how the rubber was finally selected as to be the thermal storage components in the developed envelope construction.

5.2 Thermal Mass material selection.

To find and propose a good alternative to the brick and the concrete materials, it was important to firstly understand why they have been employed as thermal mass materials in the first place. In this regard, it is to highlight that the identification of a suitable heat capacity material and its associated thermophysical characteristics have been partially covered previously in the literature review. Here, it is to elaborate that the definition of the heat capacity has been addressed in various ways. For example, the thermal diffusivity concept, as an opposite (reciprocal value) of the heat capacity, is identified by (Kalogirou et al. 2002) in the cooling equation;

$$a = k/\rho C_p$$

Where;

a = the diffusivity

k = thermal conductivity (W/m K)

ρ = density (kg/m³)

C_p = specific heat (J/kg K)

Hence, by the inversion of this equation, it can be deduced that the thermal mass is improved by having dense and high specific heat materials, but it also should be at low thermal conductivity so it can store the heat rather than pass it directly to another side. Also, it can be deduced that the heat capacity unit is (s/m²).

Moreover, as per SAP, the Standard Assessment Procedure, and (SBEM) Simplified Building Energy Model (Designing Buildings Ltd. 2016), the thermal capacity is addressed as a measure called Kappa value. The Kappa (k-value)³ refers to the heat capacity of each meter square of a material and is measured in (J/m²K). Whereas the thickness of the material is considered while its heat conductivity is not incorporated, as can be seen in the equation below provided by (BuildDesk 2016);

³ The Kappa value (k-value) should not be confused with the thermal conductivity (K-value).

$$k = 10^{-6} \sum (d_j r_j c_j)$$

Where;

d_j = the thickness of layer (mm)

r_j = density of layer (kg/m³)

c_j = specific heat capacity of layer (J/kg·K)

Therefore, in conclusion, it is agreed that the core the thermophysical properties that affect the heat capacity of material are the Density (kg/m³) by the Specific Heat (J/kgK) and the conductivity (W/mK). Moreover, based on such definitions, (Asan & Sancaktar 1998) have studied the heat capacity, the Time Lag nad Decrement Factor capabilities of some materials that can be seen in Figure 5-3. From this list, the best five materials that have the highest heat capacity capabilities are highlighted. Whereas from this list, the granite is excluded, since it has the same applicability problems that are found in brick and concrete i.e. can not be produced at fragile layers. Moreover, the asbestos is also excluded of its health hazardous implication issues.

Building material	Density ρ (kg/m ³)	Specific Heat C_p (J/kg K)	Conductivity k (W/m K)	Heat Capacity= Density x Specific Heat x Thickness C (kJ/K m ²)	Time Lag ϕ (h)	Decrement factor f
Cement sheet	700	1050	0.36	735	0.26	0.544
Concrete block	1400	1000	0.51	1400	0.44	0.588
Brick block	1800	840	0.62	1512	0.46	0.609
Gypsum plastering	1200	837	0.42	1004	0.28	0.564
Granite (red) block	2650	900	2.90	2385	0.59	0.701
Marble (white) block	2500	880	2.00	2200	0.56	0.689
Sandstone block	2200	712	1.83	1566	0.40	0.688
Clay sheet	1900	837	0.85	1590	0.45	0.639
Asphalt sheet	2300	1700	1.20	3910	1.03	0.647
Steel slab	7800	502	50.00	3916	0.89	0.179
Aluminum slab	2700	880	210.00	2376	0.55	0.733
Cork board	160	1888	0.04	302	0.32	0.174
Wood block	800	2093	0.16	1674	0.79	0.403
Plastic board	1050	837	0.50	879	0.27	0.587
Rubber board	1600	200	0.30	3200	1.17	0.501
P.V.C. board	1379	1004	0.16	1385	0.65	0.406
Asbestos sheet	2500	1050	0.16	2625	1.23	0.396
Formaldehyde board	30	1674	0.03	50	0.06	0.139
Thermalite board	753	837	0.19	630	0.28	0.439
Fibreboard	300	1000	0.06	300	0.24	0.234
Siporex board	550	1004	0.12	552	0.26	0.355
Polyurethane board	30	837	0.03	25	0.03	0.139
Light plaster	600	1000	0.16	600	0.28	0.408
Dense plaster	1300	1000	0.50	1300	0.41	0.586

Figure 5-3 Compound Decrement Factors and Time Lags for different building materials. The highlighted materials have high heat capacity capabilities, great time lag and low decrement factor values.

Source: (Asan & Sancaktar 1998)

Moreover, from the same reference and form Figure 5-3 above, the potential materials i.e. the rubber and the asphalt sheets are noted for further investigation. A list of materials with similar characteristics was obtained from various resources (Asan & Sancaktar 1998),(Thermtest Inc. 2016)

and (MakeltFrom.com 2009), and their thermal capacities were calculated and evaluated concerning the traditional brick, concrete and some fire rocks as well. The list is shown in Figure 5-4 and is sorted based on the heat capacity properties where the highest is at the top of the list. Subsequently, it can be confirmed that the asphalt and rubber (with its various types) does have a very high heat storage capabilities. It also to note that the concrete, brick and the marble are at the very bottom of the performance ranking order. Meaning that, the rubber and the asphalt materials are way much better regarding heat storing capabilities when compared to the conventional thermal mass materials.

Material Name	Denisty (kg/m3)	Cpecific Heat (J/kgK)	Conductivity (W/mK)	Claculated Heat Capcity (s/m ²)
butyl rubber	900	1966	0.088	20.1
rubber, butyl	900	1966	0.088	20.1
neoprene rubber	1250	2176	0.192	14.2
rubber, neoprene	1250	2176	0.192	14.2
rubber, natural	930	2092	0.138	14.1
silicone rubber, low k	1300	1255	0.138	11.8
rubber, dielectric mix	1100	2092	0.209	11.0
nitrile rubber	1000	1966	0.243	8.1
rubber, nitrile	1000	1966	0.243	8.1
rubber, high k	1100	2092	0.293	7.9
rubber, buna, with carbon black	1000	1757	0.243	7.2
styrene-butadiene rubber + carbon blk	1000	1757	0.243	7.2
polyurethane rubber l-100	1250	1674	0.293	7.1
rubber, polyurethane elastomer l-100	1250	1674	0.293	7.1
silicone rubber, rtv 521 and 093-009	1400	1255	0.272	6.5
Silicone rubber sheet [MIn]	1100	1050	0.2	5.8
rubber, natural, foam	100	2092	0.042	5.0
silicone rubber, medium k	1300	1255	0.335	4.9
butadiene-acrylonitrile rubber + c	1340	1443	0.418	4.6
Asphalt sheet	2300	1700	1.2	3.3
Concrete block	1400	1000	0.51	2.7
Brick block	1800	840	0.62	2.4
silicone rubber, high k	1300	1255	0.753	2.2
Marble (White)	2500	880	2	1.1
Rubber board	1600	200	0.3	1.1
Granite (red) block	2650	900	2.9	0.8
Marble (Red)	2650	900	2.9	0.8

Figure 5-4 The heat capacity capabilities of a selected list of materials including various types of rubber and asphalt, together with the conventional thermal mass materials i.e. brick concrete and some rock types. Data are obtained from (Asan & Sancaktar 1998),(Thermtest Inc. 2016) and (MakeltFrom.com 2009).

* Shaded materials are the conventional thermal mass materials

At a later stage, the asphalt was excluded from the list because of testing technicalities issue. That is, the asphalt has a rough texture that would prevent perfect layers attachments and will create lots of air pockets. Besides, it the asphalt sheets can not be in direct contact with the heat flux generators and meters as well. As a result, and as can be seen in Figure 5-5, the final list is confined to rubber products whereas the best four rubber products that have the highest heat capacities are; Butyl rubber, Isoprene rubber(IR,NR), Chloroprene Rubber (CR, Neoprene)and Silicone rubber sheets, respectively.

Material Name	Density (kg/m ³)	Specific Heat (J/kgK)	Conductivity (W/mK)	Calculated Heat Capacity (s/m ²)
Butyl rubber	900	1966	0.088	20.1
Isoprene rubber	1000	1550	0.14	11.1
Chloroprene Rubber (CR, Neoprene)	1500	1120	0.19	8.8
Silicone rubber sheet [MIn]	1100	1050	0.2	5.8

Figure 5-5 The heat capacity capabilities of four best-performing types of rubber. Materials thermophysical property data are obtained from (Thermtest Inc. 2016) and (MakeltFrom.com 2009).

Another important property that is unique about rubber as a possible thermal mass material is its flexible nature. As stated before, the mass materials are usually rigid in nature, since they require high density “material” to store the heat within, in turn, this high density is associated with high rigidity and stiffness. To further check this property, i.e. the elasticity, Young’s modulus chart is brought to the discussion. As can be seen in Figure 5-6 the rubber is found to be among the materials that have high elasticity while having a high density at the same time. Here, it is to emphasise that the rubber elasticity is imperative for the serving the purpose of having very thin construction layers. Moreover, as being flexible, the elastic materials can be incorporated into large panels, similar to the SIPS (Structural Insulated Panel Systems). In turn, the large panels are very efficient in reducing the heat flux through thermal bridges. Not to forget that such smooth surface materials will have leaves no air gaps and be in better contact to with each other in the experimental rig.



Figure 5-6 Young’s modulus, E , against density, ρ . The design guidelines assist in the selection of materials for minimum weight, stiffness-limited design. (Data courtesy of Granta Design Ltd) Reference: (Cambridge University Engineering Department 2003)

Furthermore, the elasticity character makes the rubber not only produce at thin layers, up to few millimetres but also it offers many other privileges. The first thing is that it offers a much better acoustics when compared to other stiff materials like concrete. This specific property adds much value to use the rubber materials as facings without the fear of echoes and sound waves reflections. In another word, some conditions dictate that the thermal mass material needs to be exposed directly to space as to act as a heat reservoir. In such cases, the concrete and brick materials incur acoustical problems that will no longer exist with the use of rubber as a thermal mass components.

In another respect, it is worth to mention that some rubber materials are commercially produced as a fire retardant and fire resistance materials. In fact, some rubbers are used in very extreme pressure and heat conditions, e.g. the Butyl rubber is used at the internal part of the automobile tyres. Also not to forget that rubber materials are foldable, easy to cut and customise, therefore, they would be easy to transport, and easy to be installed and joined with other parts of the building construction materials. Moreover, they can be attached using adhesive materials, hence, can be easily combined with the insulation materials as to compose the multi-layered construction panels and components.

The last thing to address about the rubber material is about its cost. As in general, the rubber materials are expensive and therefore, might not be feasible in an initial cost point of view. However, a good analogy to the payback and the long-term financial benefits could be the high price of the Vacuum Insulated Panels (VIP). These superinsulation panels are also very expensive. However, as per a comparison made by (Schiavoni et al. 2016); if the land price is high, as in their case is above 3000 €/m², then the area saving benefits when replacing a 35 cm mineral wool with a 6 cm of the VIP, will compensate for the VIP's very high installation costs. Likewise, the use of the very thin rubber materials as a heat storage medium instead of the thick brick and concrete blocks may also sound economically feasible. In conclusion, it is assert that the short list, shown in Figure 5-5 seems promising in replacing the conventional thermal mass materials. However, due to time and budget limitations, the experiment could only be conducted with only one rubber material. In the end, the rubber with the highest heats storage potentials i.e. Butyl rubber was supplied and was used in the experiment.

5.3 Experimental setup

Before is commencing the experiment of testing the rubber materials exploitation as a heat storage mediums in the building envelope, core issues had to be considered and well addressed. This issue is about the availability of the experimenting device, which was not readily available and can be used for a limited time. This consideration was important since the experiment was intended to investigate a different number of the layer arrangements. Therefore, the layer arrangements permutations are almost confined to three to four setups. This point is elaborated in the following three sections.

Also, it is important to mention the complete description about the thermophysical properties of the butyl rubber materials was not available for commercial products. Therefore the material was purchased and then sent to the Japan Testing Center for Construction Materials (JTCCM) to test the

conductivity and the specific heat. The test results are plotted against the expected performance early introduced in Figure 5-5. Subsequently, and as can be seen in Figure 5-7, the procured Butyl rubber seems to have a much less heat storage capabilities.

Material Name	Density (kg/m ³)	Specific Heat (J/kgK)	Conductivity (W/mK)	Calculated Heat Capacity (s/m ²)
Butyl rubber	900	1966	0.088	20.1
Isoprene rubber	1000	1550	0.14	11.1
Chloroprene Rubber (CR, Neoprene)	1500	1120	0.19	8.8
The tested Butyl Rubber	1350	1470	0.24	8.3
Silicone rubber sheet [MI]	1100	1050	0.2	5.8

Figure 5-7 The heat capacity of the procured Butyl rubber compared to the base information.

5.3.1 The base configurations

In the beginning, the rubber material investigation was aimed to include multiple numbers of the settings. The reason behind this is not only to explore its efficiency ranges but also to compare the experimental results with the simulation and literature findings. The holistic investigation plan is represented in Figure 5-8. In the full inaugural scenario, the configurations of [MI] and [IM] are proposed to be the reference cases and then to develop the number of permutations that disperse the layers but maintain their “mother” boundary conditions. In this regard, deciding the number of rubber and insulation layers was an important issue, and it was proposed to be 12 layers. By having 12 layers, it is possible to have four descendant scenarios that have an equal (homogeneous) distribution of the insulation and rubber across the wall. For example, if the base configuration is [MI], then, this base configuration wraps all the eight insulation layer segments at the inner side while the eight rubber segments will perform the external face. The next setup will be having four insulation layers on the inner face, followed by four rubber segments, then followed by another four insulation segments and ending up with the last set of 4 rubber segments. The same pattern is repeated for the groups of 2 and one segment, resulting in four setups as shown in Figure 5-8.

However, as stated earlier, due to experimenting device availability issue, only three of these configurations was to be selected. That is, the device was only available for less than one month, and since each setup requires 4~5 days to investigate – as will be seen later- this means that in total four configurations can be tested in total. Therefore, in the end, and as to leave a margin of one experiment failure, three layer configuration has to be selected out of the initially-proposed eight scenarios. To choose these three configurations, a step back decision was needed. That is, what are the most important and significant configuration that can be tested. Moreover, in this regard, the settings [MI] and [IM] was initially chosen. The reason behind this is the findings of Chapter 3 and the literature survey – introduced in Chapter 1.

In Chapter three it was confirmed that the least number of layers usually produces the least dynamic resistance (reflected as high-anti insulation mitigation capabilities). Besides, in the literature, and although there is no rigorous outline of which configuration is best for decrement factor or time lag, some articles have derived at the configuration [MI] entail the least time lag (Asan 1998), (Al-Sanea & Zedan 2001) and (Asan 2000). Lastly, For the remaining (third) configuration, it was decided to go for the maximum number of layer segmentations (layers grouping) i.e. each sheet of rubber is sandwiched between two single sheets of insulation. This decision was made as to explore the variation between the minimum number of segments i.e. two groups of layers as in [IM] and the maximum number of layer's groups e.g. [IM x 8]. The last decision to report is that having seven layers of insulation instead of eight while maintaining the rubber layers at eight layers in all the three configurations. That is to investigate the dispersed configuration as if it was derived from the [MIM] configuration instead [IM] and [MI], and by this mean, it is to test the dispersed settings in a neutral position (half way) between the [IM] nad [MI] configurations. Figure 5-9 shows the three configurations that have been selected for the investigation. Noting that one layer of insulation was taken out as to have the disperse configuration with external rubber layers i.e. [MIM x 8].

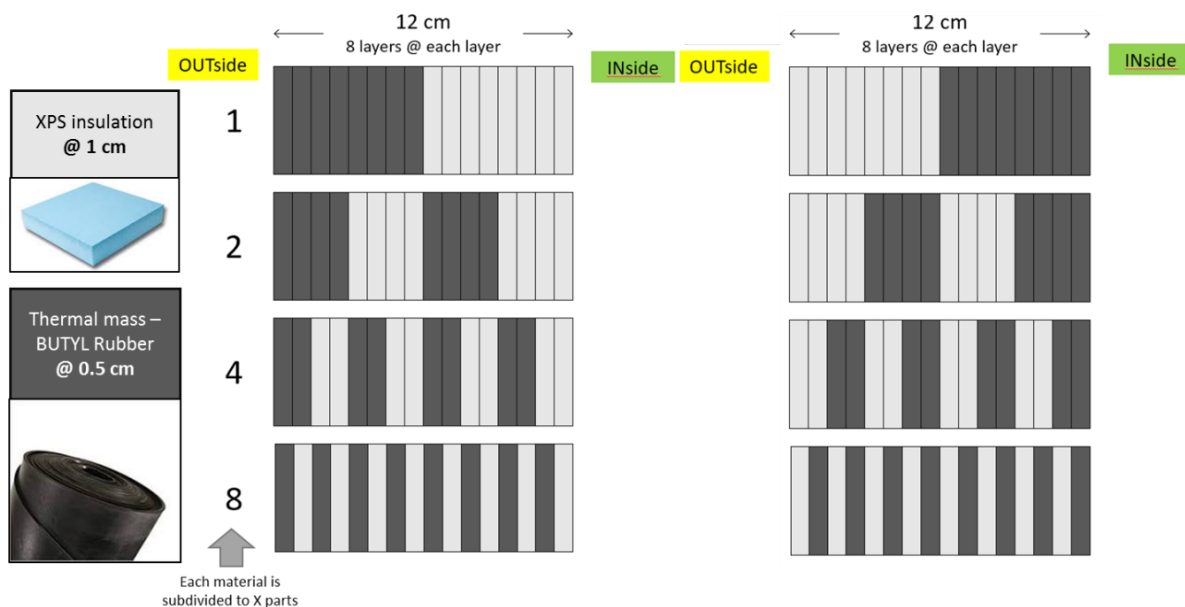


Figure 5-8 Two first sets were proposed for the experiment, where configuration either have an internal mass (rubber) or external mass.

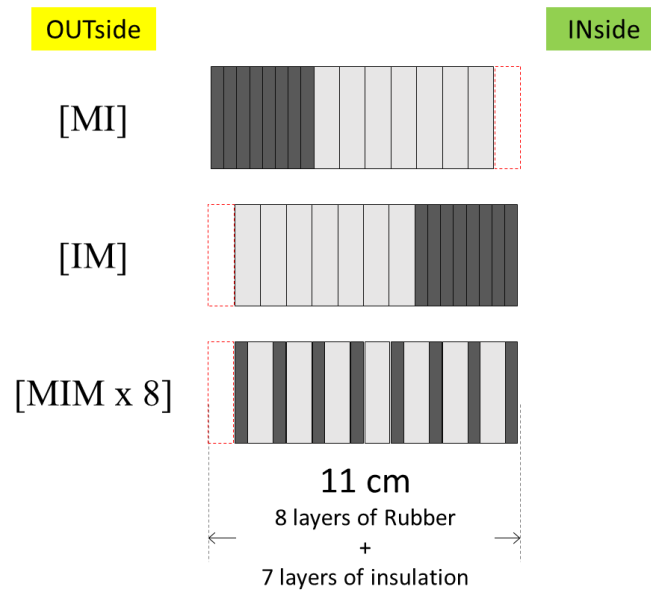


Figure 5-9 the experimented configurations.

Note: one insulation layer is excluded as to provide a neutrally dispersed-configuration i.e. [MIM x8] that is halfway between [IM] and [MI] arrangements.

5.3.2 The Peltier device, and the Rig setup

The experimental device used in this study is based on simple principles of controlling the heat flux subjected to the specimen internal and external sides, as to maintain a specified temperature, whereas the heat flux is measured and recorded during the process. The heat flux is generated by thermoelectric Peltier plates which use electricity to act as a heat pump and conveys the heat from one side of the plate to the other. Hence based on this Peltier effect, the device is commonly known as a “Peltier Device” and is shown in Figure 5-10. Similar devices that work in the same principle are commonly found in the material measurements industry. e.g. the same Peltier Device is used by Japan Testing Center for Construction Materials (JTCCM). However, the Peltier device employed in this study is developed in Mae Laboratory – the department of architecture, University of Tokyo, and it was calibrated and validated by the JTCCM. In Mae Laboratory it is used for testing the Phase Change Materials (PCM) materials. Whereas the heat flux and temperature changes are used to calculate the enthalpy and specific heat changes over time and in accordance to the external heat flux manipulations.



Figure 5-10 The Peltier device controlling dashboard and experimental units.

Courtesy: Tatebayashi, Keisuke, Mae Laboratory – Dept. of Architecture, UoT.

In this experiment, the targeted parameters are the time lag and decrement factor. In this regard, it is essential to state that the herein device can not be used to evaluate the natural temperature change at the inner side, which would be a perfect condition to test the natural temperature fluctuation regarding the external heat flux. Then, the time lag could be obtained by monitoring the change of the internal face temperature in regards to the external changes. Rather, using this device, the time lag could be achieved by monitoring the internal heat flux wave and reference it with the external heat flux sinusoidal curve. That is, it is to monitor the time of the peak internal heat flux that is generated by the device to maintain the inner surface temperature, which in turn is replicating that internal temperature peaks. Likewise, the decrement factor can be obtained by calculating the ratio of the internal heat flux range over the external heat flux ranges, rather than temperature fluctuation ranges. The thermal heat flux metre is shown in Figure 5-11. However, the Temperature of the inner layers is also monitored over the time, where it is recorded to show the heat wave amplitude pattern over the different layer setups. Such monitoring is aimed to visualise the influence of the insulation and the thermal mass (rubber) materials on the heat wave behaviour.

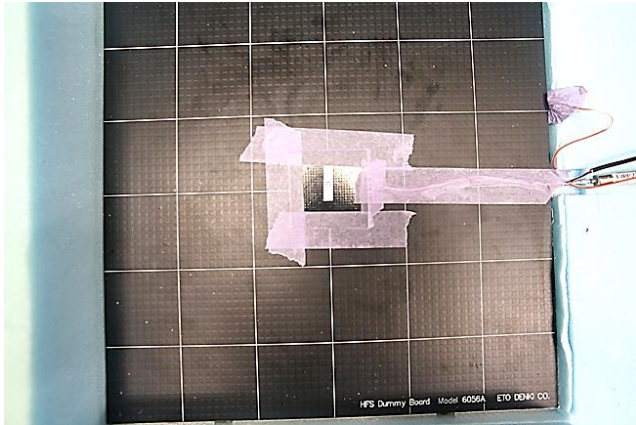


Figure 5-11 The heat flux meters are attached to the internal and external faces of the wall specimen.

Lastly, it is to elaborate the descriptive information about the experimental setup. Here, it is to mention that the Butyl rubber and the insulation sheets are initially prepared in a 30cm by 30cm tiles. These tiles are then arranged according to the investigated configuration and positioned between the Peltier plates; where they are surrounded by an Extruded Polystyrene and a mineral wool insulations as can be seen in Figure 5-12. For the experiment, the employed insulation is an XPS (Extruded Polystyrene) of a one centimetre thick and have a K-value of about 0.028 (W/mK). The XPS heat capacity value was not provided by the seller. However, it is not expected to contribute to the heat storage of the examined specimen since it has a very low density and it is just 25 kg per meter cube. The data logger is a HIOKI LR 8401 that can register a time interval up to one second. The experimental setup of the configuration [IM], the controlling dashboard, the data logger and the measurement probes are all can be seen in Figure 5-13.

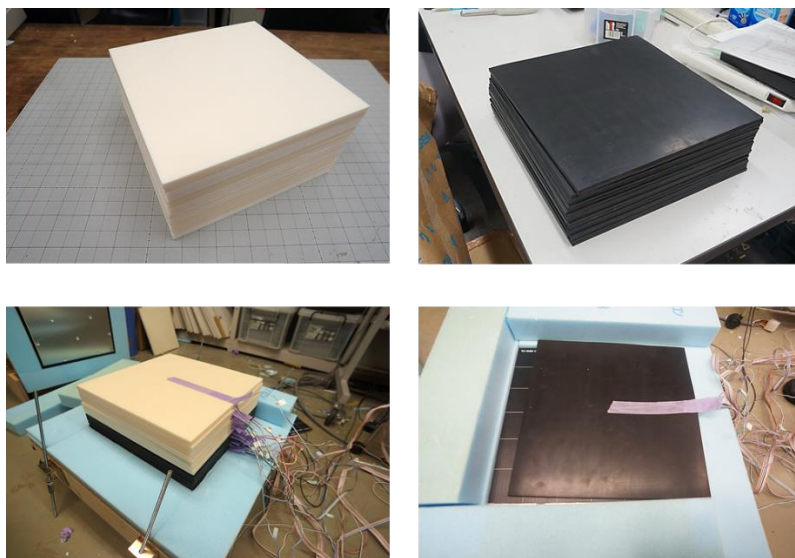


Figure 5-12 The Butyl rubber and the Extruded Polystyrene (XPS) preparation and positioning of the Peltier device.

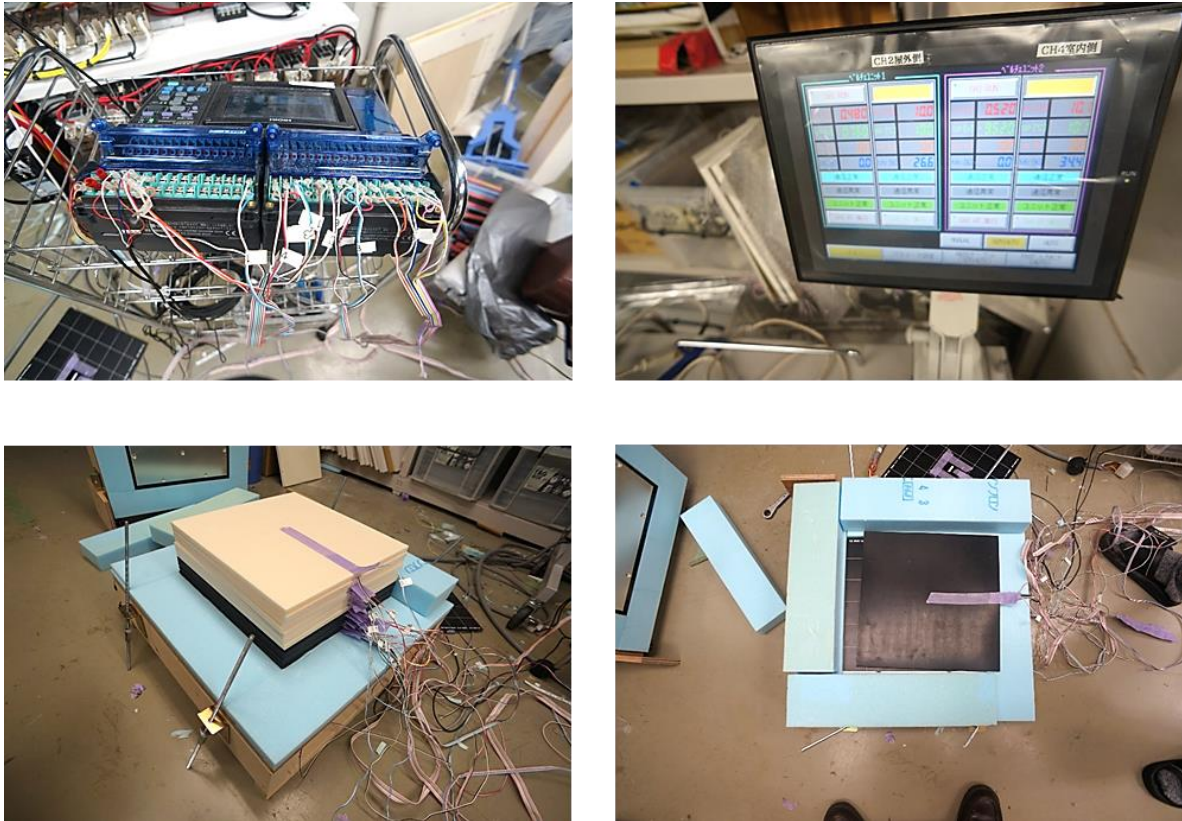


Figure 5-13 Various experimental device components

Top Right: the device dashboard. Top Left: the data logger. Bottom right: the temperature thermocouple meter attached to an intermediate rubber material. Bottom left: The group of the insulation materials in the configuration [IM].

5.3.3 Thermal conditions setup

Based on the device controlling parameters and based on the purpose of the experiment, it was concluded that the temperature profile should be maintained constant at the internal temperature while fluctuating on the other side (outer side). It should be set like this because the core purposes of the experiment are to test the Time Lag competence of the three configurations, in the first place, and then, to estimate the Decrement Factor and other dynamic performance evaluation measures. The constant inside temperature then resembles an air-conditioned space with a fixed thermostat value. On the other hand, the external temperature is set to follow a sinusoidal pattern of a 24 hours cycle. This sinusoidal can be thought of as the ambient temperature fluctuation rather than the sol-air temperature since the Sol-air usually has sharp peaks at the midday -depending on the wall orientation and shadings- and a smooth sinusoidal curve can not resemble it (refer to chapter 1 for the Sol-air temperature profiles).

The sinusoidal equation, given below, is a basic Sin curve equation and is typically found in many types of research e.g. (Al-Sanea & ZEDAN 2001). Another example is equation No four provided

by (Asan & Sancaktar 1998) P. 161 is a mathematical equation that is used for the same purposes, despite that authors used it to mimic the Sol-air temperature.

$$T_{out}(t) = A \cdot \sin(\omega t - \phi) + T_{Omean}$$

Where;

T_{Omax} = The Maximum outdoor temperature

T_{Omin} = The Minimum outdoor temperature

T_{Omean} = is the mean outdoor temperature which equals $T_{Omax} - T_{Omin}$

A = is the temperature amplitude; which equals $(T_{Omax} - T_{Omin})/2$

ϕ = the phase; where midnight is assumed to be the lowest Temperature

ω = is the Frequency which equals a one day cycle

The induced temperature (T_{out}) is assumed to range from (10 ~ 40°C), while the internal temperature is fixed at 10°C . and it can be noticed that the minimum external equals the internal temperature. The temperature variation between both wall sides is set in this way as to be a challenging condition that could pronounce variation of the dynamic capabilities of the different configurations. That is to examine the heat storage capacity of the walls and how they would maintain the minimum temperature that occurs on the external temperature.

Consequently, for the outer temperature equation, the amplitude (average outdoor) temperature well then equals 25°C, and the amplitude will, in turn, equals 15°C. Here it is to mention that, due to device input limitation, which is up to 80 cells, the temperature signal is sent every 20 minute. As a result, for every day there will be 72 temperature updating signals. Besides, it is also assumed that the peak temperature occurs at the midday ($\pi/2$). The resultant curve and the last sinusoidal equation parameters are shown in Figure 5-14 below.

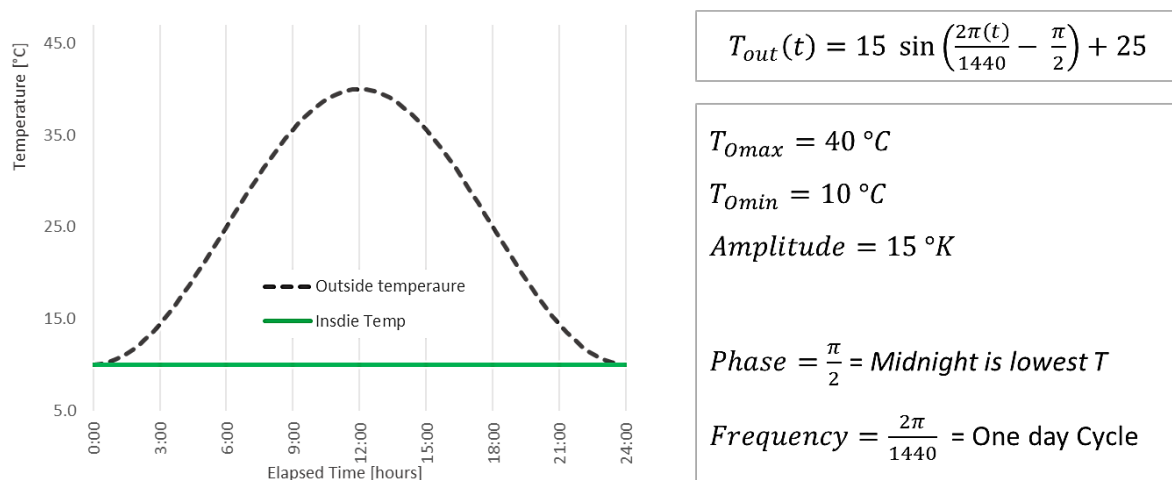


Figure 5-14 The Experimental conditions, where the internal temperature is fixed, and the Sinusoidal Curve resembles the external temperature.

After the whole setup is done, the experiment starts by running the device to meet a specified one temperature that resembles both, the internal and external temperature. This first temperature is either the average value of the outer temperature fluctuation range, or it can also be set to equal the internal (resembling the thermostat) temperature. In this experiment, the initial temperature equalled the internal temperature i.e. 10°C. The device is kept operating at this setup until this initial temperature is found in all the inner faces of the wall, here, the importance of the thermocouple sensors appears well. Subsequently, after all, the layer reaches the 10°C, the external Peltier plate is operated in the sinusoidal mode and is kept to run in a continuous cycle for about four days as to assure that the heat fluctuation is steadily repeating every 24 hours.

5.4 Results and discussion

Before delving into the results and discussion, it is to mention that the heat direction inside the Peltier device can be changed. That is, for a given setup of a right-hand insulation and left-hand rubber materials, the heat can be set to flow from the right plate to left one. Hence the configuration can be perceived as [IM], on the other hand, if the heat is set to flow from the plate left to right plate, then the configuration can be viewed as [MI]. As a result, the investigated configurations with the same group of the layer but with different boundary conditions can experiment without rearranging the layers on the device. Subsequently, the investigated configurations can be well depicted as in Figure 5-15 based on the fixed and fluctuated temperature settings, rather than the wall specific orientation.

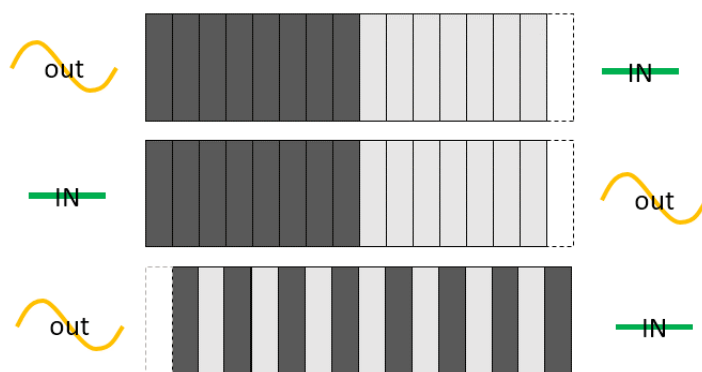


Figure 5-15 In the Peltier device the configuration can be altered by changing the heat flux direction instead of rearranging the layers.

After running each configuration for about three and half days, where the sinusoidal curve is at least repeated for the three time, the results of a 10 seconds interval are collected and ran through a series of processes. The important process is to convert the flow meters recorded Volt values into a (W/M²) values. However, the temperature values are directly obtained and plotted to give an initial idea about the temperature distribution profile “print” of each configuration. In addition, the temperature profile is also used to monitor the and assure that the device is maintaining the desired internal and external temperatures. Not to forget, it is also important to ensure that sinusoidal curve is smooth enough since the temperature is updated every 20 minutes. Altogether, the temperature profiles of the three configurations I spotted in Figure 5-16. From this figure, the effect of the mass can be recognised in the first and third configuration, i.e. [MI] and [MIM x 8] where it can be seen that there is a slight shift of the temperature wave -a horizontal change in the time axis. While the effect

of the insulation is found on the high temperatures difference between the insulation layers and can be well seen in all the configurations as a vertical gap – temperature differences. This temperature gap well resembles the Decrement Factor properties across the settings. In addition, it can be noticed that The third configuration i.e. [MIM x 8] have a combined effect of both the insulation in reducing providing the vertical gap and the rubber in providing the vertical shift, and this synergic effect occurs for each set of insulation and mass layers.

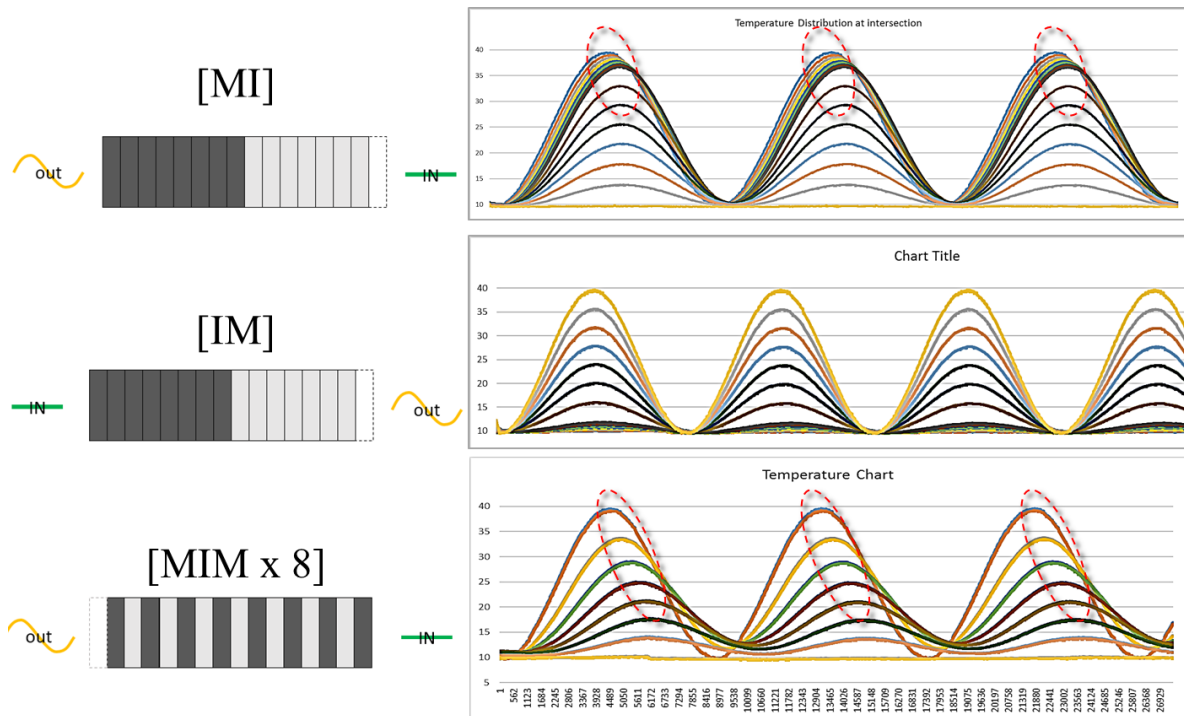


Figure 5-16 The temperature distribution profiles for the various configurations. The effect of the rubber appears a Time Lag which is the slight shift between the peaks. While the insulation prevails in reducing the temperature -vertical gap (Decrement Factor).

Additionally, The heat flux waves variation between the internal and outer faces are developed. The analysis results of the heat flux are the base evaluation measure that used to identify the dynamic thermal performance of the walls. As to plot the heat flux in an understandable and smooth traceable curves, the heat flux 10 seconds interval data are averaged over 20 minutes. After plotting the refined heat flux curve, it is important to realise that for the interior face flux, the less amplitude means much more stable interior and less cooling load will then be required. On the other hand, for the external heat flux curve, the higher amplitude means greater thermal capacity since the device is applying much heat to meet the required temperature. In other words, the higher the external heat flux amplitude, the more resistance the configuration is opposing to the obvious weather changes. Figure 5-17 is sample case of the [MI] that is used to demonstrate this issue, where the green colour represents the heat flux at the internal face, while the orange represents the external heat flux.

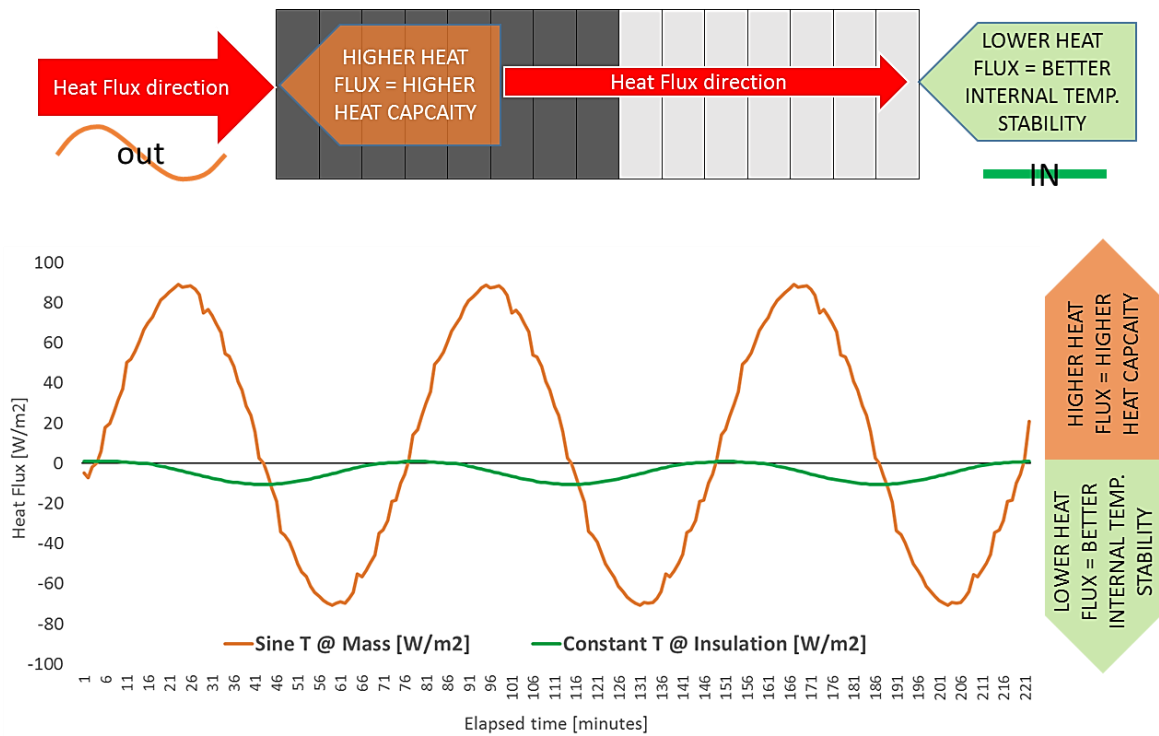


Figure 5-17 The heat flux curves of a sample configuration of [MI].

It is to note that the higher flux at inner face means that configuration has higher heat capacity and is resistive to severe weather conditions. While lower heat flux at inner face means that less heat is getting inside.

Based on this definition, the three configurations are individually potted as can be seen in Figure 5-18. It is apparent that the highest heat storage abilities are found at configuration [MI], since it have the highest external heat flux patterns, followed by the [MIM x 8] configuration, and the worst among this group is the [IM] configuration. On the other hand, the internal heat flux seems to be equal among all the configurations. However, if the internal heat flux is similar to all the configurations does not mean that their performance is the same. Figure 5-19 is made to compare the three configurations inner and outer heat fluxes better on shared graphs. For example the [MI] configuration have stored much heat while [IM] did not, hence if they demand the same internal heat flux (cooling) then, in fact, the configuration [MI] have dissipated back (to the outside) a lot of the stored heat, hence its dynamic thermal performance is much better than the [IM].

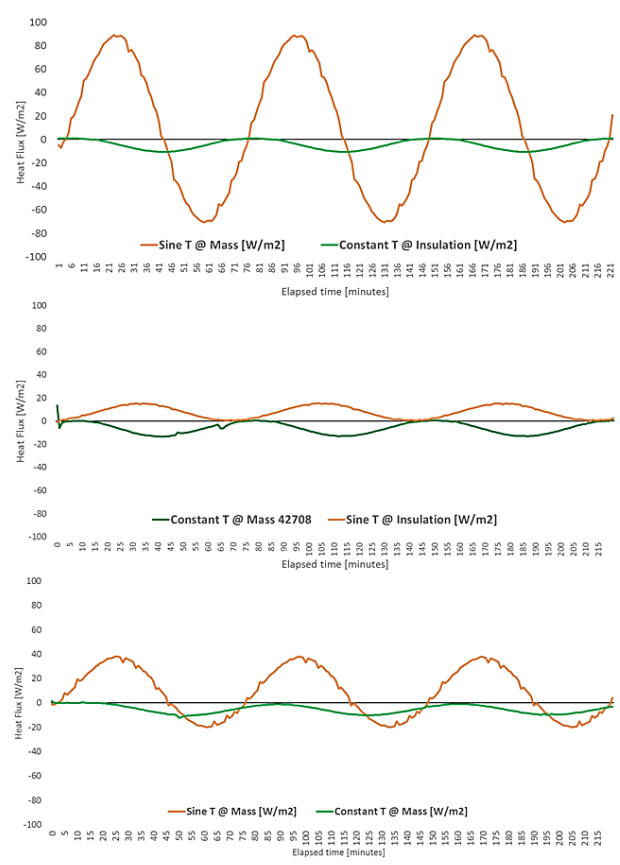
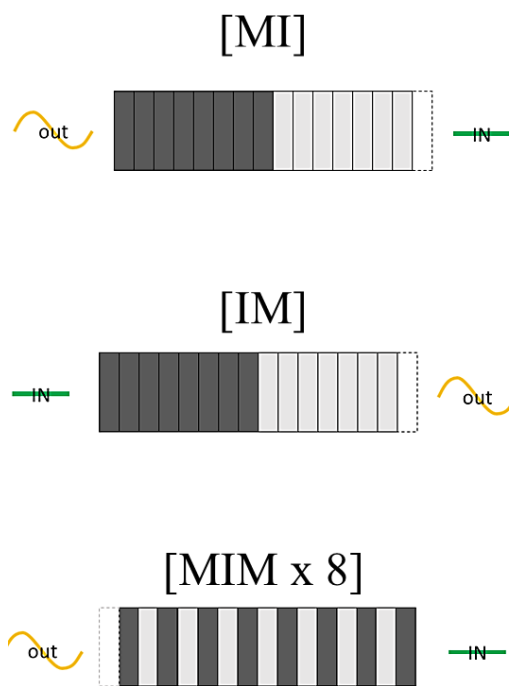


Figure 5-18 The individual internal and external heat flux patterns of the investigated configurations.

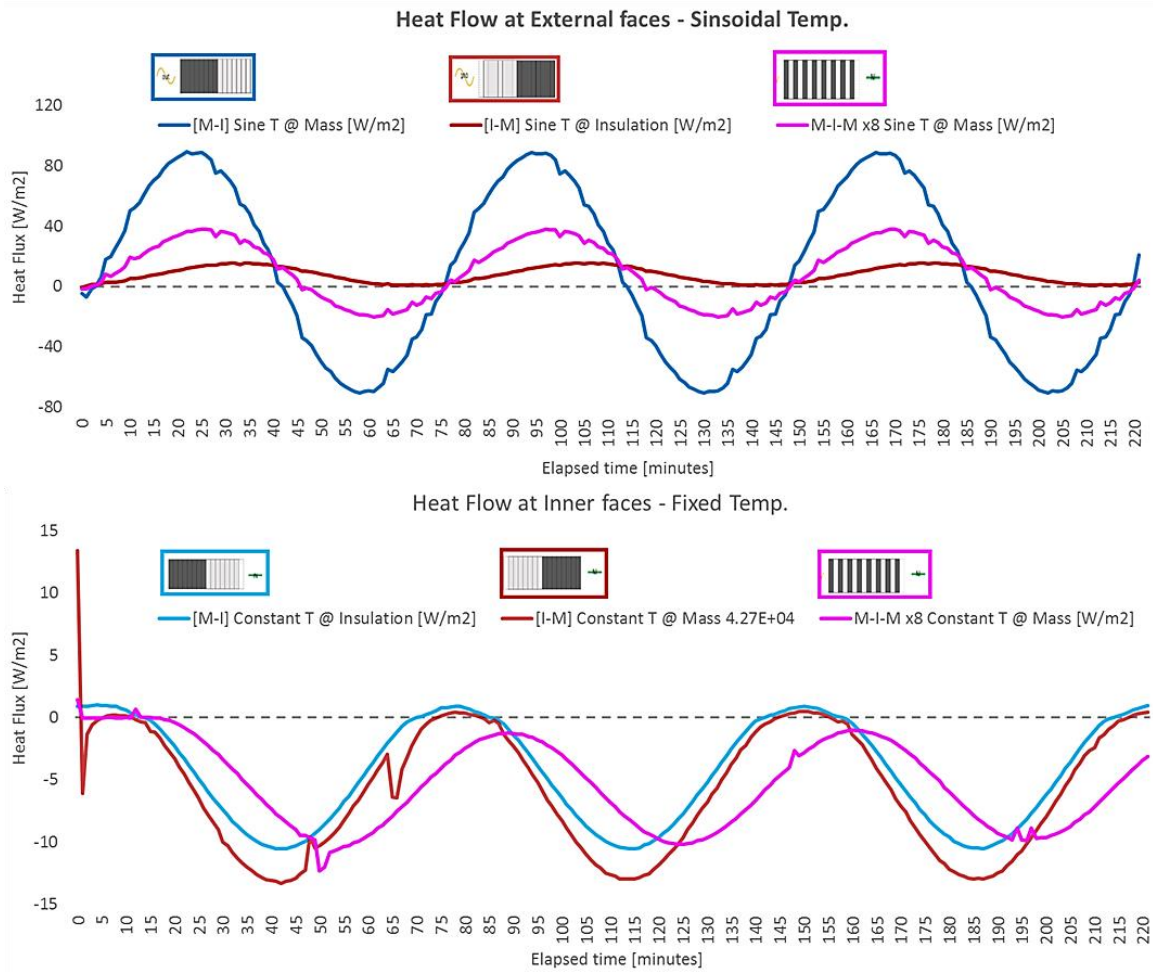


Figure 5-19 The outer and internal heat flux of the various configurations are plotted n the same graph for better referencing and comparison.

To express the relation between the external and internal heat flux magnitudes, the Decrement Factor value is obtained. For each configuration, the decrement factor calculation starts by finding the minimum and maximum heat flux values for the internal and the external surfaces, over a three complete days cycle. Afterwards, the decrement factor ratio is obtained by subdividing the internal heat flux range (i.e. maximum minus minimum) over the external heat flux range. The decrement factor values for the three configurations is displayed in Figure 5-20.

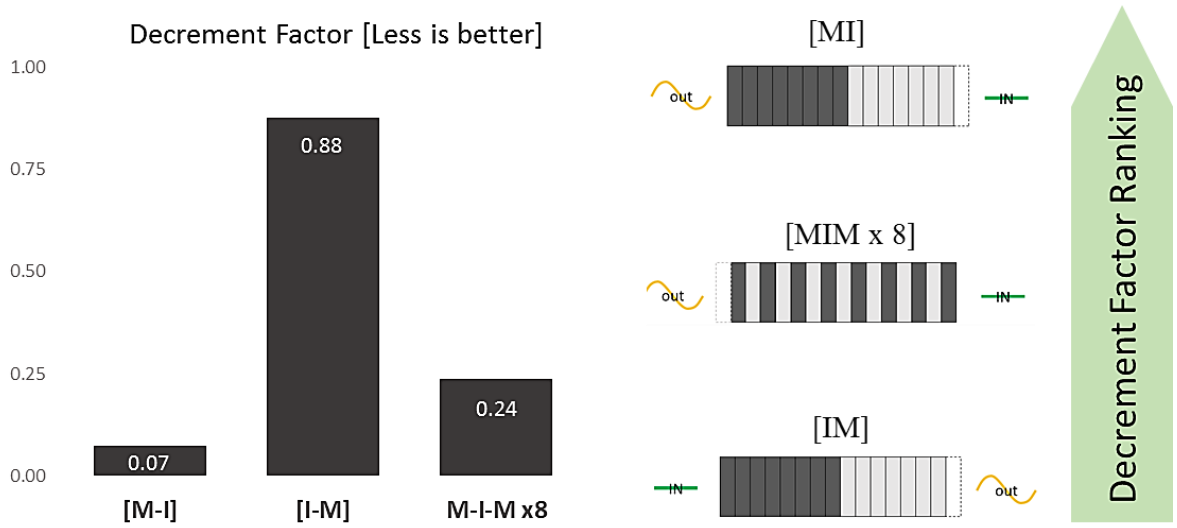


Figure 5-20 The Decrement Factor values and ranking for the various configurations.

Likewise, the Time Lag is also identified for all the three configurations. Inaugural, for illustrate the Time Lag in a graphical presentation, the heat flux profiles of the three configurations are recalled, but with a small modification to the internal heat flux curve. That is, as to visually identify the heat flux peaks (either minimum or maximum) the internal heat flux curve is multiplied by minus one, as to “flip” mirror the curves around the y-axis. The resultant curves are shown in Figure 5-21, and it can be seen that the multi-layered configuration i.e.[MIM x8] yields a clear gap between the peak fluxes. Moreover, it is apparent these fluxes are repeated on the same sequence over the three-day cycle.

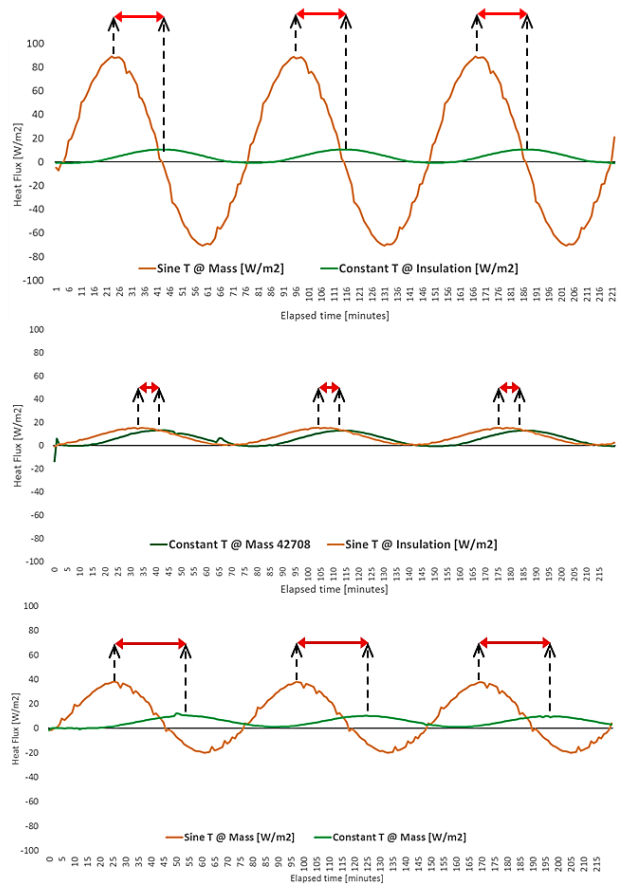
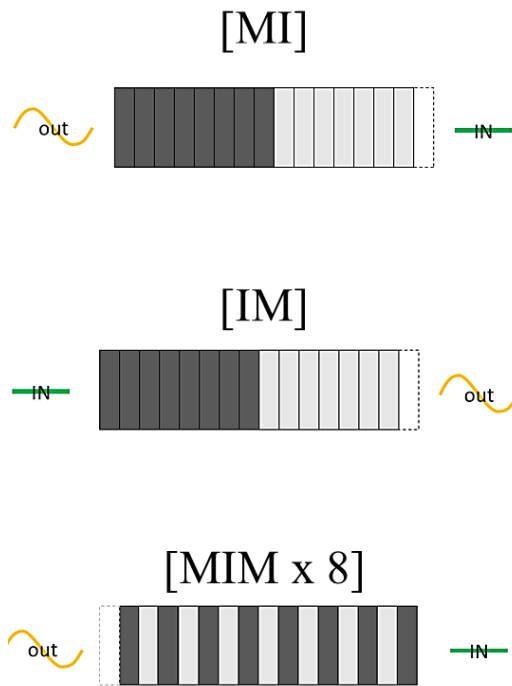


Figure 5-21 The internal heat flux curves are inverted as to better visualise the Time Lag (heat wave peak delay) about the external heat flux curve

In addition to the graphical presentation, the Time lag was also calculated based on its simple definition, i.e. what is the time gap between the peak (Min/Max) external temperature and its next immediate peak (Min/Max) at the internal heat flux curve. The Time Lag ranking of the various configurations is shown in Figure 5-22. Similar to what was observed earlier, it is evident that the maximum Time Lag was obtained by the dispersed (multi-layered configuration), where it is estimated by eight and a half hours. The second longest Time Lag was found for the [MI] configuration while the [IM] configuration has provided a Time Lag of about three hours only.

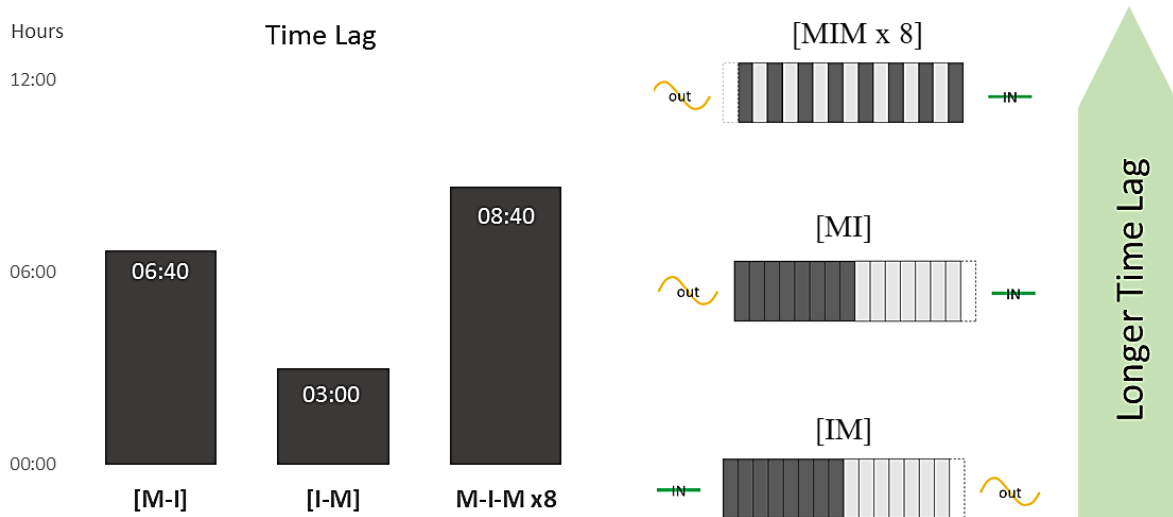


Figure 5-22 The Time Lag values and ranking for the various configurations.

Another factor that can reflect the dynamic thermal performance of the different layer configurations is the effective R-Value. Hence, an attempt was aimed at calculating the dynamic R-Value, using the same basic heat flux equation which is used in the static conditions, where the wall resistance (R-Value) equals the heat flow (Q) over the Temperature difference between the two faces of the wall (ΔT). In the same respect, the effective R-value can also be calculated by converting the direct relation into a second order equation relation and implementing a definite integration of the heat flux and the temperature difference. Such equation is found in literature, where (Al-Sanea & ZEDAN 2001) define the Dynamic R-value in the following formula;

$$R_e = \int_0^{24hr} (T_{f,o} - T_{f,i}) dt / \int_0^{24hr} q_i dt$$

Based on this equation, the Temperature difference and the heat flux can be calculated instantly over the 24 hours without the need for integration. Hence, the total temperature variation (external surface temperature minus the internal surface temperature) and the total heat flux at the inner surface are used to calculate the Dynamic R-Value. On another hand, the nominal (steady state) R-value is obtained from the conductivity and thickness values of the insulation and rubber materials in the very basic way. In the end, the results of the Dynamic R-value are plotted in Figure 5-23 against the nominal R-value. Moreover, it can be seen that all the configurations have shown a better dynamic R-value compared to the nominal one (that is usually prescribed in the building codes and references). However, it is paramount to state this dynamic R-value is plotted for the sake illustrating that the dynamic R-values is varied between the various configuration although they have the sam amount of insulation and rubber materials. Also, the Dynamic R-values are different from the nominal R-value. However, the Dynamic R-value calculation is not a reliable measure when using such experimental setup since the experimental device operates to maintains the temperature within a certain range. Hence, the temperature difference is same in all the configurations while they only vary in their internal heat flux values.

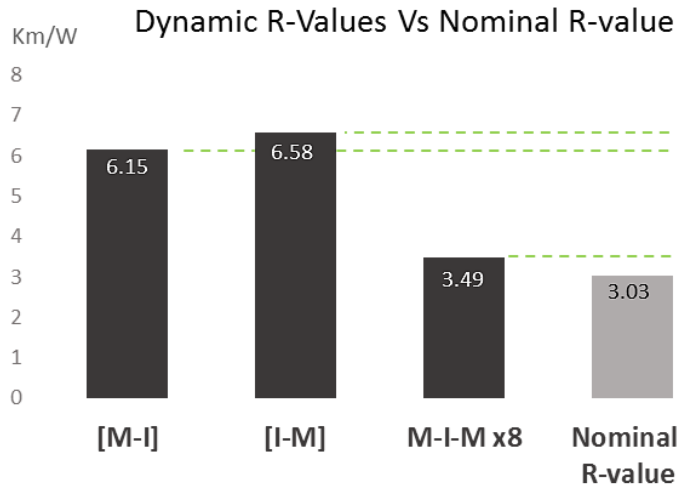
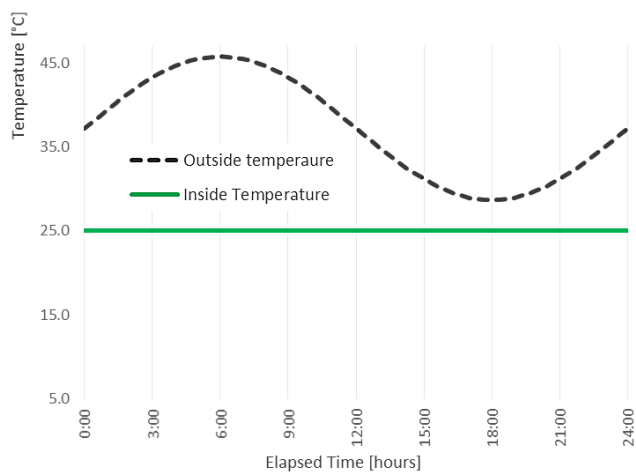


Figure 5-23 The Dynamic R-values of the various configurations compared to their (shared) nominal R-Value.

Besides all, it is important to state that this experiment was conveyed on a sinusoidal (steady periodic) conditions. However, as shown in Chapter 1 the HVAC system operation and load can either be steady periodic or instantaneous. Each of which has its implications on the dynamic behaviour of the investigated configuration. Moreover, for the sake of elaboration, one case the last case was prepared to study the effect of initial transient operation on the resultant curves, where the whole experimental conditions were changed. That is the internal temperature is now raised and fixed at a 25°C. Meanwhile, the outside temperature sinusoidal curve parameters are modified to fit a Maximum temperature of 45.7 °C, and a minimum outdoor temperature of 28 °C. Moreover, it can be noticed that the starting point occurs at midnight while the peak temperature arrives at 6 pm, i.e. after six hours rather than twelve hours compared to the first sinusoidal curve. As can be seen in Figure 5-24. Moreover, it is to state that the configuration used for this first transient sample investigation is kept at the dispersed arrangement but with adding another insulation layer at the internal face, as can be seen in Figure 5-25. Hence the subject configuration would appear as if it is derived from an [MI] rather than the [MIM] configuration.



$$T_{out}(t) = 8.55 \sin\left(\frac{2\pi(t)}{1440} - \pi\right) + 37.2$$

$T_{Omax} = 45.75^{\circ}C$
 $T_{Omin} = 28.65^{\circ}C$
 $Amplitude = 8.55^{\circ}K$

 $Phas = \pi$
 $Frequency = \frac{2\pi}{1440} = \text{One day Cycle}$

Figure 5-24 The Experimental conditions of a proposed initial transient experiment, where the internal temperature is fixed, and Sinusoidal curve resembles the external temperature.

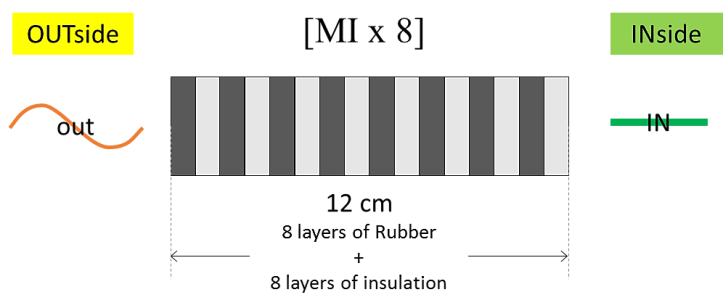


Figure 5-25 The sample case (configuration) that is used for testing the effect of the initial transient operation.

The resultant heat flux curve is shown in Figure 5-26. Moreover, from this number, the initial transient conditions can be distinguished from the steady-periodic conditions. Where the latter appears after the experiment is run for a while and is very typical of what was seen in the earlier results. Meanwhile, the initial transient conditions are the configuration dynamic behaviour that occurs immediately after the initial fixed conditions, i.e. immediately occurred after the experiment starts running. Given these points, it can be seen that dynamic thermal behaviour of the wall configurations under the initial transient conditions is quite different from the steady periodic operation and requires further analysis.

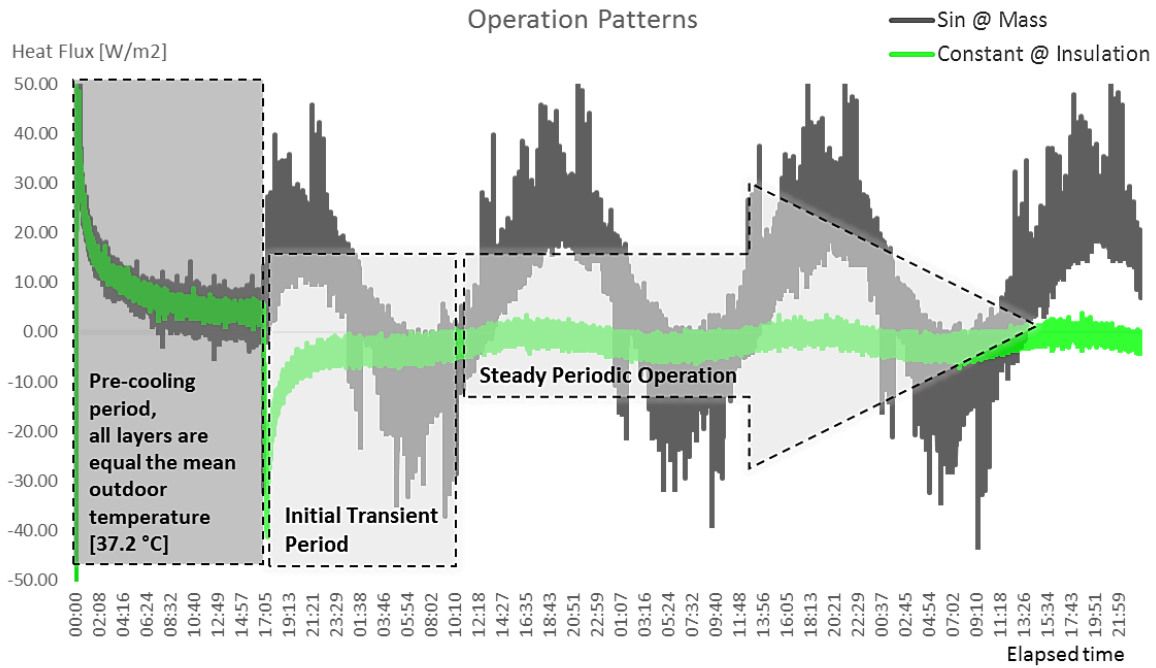


Figure 5-26 The experimental situation of a proposed initial transient experiment, where the internal temperature is fixed, and the Sinusoidal Curve resembles the external temperature.

5.5 Conclusion

In this Chapter, it was hypothesised that the rubber materials could be utilised to compensate for the use of the conventional thermal mass materials in the building envelope. The various wall specimens “configurations” is subjected to a predetermined temperature – either constant or changeable - on its both faces (sides). This temperature is met by a device that imposes the appropriate heat flux via plates attached to the wall external and internal faces. In turn, the employed device relies on what is so called a “Peltier” effect, where change the electrical current works as a heat pump to transfer the heat from either side of the plates to the other. Hence the device is known as a Peltier device. In the end, it is to state that the instrument has efficiently met the desired temperatures, which is fixed at one side and fluctuated following a sinusoidal pattern that closes its cycle every 24 hours with an interval of 20 minutes between each temperature variation.

All things considered, it is said that all the rubber walls have yielded the anticipated dynamic performances, regarding providing a high lag compared to its thickness when compared to results found in literature, namely when compared to the results of work provided by (Ozel 2014). In Ozels’s work the same insulation material (XPS) was integrated into three wall configurations that are 20cm thickness and have a brick as a heat storage medium. In (Ozel 2014) article Table 3., it can be seen that the Time Lag for walls 1 and 2, herein named [IM] and [MI] had time lags of 9.21 and 8.84 hours respectively. In comparison to similar walls in this study, the experimented Time Lag for the same corresponding wall configurations was 3 and 6.4 hours, respectively. Here, it is to remind that the walls overall thickness were just 11 cm which is almost half of Ozel’s experimented walls. Also not to

forget, that the dispersed configuration, have approached 9 hours of Time Lag, which is a very close value for the results shown by (Ozel 2014). In other words, it can be well said that incorporating the rubber sheets as a heat storage mediums in the wall structure can provide the same effect of using the brick but with a privilege of saving the space and cutting the wall thickness to the half. Moreover, as per what was hypothesised and provided by (Bond et al. 2013), the rubber layers dispersion over the wall would even lead to a much better Time Lag performances.

On another aspect, and concerning the Decrement Factor, it is to say that the layer configurations had a very profound effect on the Decrement Factor performances. As when the external insulation arrangement [IM] lead to relatively small decrement ratio i.e. 0.07, the different settings i.e. [MI] that have an internal insulation instead had a decrement factor of 0.88. In this regards, and when comparing this result with the same research reviewed above i.e. Ozel's results, the Decrement ratios are very high, especially when recognizing the at the same insulation material (with very similar properties) and almost the same thickness i.e. 8cm and 7cm have been utilized in Ozel work and the study herewith, respectively. However, this bug variation in the decrement factor values might be ascribed to the change in decrement factor calculation method. As in Ozel's study, the decrement factor is obtained from the natural temperature fluctuation, while in this study, the same value is achieved by calculating the ratio between the internal and external heat fluxes instead. It can also be argued that this variation might be caused by the nonlinear relation between the wall thickness and the decrement factor reduction. Meaning that, if the experimented walls are increased from 11cm to 20cm they might have shown much smaller decrement factors. To settle this issue, another set of wall configurations at a wall that is 20 thick and with an 8cm insulation needs to be investigated for the sake of better calibration with the study carried by (Ozel 2014).

Form the Decrement Factor and the Time Lag rankings, shown in Figure 5-20 and Figure 5-22, respectively; it is to highlight that the configuration [IM] does not provide any advantages over the [MI] or over the [MIM x8]. This inferior performance of the [IM] configuration might not differ if it is investigated under an initial transient operation. As per literature, namely the article of (Al-Sanea & ZEDAN 2001), one can support that having an internal mass would not help in reducing the instantaneous load unless the initial conditions are similar to the internal thermostat settings. That is, if the mass material (rubber) is placed inside and is cooled to 25°C, per say, and the internal conditions are to be maintained at the same 25°C- but not much less- then the mass will not require much instantaneous cooling load.

Chapter 6:

6. Reflective paints study

The contents of this chapter are concerned with the external surface properties of the building envelope, whereas all the previous chapters were oriented to investigate the envelope core configurations. Therefore, the main parameters studied herewith are not dealing with the dynamic thermal behaviour measures e.g. the Decrement Factor and the Time Lag. Rather, the temperature variation behaviour over the ambient conditions is the main evaluation criteria of this chapter. In brief, two solar paint experiments were conducted to test four key parameters. That is, in the first experiment, evaluating the performance of the solar paint compared to the conventional paint was the base target. In addition, the influence of the base sealer on the performance of the solar paint itself was studied as a second parameter. The solar paint colour was investigated as a third parameter. On the other hand, the Second experiment added a fourth parameter to the evaluation i.e. is the influence of the glossiness of the paint on its temperature reduction performance over the various weather conditions. The results of both studies are presented and discussed wehars a collective conclusion was finally presented regarding the use of the solar paint as a heat protection measure.

6.1 Introduction

After exploring and testing the un-exploited potentials of the core components of the building envelope, the experiments conveyed in this chapter are concerned with the external properties of the envelope, i.e. the skin “facial” properties. Initially, the objective of studying the skin was aimed at utilizing the building skin to serve as a cooling device, which is mainly achieved through nocturnal radiative properties of the walls. However, since the measurements for such kind experiments are very expensive and falls beyond the financial status, the skin properties have been conceived in a different way. That is, the building skin study is oriented to examine the protection capabilities of typical – commercial- solar paint products.

Both qualities, i.e. utilising the skin as a protection measure or as a cooling medium are a major part of the passive cooling overall strategies. In Figure 6-1, both strategies, i.e. skin as a protection measure and as a cooling measure are highlighted and traced back to their upper-class definitions. It is to highlight that the experimental investigation was carried in tow stages, where the first stage can be conceived as an exploration of the solar paint general protection capabilities. The second experiment has reduced the forces on two basic paint properties to investigate, i.e. the colour and the glossiness of paint, which are introduced in the second part of the chapter herein. Not to forget, that in the literature survey, which thoroughly covered in section 3-, it was highlighted that the study of the external skin properties could be decoupled from the envelope-core studies, although they have an interactive influence across each other in the overall determination of thee buiding envelope characteristics.

6.2 First experiment (inspection)

The First Solar paint experiment was carried out in August 2014; The experiment was intended to test the application of the so-called reflective paint or a Solar Paint, on flat roof tiles. It aimed to identify mitigation capabilities of solar paint to prevent the sunlight penetrating through the roof, and thereby, to recommend its application feasibility to the OM Solar project – at Okinawa. The key thing is, the findings of the first experiment was a base to develop the second experiment that avoided many of the error sources, as well as investigating other parameters under certain climatic conditions. However, the first experiment setup, data analysis and results are presented as the following.

6.2.1 Experimental setup and methodology

There were three main targets behind the first solar paint experiment. The first objective is to gauge the solar radiation reduction by using different Solar Paint types and comparing it with normal (commercial) paint, and bare roof tiles. Secondly, it is to identify the influence of using the supplied white paint base “sealer” on the performance of the solar paints. Finally, is to explore the influence of the colour tone on the solar paint performance, especially when thinking about dark solar paints. This experimental research is described as in the following points.



Figure 6-1 The importance of the external Skin – and its effect on the envelope performance.

Base Source: (N. B. Geetha 2012)

For the data collection and measurement, a tool named HIOKI 8422-50 is used to collect and store the measured data, whereas thermocouple wire of Type-K are used to measure the surface temperature of the specimens. Ten ventilated roof blocks of a 37cm by 37cm and about 5cm thick was used as the testing medium. These tiles are placed on the building roof in two rows as can be seen in Figure 6-2. The roof tiles are relocated in the roof in way to minimize the shading effect of the adjacent buildings as can ve seen in Figure 6-3. Inaugural, there was a sided tested that aimed to calibrate and check if all the selected device sensors are reliable and have the same readings. Moreover, this inaugural test have also checked if the adhesive tapes (tapes that are used to place the probs on its place on the top of the tiles) have an influence on the device readings.

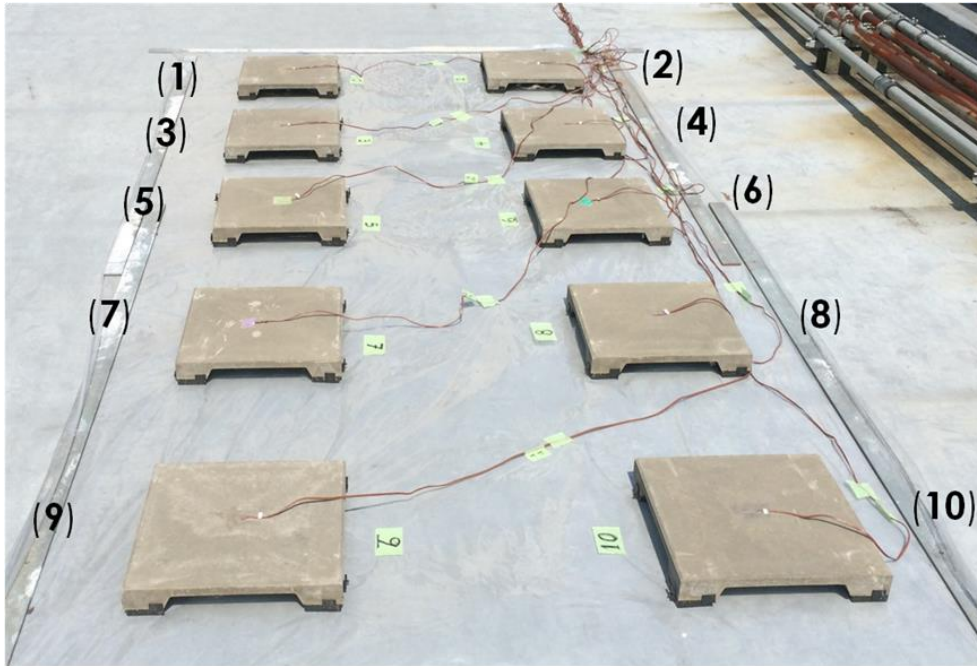


Figure 6-2 The bare concrete tiles are used to investigate the measurement tool (Hioki 8422-50) reliability and error margin.



Figure 6-3 The roof tiles are located in a way to minimise the shading effect of the surrounding context.

In order to estimate the shading effect throughout the day, the four tiles located at the far corners are kept plain (unpainted) as can be seen in Figure 6-4. As by comparing the temperature variation of these tiles, one can deduce if some parts are getting shaded at specified time of the day. For example, when the two or one tile located at the eastern side of the experimental rig are having a lower temperature when compared to their counterparts tiles on the western side, these means that the early morning sun has stricken part of the tiles while the others are still shaded by the eastern buildings.

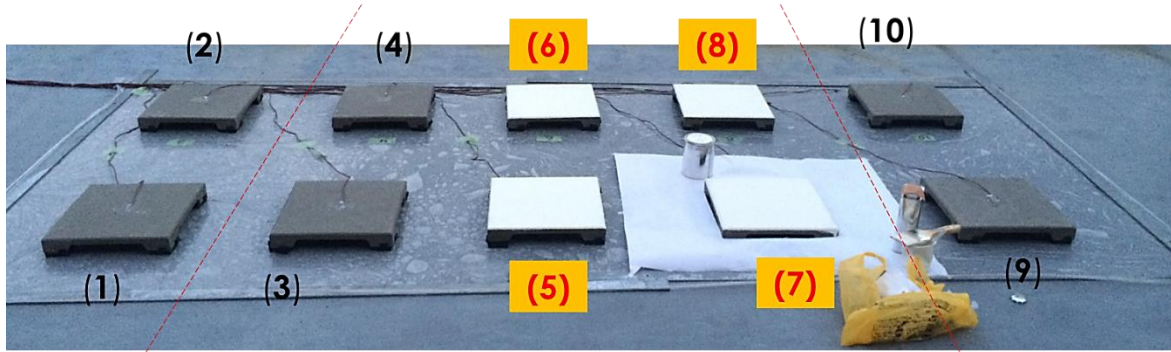


Figure 6-4 The cornered tiles (1, 2, 9,10) are kept plain to monitor the shading effect. Meanwhile, the sealer base is applied over four tiles of the six tiles that will be painted.

Subsequently, as can also be seen in Figure 6-4, the second stage was to apply the sealer (paint base) on four tiles numbered (5,6,7 and 8). The influence of the sealer itself is studied by implementing it to some tiles while applying paint directly to others. This investigation is decided during the sealer application to the first tile. And the reason behind this decision, i.e. to investigate the sealer effect on the solar paint performance, is that after taken Infrared photos, as in Figure 6-5, it was realised that the application of the sealer (as being opaque and white) have an immediate effect on the tiles surface temperature as can be seen in Figure. Hence, it was of interest to investigate if the solar paint sealer is contributing to the paint's performance.

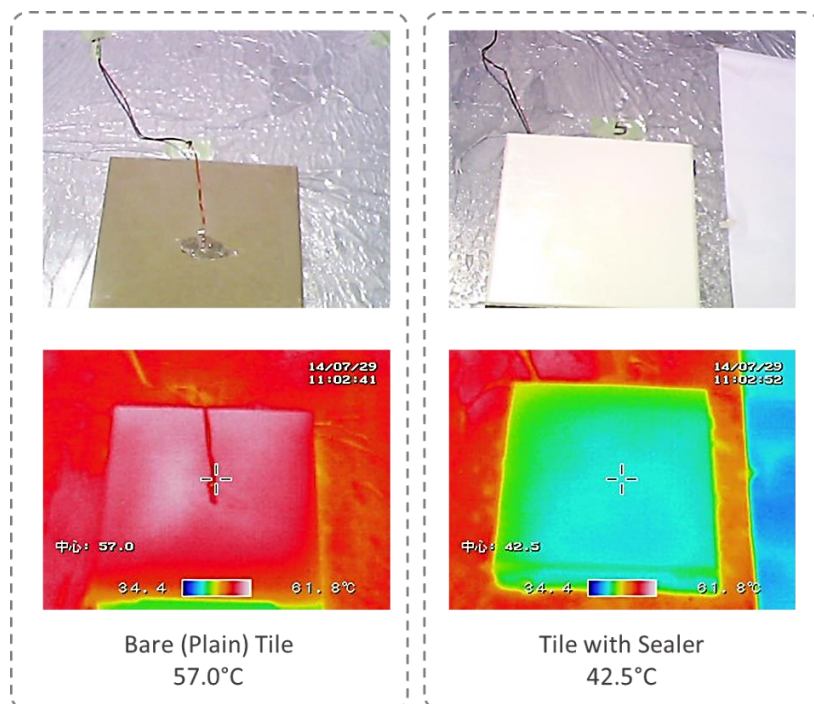


Figure 6-5 The application of the paint base "Sealer" have an immediate influence on the surface temperature, where the difference between the plain tile and the tile with a sealer is about 15°K.

After applying the sealer bases, four oil based paints are applied on top of these tiles i.e. (5,6,7 and 8), whereas three of these were Solar Paints while the other is conventional paint. The solar paints used are the black, grey, and white colour of the same paint manufacturer. The conventional paint is chosen to be a grey colour. For the remaining two tiles, i.e. (3, and 4) solar black and solar white paints are applied directly to these two tiles with and without sealer. As shown in Figure 6-6, a matrix of six cases is then obtained. Where it can be noticed, that the regular grey paint is used as a reference base to compare the paints thermal performance. Meanwhile, the four plain tiles can also be used as reference cases as well as assessing the performance of the paint application in general on reducing the temperature of the tiles. Besides, it is to mention that the tiles temperature are measured on both sides, top and bottom, and as can be noticed in Figure 6-6, each tile has two numbers, where the first number indicates the top surface temperature probe number and the second indicates the soffit (bottom) probe number. This step is taken to calculate the temperature difference between the tile surface and soffit, and thus having an idea about the convention effects on the heat removal from the tiles surface.

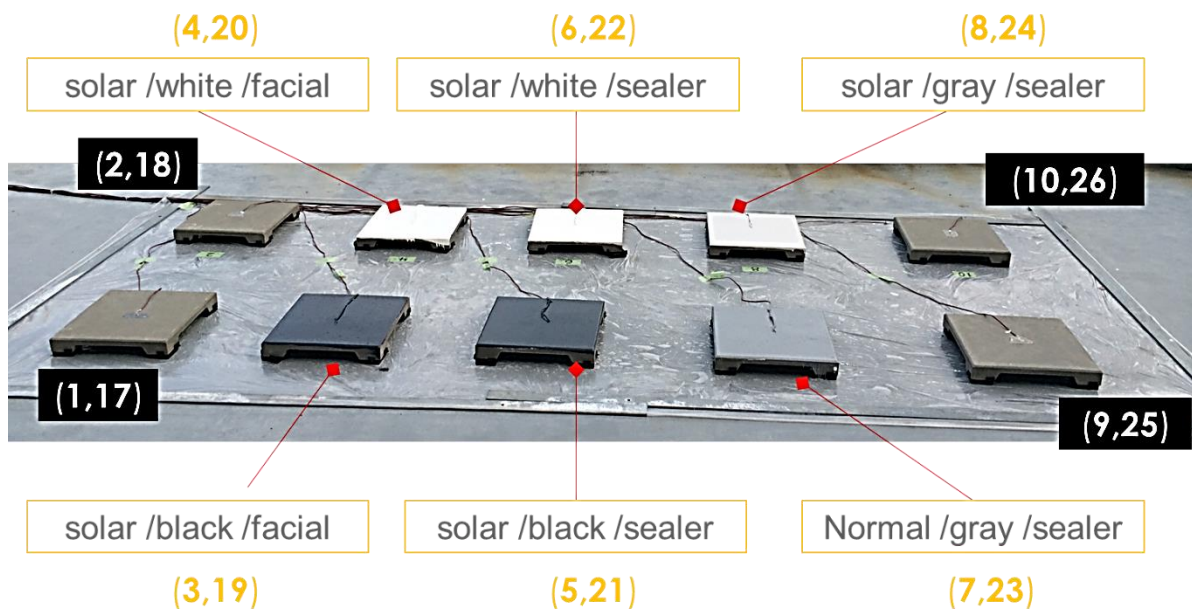


Figure 6-6 The six cases (permutations) are a named basis on the three parameters being investigated. The first parameter is the paint type either Normal paint or Solar paint. The second parameter is the paint colour (White, Grey and Black). The third parameter is either the paint is directly applied to the tile or applied on top of a sealer base.

6.2.2 Results and Discussion

As a start, and before collecting the data from the data logger, Infrared thermal Photos are taken to have an inaugural idea about the paints thermal performance. Figure 6-7 shows that all the painted tiles, including the regular grey tile and the black/grey solar tiles, are cooler than the base reference, i.e. the bare (plain) concrete tile. Also, the following points were also noted;

- The best Temperature reduction is achieved when using White Solar on Sealer $\Delta T = 11.4^\circ\text{K}$.
- The worst result among the painted tiles is when using Black Solar without a sealer base.
- Paints on sealer showed better temperature reduction. That is, when comparing the White solar paint with the ad without the base sealer, the one with the sealer is cooler by 0.9°K than the solar paint that is directly applied to the tile without the sealer base. Similarly, for the Balck solar tiles, the one that has a sealer base is colder by 1.6°K .
- The Black Solar paint on sealer performed better than normal grey paint that is also applied on top of a sealer base.

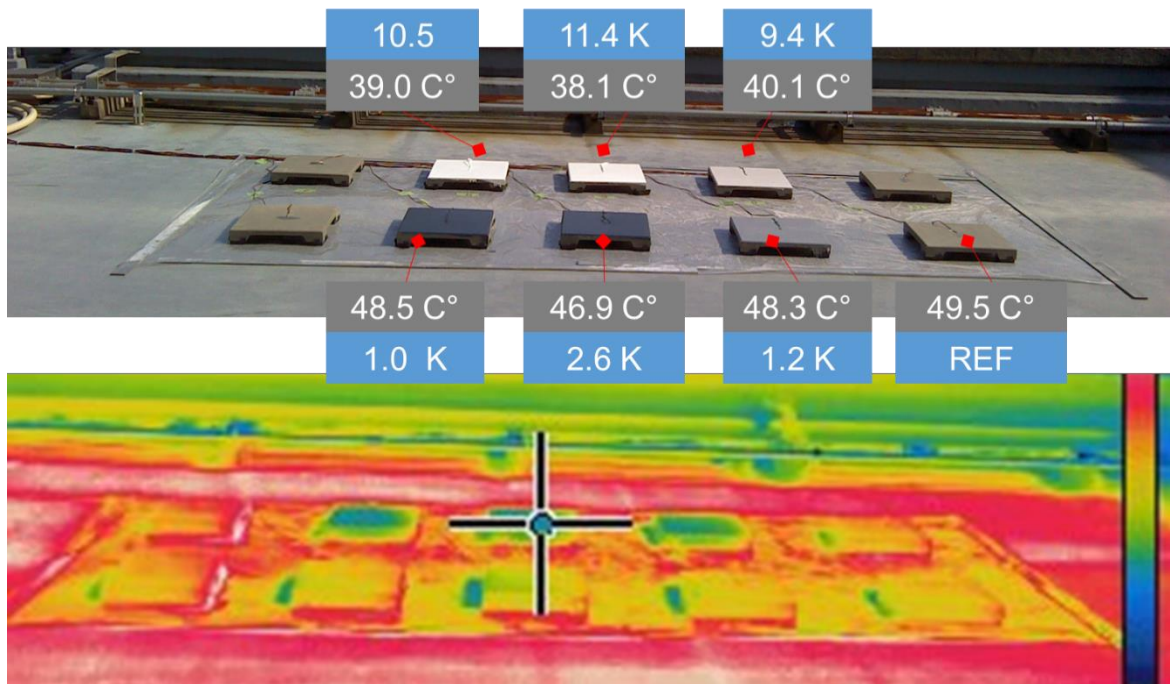


Figure 6-7 The first Infrared thermal photos showing the surface temperature variation than the reference tile i.e. the bare tile. Note that all the painted tiles are cooler than the bare concrete tile.

Another important issue to point out is that some unseen errors have led to the exclusion of some results. The employed data logger does not have the capability to view the collected data from a remote location. Hence, some probes seem to have damaged after a few days of readings. The cause of these errors reading appears to be due to the excessive temperatures, since the experiment was conducted in August for 21 days starting from the fifth, and bearing in mind that the errors occurred in probes of the soffit temperature of Solar Black tile that has no seal base, labelled as (S-B-F) and the soffit temperature of the Solar White on sealer (S-W-S). However, the cool temperatures data, that has an interval of 10-second records have been averaged on an hourly basis. Afterwards, the results are produced whereas the central objective was to conclude the influence of using the solar paint, the paint colour, and the sealer base application are highlighted. Not to forget that the general behaviours and global observations are all addressed as per the following.

For the surfaces' temperature recorded data (not the average data), it is noticed that the conventional grey paint resulted in a significant temperature fluctuation. The conventional grey paint

on a sealer (N-G-S) have a recorded a minimum temperature of 21.4°C and a maximum of 63.8°C. Hence it has a fluctuation range of 42.4°K, over the specified time course. Meanwhile, the white paint without a sealer base/ facial (S-W-F) had the most stable temperature fluctuation that was only 21.8°K. What the temperature ranges for the other cases is shown in Figure 6-8. Moreover, it is also to highlight that all paints surface temperatures did not drop below the minimum temperature of the plain tiles. Meaning that, there are a winter heating penalties when using the solar paint is not likely to occur, despite that the measurements are taken during the summer.

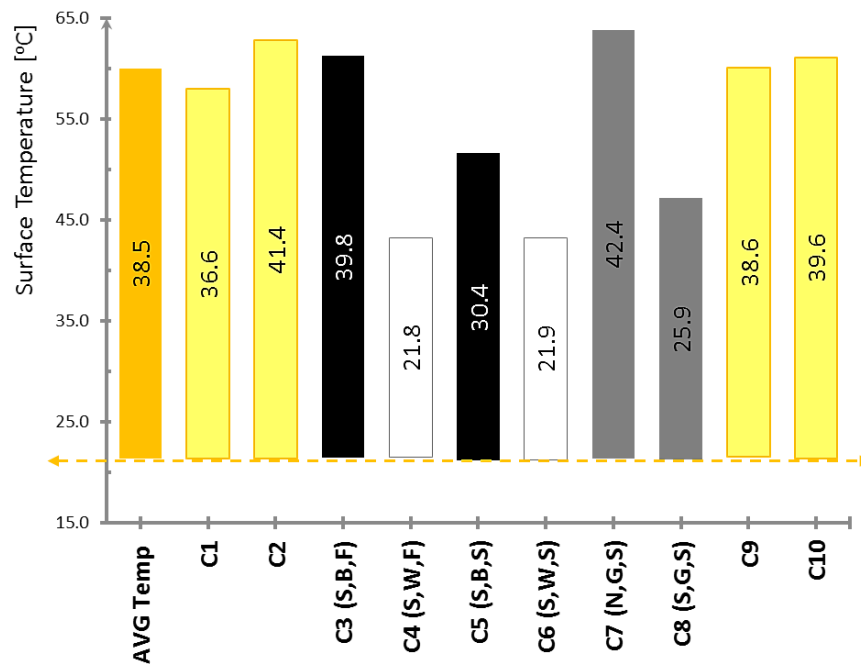


Figure 6-8 The fluctuation range of surface temperatures. The average temperature is for the bare concrete tiles i.e. (C1, C2, C3 and C4)

For the soffit temperatures profiles, it can be noted, and as normally expected, that the overall soffit temperatures are lower than the surface temperature. It can also be noticed that there is an error in the probes of the Solar Black paint without sealer (S-B-F) was excluded from the results and from Figure 6-9 results due to continuous errors. Similarly, the Solar White paint with a sealer base (S-W-S) have shown an errored reading most of the time, but it is kept in the graph to illustrate the errors. Beside these errors, it can also be seen that there is a minor change in the temperature fluctuation range orders. That is, similar to the surface temperature profiles, the minimum temperature fluctuation range was gain recorded in the case of (S-W-S). However, on the other hand, the maximum fluctuation for the soffit temperature is found in the reference cases average temperature which is ranged from 22.1°C to 55.6°C. Here, it is worth noting that the base cases (C1, C2, C3 and C4) where expected to show very close temperature profiles which is not the case. Moreover, this temperature variation on similar cases may be ascribed to the shading effects, since the shading period of each tile is likely to be different from the others due to their placement. However, From the previous points and Figure 6-8 and Figure 6-9, it is was seen that the soffit temperature have cooler temperature records and lower temperature fluctuation ranges. Figure 6-10 is prepared to investigate the relation

between the surface temperatures furtherly and the soffit temperatures profiles. In this manner, and from the beginning, it is noted that there is no temperature time delay between those two temperatures, i.e. the soffit temperatures are typically in offset from the surface temperature. Overall, the difference between the surface averaged temperatures and the soffits average temperatures can reach 16.8°K at maximum, add the minimum is found to be 3.6°K, whereas the mean of the variation is calculated as 6.6°K.

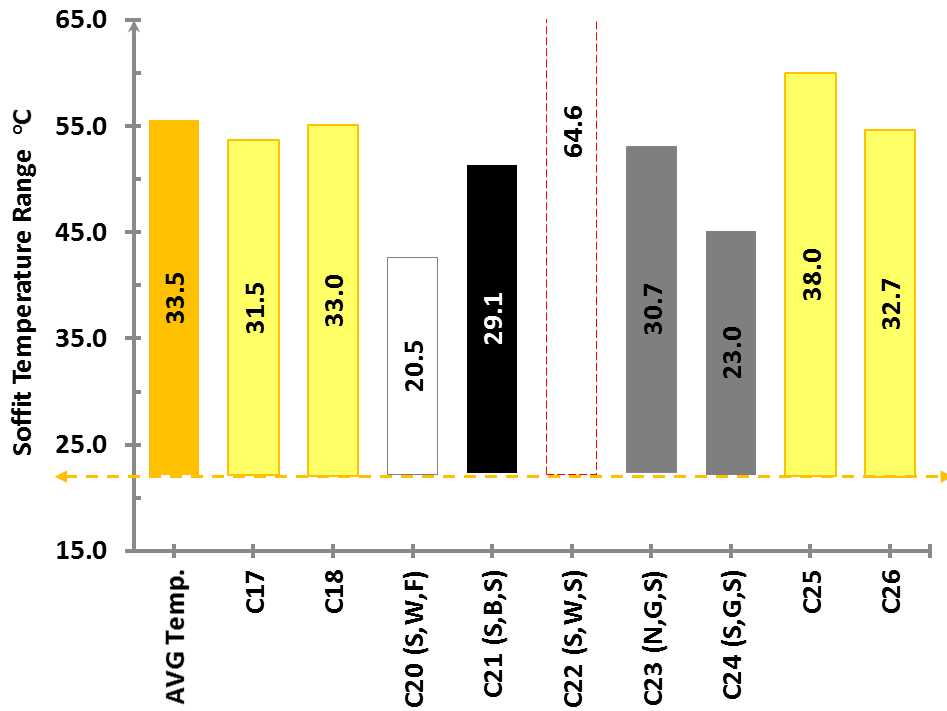


Figure 6-9 The fluctuation range of soffit temperatures. The average temperature is for the bare concrete tiles i.e. (C1, C2, C3 and C4). The results of the case of the Black Solar paint without sealer (S-B-F) are excluded due to reading errors., similar to what is seen in the solar white paint on a sealer, i.e. case (S-W-S).

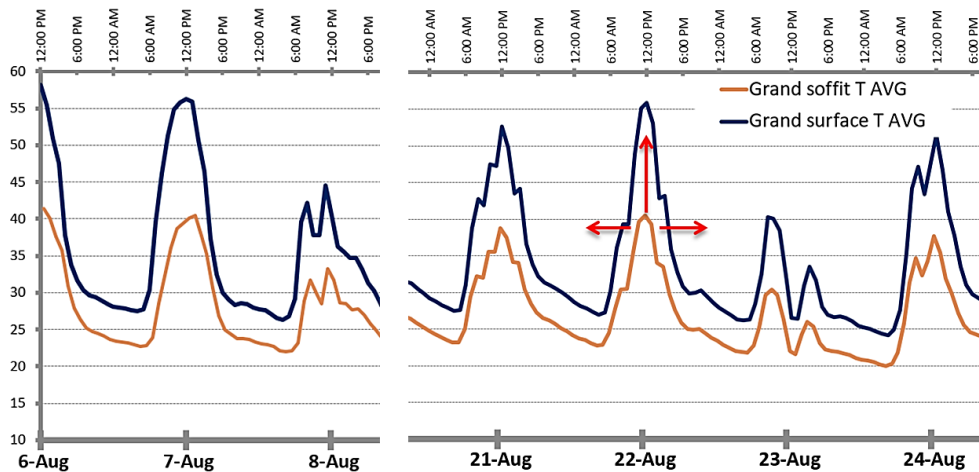


Figure 6-10 The tiles surface and soffit temperature averages are showing that the soffit temperature instantaneously follows the surface temperatures.

After covering the general temperature trends, the following paragraphs are oriented to discuss the specific parameters that are set to investigate (listed earlier at the introduction). As a start, the impact of using the solar plant on reducing the surface temperatures is investigated. This investigation is made by comparing the surface temperatures of solar grey paint from one side, with the conventional grey paint and the bare tile averages from the other. The temperature profile of the period 8~26 August is presented in Figure 6-11. In this regard, it is important to state that the compared grey colours tone/value are not typically the same. Besides, results showed that the normal grey paint temperatures are almost conforming with the plain (bare) concrete tiles, even it got hotter than it in many peak hours and exceeded 55 °C. On the other hand, the solar paint has shown a much lower peak temperature that remained below 47°C.

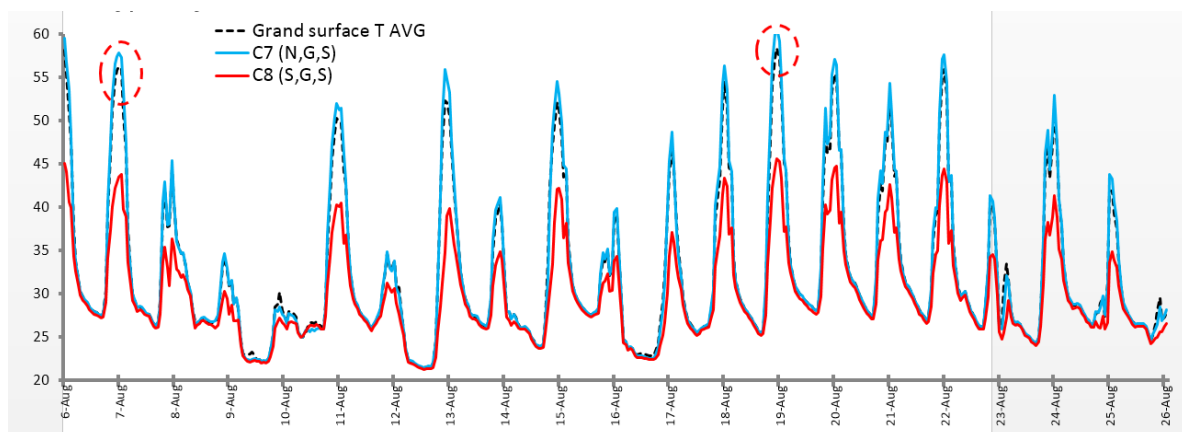


Figure 6-11 the impact of using solar paint is studied by comparing the normal grey and solar grey paints in reference with the bare concrete tiles; where both are applied over a sealer base.

Subsequently, and as the impact, if the solar paint is being realised, the color of the solar paint is studied when these paints are applied on a sealer base. The cases of white, grey and black solar paints on sealer are collectively compared, whereas the bare tiles average is also being plotted as can be seen in Figure 6-12. The results showed unexpected behaviours, whereas the (S-B-S) Solar Black on sealer shows the minimum peak temperature in many days when compared to the other solar paints, meanwhile, inverted cases where the grey solar paint yields a lower peak are also recorded. Furthermore, it is to highlight there was also an unexpected disorder of temperature peaks order and the colour tones. In other words, it is expected that the colour should have performed as white, grey, and black or vice versa, but the temperature peaks ranking, for most of the days was grey, white then black as the lowest peak temperatures. There is no clear justification for this behaviour, but it may be assumed that the solar paints may have been influenced by the Infrared portions that they block from the sky where the paint colours do not interact with this solar spectrum component.

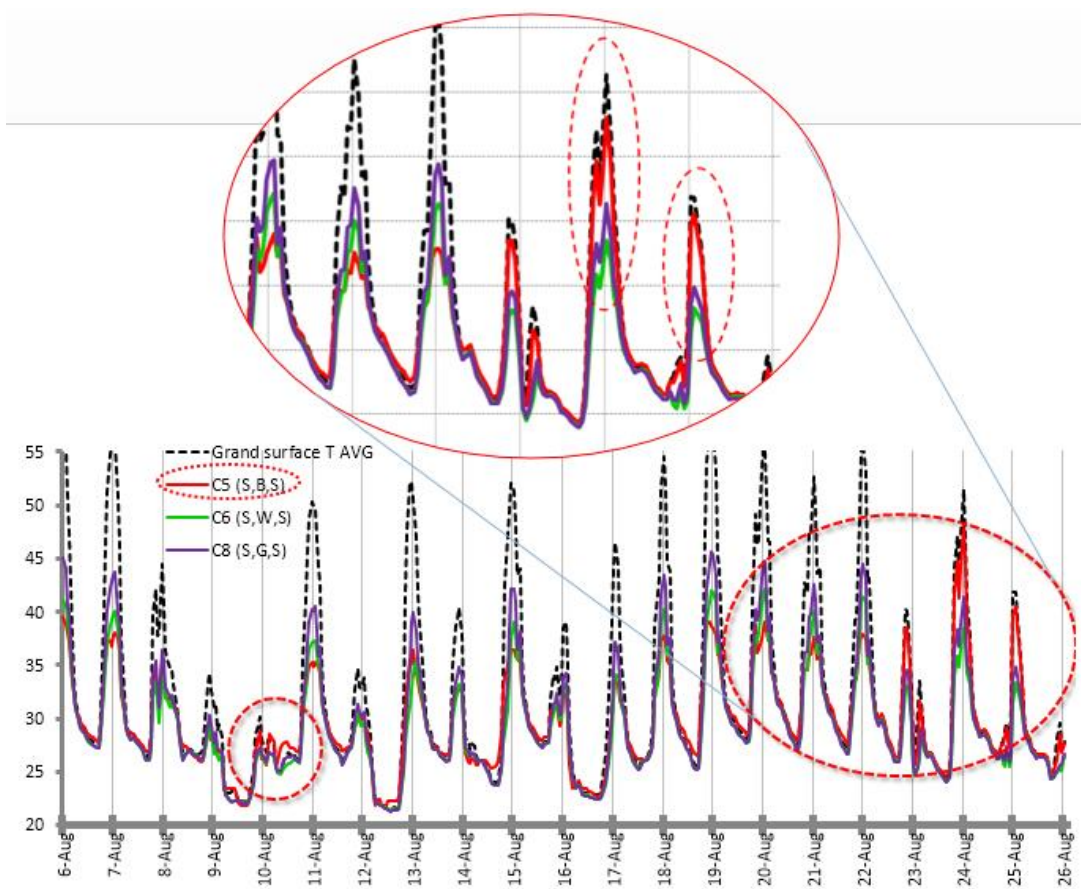


Figure 6-12 the impact of using solar paint colour is studied by comparing the three colours of solar paints when applied over a sealer base.

Likewise, the influence of the colour paint is studied but for the cases that have no sealer on the base and the solar paints are being applied directly to the concrete tiles. For this investigation, and since there is no such case of solar grey on facial (S-G-F), only the black and white cases of (S-W-F) and (S-B-F) are compared and plotted along with the bare concrete tiles average temperatures. Unlike the previous case, the Black Solar paint applied directly to surface resulted in temperatures as high as or

higher than the bare tiles, as can be clearly seen in Figure 6-13. In another respect, it was monitored that the at days with low temperatures, the white paint have a tendency to fatherly decrease the surface temperature. This issue may raise back the winter heating penalty issues. Hence, it might be deduced that the heating penalties require another study that focuses on such tradeoff between the cooling load/temperature reduction on summer and heating load increase in the winter for the various solar paint cases.

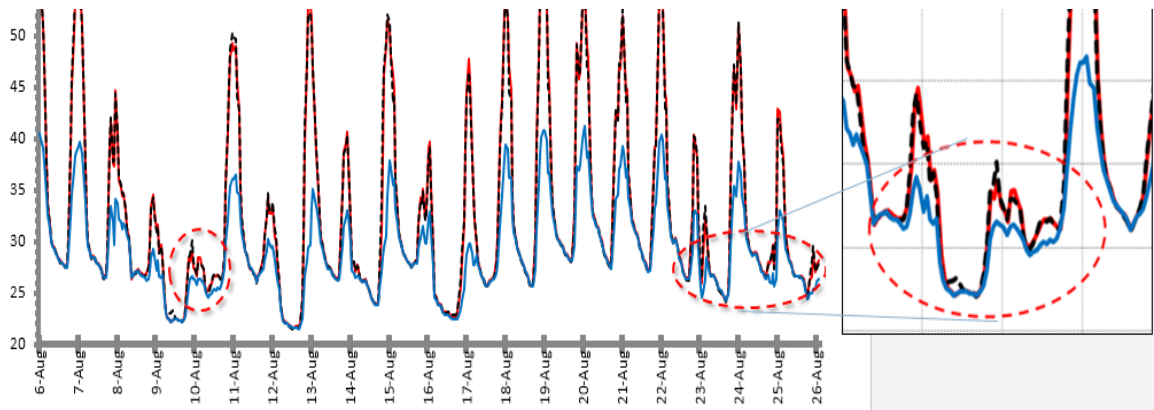


Figure 6-13 the impact of using solar paint colour without a sealer base is studied by comparing the white and black colours of solar paints.

Having shown that solar paint is highly influenced by the presence of the sealer on its base, the specific solar paint colours are studied apart. That is, for the black solar paint, the cases of the application with the sealer base i.e. (S-B-S) and without the sealer base (S-B-F) are compared. From what is seen in Figure 6-14, it is very clear that the application of the black solar paint without a sealer base is meaningless. In another word, when the black solar paint is secretly applied to the tile, it yields temperature peaks that is equal the bare tile itself. On the other hand, despite the anomaly found on the 24th, the application of the black solar paint over a sealer base has maintained a peak temperature below the 40°C.

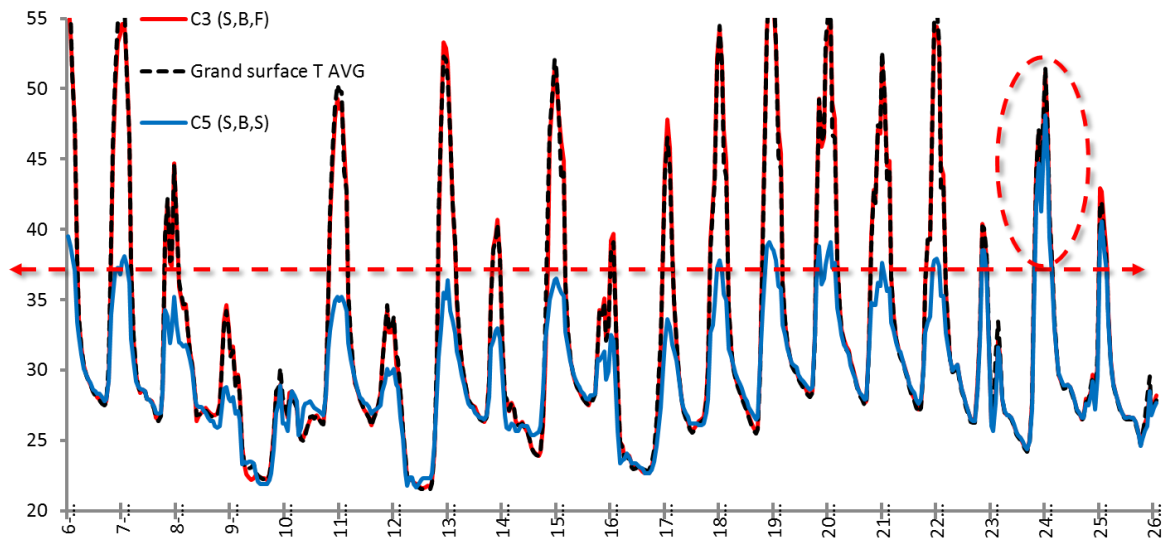


Figure 6-14 the impact of having a sealer base on the black solar paint is studied by comparing the cases (S-B-S) solar black on sealer and (S-B-F) solar black on facial surface.

In the same manner, the influence of the sealer application on the white solar paint was also studied. The cases of solar white on sealer (S-W-S) is weighed against the (S-W-F) solar white on facial base while accompanying the overall average concrete tiles average temperature. The result of these case are plotted in Figure 6-15, and from the first sight, it can be concluded that the white solar paint performing is not affected by the presence of the sealer on the tile base. The temperature profile of the cases (S-W-S) and (S-W-F) is almost conforming, with very few days (usually on cold days) e.g. 10th of August) where the solar white with no sealer (S-W-F) records a slight extra drop in the minimum temperature.

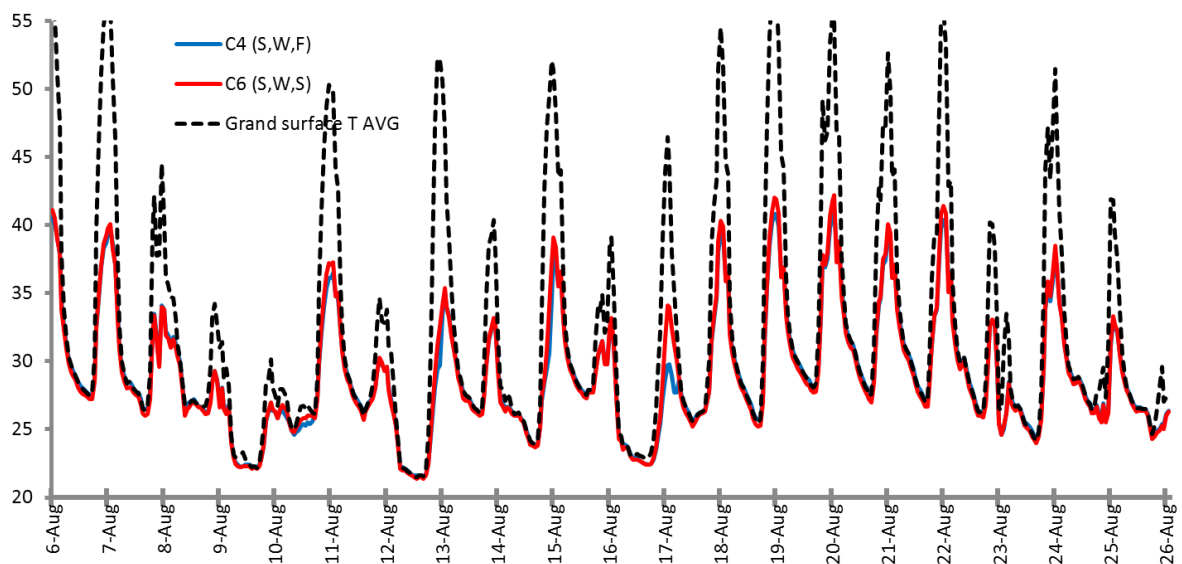


Figure 6-15 the impact of having a sealer base on the white solar paint is studied by comparing the cases (S-W-S) solar white on sealer and (S-W-F) solar white on the facial surface.

6.3 Second experiment

As per the results and finding from the first experiment, The objective of the second solar paint experiment herewith is to examine the role of the glossiness of the colour paint on its temperature profiles. Also, the experiment has also conveyed the colour, the application of the sealer, as well as the paint type (i.e. Normal and Solar) as investigated factors. With a little bit of attention to the seal effect on the temperature profiles. Moreover, it is worth t mention that the first experiment has raised many unseen issues that may have affected the results, and as well be explained in the following section, this error causes issues have been fully considered in the new (second) experimental setup.

6.3.1 Methodology

The second solar paint experiment inherited the same objective of the first one, as to utilise the solar paint as a heat mitigation measure rather than a heat dissipation measure (cooling). Therefore, the second experiment has commenced forming the first of September 2016 up to the end of that month. The experiment starting time was delayed due technicalities, however, the ambient temperature over the experiment period had some summer-featured days as well be seen later. Alos as stated earlier, the second experiment is done with a wider number of cases and permutations that would enable comparing the various factors in a detailed manner. In this regards, and as can be seen in Figure 6-16, the experiment consisted of 16 cases and where 18 tiles have been used – the plain/bare tiles are three tiles. In these 16 cases, the variables where The sealer application as a base, the Glossy and matt paint and the paint colour.

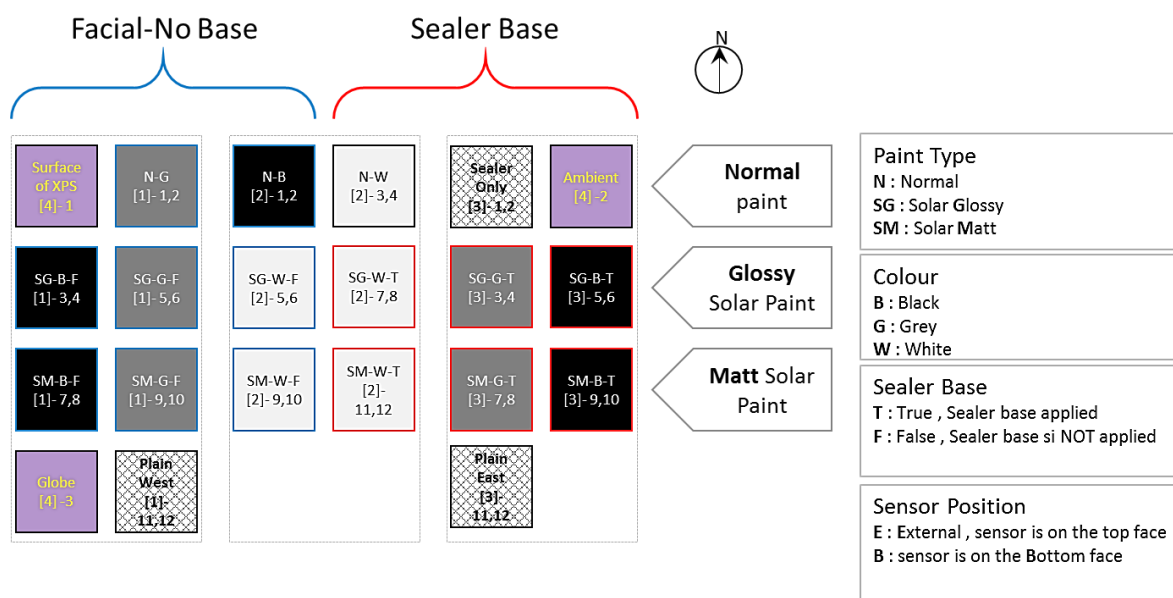


Figure 6-16 The second experiment investigated factors and the resultant permutation (cases) matrix

Since the number of the cases was huge, a coding name was developed as to ease tracking and understating of the case properties and base formation factors. The name coding methodology is shown in Figure 6-17.

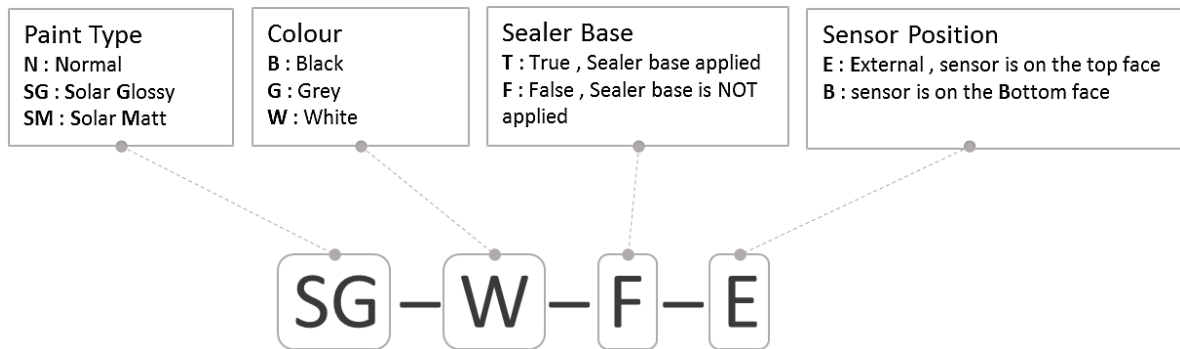


Figure 6-17 The cases/permutations name coding methodology

Additionally, as stated earlier, there were some issues that may have lead to errors or may have affected the overall results of the first experiment. These issues are expected to be listed as the following. Firstly, it is anticipated that the contextual shading has a limited the time when all the tiles are equally exposed to the sun radiation. Since on the early morning hours and during the late afternoon hours, the tall surrounding buildings cast shadows on the sided tiles while leaving the others under the solar radiation. For this reason, the experimental rig has been moved to the further northern part of the available roof area. Also, a previous solar exposure test was made using the Solmetric SunEye 210 tool. Moreover, despite the sunrise and sunset moments, the results have revealed that the experiment area (based on its four corner points) is not subjected to any contextual shading during the experiment period, i.e. September.

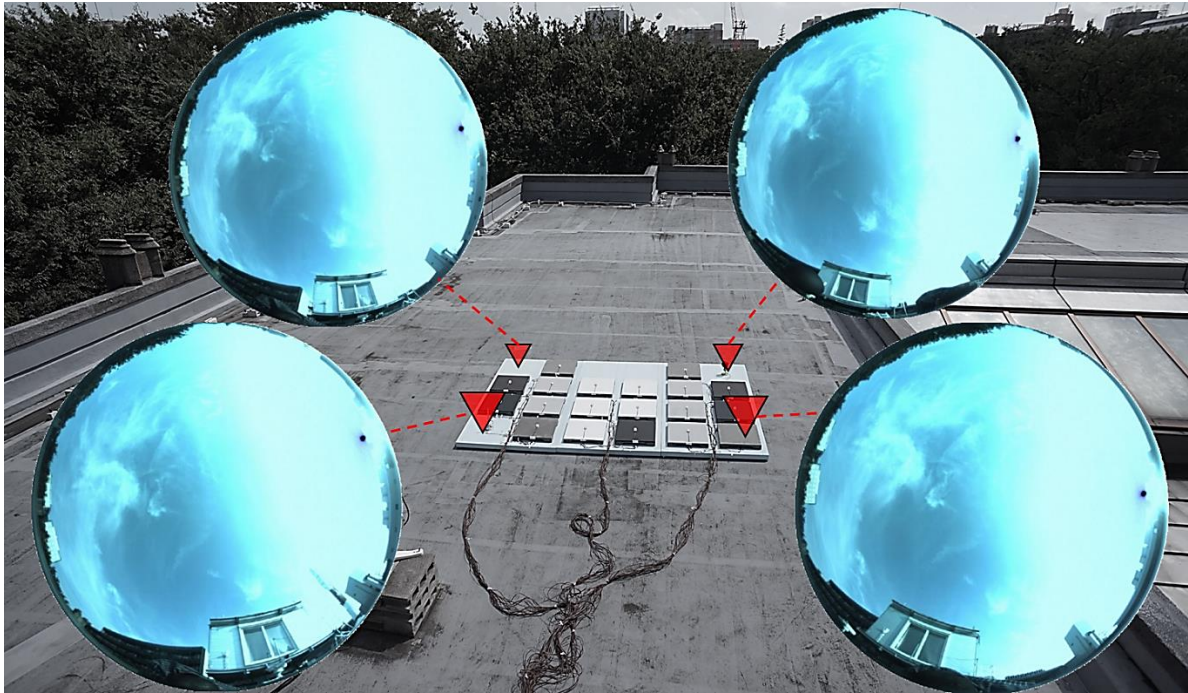


Figure 6-18 The second experiment is located at the less shaded area, where the sun exposure analysis confirmed that the location has full access to the solar radiation during the experimental period.

Another important factor that is thought to have a significant impact on the soffit temperatures of the first experiment is the direct contact between the concrete tiles and the roof slab finishes. This direct contact may have contributed to raising the tiles temperature by two means. The first is by the direct conduction at the relatively mild/cold periods of the day, where the roof slab retains and stores much more heat compared to the small tiles that have a higher tendency to dissipate the heat. Moreover, through the radiation between the tiles soffit (that host the soffit probs) and the roof slab, and since the latter is mostly hotter than the tiles, then it does not allow collect accurate results of the tiles soffit as well as surface temperatures. For this reason, a base of a 5cm XPS insulation sheet is located beneath the tiles as can be seen in Figure 6-19. Also, this XPS is suspended from the roof slab by a small Styrofoam legs as to allow for ventilation and reduce the contact area between the XPS base and the roof to the minimum possible degree. Such technique was found in literature, namely, in the roof experiment carried by (Synnefa et al. 2006).

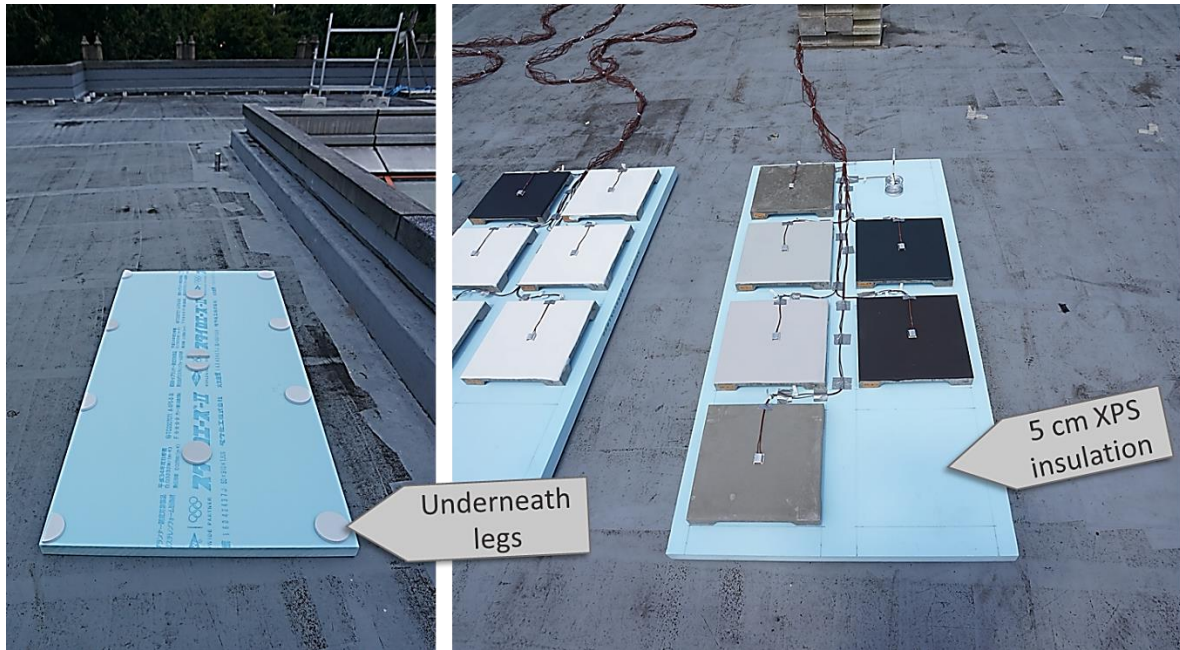


Figure 6-19 The tiles are placed over a cm XPS sheet that is suspended for the roof slab by a Styrofoam legs as to reduce the heat transfer for the roof to the tiles to the minimum degree.

From the first experiment and based on the experiment concerns forwarded by (Synnefa et al. 2006), it was realised that the probes / sensor needs to be protected from direct solar radiation. The thermal couple naked heads are prone to report higher temperatures due to their metallic nature, despite their finite size. Therefore, an in-home made plastic hoods/caps with an aluminium foil being attached to their outer face. These caps are placed in a way to protect the probes from the low angle solar radiation as well as the noon solar radiation. The caps can be seen in Figure 6-20, where it can also be seen that they allow for air flow to pass over the probes.



Figure 6-20 A custom made plastic caps with an aluminium foil finishing are placed to protect the thermocouple probes from the direct sunlight throughout the day.

Regarding the protection caps and the measurement probes, it is a norm that the probes are placed at the centre of the tile. However, this norm is not solely derived from a geometrical point of view, but also from a thermal distribution perspective. That is the probes are placed at the tiles centre as to avoid the heat that is accumulated at the tile edges. As can be seen in Figure 6-21, the thermal camera images shows that there is a very tangible temperature variation between the center and the edges of the tile. This variation, or so called the standard deviation of the temperature difference between the centre, and the edge is over one-degree celsius among all the cases. This variation is quite high when considering that the distance between the tile centre and edge is less than 20 cm.

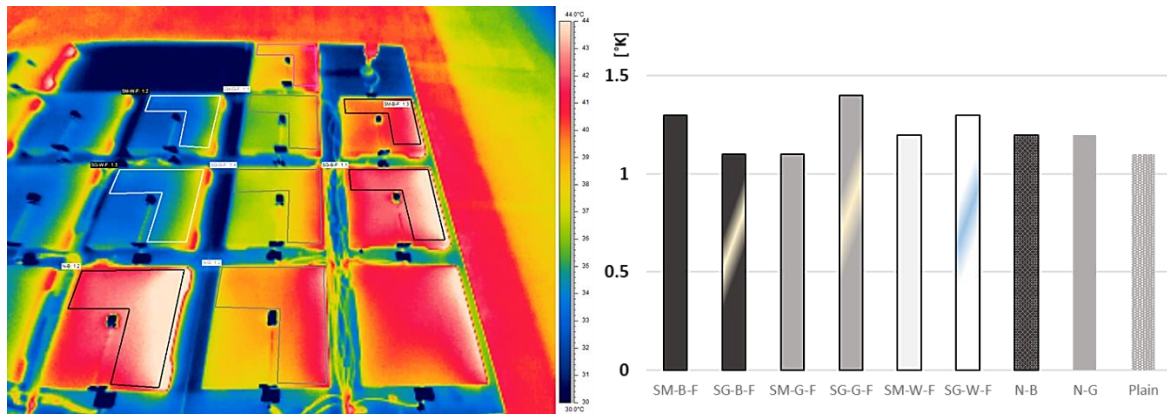


Figure 6-21 Temperature distribution Standard Deviation for sample tiles.

In the same regards, and concerning the significant temperature variation across the tiles surface, it is also important to consider that the tile sides is also very prone to a dramatic temperature rises when the sun leans toward the before and afternoons. Figure 6-22 shows that such a difference in a sample case of a plain concrete tile may reach a 5.4°K. On the same figure, it can be seen that the whole row of the tiles. Here, it is to state this variation issue can only be solved by having a fairly large experimental surface rather than small tiles, whereas this was not feasible on this experiment. Lastly, it is shown that a better data recorder was used to collect the data on an interval of 10 seconds. The Hioki data logger type LR 8401 can send and store the data in an FTP site which have eased data monitoring which enabled instantaneous errors debugging.

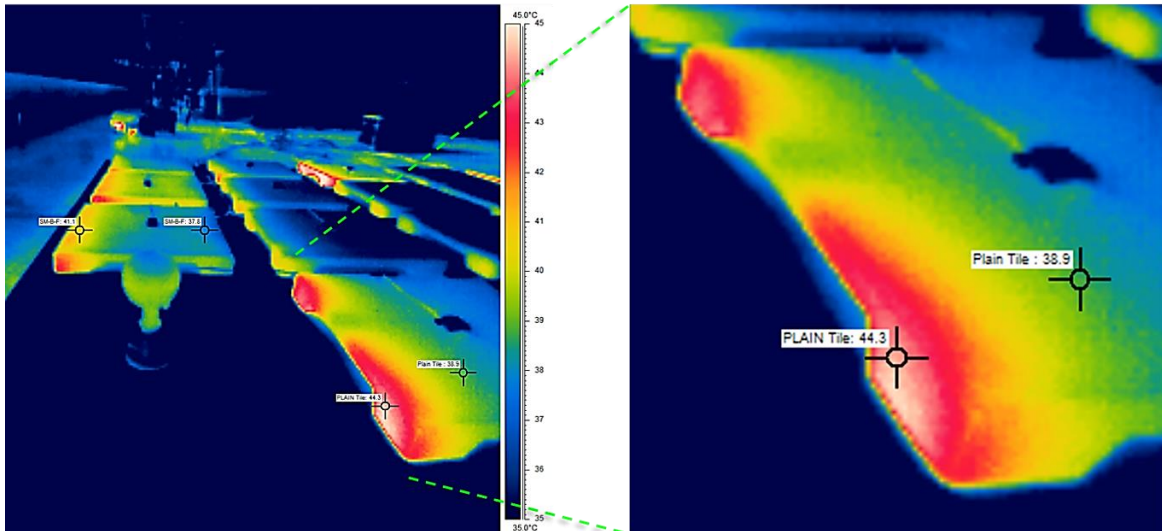


Figure 6-22 Temperature variation between the tiles surface and edges may exceed 5°K

6.3.2 Results and Discussion

In addition to the collected temperature data, another meteorological data set was obtained from AMEDAS (Automated Meteorological Data Acquisition System) (Japan Meteorological Agency n.d.). These data first analysed to select the most appropriate sample days that serve the purpose of the research. The objective of this exercise was to have two days conditions. The first is to be a sunny day with minimum clouds, whereas the second is to be the most cloudy day (overcast condition) but without any precipitation. Based on this definition, The first ten days of September was selected as a sample range, and as can be seen in Figure 6-23, these days have had many sunny days and had least rain as well.

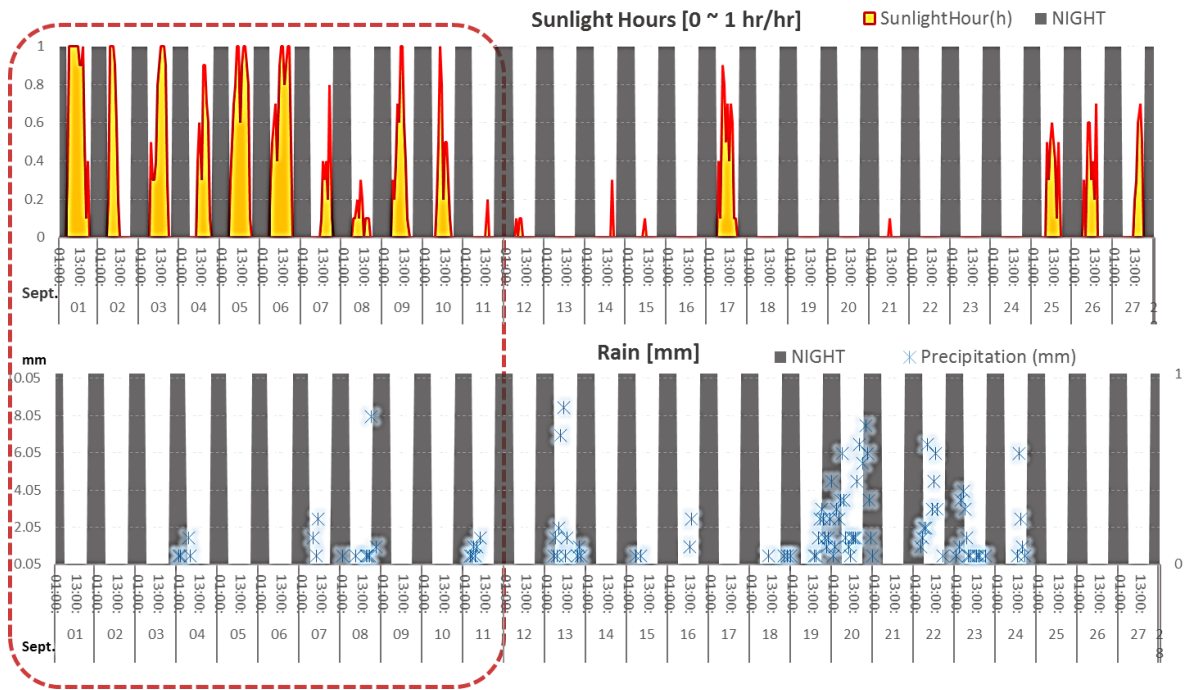


Figure 6-23 Selecting the sample days through September 2016.

After selecting the sample days, the next step was to check the variation between the surface and soffit temperatures for each tile (case). The temperature variation is displayed for each day of the selected sample 10 days, and the outcomes are shown in Figure 6-24. The results indicate that there is no clear general definition or preference for which side of the tiles gets hotter i.e. in some cases the soffit is hotter than the surface temperature across the whole days. It is noticed that the soffit of the black paints, conventional paint and tiles without paint is even hotter than their surfaces, with just an exception of the Glossy Black paint. This grouping can be seen in Figure 6-25. However, Here it is noted an important key thing, which is this phenomenon did not show up in the first experiment whereas all the soffit's temperatures were cooler than the surface temperatures. This behaviour can then well be linked with the usefulness of the XPS platform since it has allowed for the tiles to be independent of the roof temperature profile and behaviour. However, the group of the cases that have a hotter soffit can be ascribed to the fact that their surfaces temperature have an excessive heat which can then be dissipated through convection, as illustrated in Figure 6-25. Meanwhile, the soffit is left at it is at a higher temperature. On the other hand, the relatively colder white tiles may have heat gain by convection instead while their soffits are protected from that heats gain source. In conclusion, it can be seen that the soffit temperatures are more stable and seem to be more realistic. Hence it can be used for the future analysis.

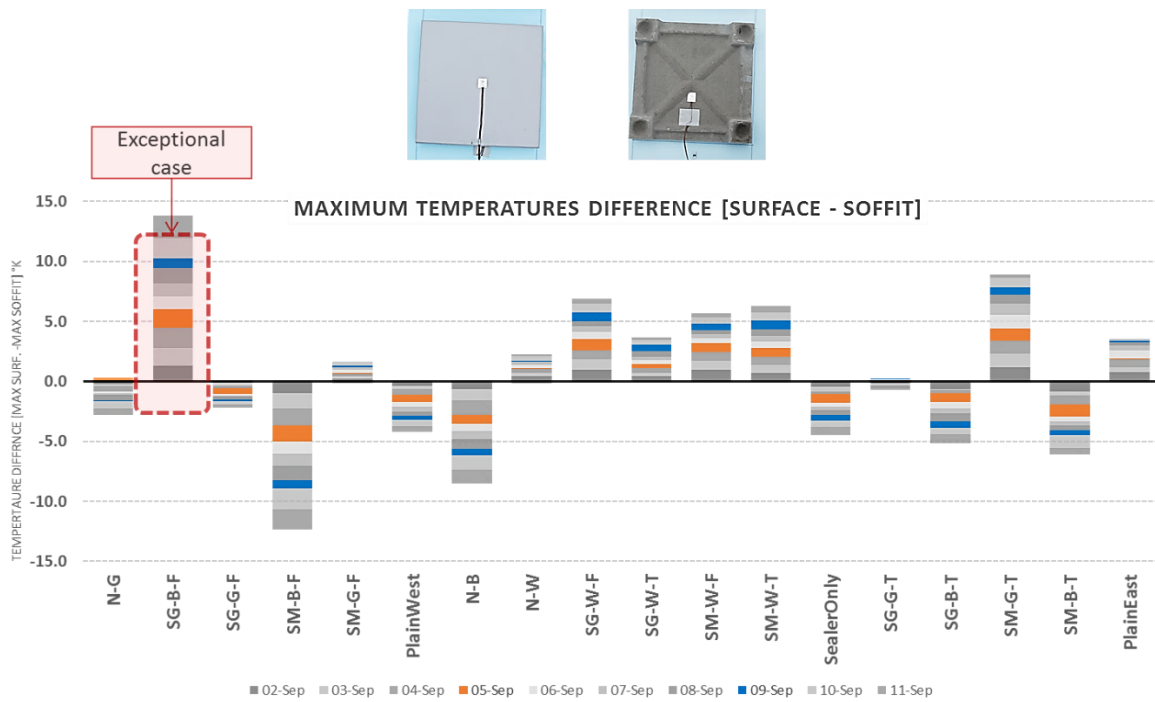


Figure 6-24 The Top and bottom temperatures variation

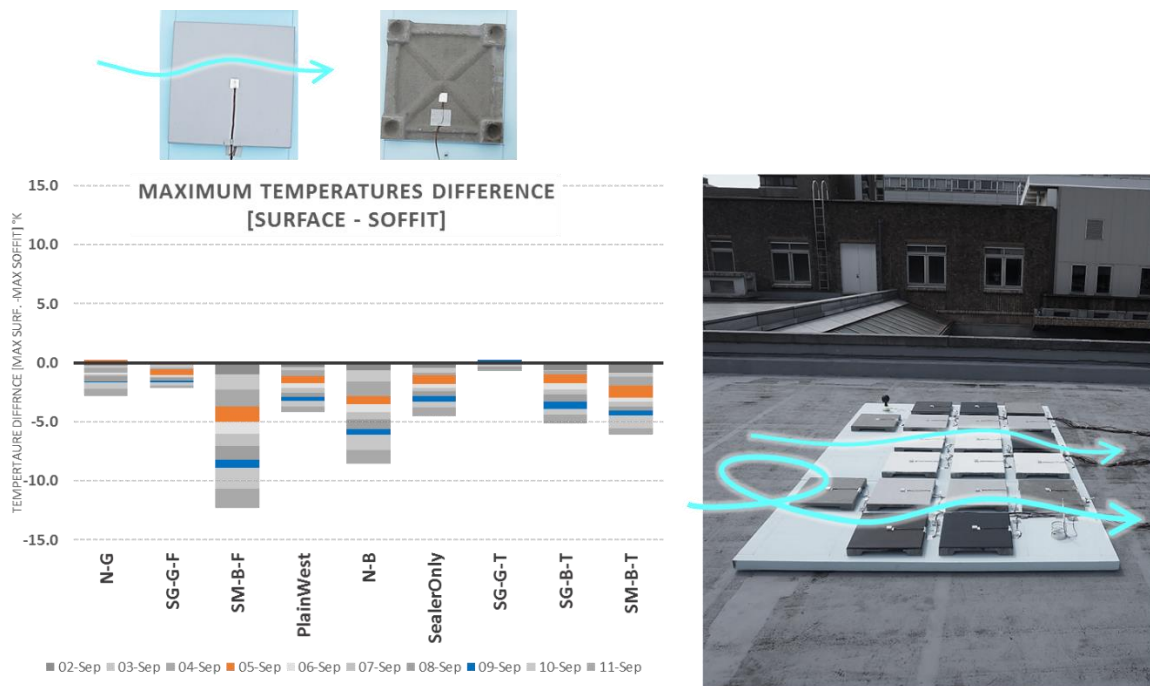


Figure 6-25 The group of cases that have a soffit temperature that is hotter than their surface temperatures. The group consists of black paint, conventional paint and tiles without paint.

The next analysis was concerned with the influence of the sealer application in the tiles temperature reduction. However, it is to state that the sealer used for this experiment was transparent, unlike the first experiment which incorporated a white sealer. However, to confirm the influence of the sealer,

and if it can reduce the temperature by itself, the tile that only has a sealer was compared with the plain tile on the eastern side, the location of both tiles can be seen in Figure 6-26 below. The results of this investigation are plotted in Figure 6-27, and it is clearly seen that the tile that has a sealer only on its surface have yielded a higher temperature over the ten days when compared to the bare/ base concrete tiles. Not to forget that this temperature profile is on both sides of the tiles i.e. the surface and the soffit as well. When comparing these results with the first experiment, whereas the sealer application has led to reducing the surface temperature, it is to remind that the seal used in the first experiment had a white colour while the sealer in the second experiment was transparent, as can be seen, on Figure 6-28.

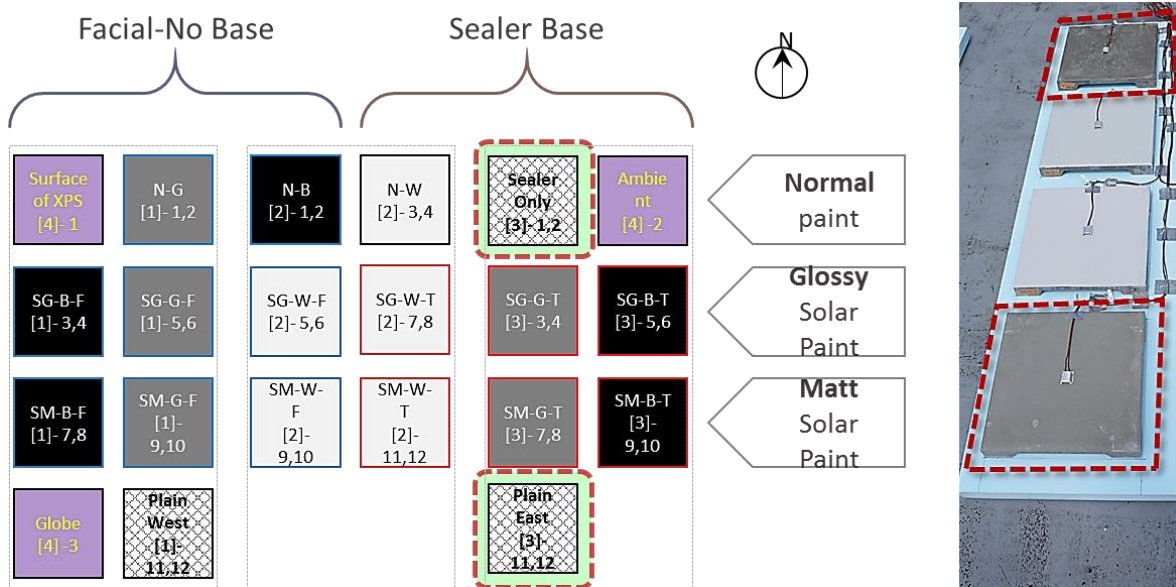


Figure 6-26 The influence of the sealer is made by comparing the tile that only has a sealer together with the plain tile located on the eastern side

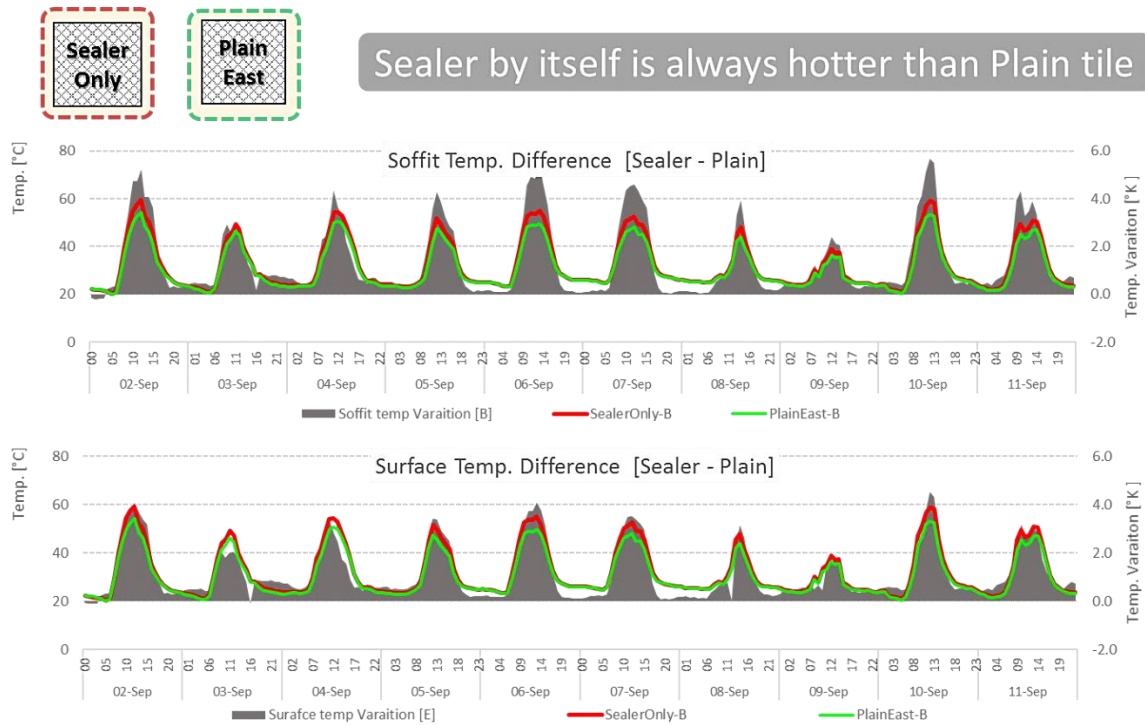


Figure 6-27 The result of the comparison between the plain (bare) concrete tile and the tile with sealer only.



Figure 6-28 The sealer that was used in the second experiment was transparent. Unlike the first experiment where the sealer was white

On the same aspect, the sealer influence was tested using another technique which is based on incorporating all the solar paint tiles configurations. That is, comparing two sets of tiles, one with sealer bases and the other set of tiles are applied without sealer, where the maximum temperature difference between these two sets is calculated. Figure 6-29 is developed to give a visual idea of these two sets (Groups). The result is plotted in the following chart, shown in Figure 6-30, whereas for any paint case if the data column is above zero (positive) it means that when that specific paint is applied without a sealer, it will yield higher soffit temperatures.

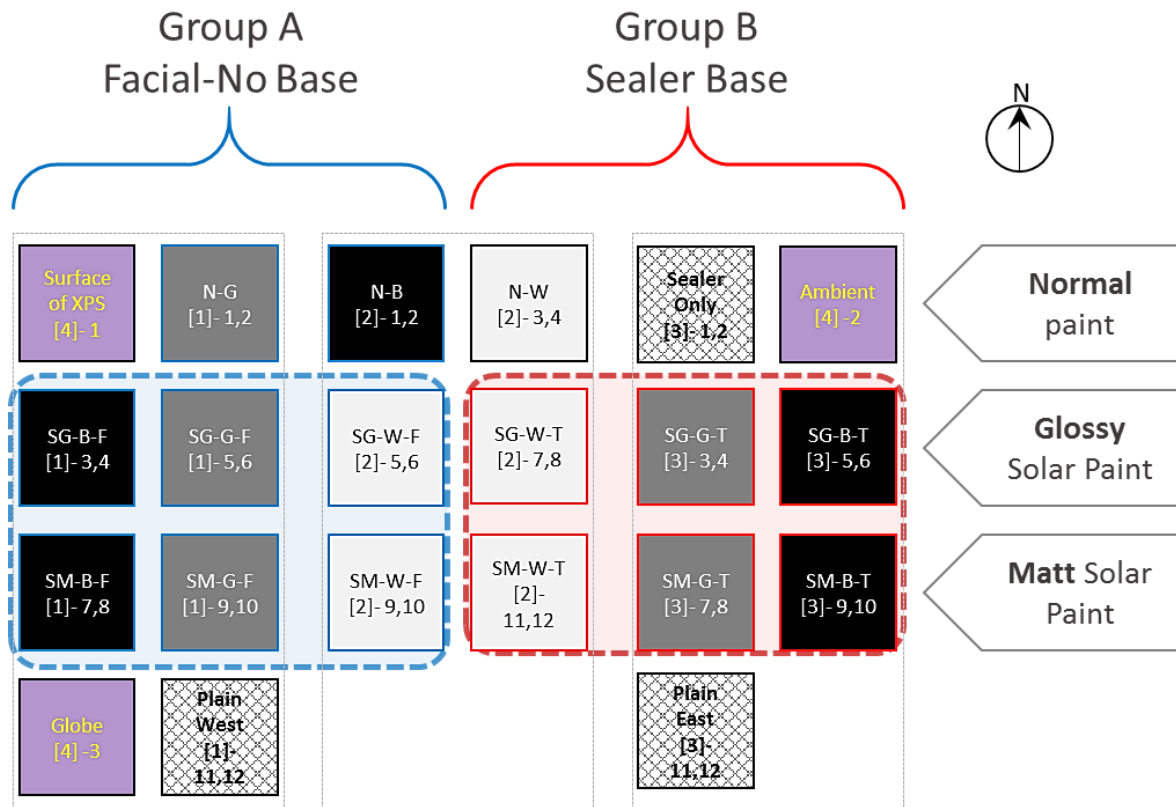


Figure 6-29 Two sets (Group) of cases that either applies the sealer or without the sealer base (facial) are compared to study the influence of the sealer application on the solar paint temperature profiles

Therefore, based on the above definition, together with monitoring the weather conditions, two things can be deduced from Figure 6-30. Firstly, the biggest variation between the sealer and facial application have been observed in rainy days, which are third, fourth and 11th. For this observation to be made clear, Figure 6-31 is meant to highlight the rainy days with warm colours. The second important note is that all of the glossy paints, i.e. labelled with [SG-xx], are negatively influenced by the presence of the sealer. That is, the glossy paints will not perform well unless they are applied on a sealer. On the other hand, the matt paints i.e. labelled [SM-xx] they performed better when they applied directly on the tile without the need for a sealer base. This finding may address the question of the need for buying the sealer if the matt paint is to be used.

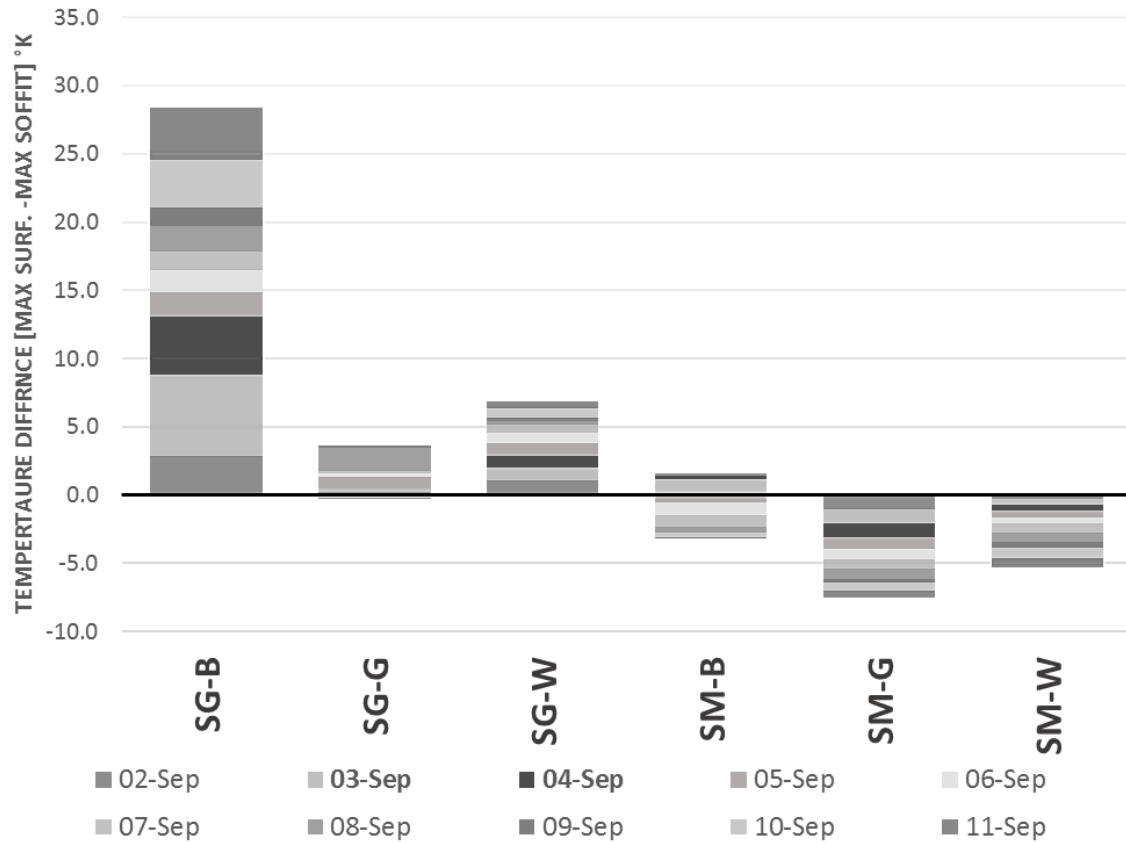


Figure 6-30 Maximum temperatures difference [without sealer - sealer base].

- The Highest variation occurs in **Rainy Days** [3rd , 4th and 11th].

- for GLOSSY paints , the Sealer is a must
- for MATT tiles , the Sealer may hinder its performance

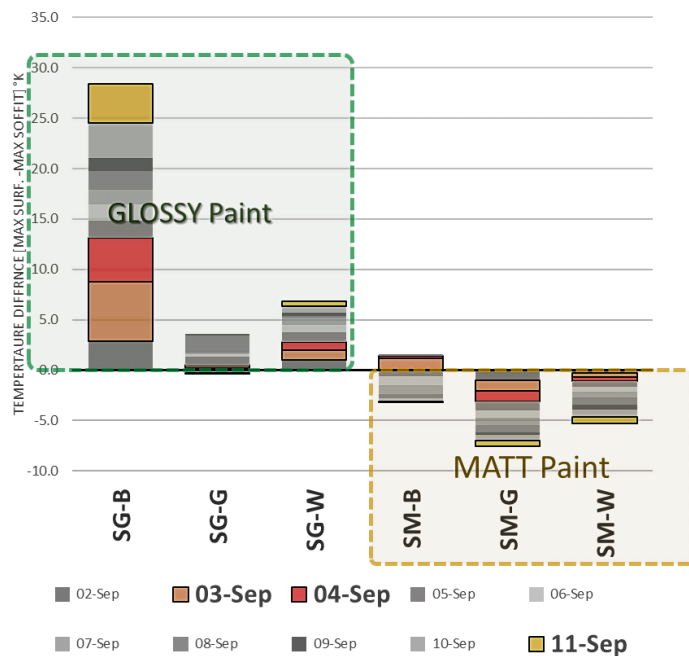


Figure 6-31 Maximum temperatures difference [without sealer - sealer base] with weather conditions being considered.

From the previous point, it was highlighted that the performance variation between the various cases has shown to be influenced by the weather. Therefore, It was logical and interesting to check the performance of each paint type in clear and overcast day. In other words, a derived objective was to To investigate the role of the glossiness of the paint on its performance at various conditions. In this point, it is to highlight one important fact that would relate to the weather, which is the optical properties of the glossy and the matte paints. In Figure 6-32, the manufacturer's specification of both paints shows that the matte finish paints should yield the best mitigation performance since its reflection rate on the near infrared as well as the overall wavelength is higher than reflection values fro the glossy paints.

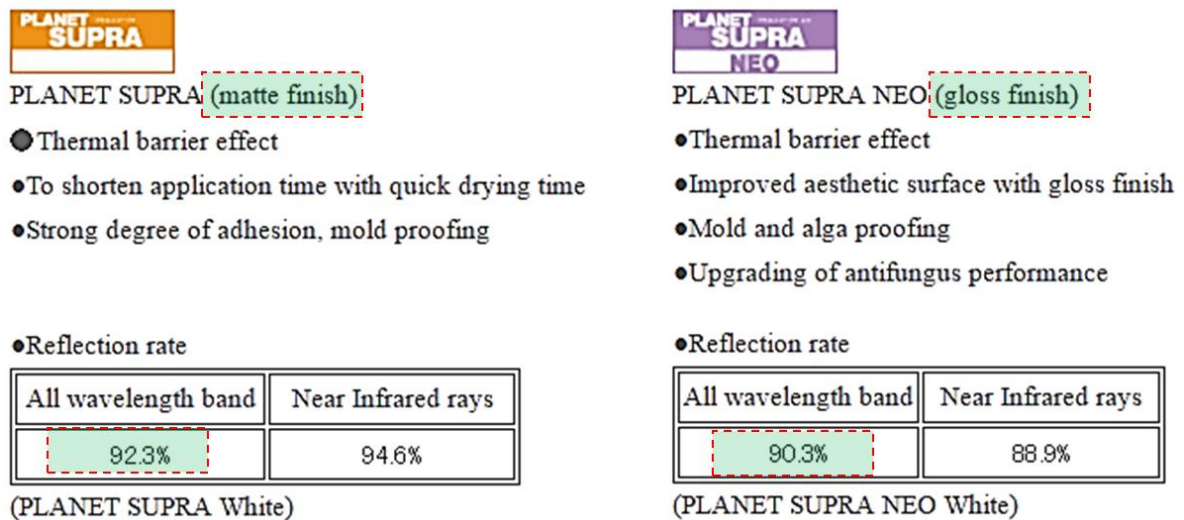


Figure 6-32 The solar paints reflection rates as per provided by the manufacturer. Source:(SCI-PAINT JAPAN INC. 2008).

In order conducting the paints glossiness sensitivity to the weather conditions, two specific representative days needs to be selected among the initial ten days. As one to specifically represent the sunny day, and the second should be a cloudy day – preferably without any precipitation (rain). For this purpose, Figure 6-33 is prepared to visualise to conditions that helped in identifying those two representative days, i.e. the sunlight hours, cloud cover and the precipitation. Whereas the sunlight hours would hit the clouds of the sky as well, and the precipitation will give an idea about the general weather conditions around the specified days. In the end, September the 5th was selected as a sample of sunny day conditions, while the 9th is used as an overcast condition representative day.

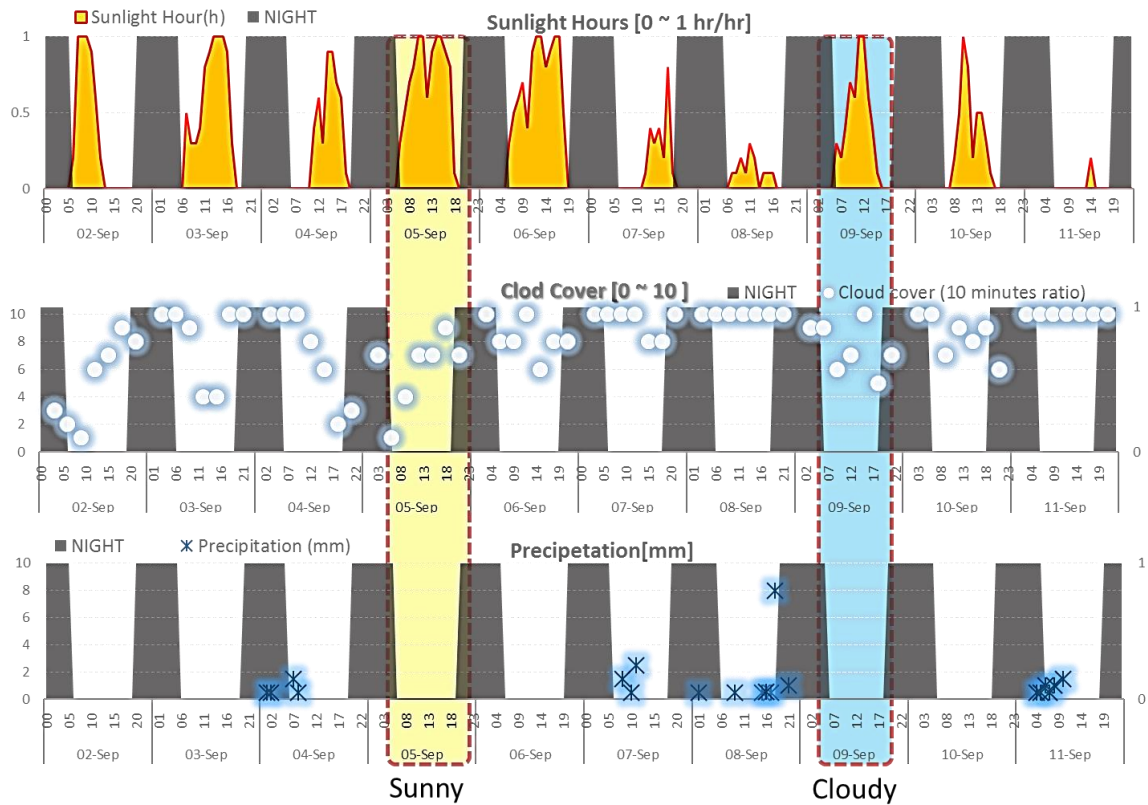


Figure 6-33 Identification of the representative sunny (clear) and cloudy (overcast) days.

The temperature profile of the three colours is plotted for the sampling sunny and cloudy days. As can be seen in Figure 6-34, and anticipated as per the manufacturer provided information, the matt paints for any given colour are better (colder) their counterparts of glossy paints, on both days. Moreover, as in Figure 6-35, the matte paint have yielded cooler temperatures over the course of the whole ten sampling days.

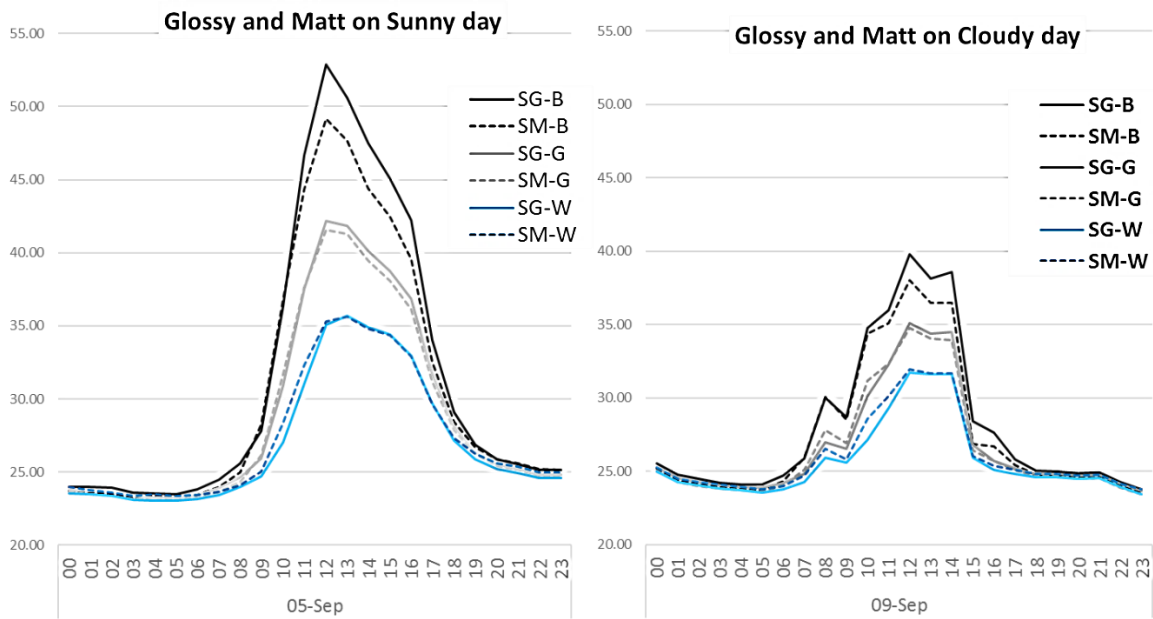


Figure 6-34 Comparing the temperature profile for the glossy and matte finishes in a sunny and cloudy days.

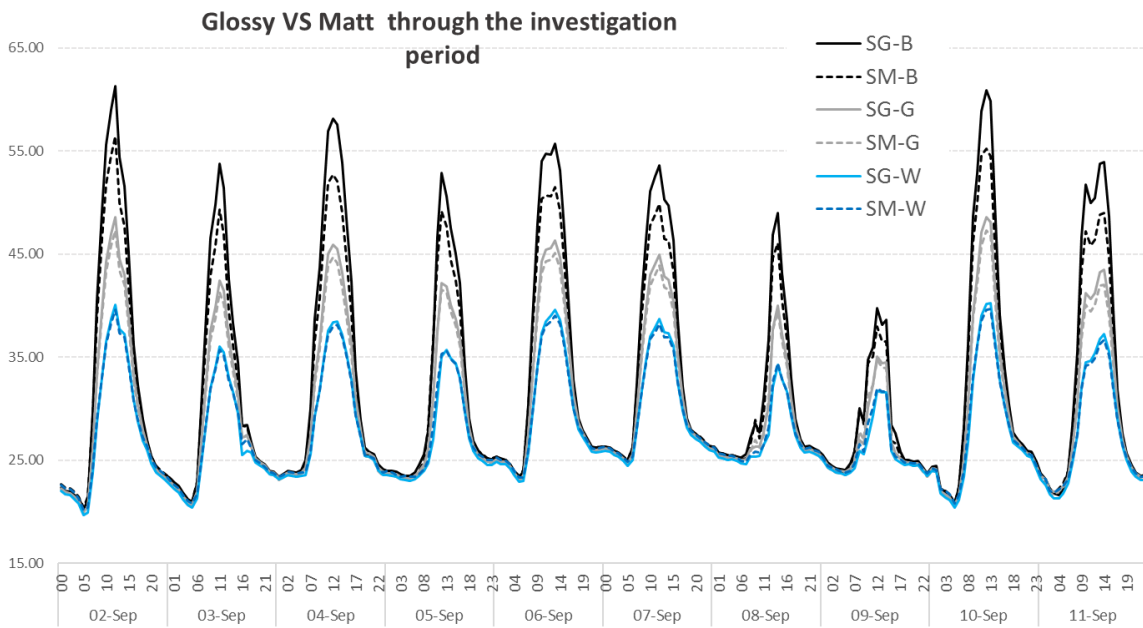


Figure 6-35 Comparing the temperature profile for the glossy and matte finishes in all the sampling ten days

A small interesting observation was noted during the early morning of the cloudy days. That is, there is a minor adverse change in the temperature profiles that exclusively occurred during the early morning hours of cloudy days. In these few hours, the glossy paint recorded cooler temperatures when compared to the matte paints, in particular for the bright colours, i.e. white and grey. To vivid this observation, Figure 6-36 is made by subtracting the glossy paints temperature from their

counterpart (same colours) of a matte nature. As a result, it can be seen that there some parts of the day where the glossy paint yields a better performance. Moreover, as noted earlier, this inverted effects further pronounced at the cloudy conditions. Subsequently, a closer look at the cloudy day conditions, which can be seen in Figure 6-37, may reveal this inverted behaviour as well. Moreover, it can be highlighted that it typically occurs for the white and grey colours.

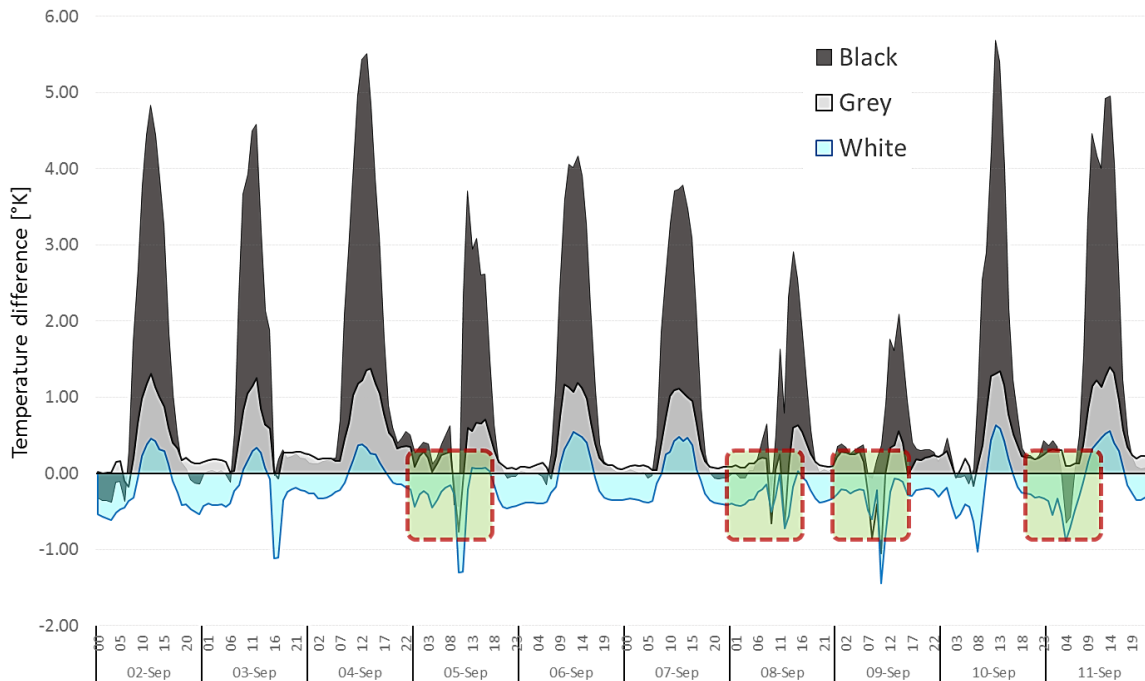


Figure 6-36 The temperature variation is calculated by subtracting the glossy minus the matte Temp for all the three paint colours.

The interpretation of this observation could be started by pointing that the portion of the Infrared and visible components of the solar spectrum vary by the variation of the day time as well as it is changed by the modification of the cloudiness conditions of the sky. In literature, many studies have shown that the Infrared radiation share of the solar spectrum is reduced by the sky conditions e.g. the study of (Escobedo et al. 2009) have pointed out this fact in many parts of their article. Also, and as per what can be seen from the time laps of a video provided by the (National Institute of Standards and Technology 2015) and reproduced here within Figure 6-38. In this figure, it is apparent that the infrared also dominates during the early morning and starts decaying when the sun moves towards the noon. Figure 6-39 is produced to summarise these two factors that change the NIR percentage of the overall solar radiation spectrum. In conclusion, it can well be said that the reason behind the change in the glossy paint performance was it becomes better than the matte paint during the early morning of the cloudy days, could be due to the significant drop in the Near-infrared NIR radiation percentage of the solar spectrum, and that is where the matte paint reflects the most of the heat. Hence, the matte paint efficiency drops since the major portion of the solar spectrum become the visible light where the glossy can better reflect the solar rays.

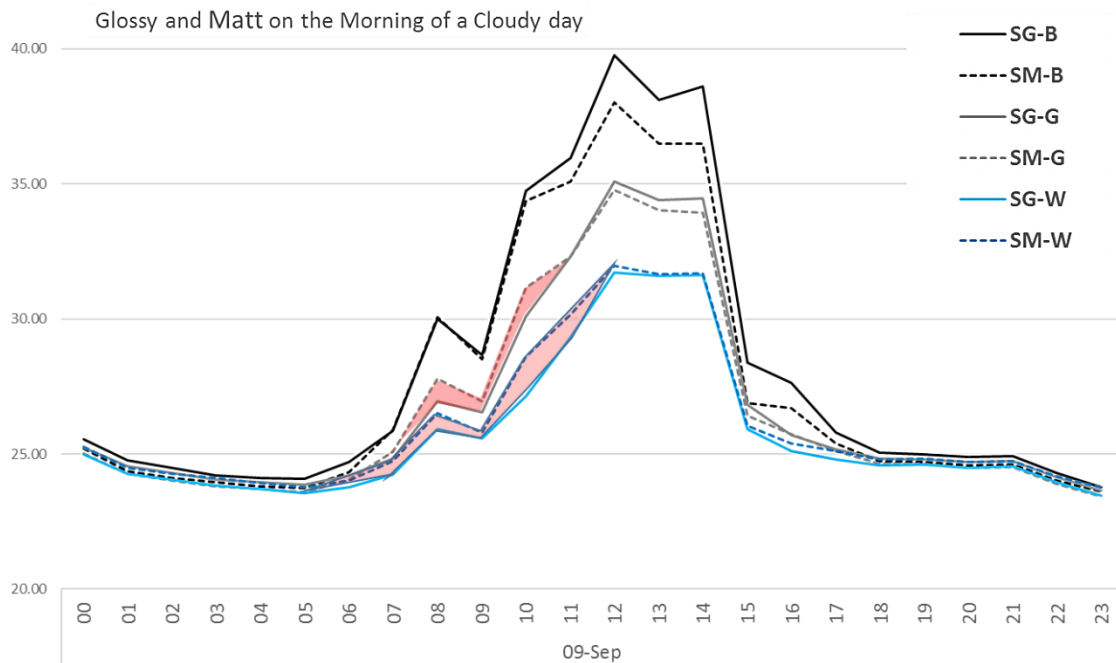


Figure 6-37 A closer look at the Glossy and matte paints temperature profile in the morning of the cloudy day.

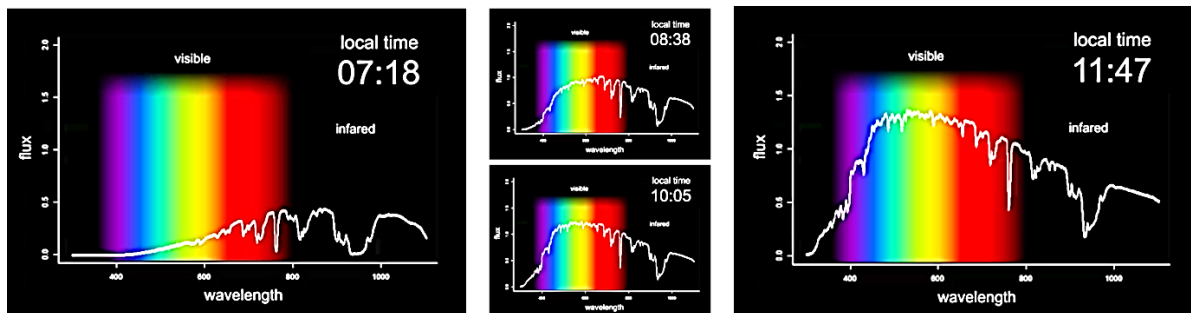


Figure 6-38 The infrared portion of the solar spectrum is high in the early morning and overwhelmed by the visible components at noon. Source:(National Institute of Standards and Technology 2015).

The NIR Radiation percentage Drops at:
 1- in the presence of cloud
 2- at the early morning hours

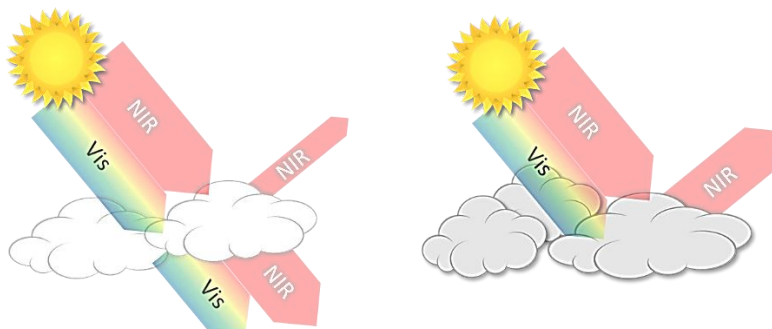


Figure 6-39 The change in the solar spectrum portions in the various conditions, i.e. the NIR portion drops by the presence of the cloud.

On the last thing to confirm about the solar paint, performance is that there is usually a risk of heating penalty in winter when using such solar reflective paints. Despite that such investigation requires a winter time measurement, But however, the results herewith (for September) Initial results shows that the minimum temperature of all the paints does not drop beyond the plain tiles, or below the normal paint temperatures. This observation can be seen in the overall layered chart that is plotted in Figure 6-40 below.

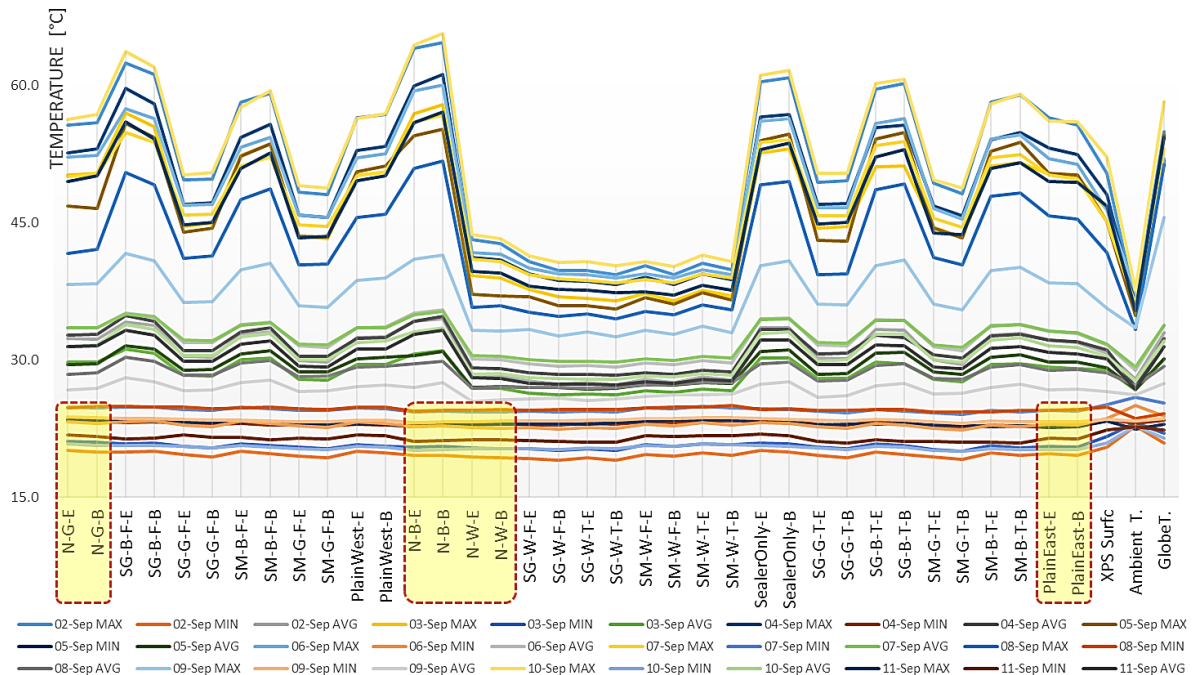


Figure 6-40 Average, Maximum, and Minimum Temperature for the period (2nd~11th Sept.) for all the experimental permutations compared to the base cases i.e. the bare (plain) concrete tiles and the normal paints

6.4 Conclusion

This conclusion covers the first and the second experuimntIn findings, where the investigated factors and the main aim of utilising the solar paint are addressed. As a reminder, the incorporation o the solar paint was intended to work as a heat mitigation measure only and is not extended to use solar radiative paints. Also, the first and second experiments have three common parameters that have experimented, which are the usefulness of suing the solar paints. The influence of the sealer base on the paint performance. Moreover, the effect of the paints colours on its temperature reduction performance. However, it was found that these factors are interactive and one factor may change the other performance, as will be seen in the following. On the other hand, the second experiment is meant to address a fourth factor, which is the effect of the paint glossiness on its heat reduction performance.

To start with, it is to confirm that the solar paint has a profound effect on reducing the temperature of the surface which host them. However, however, this is affected by a combined

influence of the colour and the sealer type and application. Meaning that, if the sealer is a white type, then the application of the sealer is indispensable for the dark colours. Meanwhile, it does not affect the light colours performances. On the other hand, if the sealer is transparent, then it will negatively influence the performance of the matte paints, meanwhile, if a glossy solar is to be applied, then they must be painted over a sealer base.

From another point of view, the role of the paint colour is generally within expectations, as the light colours have shown a good potential in reducing the tiles temperature. However, the use of the light colour may affect the performance of the matte paint during cloudy weather as well as early morning hours where the NIR radiation is subsided. In this regards, it is recommended that further research may have a look at the inclination of the surface where the paint should be applied. That is, and based on the initial finding from the second experiment, it is expected that the glossiness of the solar paint may have various contributions if the surface is made vertical.

In conclusion, it is to state that solar paints have shown a high abilities as a heat mitigation measures, as they have contributed to mostly keep the painted tiles below the tiles with conventional paints. When bearing in mind that such heat mitigation strategy is totally passive and is easy to apply, then it is recommended that it should be prescribed as part of the envelope description, especially in the cooling dominant climates. For the mild climates, the winter heating penalties are to be considered, despite that in both experiments, there was no significant risk of heating penalties, since the paint have only contributed to dampening the maximum temperature, and did not extend to lower the minimum daily temperatures.

Chapter 7:

7. Conclusion

In this chapter, the main findings that directly address the research hypothesis and objectives are summarized, then incorporated in the proposed framework structure. Later on, the research limitations are highlighted while showing the potential research fields that may hand over from this research. In more detail, The first section, that is intended to briefly summarize the main conclusions across the various chapters. The second section, in turn, is represented by a single chart that explains the proposed roadmap toward having a better envelope specification, that account for the cooling load as a genuine part of the building needs. Lastely, the third part is also aimed to summarize the key obstacles and limitations that may have affected the research results, and starting from these limitations, the suggested future works areas are emerged.

7.1 Summary of the findings

From the beginning of the literature review, it can be fairly said the building envelope and how is described in the various standards and codes has a clear lack of vital information, and seemed to be repeatedly viewed from the same direction that prioritized the heating load over the need for the cooling loads, misunderstanding the local climatic needs and conditions. This global perception has resulted in disregarding the dynamic thermal behaviour that the building envelope is -in reality- subjected to. In turn, perceiving and assist the building envelopes in the static bases have by all means excluded the massive potentials of exploiting the thermal mass materials in reducing the cooling loads, as well as the heating loads. However, among the literature survey, that there is also many promising concepts, like the “critical thermal mass thickness” concept, in addition to other concepts that may ameliorate the building energy and comfort conditions alike. Still, with the literature review, it was found that there is an imperative topic that had a minor attention, even from the scientific respecting side, which is the anti-insulation.

Moving from hypothesis to test and validation, and before commencing the simulations, it was of important to explore the simulation tools and its related means. That is, an integral investigation was concerned with the selection of the simulation software based on many factors that are linked and crucial to the research purpose. Here, it can be concluded that the EnergyPlus software serves all the critical research points and requests from the simulation tool. That is, the EnergyPlus have been found reliable in simulating advanced heat storage mediums, with is a genuine part of the research investigation. Also, it has many other privileges that made it perfectly suited for simulation the layer configurations, checking the results in various ways, well control over the inputs, as well as being able to run many sets of simulations using its parametric tools. On another aspect, the weather files are also investigated in this chapter, where it was found that most of the weather files out of the US are likely to have customised values, specifically for the cloud coverage and the horizontal infrared radiation values. Hence, it is advised that if a weather data of a site out of the US borders, it needs to be double checked. Lastly, in this chapter, and after identifying the simulation tool and the reliable weather data, an initial simulation test was carried out to check if the EnergyPlus, with its default settings, will be able to simulate the layer segmentation only – without layer rearrangements- would be stable and produce reasonable errors. This innovative exploration was also repeated in the next chapter under different simulation conditions. and the results in both chapters showed that it could safely simulate the layer configuration rearrangements.

All points considered, the third chapter has directly delved into providing a mitigation measure for the anti-isolation behaviour. In this regards, it was hypothesised that if the building layers configuration have significant effects on the various dynamic thermal behaviour measures, then it would also likely affect the anti-insulation behaviour. The hypothesis was developed, and the proposed six different layer configurations were tested under a vast number of permutations that hit 1,000 permutations, where the various climates and occupancy schedules have performed the examination mediums. The results have been positive, and it was proven that the anti-insulation negative behaviour can be mitigated by reconfiguring (re-arranging) the envelope layers. This finding

is deemed to be critical for all the building stakeholders, because, simply, it will allow maintaining the same insulation thickness if the overheating (anti-inflation) risk may have appeared. In another word, designers are had another tool instead of going directly to a tradeoff between the cooling and heating loads when the insulation becomes the tweaking measure. Also, the founded mitigation measure also facilitates another genuine part of the anti-insulation equation. That is, since the anti-insulation is a product of high cooling setpoints and great insulations, designers can have access to another mean of increasing the cooling set-point with a clear threshold of the upper increment limits. Not to forget, that in the findings of chapter two, there was a clear relation between the best performing layer configurations and the occupancy profiles of the subject budling. Also, it was also shown that the mild climates are more prone to the anti-insulation behaviour, which is a point that is usually understood in a serious way. All in all, the findings and the data are prepared as an article and submitted to the Energy and Buildings Journal with a title of “Anti-insulation Mitigation by Altering the Envelope Layers’ Configuration”.

Moving in the same anti-insulation track, another hypothesis to mitigate the anti-insulation was to change the number of the layer segments of the envelope. This assumption was based on recent research (as shown in literature review) which concluded that if the number of the layer segments is increased, then this increment (layer dispersion) would enhance the dynamic thermal performance of the derived multi-layered configuration. Taking this finding into consideration, the chapter was oriented to test the layer dispersion on the conclusions of the previous chapter i.e. chapter three. That is, the best performing configurations have been taken from chapter 3 and subjected to further layer dispersion, where a two-layer configuration is developed to be a four, six and eight layer configuration while maintaining the external boundary conditions of the base “mother” configuration. The findings of this chapter were to somehow unpredictable and inconsistent. As the segmentation may increase the Point of thermal inflexion at one schedule, but it may reduce it on the same schedule when applied in different climates. Therefore, two points were concluded from that chapter. Firstly, it is to confirm that the layer segmentation has a good ability to manipulate the Point of thermal Inflexion when anti-insulation is founded. Secondly, it is recommended if a layer segmentation is to be used as an anti-isolation measure, then the specific climatic and occupancy profiles have to be individually studied for the specific subject case.

The third chapter has inherited the concept of the layer segmentation from its preceding chapter, but this time, with an experimental methodology to test the segmentation effect on the dynamic thermal behaviour of the walls. Moreover, and most importantly, the main objective of this chapter was to provide a practical solution for incorporating the thermal mass materials at a reasonably small thicknesses. In addition, it is also to provide a reasonable solution if the layers are to be dispersed along the wall at small thicknesses. In another word, investigating the use of the rubber materials a heat storage mediums would enable the designers to employ the thermal mass without thinking about his great thickness that may not comply with the aesthetic or space measures. Also, the use of the rubber has other two significant privileges. The fist is the ability to mobilise it at ease. Such value is paramount in supporting the emerging concepts of the portable and remote buildings. The mobility issue might also be conceived as a disaster architecture where the buildings have to be

flexible enough to travel. The second important issue that the rubber may help to supply for isolated to the acoustics. That is, it is very common that designers may want to expose the thermal mass to the internal environment as to serve as a coolth/heat reservoir, especially when this mass is associated with night ventilation, and in such cases, the designers may hesitate from the echo and the poor acoustical environment that is incurred by employing and exposed thermal slabs and walls. Therefore, the utilisation of rubber, as an elastic material would enable using it as an internal heat storage medium while tolerating the acoustical issues. In conclusion, it has shown that the rubber material can provide reasonable decrement factors and substantial time lags when correctly incorporated within the layering structure. Also, it was confirmed that produced 11cm wall have similar capacities of a brick wall with a 20cm of thickness.

The last chapter that has experimental contents is the dealing with solar paints experiments. In general, the contents of this chapter may have, to some extent, decoupled from the other chapters, since its contents are not borrowing concepts and findings from earlier chapters. In fact, the solar paint experiment can be studied in an individual research, because the nature of the solar paint is dealing with the facial properties of the building envelope. However, studying the facial properties of the skin are indisputably when describing the envelope properties since the skin optical properties dictate how much of heat does the envelope have to handle afterwards. Therefore, in this study, the solar paint have been investigated at two discrete experiment, where the first one can be considered as an exploratory investigation where some of the paint properties are examined. Moreover, the second experiment was developed to assert the findings of the first experiment and exploring another paint properties. Collectively, it was confirmed that the solar paints have good potentials to reduce the surface temperature that will subsequently affect the envelope core be with it. However, as per the investigated parameters, it was found the solar paint colour is governed by the type and the presence of the base sealer. For example, It was found that the Glossy paints do not perform well if no sealer is applied at its base, on the another hand it was found that for matte paints the sealer may hinder its solar protection performance. Moreover, and as expected and specified by the paint manufacturer, the matte paint has shown better temperature reduction. However, interestingly, it was also found that at some specific times, namely, at the early mornings of the cloudy days, the glossy paints perform better than the matte paints. Moreover, to interpret this paints behaviour, it was deduced that the glossy paints work better if the NIR components of the solar spectrum are subsided. Lastly, it was found that, unlike the solar cooling paints, the solar protection paints may have little risk of winter heating penalties if applied in mild climates where both cooling and heating are of equal importance.

7.2 The concluded framework

This section is composed of one graph, that is shown below, where the roadmap to improve and incorporate the various factors in the envelope specification is listed in chronological order. That is, if a legislation body that is concerned with developing an envelope specification for a given location and parameters, it might use this figure, together with this research, to come up with adequate specifications that take into account the various measures being studied and developed in this research.

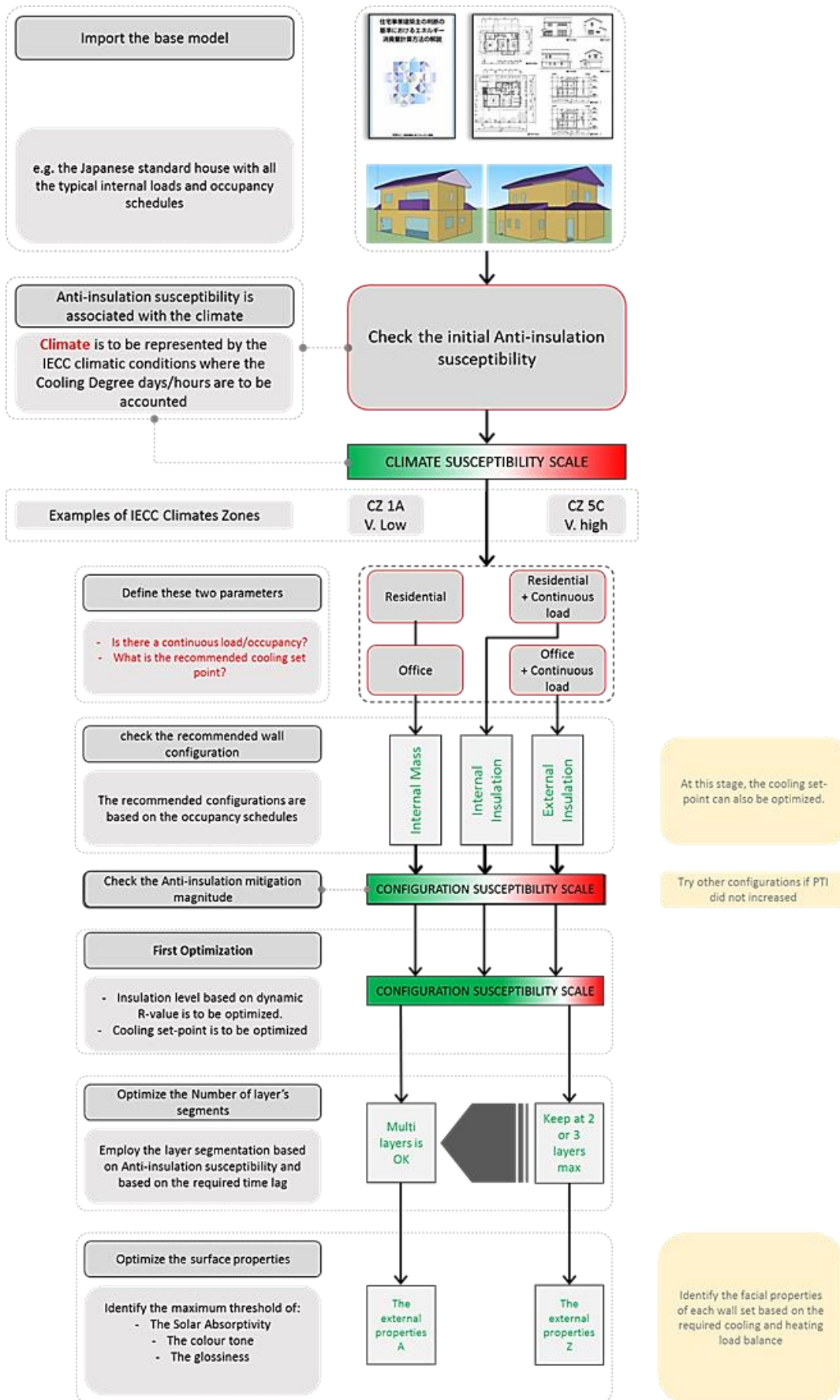


Figure 7-1 the framwrok formulation.

7.3 Limitation and further work

In this part, it is to overview the issues that may have contributed to the limitation of the findings or may have lead to some errors in the experiments or simulation. In the beginning, it is to say that since the second chapter is meant to be an initial error tracing for itself, this section will move to list the work limitation starting from the third chapter that is concerned with the anti-insulation mitigation. In that chapter, the major applicability comes from the early simulation assumptions, where the experimental subject was a simple box that has no windows and so on. Therefore for the wider range of applying the findings of chapter three it is to consider that each building has its thermal behaviour, due to the unique occupancy and internal gains, material properties, windows to wall ratios, internal mass and heat storage, and so on. Therefore, the recommended configurations for each building might differ from what is found herewith in this study.

Indeed, as by taking the Japanese residential building types, i.e the flats and the detached housing, we can anticipate -based on earlier conclusion- that anti-insulation is likely to occur on flats but less likely to arise in the detached houses. As in one hand, the flats might be susceptible to the anti-insulation behaviour, as one of things that have been advocated in the article paper, is that even in a very typical residential building, like in flats, which can be presented by the Hong Kong example, it can facilitate rising the anti-insulation behaviour. This is because such spaces are majorly located in the mid-floors of the building and they are protected from direct external heat and their cooling loads become dictated by internal gains instead, therefore, the privilege of having insulation to cut the external heat transmission loads diminishes, and this is where they become more likely to give rise to anti-insulation. On the other hand, for regular houses it is much less likely to encounter anti-insulation, because firstly, the occupancy in typical Japanese houses is small (the number of the family members is not so big) which will result in having less internal gains, meanwhile the envelope external surface area inflates in relation with the internal air volume, making the external transmission load greater, which will give benefit to the insulation where it becomes a more of pro-insulation rather than anti-insulation.

Also, this research was solely concerned with the cooling energy consumption. Therefore, some configurations might not agree with the recommendations when other measures are used, the time lag, the decrement factor, the damping effect, as examples. It also might disagree with the configurations recommended by studies concerned internal thermal comfort models, where the heat radiation to occupants is considered, and internal thermal mass, for example, might not be welcomed, while the optical properties (e.g. emissivity) is fixed in this study. Importantly, it is to highlight that similar comprehensive studies are required to account for the winter heating loads as to evaluate the drop in the anti-insulation behaviour when the the annual energy consumption is considered.

On the other hand, The founded results of the third chapter can also be a good incentive to study more about anti-insulation and exploring other mitigation concepts. For example, as an analogy to this research, an inspiring and promising concept could be investigating the influence of changing the surface optical properties (e.g. emissivity) to mitigating anti-insulations. (Huang et al. 2013) Showed that high reflectivity coating could significantly reduce cooling load. Therefore, the effect of

implementing the Reflective to manipulate anti-insulation can be studied. Moreover, this is the ongoing research topic.

Concerning the fourth chapter that is dealing with anti-insulation, where the same points above are also applied, but the main concern about this chapter was the time limitation to conduct another set of 6500 simulations. Which is the required number of permutations for the layer segmentation to cover the same possibilities that were involved in the previous chapter? Here, it is stated that at the beginning of the research planning, and based on the previous chapter findings, it was expected to find a consistent behavioural pattern over a reasonably small number of cases. However, there was no clear and distinguished pattern to describe the layer segmentation behaviour. Therefore, it is suggested the layer segmentation exercise can take a step further, since it showed a good potential in mitigating the anti-insulation, but it needs much more simulation permutations to come up with clear guidelines for the layer segmentation rules of thumbs.

Moving to the rubber experiment, there are few points that were of concerns and may have caused a series of limitations during the experiment as well as for the use of the rubber as a heat storage medium afterwards. Firstly, it is to highlight that the developed rubber and insulation systems cannot be used directly on flat roofs, due to their elastic nature. However, it can be argued that such a system can be part of the construction, i.e., to be integrated into concrete slabs instead of the insulation material alone, but in such cases, it will require further assessments and investigations. The second issue that might arise with the use of the rubber is that it blocks the vapour transportation and wall breathing. Therefore, the humidity issue needs to be validated using experimental and specialised humidity simulation tools, like Wufi for example. Moreover, and despite that the rubber cost issues have been argued and addressed in the discussion, the cost implications need to be studied under an economic model. Whereas this feasibility model is to be explored in a holistic payback point of view, i.e. the land price, the HVAC equipment size, their corresponding installation, maintenance and capacity are to be incorporated in the financial model. In another aspect, further studies may look at the real manufacturing and build a mock model of the rubber wall as to test factors like the homogeneity and the erection of the developed wall, whereas technical details like a variation of the expansion rates between the insulation and rubber may arise, and so on. The last issue to consider about the rubber is that the behaviour of the rubber configurations needs more experimental tests under the initial transient operation modes. Since the recommended wall “best beefing over a dynamic measure” is likely to differ from the ones, have been seen in the steady periodic tests.

For the solar paints, the major experimental constraint was the size of the tiles where the paints are applied. As it was seen that these small tiles have very high-temperature variations on their surfaces. Also, their small size made them more susceptible to be influenced by the surrounding context, as they rapidly respond to a small contextual shading, and so forth. Besides, the major issue about the applicability of the solar paints, which was repeatedly raised in many points of this study, is the heating loads penalties that might arise when employing this paint technique. Moreover, for this issue, it is recommended that a further study is to be carried out to test the difference between the solar protection paints and the solar cooling paints as to clarify the heating penalties behind each. Other than that, it might be interesting to further investigate the note that the glossy paints are better

performed under the cloudy conditions and at early in the morning. To take this note further, another experiment can look at the application of the solar paints (matte and glossy) on the various wall orientations. That is based on the notion that if the glossy paint is good at mitigating low sun angles, it might be interesting to see how it performs when the sun is at low altitudes during the early morning.

Finally, it is to show that that, the first aim of this research was to find a holistic and collective recommendation for the envelope based on the outcomes of each study (represented in the chapters), that is, to link all the experiments and simulations findings as to develop a perfect envelope, if to say. However, that collective recommendation concept seemed to be illogical because of the following aspects. Firstly, the factors that influence each measure is different from others, e.g. The layer configurations' performance is affected by the occupancy profile which can not be experimented in the Peltier device. On the other hand, the solar paint performance is facial and is dependent on the solar radiation and clouds coverage, where simulating this effect would be inaccurate due to the lack of accurate cloud cover measurements, and so forth. Moreover, for these reasons, developing a framework, where the findings are formulated as guidelines that can be adjusted to match the specific and local needs is thought to be more universal and can be reasonably adopted by local authorities and sustainable bodies to develop the local codes with respecting to the cooling demands of their buildings. For the future researchs, and starting from this framweork, the other factors that have signifcant effects on the building's energy consumption can be examined. For example, the buidling shape and vloume to wall area ratios is a rcih study area, that can be linked with the effects of the walls configurations and with the surface properties as well. Not to forget, another invistigation field is to explore the influcne of adding the window to the equations, either by studing their solar heat gain or the heat loss through this weak envelope points.

Bibliography

- Akbari, H. & Levinson, R., 2008. Evolution of Cool-Roof Standards in the US. *Advances in Building Energy Research*, 2(1), pp.1–32.
- Akbari, H. & Matthews, H.D., 2012. Global cooling updates: Reflective roofs and pavements. *Energy and Buildings*, 55, pp.2–6. Available at: <http://www.sciencedirect.com/science/article/pii/S0378778812001491> [Accessed January 16, 2015].
- Albatici, R. & Tonelli, A.M., 2010. Infrared thermovision technique for the assessment of thermal transmittance value of opaque building elements on site. *Energy and Buildings*, 42(11), pp.2177–2183. Available at: <http://www.sciencedirect.com/science/article/pii/S0378778810002264> [Accessed August 2, 2015].
- Al-Regib, E. & M.Zubair, S., 1995. TRANSIENT HEAT TRANSFER THROUGH INSULATED WALLS EMAD. *Energy*, 20(7), pp.687–694.
- Al-Sanea, S.A., 2012. State of the Art in the Use of Thermal Insulation in Building Walls and Roofs – Part II.
- Al-Sanea, S.A. & ZEDAN, M.F., 2001. Effect of Insulation Location on Initial Transient Thermal Response of Building Walls. *Journal of Thermal Envelope and Building Science*, 24(4), pp.275–300. Available at: <http://jen.sagepub.com/content/24/4/275> [Accessed March 17, 2016].
- Al-Sanea, S.A. & Zedan, M.F., 2001. Effect of insulation location on thermal performance of building walls under steady periodic conditions. *International Journal of Ambient Energy*, 22(2), pp.59–72. Available at: <http://www.tandfonline.com/doi/abs/10.1080/01430750.2001.9675389> [Accessed March 27, 2016].
- Al-Sanea, S.A. & Zedan, M.F., 2011. Improving thermal performance of building walls by optimizing insulation layer distribution and thickness for same thermal mass. *Applied Energy*, 88(9), pp.3113–3124. Available at: <http://www.sciencedirect.com/science/article/pii/S0306261911001486> [Accessed February 14, 2016].
- Al-Sanea, S.A. & Zedan, M.F., 2008. Optimized monthly-fixed thermostat-setting scheme for maximum energy-savings and thermal comfort in air-conditioned spaces. *Applied Energy*, 85(5), pp.326–346.
- Al-Sanea, S.A. & Zedan, M.F., 2002. Optimum insulation thickness for building walls in a hot-dry climate. *International Journal of Ambient Energy*, 23(3), pp.115–126. Available at: <http://www.tandfonline.com/doi/abs/10.1080/01430750.2002.9674880> [Accessed March 27, 2016].
- Al-Sanea, S.A., Zedan, M.F. & Al-Hussain, S.N., 2012. Effect of thermal mass on performance of insulated building walls and the concept of energy savings potential. *Applied Energy*, 89(1), pp.430–442. Available at: <http://www.sciencedirect.com/science/article/pii/S0306261911005058> [Accessed December 2, 2015].
- Amari, H. et al., 2007. Thermal sensation and comfort with different task conditioning systems. *Building and Environment*, 42(12), pp.3955–3964. Available at: <http://www.sciencedirect.com/science/article/pii/S0360132306003660> [Accessed March 4,

2016].

- Asan, H., 1998. Effects of wall's insulation thickness and position on time lag and decrement factor. *Energy and Buildings*, 28(3), pp.299–305.
- Asan, H., 2000. Investigation of wall's optimum insulation position from maximum time lag and minimum decrement factor point of view. *Energy and Buildings*, 32(2), pp.197–203. Available at: <http://www.sciencedirect.com/science/article/pii/S03787788000044X> [Accessed March 18, 2016].
- Asan, H., 2006. Numerical computation of time lags and decrement factors for different building materials. *Building and Environment*, 41(5), pp.615–620. Available at: <http://www.sciencedirect.com/science/article/pii/S0360132305001046> [Accessed January 27, 2016].
- Asan, H. & Sancaktar, Y.S., 1998. Effects of Wall's thermophysical properties on time lag and decrement factor. *Energy and Buildings*, 28(2), pp.159–166. Available at: <http://www.sciencedirect.com/science/article/pii/S0378778898000073> [Accessed January 27, 2016].
- ASHRAE, 2013. ANSI/ASHRAE/IES Standard 90.1-2013: Energy Standard for Buildings Except Low-Rise Residential Buildings.
- ASHRAE, 2012a. *ANSI/ASHRAE Standard 169-2006, Proposed Addendum b to Standard 169, Climatic Data for Building Design Standards*, Atlanta GA 30329-2305. Available at: www.ashrae.org.
- ASHRAE, 2007. Energy Standard for Buildings Except Low-Rise Residential Buildings.
- ASHRAE, 2012b. Proposed Addendum b to Standard 169, Climatic Data for Building Design Standards. Available at: www.ashrae.org/bookstore.
- ASHRAE HOF, 2013. ASHRAE Handbook Online. *ASHRAE® HANDBOOK - FUNDAMENTALS*. Available at: <http://handbook.ashrae.org/Handbook.aspx> [Accessed February 17, 2016].
- Attia, S. et al., 2013. Assessing gaps and needs for integrating building performance optimization tools in net zero energy buildings design. *Energy and Buildings*, 60, pp.110–124.
- Azemati, A.A. et al., 2013. Thermal modeling of mineral insulator in paints for energy saving. *Energy and Buildings*, 56, pp.109–114. Available at: <http://www.sciencedirect.com/science/article/pii/S0378778812004914> [Accessed June 18, 2014].
- Bauman, F. & Arens, E., 1996. Task/ambient conditioning systems: Engineering and application guidelines. *Center for Environmental Design Research, UC Berkeley*, (6), pp.0–13. Available at: <http://eprints.cdlib.org/uc/item/0r36z48d>.
- Berdahl, P. & Bretz, S.E., 1997. Preliminary survey of the solar reflectance of cool roofing materials. *Energy and Buildings*, 25(2), pp.149–158.
- Bojic, M., Yik, F. & Sat, P., 2001. Influence of thermal insulation position in building envelope on the space cooling of high-rise residential buildings in Hong Kong. *Energy and Buildings*, 33(6), pp.569–581. Available at: <http://www.sciencedirect.com/science/article/pii/S0378778800001250> [Accessed March 18, 2016].
- Bojić, M.L. & Loveday, D.L., 1997. The influence on building thermal behavior of the insulation/masonry distribution in a three-layered construction. *Energy and Buildings*, 26(2),

- pp.153–157. Available at: <http://www.sciencedirect.com/science/article/pii/S0378778896010298> [Accessed March 18, 2016].
- Bond, D.E.M., Clark, W.W. & Kimber, M., 2013. Configuring wall layers for improved insulation performance. *Applied Energy*, 112, pp.235–245. Available at: <http://www.sciencedirect.com/science/article/pii/S030626191300531X> [Accessed June 9, 2015].
- BuildDesk, 2016. Thermal mass. Available at: <http://www.builddesk.co.uk/software/builddesk-u/thermal-mass/>.
- Bullett, T.R. & Prosser, J.L., 1983. Paint: a surface modifier. *Physics in Technology*, 14(3), pp.119–125. Available at: <http://stacks.iop.org/0305-4624/14/i=3/a=301?key=crossref.55f1a79f77d4aa18dc70d5705d8beebea> [Accessed November 1, 2016].
- Burns, P.J., Han, K. & Winn, C.B., 1991. Dynamic effects of bang-bang control on the thermal performance of walls of various constructions. *Solar Energy*, 46(3), pp.129–138.
- Cambridge University Engineering Department, 2003. Materials data book. *Materials Courses*, pp.1–41.
- Catalanotti, S. et al., 1975. The radiative cooling of selective surfaces. *Solar Energy*, 17(2), pp.83–89. Available at: <http://www.sciencedirect.com/science/article/pii/0038092X75900626> [Accessed February 18, 2015].
- Contribution of Working Groups I, II and III to the F.A.R. & IPCC, 2014. *Climate Change 2014 Synthesis Report*, Geneva, Switzerland.
- Corrado, V. & Paduos, S., 2016. New equivalent parameters for thermal characterization of opaque building envelope components under dynamic conditions. *Applied Energy*, 163, pp.313–322. Available at: <http://www.sciencedirect.com/science/article/pii/S030626191501363X> [Accessed December 11, 2015].
- Crawley, D.B. et al., 2001. EnergyPlus: creating a new-generation building energy simulation program. *Energy and Buildings*, 33(4), pp.319–331.
- Crawley, D.B., 1998. Which Weather Data Should You Use for Energy Simulations of Commercial Buildings?, p.ASHRAE 1998 TRANSACTIONS 104 Part 2.
- Daouas, N., 2011. A study on optimum insulation thickness in walls and energy savings in Tunisian buildings based on analytical calculation of cooling and heating transmission loads. *Applied Energy*, 88(1), pp.156–164. Available at: <http://www.sciencedirect.com/science/article/pii/S0306261910002990> [Accessed February 22, 2016].
- Designing Buildings Ltd., 2016. Kappa value - Designing Buildings Wiki. Available at: https://www.designingbuildings.co.uk/wiki/Kappa_value [Accessed November 7, 2016].
- Dias, D. et al., 2014. Impact of using cool paints on energy demand and thermal comfort of a residential building. *Applied Thermal Engineering*, 65(1–2), pp.273–281. Available at: <http://www.sciencedirect.com/science/article/pii/S1359431113009538> [Accessed June 18, 2014].
- ECCA, ECCA – European Coil Coating Association. Available at: www.eccacoil.com.

- Energy, U.D. of, 2015. EnergyPlus Documentation, Engineering Reference.
- Escobedo, J.F. et al., 2009. Modeling hourly and daily fractions of UV, PAR and NIR to global solar radiation under various sky conditions at Botucatu, Brazil. *Applied Energy*, 86(3), pp.299–309.
- Etzion, Y. & Erell, E., 1991. Thermal storage mass in radiative cooling systems. *Building and Environment*, 26(4), pp.389–394. Available at: <http://www.sciencedirect.com/science/article/pii/036013239190065J> [Accessed June 27, 2014].
- Ghahramani, A. et al., 2016. Energy savings from temperature setpoints and deadband: Quantifying the influence of building and system properties on savings. *Applied Energy*, 165, pp.930–942. Available at: <http://www.sciencedirect.com/science/article/pii/S0306261915016888> [Accessed January 17, 2016].
- Granqvist, C.G., 1981. Radiative heating and cooling with spectrally selective surfaces. *Applied optics*, 20(15), pp.2606–15. Available at: <http://ao.osa.org/abstract.cfm?URI=ao-20-15-2606> [Accessed February 18, 2015].
- Griggs, E.I. & Shipp, P.H., 1988. *The impact of surface reflectance on the thermal performance of roofs: An experimental study*,
- Gunde, M.K., Orel, Z.C. & Hutchins, M.G., 2003. The influence of paint dispersion parameters on the spectral selectivity of black-pigmented coatings. *Solar Energy Materials and Solar Cells*, 80(2), pp.239–245.
- H. E. Ashton, 1966. Canadian Building Digest - National Research Council. Available at: [http://ip51.icomos.org/~fleblanc/projects/1983-1992_HC/brochures & publications/technical dossiers series/paint/i_p_hc_tech_paint_CBD_no76.pdf](http://ip51.icomos.org/~fleblanc/projects/1983-1992_HC/brochures%20&%20publications/technical%20dossiers%20series/paint/i_p_hc_tech_paint_CBD_no76.pdf) [Accessed November 1, 2016].
- Haavi, T., Jelle, B.P. & Gustavsen, A., 2012. Vacuum insulation panels in wood frame wall constructions with different stud profiles. *Journal of Building Physics*, 36(2), pp.212–226. Available at: <http://jen.sagepub.com/cgi/doi/10.1177/1744259112453920> [Accessed November 1, 2016].
- Hirsch, J.J., Weather Data & Weather Data Processing Utility Programs. Available at: http://doe2.com/index_wth.html.
- Huang, Y., Niu, J. & Chung, T., 2013. Study on performance of energy-efficient retrofitting measures on commercial building external walls in cooling-dominant cities. *Applied Energy*, 103, pp.97–108. Available at: <http://www.sciencedirect.com/science/article/pii/S0306261912006435> [Accessed March 7, 2016].
- Idris, Y. & Mae, M., Data on anti-insulation detection via Point of Thermal Inflexion (PTI) in 1248 cases; 13 climates, four occupancy profiles, six wall configurations and four insulation levels. *Data in Brief*, (under revision).
- International Code Council, 2015. *International Energy Conservation Code*, USA.
- Japan Meteorological Agency, Past weather data download 気象庁|過去の気象データ・ダウンロード. Available at: <http://www.data.jma.go.jp/gmd/risk/obsdl/index.php#!table>.
- Japan Sustainable Building Consortium, 2011. *energy conservation standards of housing*,
- Jelle, B.P., Kalnæs, S.E. & Gao, T., 2015. Low-emissivity materials for building applications: A state-of-the-art review and future research perspectives. *Energy and Buildings*, 96, pp.329–356. Available at: <http://www.sciencedirect.com/science/article/pii/S0378778815002169> [Accessed July 29, 2015].

- Jentsch, M.F., Bahaj, A.S. & James, P.A.B., 2008. Climate change future proofing of buildings— Generation and assessment of building simulation weather files. *Energy and Buildings*, 40(12), pp.2148–2168. Available at: <http://www.sciencedirect.com/science/article/pii/S0378778808001400> [Accessed April 6, 2015].
- Kalogirou, S.A., Florides, G. & Tassou, S., 2002. Energy analysis of buildings employing thermal mass in Cyprus. *Renewable Energy*, 27(3), pp.353–368. Available at: <http://www.sciencedirect.com/science/article/pii/S0960148102000071> [Accessed January 11, 2016].
- Kaynakli, O., 2012. A review of the economical and optimum thermal insulation thickness for building applications. *Renewable and Sustainable Energy Reviews*, 16(1), pp.415–425. Available at: <http://www.sciencedirect.com/science/article/pii/S1364032111004163> [Accessed April 14, 2015].
- Kazanci, O.B. & Olesen, B.W., 2013. The Effects of Set-Points and Dead-Bands of the HVAC System on the Energy Consumption and Occupant Thermal Comfort. In *Proceedings of the 7th Mediterranean Congress of Climatization*. Istanbul, Turkey. Available at: http://orbit.dtu.dk/fedora/objects/orbit:124250/datastreams/file_69e437b5-cbd8-4264-8268-13d75d543866/content [Accessed March 8, 2016].
- Kontoleon, K.J. & Bikas, D.K., 2007. The effect of south wall's outdoor absorption coefficient on time lag, decrement factor and temperature variations. *Energy and Buildings*, 39(9), pp.1011–1018. Available at: <http://www.sciencedirect.com/science/article/pii/S0378778806002775> [Accessed September 21, 2016].
- Kontoleon, K.J. & Eumorfopoulou, E.A., 2008. The influence of wall orientation and exterior surface solar absorptivity on time lag and decrement factor in the Greek region. *Renewable Energy*, 33(7), pp.1652–1664.
- Kossecka, E. & Kosny, J., 2002. Influence of insulation configuration on heating and cooling loads in a continuously used building. *Energy and Buildings*, 34(4), pp.321–331. Available at: <http://www.sciencedirect.com/science/article/pii/S0378778801001219> [Accessed June 9, 2015].
- Kuin, T.H., Ramsey, W. & Threlkeld, J.L., 1998. *Thermal environment Engineering*.
- Ladybug + Honeybee & Github, epw map. Available at: <http://www.ladybug.tools/epwmap/> [Accessed November 3, 2016].
- Lakeridou, M. et al., 2012. The potential of increasing cooling set-points in air-conditioned offices in the UK. *Applied Energy*, 94, pp.338–348. Available at: <http://www.sciencedirect.com/science/article/pii/S0306261912000700> [Accessed January 18, 2016].
- Levinson, R., Akbari, H. & Gartland, L., 1996. Impact of the temperature dependency of fiberglass insulation R-value on cooling energy use in buildings.
- MakeItFrom.com, 2009. Material properties. Available at: <http://www.makeitfrom.com/material-properties/Chloroprene-Rubber-CR-Neoprene>.
- Masoso, O.T. & Grobler, L.J., 2008. A new and innovative look at anti-insulation behaviour in building energy consumption. *Energy and Buildings*, 40(10), pp.1889–1894. Available at: <http://www.sciencedirect.com/science/article/pii/S0378778808000923> [Accessed December 16, 2014].

- MATTHEWS, J., 2000. *THERMAL COMFORT IN THE HAVELIS OF JAISALMER – A STUDY OF THE THERMAL PERFORMANCE OF AN URBAN COURTYARD HOUSE*. University of East London.
- Mazzeo, D. et al., 2015. Dynamic thermal characteristics of opaque building components. A proposal for the extension of EN ISO 13786. In *Energy Procedia*. pp. 3240–3245.
- McLeod, R.S., Hopfe, C.J. & Kwan, A., 2013. An investigation into future performance and overheating risks in Passivhaus dwellings. *Building and Environment*, 70, pp.189–209.
- Meinel, A.B. & Meinel, M.P., 1976. *Applied solar energy. An introduction*, Addison-Wesley Publishing Co., Reading, MA.
- METEOTEST: et al., 2014. Meteoronorm Global meteorological database V7 Handbook Part1: Software. Available at: www.meteororm.com.
- Ministry of Industry and Electricity, K. of S.A., 2002. *Studies and Statistics Department, Electrical Affairs Agency: Electricity Growth and Development in the Kingdom of Saudi Arabia up to the year 1420 H (1999/2000 G)*, Saudi Arabia.
- Muselli, M., 2010. Passive cooling for air-conditioning energy savings with new radiative low-cost coatings. *Energy and Buildings*, 42(6), pp.945–954. Available at: <http://www.sciencedirect.com/science/article/pii/S0378778810000125> [Accessed February 9, 2015].
- N. B. Geetha, R.V., 2012. Passive cooling methods for energy efficient buildings with and without thermal energy storage – A review. *Energy Edu. Sci. Technol. Part A*, 29 (2) (20), pp.913–946. Available at: http://www.silascience.com/journals_detail.aspx?j_id=2&v_no=67.
- National Institute of Standards and Technology, U.S.C.D., 2015. Top-of-the-Atmosphere Sunlight — As Seen from Earth | NIST. Available at: <https://www.nist.gov/news-events/news/2015/10/top-atmosphere-sunlight-seen-earth> [Accessed November 5, 2016].
- Orel, B. et al., 1990. Coil-coating paints for solar collector panels—I. Characterization and performance tests. *Solar & Wind Technology*, 7(6), pp.699–705. Available at: <http://www.sciencedirect.com/science/article/pii/0741983X90900443> [Accessed July 17, 2014].
- ORNL ((Oak Ridge National Laboratory)), ORNL Thermal Mass Calculator. Available at: <http://web.ornl.gov/sci/roofs+walls/AWT/InteractiveCalculators/download.htm> [Accessed July 8, 2016].
- Ozel, M., 2014. Effect of insulation location on dynamic heat-transfer characteristics of building external walls and optimization of insulation thickness. *Energy and Buildings*, 72, pp.288–295. Available at: <http://www.sciencedirect.com/science/article/pii/S037877881300697X> [Accessed September 1, 2016].
- Ozel, M., 2012. The influence of exterior surface solar absorptivity on thermal characteristics and optimum insulation thickness. *Renewable Energy*, 39(1), pp.347–355. Available at: <http://www.sciencedirect.com/science/article/pii/S0960148111004988> [Accessed March 25, 2016].
- Passive House, 2016. Building Envelope. , p.312. Available at: https://passipedia.org/planning/thermal_protection [Accessed October 21, 2016].
- Priyadarsini, R., Hien, W.N. & Wai David, C.K., 2008. Microclimatic modeling of the urban thermal environment of Singapore to mitigate urban heat island. *Solar Energy*, 82(8), pp.727–745.
- Raman, A.P. et al., 2014. Passive radiative cooling below ambient air temperature under direct

- sunlight. *Nature*, 515(7528), pp.540–4. Available at: <http://dx.doi.org/10.1038/nature13883> [Accessed October 13, 2015].
- Ritter, M.E., 2012. The Physical Environment: an Introduction to Physical Geography. *Manual of Remote Sensing*, 1. Available at: http://www.earthonlinemedia.com/ebooks/tpe_3e/energy/nature_of_electromagnetic_radiation.html [Accessed November 1, 2016].
- Roaf, S., Fuentes, M. & Thomas, S., 2007. *Ecohouse* Third., Chennai, India: Elsevier Ltd.
- Rosenfeld, A.H. et al., 1995. Mitigation of urban heat islands: materials, utility programs, updates. *Energy and Buildings*, 22(3), pp.255–265.
- Saidur, R. et al., 2007. Energy and associated greenhouse gas emissions from household appliances in Malaysia. *Energy Policy*, 35(3), pp.1648–1657.
- Samuel, D.G.L., Nagendra, S.M.S. & Maiya, M.P., 2013. Passive alternatives to mechanical air conditioning of building: A review. *Building and Environment*, 66, pp.54–64. Available at: <http://www.sciencedirect.com/science/article/pii/S0360132313001212> [Accessed May 25, 2014].
- Sathish Kumar, P. et al., 2016. Paints and Coating of Multicomponent Product. In J. K. Kim, S. Thomas, & P. Saha, eds. *Multicomponent Polymeric Materials*. Dordrecht: Springer Netherlands, pp. 157–226. Available at: http://dx.doi.org/10.1007/978-94-017-7324-9_7.
- Schiavoni, S. et al., 2016. Insulation materials for the building sector: A review and comparative analysis. *Renewable and Sustainable Energy Reviews*, 62, pp.988–1011. Available at: <http://linkinghub.elsevier.com/retrieve/pii/S1364032116301551> [Accessed September 9, 2016].
- SCI-PAINT JAPAN INC., 2008. High reflection and excellent thermal barrier paint. Available at: <http://www.sci-paint.jp/en/products/supra/index.html>.
- Seth, S.P. et al., 1981. Optimum distribution of insulation and concrete in a multilayered wall of roof. *Applied Energy*, 9(1), pp.49–54.
- Smith, G.B. et al., 2003. Coloured paints based on coated flakes of metal as the pigment, for enhanced solar reflectance and cooler interiors: description and theory. *Solar Energy Materials and Solar Cells*, 79(2), pp.163–177. Available at: <http://www.sciencedirect.com/science/article/pii/S0927024802004099> [Accessed June 18, 2014].
- Sodha, M.S. et al., 1981. Thermal load levelling in a multilayered wall/roof. *International Journal of Energy Research*, 5(1), pp.1–9. Available at: <http://onlinelibrary.wiley.com/doi/10.1002/er.4440050102/abstract> [Accessed October 31, 2016].
- Stazi, F. et al., 2015. The effect of high thermal insulation on high thermal mass: Is the dynamic behaviour of traditional envelopes in Mediterranean climates still possible? *Energy and Buildings*, 88, pp.367–383. Available at: <http://www.sciencedirect.com/science/article/pii/S0378778814010123> [Accessed September 21, 2016].
- Stevanović, S., 2013. Optimization of passive solar design strategies: A review. *Renewable and Sustainable Energy Reviews*, 25, pp.177–196. Available at: <http://www.sciencedirect.com/science/article/pii/S1364032113002803> [Accessed May 8, 2015].

- Synnefa, A., Santamouris, M. & Akbari, H., 2007. Estimating the effect of using cool coatings on energy loads and thermal comfort in residential buildings in various climatic conditions. *Energy and Buildings*, 39(11), pp.1167–1174.
- Synnefa, A., Santamouris, M. & Livada, I., 2006. A study of the thermal performance of reflective coatings for the urban environment. *Solar Energy*, 80(8), pp.968–981.
- Szokolay, S.S., 2007. *Introduction to Architectural Science: The Basis of Sustainable Design* Third., Great Britain: Elsevier Ltd.
- Thermtest Inc., 2016. Thermophysical Properties. Available at: <https://www.thermtest.com/material-property-search> [Accessed November 7, 2016].
- Threlkeld, J.L., 1970. *Thermal environmental engineering*, Prentice Hall.
- Tyler, H. et al., 2009. Energy savings from extended air temperature setpoints and reductions in room air mixing. In *International Conference on Environmental Ergonomics*. Boston: escholarship University of California, pp. 0–13. Available at: <http://eprints.cdlib.org/uc/item/28x9d7xj#>.
- UNI EN ISO 13786, 2007. Thermal performance of building components - Dynamic thermal characteristics - Calculation methods. , p.42. Available at: <https://www.iso.org/obp/ui/#iso:std:iso:13786:dis:ed-3:v1:en> [Accessed July 19, 2016].
- United Nations, Department of Economic and Social Affairs, P.D. (2014)., 2016. *The World's Cities in 2016 Data Book*, Available at: http://www.un.org/en/development/desa/population/publications/pdf/urbanization/the_worlds_cities_in_2016_data_booklet.pdf.
- US Department of Energy, 2014a. Commercial Prototype Building Models | Building Energy Codes Program. Available at: https://www.energycodes.gov/development/commercial/90.1_models [Accessed April 4, 2016].
- US Department of Energy, 2015a. EnergyPlus Documentation, Auxiliary EnergyPlus Programs.
- US Department of Energy, 2015b. EnergyPlus Documentation, Getting Started with EnergyPlus.
- US Department of Energy, 2015c. EnergyPlus Documentation, Input Output Reference. , p.1317. Available at: <http://nrel.github.io/EnergyPlus/InputOutputReference/01a-InputOutputReference/>.
- US Department of Energy, 2012. Residential Prototype Building Models | Building Energy Codes Program. Available at: https://www.energycodes.gov/development/residential/iecc_models [Accessed May 8, 2016].
- US Department of Energy, Weather Data by Location | EnergyPlus. Available at: https://energyplus.net/weather-location/asia_wmo_region_2/JPN//JPN_Tokyo.Hyakuri.477150_IWEC [Accessed November 3, 2016].
- US Department of Energy, 2014b. *Windows and Building Envelope Research and Development; Roadmap for Emerging Technologies*, Available at: <http://energy.gov/eere/buildings/downloads/research-and-development-roadmap-windows-and-building-envelope>.
- Wijewardane, S. & Goswami, D.Y., 2012. A review on surface control of thermal radiation by paints and coatings for new energy applications. *Renewable and Sustainable Energy Reviews*, 16(4), pp.1863–1873. Available at:

<http://www.sciencedirect.com/science/article/pii/S1364032112000470> [Accessed June 5, 2014].

Wilcox, S. & Marion, W., 2008. *Users Manual for TMY3 Data Sets*,

Wong, N.H. et al., 2011. Evaluation of the impact of the surrounding urban morphology on building energy consumption. *Solar Energy*, 85(1), pp.57–71.

Zhang, H. et al., 2010. Comfort, perceived air quality, and work performance in a low-power task–ambient conditioning system. *Building and Environment*, 45(1), pp.29–39. Available at: <http://www.sciencedirect.com/science/article/pii/S0360132309000547> [Accessed September 9, 2015].

Zhang, Q., Lou, C. & Yang, H., 2006. Trends of Climate Change and Air-Conditioning Load of Residential Buildings in China. *Journal of Asian Architecture and Building Engineering*, 5(2), pp.435–441. Available at: https://www.jstage.jst.go.jp/article/jaabe/5/2/5_2_435/_article [Accessed February 16, 2015].

Zhu, D. et al., 2012. *Comparison of Building Energy Modeling Programs: Building Loads*,